In vivo cell reprogramming to pluripotency: generating induced pluripotent stem cells *in situ* for tissue regeneration

Irene de Lázaro del Rey

A thesis submitted in partial fulfilment of the requirements for the degree of Doctor of Philosophy

UCL School of Pharmacy

University College London

2015

Declaration of academic integrity

I, Irene de Lázaro del Rey, confirm that the work presented in this thesis is my own. Where information has been derived from other sources, I confirm that this has been indicated in the thesis.

Irene de Lázaro del Rey

London, 17.12.15

To my gran, Isabel

As you set out for Ithaka
hope the voyage is a long one,
full of adventure, full of discovery.
Laistrygonians and Cyclops,
angry Poseidon—don't be afraid of them:
you'll never find things like that on your way
as long as you keep your thoughts raised high,
as long as a rare excitement
stirs your spirit and your body.
Laistrygonians and Cyclops,
wild Poseidon—you won't encounter them
unless you bring them along inside your soul,
unless your soul sets them up in front of you.

Hope the voyage is a long one.
May there be many summer mornings when,
with what pleasure, what joy,
you come into harbors seen for the first time;
may you stop at Phoenician trading stations
to buy fine things,
mother of pearl and coral, amber and ebony,
sensual perfume of every kind—
as many sensual perfumes as you can;
and may you visit many Egyptian cities
to gather stores of knowledge from their scholars.

Keep Ithaka always in your mind.
Arriving there is what you are destined for.
But do not hurry the journey at all.
Better if it lasts for years,
so you are old by the time you reach the island,
wealthy with all you have gained on the way,
not expecting Ithaka to make you rich.

Ithaka gave you the marvelous journey.
Without her you would not have set out.
She has nothing left to give you now.

And if you find her poor, Ithaka won't have fooled you.
Wise as you will have become, so full of experience,
you will have understood by then what these Ithakas mean.

Ithaka – C.P. Cavafy
(Translated by Edmund Keeley/Philip Sherrad)

Acknowledgements

One can easily find the parallelism between the PhD years and Cavafy's interpretation of the trip to Ithaka. We are often too focused on the final destination so as to understand that what is truly important is all what happens during the journey. Now that I have understood this, I would like to thank all those who encouraged me to start the trip and the ones who helped me along the way.

Thank you Kostas for leaving this very exciting project on my hands, even if they were surely not the best prepared for it. It has been a huge jump for me. I have learned a lot, I have enjoyed it a lot and, at the times that it was not easy, it always helped to feel that you trusted me more than I trusted myself! Thanks as well for giving me freedom in the direction of the project, necessary to build my own critical thinking, while always being available for discussions that I really enjoyed. Thanks for your dedication and for being so motivational.

Many people have come to and left the Nanomedicine Lab since I first arrived as a Master student in 2010. I cannot fit so many names in these lines! But my gratitude goes to all of you for the advice and guidance on my early days and for the support, understanding, and putting up with my writing-up mood in the last few months! Dr Cyrill Bussy and Dr Açelya Yilmazer deserve however a special mention because without them this project would have never taken off. Cyrill, you have now raised a few generations of Nanomediciners, always leaving aside your own things to rescue our experiments, and I am grateful to be one on the list. Acelya, you taught me so much and took so much care of me at the beginning and I really value that you did this even in your most stressful time. And I am glad that after four years I can still have your support. We always made a good team. I would also like to thank the master and PhD students that during their training and under my supervision have had an input in this project: Sarah, for the Southern Blot experiments; Yein and Faziela, without you I would not have had enough hands to handle so many stainings. I hope I have managed to teach you something as well!

Some of the studies in this thesis would not have been possible without our collaborators. I would like to thank the staff at the Genome Centre (Queen Mary University of London) for microarray experiments, Dr Neil Humphreys and Ms. Maj Simonsen Jackson (Transgenic Facility, University of Manchester) for chimerism

experiments, Dr Adam Reid (Centre for Tissue Injury and Repair, University of Manchester) for advice and training on surgical procedures and Dr Hans Degens (Manchester Metropolitan University) for advice, training and equipment for muscle myography. I would like to especially thank Prof. Giulio Cossu (Centre for Tissue Injury and Repair, University of Manchester) and the members of his lab for sharing their expertise and giving their advice on my observations. I would also like to ackownledge Obra Social LaCaixa and UCL for a jointly funded PhD Scholarship.

To the UCL School of Pharmacy I owe not only the experience gained during the first two years of my PhD, but also getting to know many special people that, although did not have an input in the science behind this thesis, merit equal acknowledgement for their help outside the lab. Giulia, you are missed in the lab and outside. Thanks for being "my only normal friend" in this cloud of craziness. Dimitris, thanks for standing my complaints since we started our Master together, for sharing your complaints with me and for complaining together! Francisco and Katrien, thanks for making the office an awful place to get work done, but a great place to be. Álvaro, the School of Pharmacy became a better place from the moment you arrived. Thanks for calling each Sunday, making me be rational when I am not and helping me overcome my fear to heights…I want to be like you when I grow up! Nicola, we have been through this PhD together…think how many things we have done and experienced since that first Christmas ice-skating! Thanks for being there throughout this trip…I hope we keep it this way.

Thanks as well to my non-scientist friends for understanding that sometimes I had to prioritise my cells or mice and for bringing me back to the outside world when it got too much. Mayte, you helped so much when things went rough and I would not have made it without you! You have also set the best example that anything can be achieved, just with a lot of effort. Miguel, who would have told us that summer in Santander 6 years from now that we would end up as we are now… I am glad that destiny decided to send us to the same island. Dessi, Mike and Jess, the times in Ampton St were the best, I wish we could go back. Artal, you have gained a place in heaven by sharing a flat with me the last few crazy months, thanks for your patience…I guess it will be my turn soon! Thanks to my friends from home Elena (the person who understands me better for the last 15 years), Jesús, Iván, Jose, Marta, Noemí, Carmen, María, Irene, Lorena, Jessica,

Laura… for still counting me in even if I am barely present and for being close in spite the distance. You are the definition of home. Gloria, Diego, Jordi, Julian, Mufi, Culi…for the visits and for always making some time for a coffee and a chat when I am back. Dr Maria de Toro, you showed me that jumping from Chemistry to Microbiology or from Pharmaceutics to Biology was just a matter of hard work and determination, thanks for the inspiration!

And, of course, thanks to those who always encouraged me to start this trip. Dr Maribel Rodriguez Franco and the team at CSIC for introducing me to research, and encourage me to continue with it. Dr. Manuel Guzmán, Dr. Jesús Molpeceres and Dra. María Guinea for your advice, recommendation letters and for keeping a nice memory of uni times after so long. Marta, Paula, Bea, Silvia, Pablo, Jorge and everyone else at hospital, for teaching me so much. Dr Alberto Arcediano, for being a great doctor and a better person. Thanks for always being much better than me in keeping in touch and for always sparing time to catch up.

Finally, a big thank you to my family for their visits, their encouragement and their trust on me. But if someone deserves more credit than anyone else for their help and support, not only during but also long before the preparation of this Thesis, those are my parents. You have made – and still do – more sacrifices than what you certainly should so that I can be in this position today. I will never be able to thank you enough.

Abstract

Artificially induced changes of cell identity are increasingly attracting attention as potential strategies to regenerate diseased or injured tissues, but still rely heavily on *ex vivo* culture with the exception of a small number of *in vivo* transdifferentiation studies. The reprogramming of somatic cells to pluripotency *in vivo* is even less explored, partly due to fears of teratoma formation. In this thesis, we hypothesised that such twist in cell fate can be safely achieved *in vivo* provided that sufficient but transient levels of reprogramming factors are locally expressed. We also speculated that transiently pluripotent cells can be generated in different tissues, thanks to the universality of the Yamanaka reprogramming factors, and that they may contribute to replenish the injured site after an insult. *In vivo* induction of pluripotency was first described in the liver and later in the skeletal muscle of wild-type mice. In both scenarios, the fast but transient upregulation of pluripotency markers and downregulation of tissue-specific genes did not progress to teratoma formation. The *in vivo* reprogrammed hepatocytes were established as a cell line *in vitro*, the so-called *in vivo* induced pluripotent stem (i^2PS) cells, and their pluripotency was confirmed at the molecular and functional levels. Clusters of *in vivo* reprogrammed cells within the skeletal muscle tissue were found to express pluripotency and myogenic progenitor markers and to re-integrate in the normal tissue architecture after a transient proliferative stage recapitulating events of normal postnatal myogenesis. Finally, *in vivo* reprogramming to pluripotency resulted in a modest enhancement of regeneration and functional rehabilitation in a model of skeletal muscle injury. In conclusion, this work not only provides proof-of-concept of safe *in vivo* cell reprogramming to pluripotency but also presents a thorough characterisation of the *in vivo* reprogrammed cells and supports the potential of such strategy to improve regeneration after injury.

Table of Contents

List of Figures

Chapter I

Chapter II

Chapter III

Chapter IV

Chapter V

Supplementary Figures

List of Tables

Chapter I

Chapter III

Supplementary Tables

List of abbreviations

2i	Dual inhibition
ADRC	Adipose tissue-derived regenerative cell
ADSC	Adipose tissue-derived stem cell
AP	Alkaline phosphatase
ASC	Adult stem cell
BMMSC	Bone marrow mesenchymal stem cell
BrdU	5-Bromo-2'-deoxyuridine
ca.	Circa
CM	Cardiomyocyte
CNS	Central nervous system
CTX	Cardiotoxin
DIG	Digoxigenin
DMEM	Dulbecco's Modified Eagle Medium
DNA	Deoxyribonucleic acid
EB	Embryoid body
ECC	Embryonic carcinoma cell
ES cell	Embryonic stem cell
FACS	Fluorescence Activated Cell Sorting
FBS	Fetal Bovine Serum
GA	Gastrocnemius
gDNA	Genomic DNA
GEO	Gene Expression Omnibus
GFP	Green fluorescent protein
h	Hours
HBSS	Hank's Balanced Salt Solution
HTV	Hydrodynamic tail vein

HWM	Hepatocyte Wash Medium
H&E	Haematoxylin and eosin
ICC	Immunocytochemistry
ICM	Inner cell mass
IHC	Immunohistochemistry
i.m.	Intramuscular
i.p.	Intraperitoneal
iPS cell	Induced pluripotent stem cell
i^2PS cell	*In vivo* induced pluripotent stem cell
kg	kilogram
KODMEM	Knockout Dulbecco's Modified Eagle Medium
KSR	Knockout Serum Replacement
LDM	Liver Digest Medium
LIF	Leukemia inhibitory factor
mAb	Monoclonal antibody
MEF	Mouse embryonic fibroblast
mES cell	Mouse embryonic stem cell
mg	milligram
MI	Myocardial infarction
min	Minute
miRNA	MicroRNA
ml	Milliliter
mRNA	Messenger RNA
mm	Millimeter
MS cell	Mesenchymal stem cell
MyHC	Myosin heavy chain
NCBI	National Center for Biotechnology Information
NEAA	Non-essential amino acid

No.	Number
pAb	Polyclonal antibody
PBS	Phosphate buffered saline
pc	Post culture
PCR	Polymerase Chain Reaction
PD	Parkinson's disease
pDNA	Plasmid DNA
PFA	Paraformaldehyde
RNA	Ribonucleic Acid
RT	Room temperature
RT-qPCR	Reverse transcription quantitative PCR
s	Second
SAN	Sinoatrial Node
s.c.	Subcutaneous
SCNT	Somatic cell nuclear transfer
SD	Standard deviation
SE	Standard error
UCB	Umbilical cord blood
WT	Wild type
µg	microgram
µl	microliter

Chapter I.
Introduction.

1.1. Regenerative medicine and cell replacement: tackling disease at its roots.

The Western world has witnessed a remarkable increase in life expectancy in the last decades. According to the UK's Office for National Statistics (ONS), average life expectancy is 77.9 years for males and 82.0 years for females (2007-2009 data). However, healthy life expectancy is estimated in 63.0 and 65.0 years, respectively [1]. We now live longer lives, but we also live with disease for longer, and treatment of many conditions remains challenging to manage with the currently available small molecule therapeutics and surgical interventions. These strategies often target the symptoms but do not tackle the genuine cause of the disease [2]. Such is the case in the treatment of Parkinson's disease (PD), one of the most prevalent degenerative ailments of our time, in which the administration of L-DOPA alleviates motor symptoms but does not restore death of dopaminergic neurons in the substantia nigra, the major origin of the disease [3]. Eventually, the "wearing off" effect of the drug over time results in the reappearance of motor impairment [4]. Treatment limitations are not only encountered by degenerative diseases. For example, in the event of a severe muscle injury, clinically-available conservative treatment - based on rest, ice, compression and elevation (RICE) - does not replace lost myofibers, failing to fully recover muscle force [5].

In such scenario, there is an urgent need to explore new therapeutic approaches that replenish and restore the damaged or degenerated tissues rather than simply compensate their impaired or lost function. This is precisely the uttermost aim of regenerative medicine and more in particular of cell replacement strategies [6] that, following on the examples above, attempt permanent replacement of lost neurons to alleviate PD [7] and of damaged muscle fibers to recover muscle force upon injury [8]. Indeed, the treatment of conditions in which a particular cell type is damaged or degenerated could be simplified if a stock of healthy replacement cells was readily available. However, the challenge to find an optimal source to generate such a stock is daunting and has not yet been entirely resolved.

Despite the initial success of studies involving transplantation of fetal tissue [9], the limited availability of this material together with ethical considerations have narrowed its potential as convenient source for cell

replacement [10]. Primary human cells isolated from unused or rejected organs for transplantation suffer from similar limitations [11]. Autologous grafts from different tissues of the same individual were at first seen as a better alternative [12]. However, the expectations of this approach have not been fulfilled in the long term, partly due to the invasive techniques that are frequently required for their sourcing, but mainly due to excessive variability in the results, inherent to the use of a non-standardised starting material [13, 14].

1.1.1. Stem cells in regenerative medicine: sources, promises and challenges. A realistic view on panacea.

In view that scarcity of the starting material is one of the main limitations in the search for an optimal cell source, stem cells stand out as promising candidates since they self-renew (divide unlimitedly into identical undifferentiated daughter cells) and can differentiate into representatives of one or various developmental lineages (potency), as represented in **Figure 1.1**. Several types of cells that fall into such definition can be found during human development and are classified according to the developmental stage at which they occur and to their differentiation potential **(Figure 1.2)** [15].

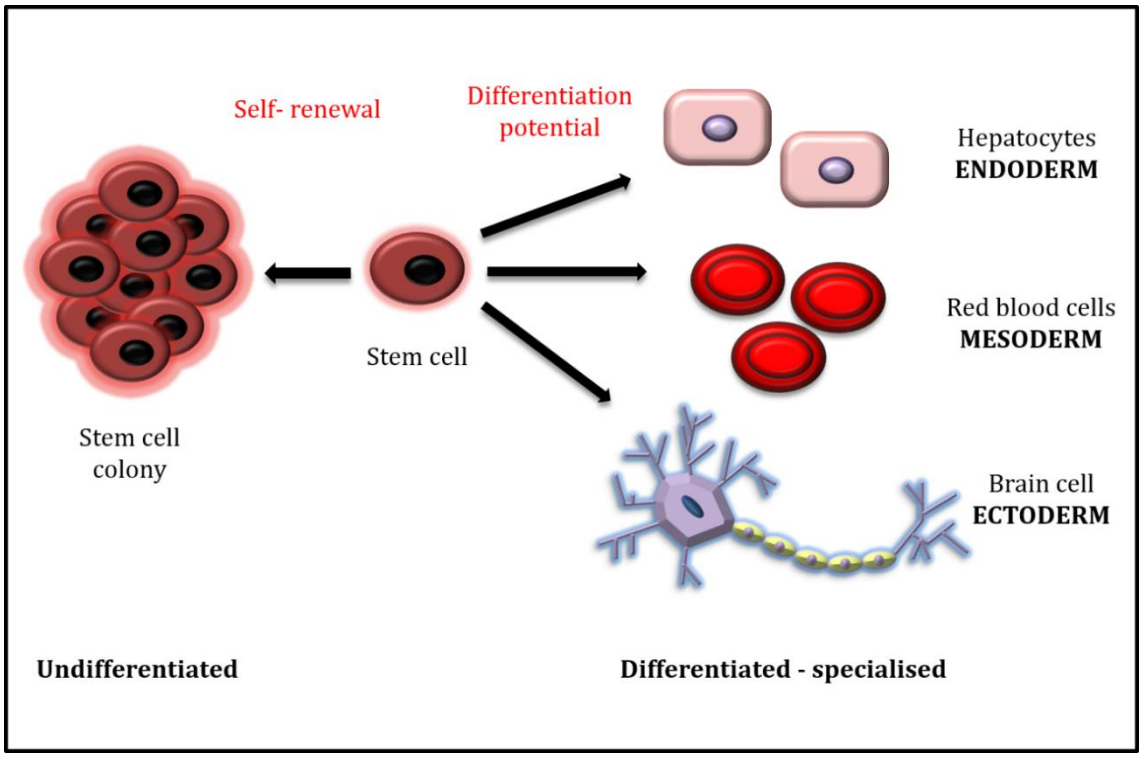

Figure 1. 1. Stem cell properties. *Stem cells are able to self-renew (divide unlimitedly remaining undifferentiated) and also to differentiate into cells from one or various developmental lineages.*

Totipotent cells are only found in the zygote and up to the 8-cell embryo. In a later stage, the blastocyst, embryonic stem (ES) cells can no longer generate extraembryonic tissues. However, they are regarded as one of the most promising sources for cell replacement strategies because they can differentiate into representatives of all three lineages (endoderm, mesoderm and ectoderm, hence termed "pluripotent") and, more importantly, because they can retain pluripotency and self-renew in culture when exposed to the right conditions. This was manifested thanks to Evans and Martin's first ES cell isolation from the inner cell mass (ICM) of mouse blastocysts in 1981 [16, 17] and to the identification of Leukemia inhibitory factor (LIF) as key to maintain pluripotency *in vitro* [18]. ES cells were finally established as the gold standard of pluripotency in 1990, when Nagy proved their functional pluripotency via tetraploid complementation studies [19].

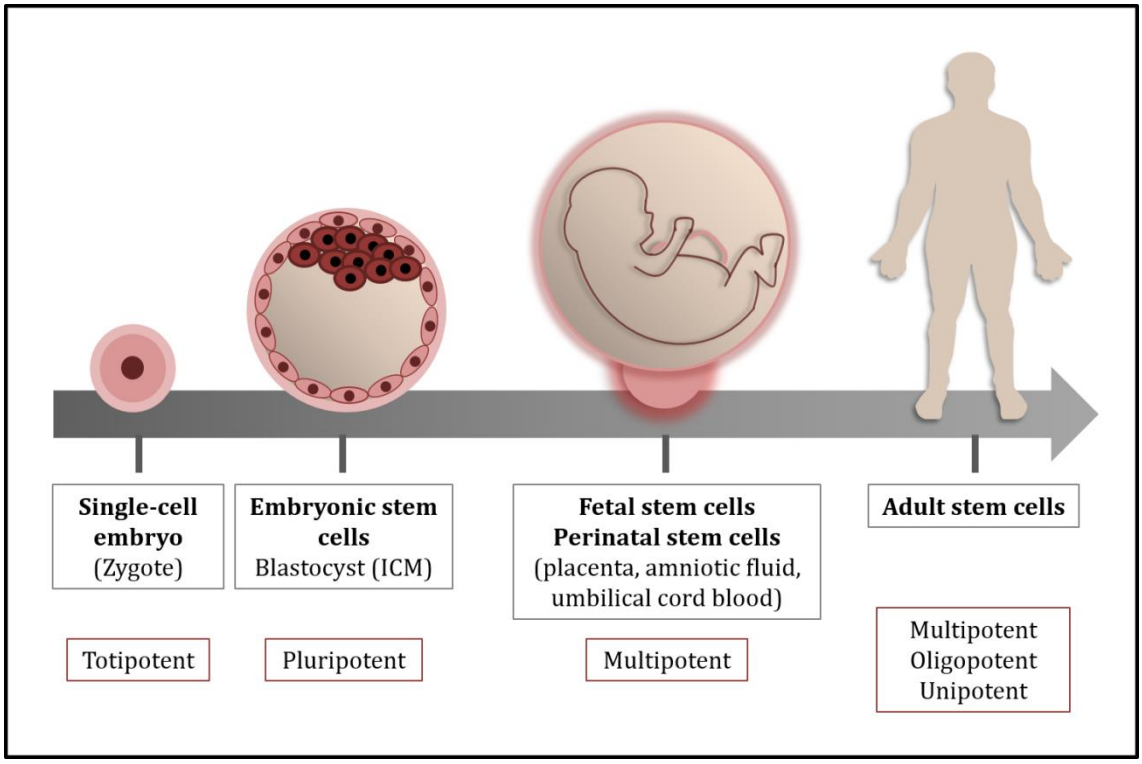

Figure 1. 2. Sources of stem cells classified according to their developmental origin and differentiation potential.

Further excitement was led by Thomson's first-ever isolation of human ES cells almost a decade later [20] that, probably too prematurely, suggested that the perfect source for human cell-based therapeutics could have been found. However,

this enthusiasm has been overshadowed by ethical constraints derived from the necessary destruction of human blastocysts. Such debate has spread beyond the scientific community and has resulted in governmental policies that limit research on human ES cells. From 2011 no process or technique involving blastocyst destruction can be patent-protected in the European Union, which might affect investor motivation for research in this area [21]. The situation has improved slightly in the US, where the ban on the use of federal funding for human ES cell research was abolished in 2009. However, such funds can still only be allocated to research on approved human ES cell lines and not for the derivation of new ones [22]. Leaving ethical and legal considerations aside, there is not a definite answer to whether the transplantation of ES cell-derived differentiated cells, which will necessarily be allogenic, will trigger an immune response and graft rejection. This may be another factor limiting the potential of such cells [23-25].

Later in development, fetal (obtained from aborted fetuses) and perinatal stem cells (harvested from placenta, umbilical cord blood and amniotic fluid) can be relatively easily accessed and their isolation does not involve the destruction of the embryo. However, their differentiation potential is restricted to certain lineages (i.e. they are not pluripotent but multipotent) and they cannot be maintained in culture for long periods of time without being coerced [26]. A lot of hope has been placed in the therapeutic application of umbilical cord blood (UCB) stem cells and numerous private and public "umbilical cord banks" have been created to preserve this tissue. However, the extremely restricted cell numbers encountered in some umbilical cords directly impede their therapeutic utilisation. Even with the most populated specimens, the amount of cells obtained from a single umbilical cord after *ex vivo* expansion is only sufficient to treat an infant up to 5 or 7 years old. In spite of the promising results of some preclinical and clinical studies, the limitations of this source must be taken into account and false hopes should be avoided [27].

Stem cells are not restricted to developmental stages prior to birth, but are also present in the adult organism, generally known as adult stem cells (ASCs). Multipotent mesenchymal stem (MS) cells are found in bone marrow and in the connective tissue of various organs [28]. Tissue-specific stem cells reside also in several organs including epidermis, liver, skin and skeletal muscle. Their role is to

maintain cellular homeostasis in the particular tissue and therefore their differentiation potential is very limited (oligo- or unipotent). In addition, they are not always sufficiently accessible to be isolated for their use in cell-based therapies. Bone marrow and adipose tissue are currently the most accessible sources ASCs [29].

In summary, different types of stem cells naturally occurring at various developmental stages offer different opportunities as sources of replacement cells. These are evidenced by the numerous clinical trials currently exploring their safety and therapeutic potential [30]. However, each and every of these sources is also accompanied by limitations and there is little consensus on which of them will perform better. Overall, this landscape confirms that a source that meets all requirements of abundance, accessibility, versatile differentiation potential, capacity to grow in culture without potency loss or coercion, immune compatibility and lack of ethical constraints has not yet been identified.

1.2. Induced cell fate changes as a therapeutic option: reprogramming meets regeneration.

1.2.1. New notions on differentiation, fate and plasticity of cell identity.

A series of findings initiated in the 1950s have shifted our views on cell differentiation from its definition as an irreversible process, to the realisation that cell identity is stable in the adult organism yet sufficiently plastic to be reset or altered when the right mechanisms are activated. Such observations have unveiled the concepts of cell reprogramming to pluripotency and transdifferentiation (direct reprogramming between two differentiated cell types) [31, 32].

The major contributions that led to this change in paradigm for developmental biology are chronologically summarized in **Figure 1.3**. Briggs and King's technical development of Somatic Cell Nuclear Transfer (SCNT), more commonly known as cloning, set the basis for John Gurdon's work on nuclear reprogramming. The initial studies introduced nuclei isolated from *Rana pipiens* frog blastula [33] and gastrula differentiating cells [34] into enucleated oocytes from the same species, and were able to generate new embryos. Gurdon's

experiments went one step further and, using the same technique, generated adult frogs from the nucleus of *Xenopus* endoderm differentiating cells [35], fully differentiated tadpole epithelial cells [36] and even fully differentiated keratinized adult frog skin cells [37].

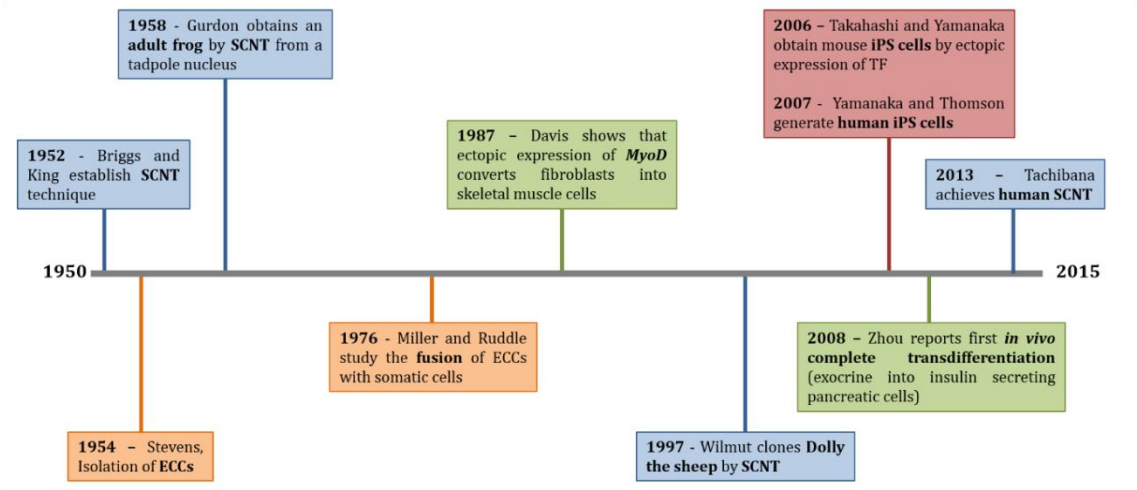

Figure 1. 3. Timeline of the studies in cell plasticity and reprogramming. Blue: *advances in SCNT.* ***Orange:*** *somatic and pluripotent cell fusion studies.* ***Green:*** *reports on transcription factor-mediated transdifferentiation.* ***Pink:*** *studies on transcription factor-mediated induced pluripotency (iPS cells).*

These findings initiated a genuine revolution in the field as they confirmed that, throughout the process of differentiation and even at the end of it, cells retain the same genetic information. They can therefore, under defined conditions, reverse differentiation – what has now been termed "reprogramming to pluripotency" – and support the generation of a new organism. Thanks to the advances in molecular biology we currently know that the process of differentiation is governed by reversible epigenetic changes rather than irreversible changes to the DNA sequence [32]. The same observation has been confirmed in mammalian organisms, although it took four decades until Dolly became famous world-wide for being the first-ever cloned mammal, generated via SCNT from the nucleus of an adult, fully differentiated, sheep mammary gland cell [38]. The births of Dolly and her offspring revolutionized thinking among the scientific community and public opinion and even triggered alarming reactions by those foreseeing the imminent misuse of human cloning [39, 40]. Such predictions were however very "optimistic". Almost two more decades were needed to reverse human cells to the pluripotent state via SCNT and such conversion is still

nowadays not fully optimised [41-43]. Thus, utilisation of this technique for therapeutic purposes is not predicted to take place in the near future.

Whilst SCNT protocols were adapted to mammalian organisms, Miller and Ruddle relied on the fusion of somatic and pluripotent cells as an alternative technique to confirm that differentiated cells could be reverted to pluripotency [44, 45]. The hybrids resulting from the fusion of thymocytes and embryonic carcinoma cells (ECCs, pluripotent cells isolated from germ cell tumours [46]) acquired biochemical and molecular characteristics of the latter while somatic cell features were lost. In conclusion, the pluripotent phenotype predominated over that of full differentiation. Currently available strategies to reprogram somatic cells to pluripotency, including SCNT and cell fusion, are illustrated in **Figure 1.4**.

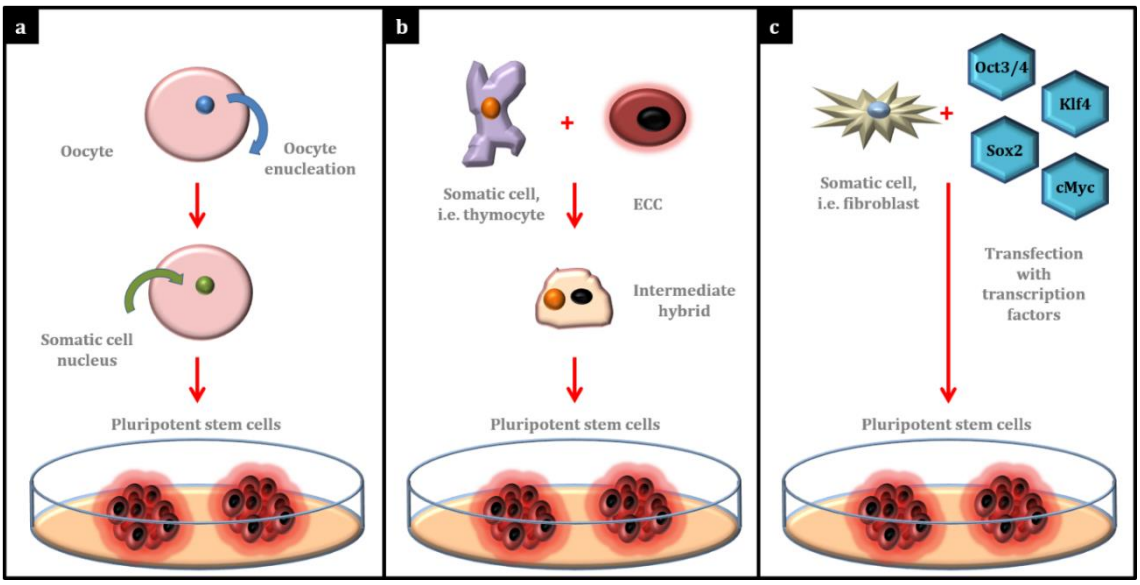

Figure 1. 4. Cell reprogramming to pluripotency strategies. *Three different approaches have been reported to reprogram somatic cells back to a pluripotent state.* ***(a)*** *Somatic Cell Nuclear Transfer: generation of pluripotent stem cells via injection of a somatic nucleus into an enucleated oocyte.* ***(b)*** *Cell fusion of somatic and pluripotent cells (ECCs), which produces hybrids that preserve the features of the stem cells.* ***(c)*** *Transcription factor based reprogramming: via forced expression of Yamanaka or OKSM factors.*

While the precise agents that drive the pluripotent conversion were still unidentified, research on transcription factors and the regulation of gene expression in the 1980s also contributed to the understanding of cell fate. Davies demonstrated fibroblast-to-myoblast conversion via retroviral overexpression of *MyoD*, a transcription factor with a relevant role in myogenesis [47]. Weintraub later confirmed the expression of muscle-related genes, albeit not complete

myoblast conversion, when the study was repeated on other cell lines [48]. These studies highlighted the capacity of lineage-specific transcription factors to induce fate changes between two differentiated cell types, which was later termed "transdifferentiation" or "direct reprogramming". Interestingly, Zhou and colleagues, followed by many others, confirmed that transdifferentiation is not restricted to the *in vitro* scenario and can also be induced in living tissues [49].

The conclusions reached from SCNT [33-38], cell fusion [44-46] and transcription factor-mediated transdifferentiation studies [47, 48, 50], led Yamanaka and Takahashi to hypothetise that transcription factors present in the oocyte and pluripotent cells could be responsible for the pluripotent conversion observed upon SCNT and cell fusion studies. With the aim to isolate those "pluripotency factors", a pool of 24 candidates was selected based on their enriched presence in oocytes and ES cells and on their previously known roles in pluripotency and its maintenance. After systematic screening of all possible combinations, a retroviral cocktail containing Oct3/4, Sox2, Klf4 and c-Myc, nowadays known as OKSM or Yamanaka factors, was able to reprogram mouse embryonic and adult fibroblasts to the pluripotent state [51]. The ectopic expression of these factors in somatic cells constitutes the most novel strategy to reverse differentiation, joining SCNT and cell fusion in the reprogramming (to pluripotency) toolbox **(Figure 1.4)**. The resulting pluripotent cells are termed induced pluripotent stem (iPS) cells and brought Yamanaka the Nobel Prize in Medicine and Physiology in 2012, jointly awarded with Sir John Gurdon for his contributions to nuclear reprogramming.

1.2.2. Opportunities offered by cell reprogramming in regenerative medicine.

The reprogramming technologies discussed above are gradually becoming more than techniques to study the mechanisms and mediators of cell plasticity, differentiation and de-differentiation. They have not only already provided invaluable research tools for disease modelling and drug screening among other applications but might also be able to offer novel alternative sources for cell replacement therapies [52]. In this respect, although at a very early stage, they have already contributed at the pre-clinical level by the:

1. **Generation of iPS cells for cell replacement interventions**: with the aim to establish a self-renewing stock of undifferentiated pluripotent cells in culture, derived from readily-available and non-ethically-controverted sources, which can generate customised differentiated cells to meet specific therapeutic needs.
2. **Induction of transdifferentiation *in vivo:*** as a means to directly manipulate cell fate in the living organism to reprogram a readily-available resident cell type into the phenotype required to alleviate a particular disease.

The achievements and limitations of these approaches are discussed in the next sections of this Chapter.

1.3. iPS cells in regenerative medicine

1.3.1. iPS cell promises: the alternative to ES cells.

The excitement brought by iPS cells to the future directions of cell-based therapies lays not only on the relative simplicity of their generation, but mainly on their similarities with ES cells. Like them, iPS cells have large nucleus, reduced cytoplasmic space and form domed-shaped compact colonies with refractive edges in culture. They express pluripotency genes at the mRNA and protein levels, including *Nanog*, *Ecat1* and *Rex1* among many others and, more importantly, grow indefinitely in culture maintaining their pluripotent properties intact under the appropriate conditions [51]. Mouse iPS cells are confirmed functionally pluripotent since they contribute to the adult tissues of chimeric mice obtained by blastocyst injection, including the germline [53]. Very importantly, iPS cells have also been generated from human fibroblasts by expression of human OCT3/4, SOX2, KLF4 and c-MYC [54], replacing c-MYC and KLF4 by NANOG and LIN28 [55] and even avoiding the tumourigenic c-MYC [56].

Commonly, iPS cells are presented not just as equivalent to ES cells but as superior alternatives that may overcome some of their associated limitations [52]. The main differences involved in the predicted use of ES and iPS cells in regenerative medicine are illustrated in **Figure 1.5**.

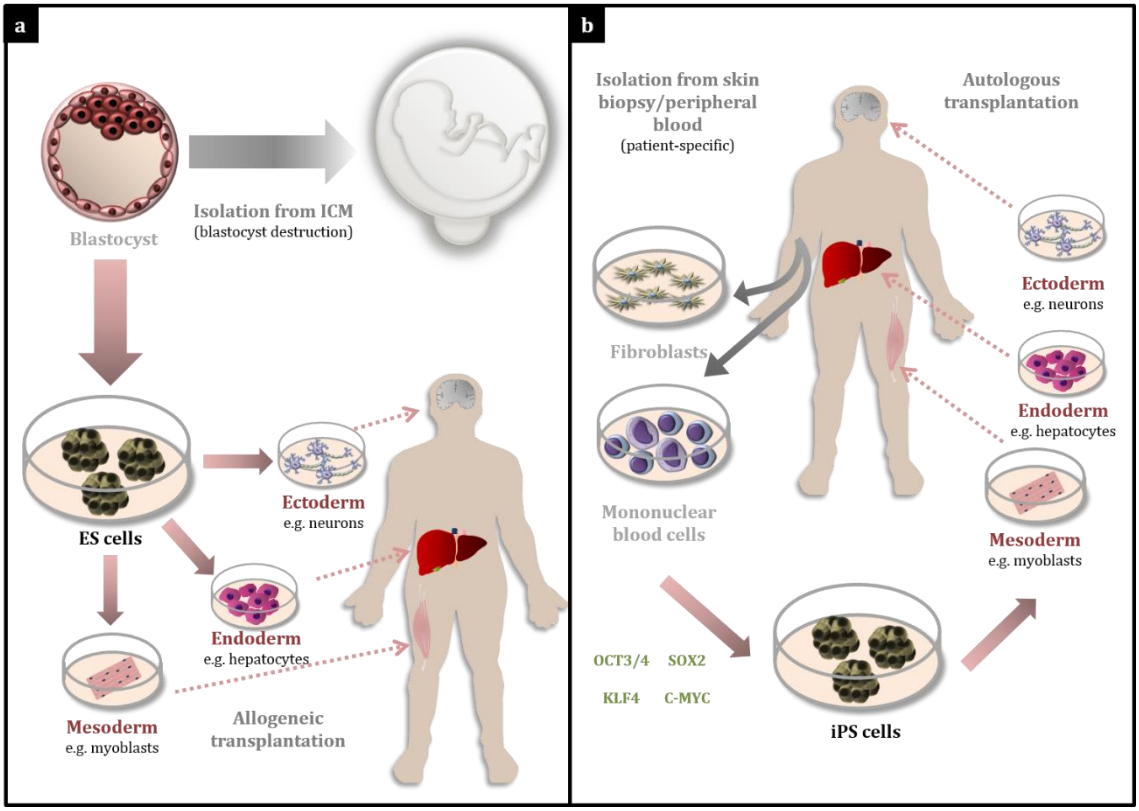

Figure 1. 5. Proposed utilisation of ES and iPS cells in regenerative medicine. (a) *ES cell-based therapy strategies involve discontinuation of the blastocyst development and rely on transplantation of allogeneic differentiated cells.* ***(b)*** *iPS cell technology allows the generation of patient-specific replacement cells for autologous transplantation, derived from easily accessible sources that do not involve handling of embryonic material.*

The first obvious benefit is the fact that iPS cell generation does not involve blastocyst destruction and therefore does not suffer from the same ethical constraints surrounding ES cell derivation. However, this is not the most relevant opportunity emerged from the way iPS cells are produced. They can be generated from a wide range of somatic cell types from all three lineages with little or no variation in the reprogramming cocktail [51, 57-65]. Dermal fibroblasts are a convenient source for iPS cell generation since they can be harvested by simple skin biopsy [62], while equally accessible mononuclear peripheral blood cells are less dependent on *in vitro* expansion to achieve sufficient cell numbers. They might also be a safer option since they are not directly exposed to environmental insults (e.g. mutations provoked by UV radiation) [57, 63, 64]. UCB cells share these advantages, however they require cord collection and banking at birth [65]. Overall, the use of these sources ensures that the procedure is minimally invasive for the donor and that they can potentially be generated from the same patient in need of the transplant. The use of patient-specific cells is predicted to minimise the

risk of immune graft rejection compared to that associated to ES cell derivatives and other cell-based therapies [23-25].

In conclusion, the envisioned application of iPS cell technology in regenerative medicine would involve harvesting easily accessible cells from a specific patient, followed by *ex vivo* induction into iPS cells, re-differentiation into the progenitor or mature phenotype required to alleviate the disease and eventual transplantation into the same patient. This sequence is illustrated in **Figure 1.5b**. In addition, it is precisely the capacity to generate patient-specific pluripotent and mature cells carrying a particular disease what makes iPS cells so valuable as tools in disease modelling and drug discovery, as discussed above. The advances in such areas fall out of the scope of this thesis but have been extensively reviewed by others [52, 66].

1.3.2. iPS cells: pre-clinical studies.

The first transplantation of iPS cell derivatives for therapeutic purposes was carried out in a murine model of sickle cell anemia only one year after the original Takahashi and Yamanaka article [67]. Since then, several other examples have highlighted the potential of iPS cell technology in regenerative medicine at the preclinical level. **Table 1.1** summarises the most relevant of these reports. The tissues and conditions targeted vary, but PD [68-70] and ischemic stroke [71-75] have attracted most interest. The interventions that aimed to alleviate genetic disorders required gene correction *ex vivo* in addition to iPS cell derivation and re-differentiation prior to transplantation [67, 76, 77]. Non-genetic diseases only involved the generation of iPS cells and their re-differentiation to the appropriate precursor or mature cell type in the culture dish before implantation. Only two studies have implanted undifferentiated iPS cells to date, one of which resulted in uncontrolled tumourigenesis [71], whereas the other showed absolute absence of tumours [78]. These discrepancies have not been further investigated. The therapeutic outcomes achieved have also varied among studies. In some reports, successful engraftment of the iPS cell derivatives did not result in functional recovery [75], while in others the alleviation of the disease was not clearly linked to the transplanted cells and may have been due to paracrine effects [72, 73]. Various reports have however shown more positive outcomes, proving not only the successful engraftment and survival of the transplanted cells but also their

functionality once integrated in the host's tissue [79, 80]. Overall, the results of these studies seem promising but there are many limitations that need to be overcome, which are discussed in **Section 1.3.4** of this Chapter.

1.3.3. iPS cells in humans: first clinical study.

Considering their brief history, iPS cells are rapidly making their way towards clinical development. The first human clinical study using iPS cell derivatives started recruiting patients in August 2013 and transplantation to the first patient was announced in September 2014 [81]. The cells to be transplanted are sheets of retinal pigmented epithelium grown in the laboratory and derived from the patient's own iPS cells. They are intended to repair the epithelium affected by age-related macular degeneration, however, the primary goal of this study is to assess the safety of such intervention [82]. The rapid progress of this technology towards clinical investigation has been received with mixed reactions among the scientific community. While some experts express excitement of the opportunities, others show concerns about the immaturity of the field and these trials [83]. Dr. Takahashi and her team at the RIKEN Center for Developmental Biology in Japan, where the sheets of retinal pigmented epithelium have been developed, have however highlighted the reproducibility of their protocol for sheet generation [84]. More importantly, they have confirmed that such cells are functional upon transplantation in diseased mice retina [80] and that they elicit no tumourigenicity or graft rejection when implanted in mice [85] and non-human primates [86].

Two other groups have also declared themselves ready to seek clinical trial authorisation in the very near future. Provided their goals are accomplished, a group in Kyoto University will implant iPS cell-derived dopaminergic neurons for PD treatment, supported by encouraging results in non-human primates [87]. The US-based biotechnology company Advanced Cell Technology will explore the potential benefits of iPS cell-derived platelets in blood clotting disorders. In theory, the latter should be a safer approach given the lack of nucleus in such cells [82].

Disease model	iPS cell derivatives	Restorative effect	Ref.
Sickle cell anaemia	Hematopoietic precursors (genetic defect corrected by gene therapy)	Normal erythrocyte phenotype restored.	[67]
Parkinson's disease	Midbrain dopaminergic neurons	Improvement of PD symptoms in behavioural tests. Positive engraftment in non-human primates.	[68-70, 87]
Muscular dystrophy (Limb-girdle)	Mesoangioblast-like cells (genetic defect corrected by gene therapy)	Restoration of α-sarcoglycan expression and of depleted muscle progenitors. Improvement of muscle force.	[77]
Muscular dystrophy (Duchenne)	Myogenic progenitors (genetic defect corrected by gene therapy)	Restoration of utrophin, replenishment of satellite cells and improvement of muscle force.	[76]
Spinal cord injury	Neurospheres	Enhanced recovery of motor function.	[79]
Ischemic stroke	Undifferentiated iPS cells	Generation of neuroblasts and mature neurons but uncontrolled tumourigenesis.	[71]
	Neuroepithelial-like stem cells	Improved functional recovery of stroke-damaged brain.	[72, 73]
	Neural progenitor cells	Improvement of somatosensory and motor symptoms.	[74]
	Neural progenitor cells	Graft survival and differentiation to neuronal phenotypes but no restorative effect.	[75]
	Neuro-epithelial-like stem cells		
Intracerebral haemorrhage		Significant recuperation of neural function.	[88]
Limb ischemia	Fetal liver kinase-1 positive cells	Revascularization of the ischemic limb accelerated via increased expression of VEGF.	[89]
	Endothelial progenitors	Neovascularization.	[90]
	Mesenchymal stem cells	Attenuation of severe ischemia.	[91]
Myocardial infarction	Undifferentiated iPS cells	Tumour free regeneration of infarcted tissue and improvement of contractile performance.	[78]
	Endothelial progenitors	Neovascularization, reduction of fibrosis and infarction site.	[90]
Cirrhotic liver	Hepatic progenitors	Liver regeneration.	[92]
Retinitis pigmentosa	Retinal pigmented epithelial cells	Improved visual function.	[93]
Age-related macular degeneration	Developing rod photoreceptors	Neural activity similar to native photoreceptors	[80, 85, 86]

Table 1. 1.Pre-clinical models of iPS cells in regenerative medicine.

1.3.4. Barriers to the applications of iPS cells in regenerative medicine.

In spite of the encouraging results shown in pre-clinical studies and their rapid progress towards clinical research, the use of iPS cells is not completely devoid of limitations.

Regarding the reprogramming methods employed, there has been a trend to first avoid the use of integrating vectors to deliver the reprogramming factors, due to the inherent risk of insertional mutagenesis, and further to completely abolish the use of DNA, which can be replaced by mRNA [94], microRNA (miRNA) [95], proteins [96] or small chemical compounds [97]. Excisable methods have also been utilised, however not all of them guarantee a 100% efficiency in transgene removal [98-101]. Unfortunately, many of the strategies considered as "safe", fail to achieve the same efficiency as the initially used integrating technology [51]. In some cases, a single technology was not enough to induce iPS cell derivation. Such was the case in the use of human artificial chromosomes, which had to be co-administered with miRNAs [102]. In **Table 1.2,** the reprogramming technologies available today for iPS cell generation are classified according to their safety/efficiency balance. We determined 'safety' based on the occurrence of genomic integration and immune complications and 'efficiency' according to the reported percentage of starting cells successfully converted into iPS cell colonies.

Reprogramming technology			Safety	Efficiency	Ref.
Viral vectors	Integrating	Retrovirus	-	++	[51]
		Lentivirus	-	++	[103]
		Inducible lentivirus	-	++	[104]
	Excisable	Excisable lentivirus	++	++	[98]
	Non-integrating	Adenovirus	++	-	[105]
	DNA free	Sendai virus	++	++	[106]
Naked DNA	pDNA		+	-	[107, 108]
	Episomal pDNA		++	+++	[109, 110]
	Mini circle pDNA		++	+++	[111]
	PiggyBac transposon		++	+	[100]
	Sleeping Beauty transposon		+	+	[101]
	Human artificial chromosome		++	-	[102]
DNA free	mRNA		+++	+++	[94]
	microRNA		+++	+	[95]
	Protein		+++	-	[96]
	Small molecules		+++	-	[97]

Table 1. 2. Reprogramming technologies available for iPS cell generation. *(+++) denotes very safe/efficient, (-) denotes not safe/not efficient.*

The transcription factors utilised to induce reprogramming might also compromise the safety of this technology. The use of Klf4 and, especially, c-Myc remains controversial due to their involvement in oncogenic pathways [53]. While initial efforts to exclude c-Myc from the reprogramming cocktail resulted in a decrease of the efficiency of the pluripotent conversion [56], it should be noted that the combination of factors required to induce pluripotency may also critically depend on the differentiation status and nature of the starting cells. For example, neural stem cells can be reprogrammed to pluripotency upon expression of Oct4 alone [61]. Hence, it is difficult to establish fair comparisons and make general statements.

Although in the early phases of iPS cell research, patient-specific iPS cell derivatives were thought to elude immune recognition, the reality is that almost ten years later there is still little consensus on the immunogenicity of such cells. Immune responses have been reported upon transplantation of undifferentiated iPS cells and subsequent generation of teratomas [112]. However, this was not observed when fully differentiated iPS cell derivatives were implanted, which suggests that the immune response may be a product of tumourigenesis rather than due to the iPS cells *per se* [113, 114]. It has also been proposed that differences among iPS cell lines generated by different protocols could be behind the discrepancies observed across studies [115]. Overall, more systematic studies are required to determine whether iPS cells may trigger immune complications.

The heterogeneity among iPS cell clones (depending on starting cell type, protocol utilised for pluripotent conversion and other factors, as reviewed elsewhere [116]) is also a matter of concern for the reproducibility of iPS cell therapies. Whether they should be considered identical to ES cells in terms of epigenetic status, genomic stability, mutational load and differentiation potential remains to be determined. Genome-wide analyses have found differences in gene expression profiles suggesting that epigenetic signatures from the tissue of origin could remain in iPS cells, which might restrict their differentiation potential [117, 118]. In addition, some studies have reported incomplete reprogramming to a pseudo-iPS cell intermediate state that, albeit similar to bona fide iPS cells in morphology and expression of certain markers, is not functionally pluripotent [119].

The capacity of pluripotent cells to generate teratomas *in vivo* has also raised some concerns on the safety of the approach. It should however be highlighted that this problem has only been encountered when undifferentiated iPS cells were transplanted [71], which is not the intended use of iPS cells in regenerative medicine, or when incomplete silencing of the reprogramming transgenes was suspected [70]. Appropriate quality control mechanisms that ensure absolute absence of undifferentiated cells among iPS cell derivatives intended for transplantation should therefore abolish this concern [120].

The use of iPS cells also suffers from limitations inherent to cell replacement therapies. Efforts have been made to simplify the long and complex culturing protocols necessary to generate iPS cell colonies, that may trigger karyotypic aberrations on the cells, and to avoid the use of xeno-biotics during this process, in order to fulfill Good Manufacturing Practices (GMP) and clinical-grade requirements [121-123]. However the subsequent differentiation protocols still rely heavily on the use of growth factors and other substances. Safety of the exposure to these molecular cues will have to be thoroughly investigated prior to any clinical application [124, 125]. Finally, and in addition to the challenges of cell delivery and transplantation, poor engraftment is often the leading cause of the absence of restorative effect at the pre-clinical level [92].

The economic resources and time-frame needed to derive iPS cells and re-differentiate them to the appropriate cell type become even more relevant if they are to be generated from specific patients. With the technologies available today, approximately 3 months are necessary to complete this process. Adding the necessary safety and quality control tests, up to six months could be required, which compromises the clinical relevance of iPS cell therapies when prompt treatment is mandatory [126]. A proposition to circumvent this problem relies in the establishment of banks of allogeneic iPS cell lines. Although at first glance this would act in detriment of the notion of personalized iPS cell therapy, it has been calculated that a stock of 75 iPS cell lines derived from homozygous human leukocyte antigen (HLA) donors would be enough to match 80% of the population in Japan without triggering any immune response [110, 127]. Similarly, it has been estimated that a pool of 150 cell lines from defined HLA donors would match 93% of the UK population [128]. This initiative is becoming a reality after the authorisation of an ambitious scheme, known as the “iPS cell Stock Project”, which

aims to generate iPS cells from samples stored in various Japanese cord blood banks [83].

In this scenario, there is still no unanimous voice in the scientific community that confirms whether iPS cells are truly a superior alternative to ES cells, or simply have different advantages to offer. What transpires from the studies presented here is that the possibility to reverse a patient's own cells back to the very plastic pluripotent state may allow new revolutionary ways of treatment, however several barriers need to be overcome before they become a reality in the clinical practice.

1.4. Transdifferentiation in regenerative medicine.

1.4.1. *In vivo* transdifferentiation: looking at Nature and escaping the dish.

Direct conversion of cells resident in a diseased or injured tissue into the replacement phenotypes needed to alleviate the particular condition would be an optimal strategy to regenerate the affected tissue. In fact, transdifferentiation occurs spontaneously after injury in certain organisms with striking capacity to regenerate. It is a substantial mechanism underlying liver [129] and heart [130] regeneration in zebrafish as well as lens regeneration in axolotls [131]. However, this ability has been lost in mammals, with the exception of very few examples restricted to neonatal stages and definitely not sufficient to restore significant damage [132]. On the contrary, spontaneous transdifferentiation in mammalian organisms is rare and mainly linked to the onset of disease. This is the case of Barret's metaplasia, whereby *Cdx2*-mediated transdifferentiation of stratified squamous into columnar epithelium predisposes to oesophagus carcinoma [133, 134]. Similarly, transdifferentiation of different starting cell types into myofibroblasts after injury or chronic damage to various tissues, including kidney [135], liver [136] and muscle [137], triggers the establishment of a fibrotic scar.

Based on the paradigm of those organisms with better capacities to regenerate and thanks to the increasing knowledge of the specific developmental regulators - mainly transcription factors - that govern each cell type, transdifferentiation has been proposed as a therapeutic strategy in different mammalian tissues and disease models. As discussed previously, Davis and

Weintraub's *MyoD* studies set the bases for this proposition, since they confirmed that transdifferentiation can be intentionally induced by the ectopic expression of such regulators [47, 48]. Their studies have been followed by others attempting to induce cell-to-cell changes *in vivo* to tackle specific conditions **(Figure 1.6)**. Most efforts have been dedicated to explore therapeutic strategies against diabetes, heart disease and, to a lesser extent, injuries and degenerative diseases affecting the central nervous system (CNS). Specific details of these studies are compiled in **Table S1**, **Table S2** and **Table S3**, respectively.

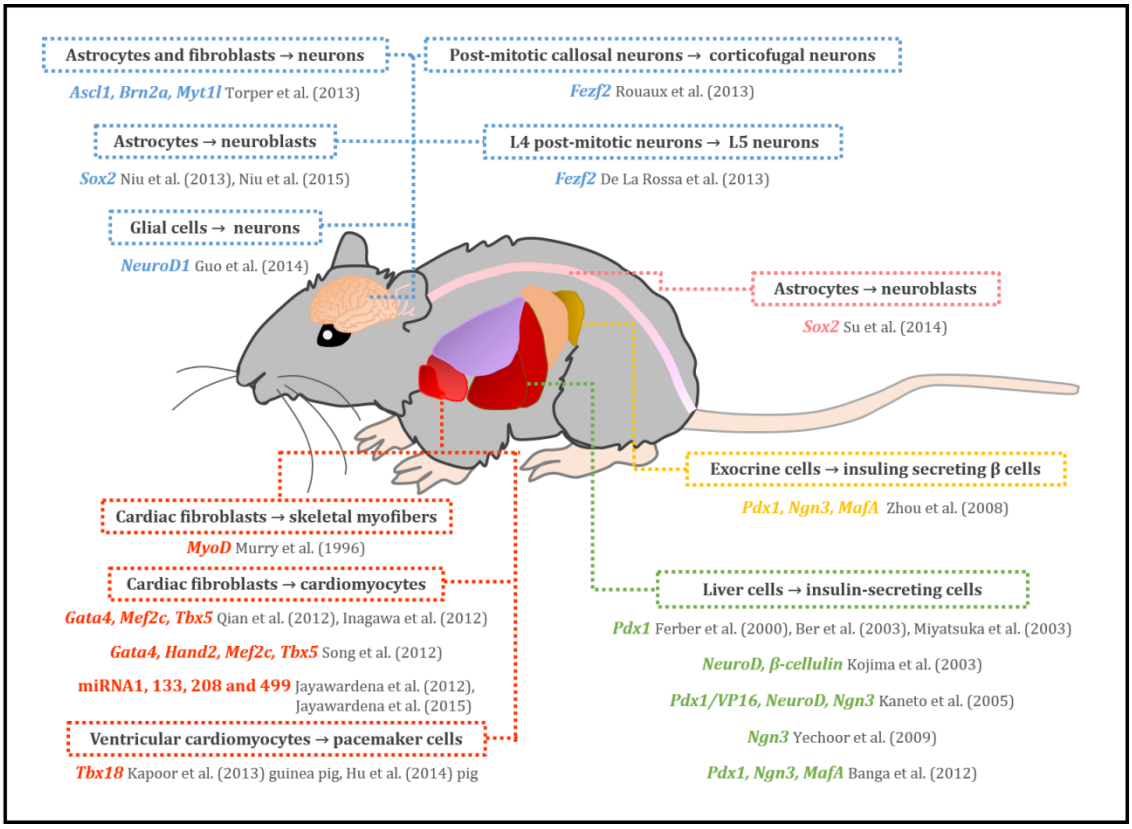

Figure 1. 6. In vivo transdifferentiation studies. *In vivo transdifferentiation studies have been so far focused on: liver and pancreas, for the treatment of diabetic disease; heart, to regenerate the tissue after myocardial infarction or to establish a biological pacemaker that corrects bradycardia; and CNS, to alleviate both neurodegenerative and traumatic conditions.*

1.4.2. *In vivo* transdifferentiation: pre-clinical studies.

1.4.2.1. *In vivo* transdifferentiation in pancreas and liver.

Efforts to alleviate diabetic disease via *in vivo* transdifferentiation have followed two different strategies: the generation of new β-cells in the pancreas [49] and the induction of insulin-secreting cells in an organ with a very similar

developmental origin, the liver [138-144]. Interestingly, the same combination of transcription factors – *Pdx1*, *Ngn3* and *MafA* - has proven the most effective reprogramming cocktail in both strategies. In the pancreas, induced β-cells resembled their endogenous counterparts very closely [49], whereas in the liver unique insulin-secreting ducts were formed [144]. Both studies achieved long-term amelioration of hyperglycaemia in diabetic mice.

1.4.2.2. *In vivo* transdifferentiation in heart.

The heart is perhaps the organ most intensively investigated for *in vivo* transdifferentiation, motivated by the high prevalence and mortality rate associated with cardiovascular disease [145]. The studies reported to date aim to generate new cardiomyocytes (CMs) after myocardial infarction (MI) or to correct bradycardia by the generation of a biological pacemaker *in situ*.

Regeneration of infarcted hearts

In the event of MI, CMs die in the infarcted area and cardiac fibroblasts migrate to the site and proliferate actively to replenish the tissue. Thanks to their abundance, cardiac fibroblasts have been considered as an advantageous starting cell type for cell fate conversions. Leaving aside a 1996 study that attempted to generate skeletal myofibers to regenerate the myocardium via forced expression of *MyoD*, with not much success [146], the increasing knowledge of the factors involved in CM development allows now to replenish the injured heart with induced CMs (iCMs).

The combinations *Gata4*, *Mef2c* and *Tbx5* (GMT) [147, 148], *Gata4*, *Mef2c, Hand2* and *Tbx5* (GMHT) [149] and the micro-RNAs 1, 133,208 and 499 [150, 151] have all confirmed generation of iCMs in mouse models of MI, however with different outcomes in the improvement of cardiac function and reduction of scar tissue.

Generation of a biological pacemaker *in situ*

The generation of a biological pacemaker via transdifferentiation has exploited the role of *Tbx18* in the embryonic development of the sinoatrial node (SAN), a small group of approximately 10,000 cells responsible for initiating the heartbeat. Transdifferentiation of ventricular CMs into induced SAN (iSAN) cells,

able to beat spontaneously and alleviate bradycardia, has been achieved in guinea pig [152] and porcine [153] models of complete heart block.

1.4.2.3. *In vivo* transdifferentiation in the CNS.

Intense efforts are also made to change cell identity *in situ* in the brain and CNS. However, the literature is more scattered in terms of starting and induced cell types, reprogramming factors used, disease models investigated and restorative effect achieved.

Various studies have explored the feasibility to reprogram astrocytes into neurons or neuron precursors (neuroblasts). Proof-of-principle of such conversion was achieved with a combination of *Ascl1*, *Brn2a* and *Myt1l* [154] and later confirmed via forced expression of *Sox2* alone [155, 156] and *NeuroD1* alone [157]. Importantly, *NeuroD1*-mediated astrocyte-to-neuron conversion was more extensive in an aged 5xFAD transgenic mouse model of Alzheimer's disease compared to young transgenics and wild-types (WT). This finding was attributed to the enriched astrocyte population triggered by neurodegeneration and highlighted the opportunities to tackle this type of conditions via *in vivo* transdifferentiation. Similarly, *Sox2*-mediated astrocyte-to-neuroblast conversion took advantage of astrocyte migration to the injury site in a model of spinal cord injury. Induced neuroblasts matured into neurons that formed synapses with resident brain cells, however functional recovery remained unexplored [158].

Fate changes between different types of neurons have also been explored, however they have proven more challenging due to the post-mitotic status of the cells. *Fezf2* induced transdifferentiation between different types of post-mitotic neurons in two different studies, however in both cases the conversion was only possible in a specific time window (from embryonic to early post-natal stages) and so far no therapeutic applications have been proposed for such approach [159, 160].

1.4.3. Opportunities and limitations of *in vivo* transdifferentiation.

Although *in vivo* transdifferentiation studies are still scarce and preliminary, they have already generated valuable knowledge regarding the plasticity of various mature cell types within their native microenvironment. They have also produced encouraging results in disease models at the early-stage pre-clinical level and are progressively unveiling the opportunities and limitations of this approach.

In vivo transdifferentiation takes advantage of the crucial role of the native microenvironment in the survival and maturation of the induced cells. Direct comparison of *in vitro* and *in vivo* transdifferentiated cells evidenced that those switched to a different phenotype within living tissue better resembled their endogenous counterparts in terms of morphology, function, degree of differentiation and interaction with neighbouring cells [49, 147]. In addition, the fact that the conversion takes place *in vivo* eliminates the challenges associated to *in vitro* culture and cell delivery or transplantation [92, 121-123]. Altogether, these facts place *in vivo* transdifferentiation in an advantageous position over traditional cell therapy.

Direct generation of the desired mature phenotype, avoiding pluripotent intermediates, is considered beneficial by many [31]. However, in some of the studies discussed above, the induced cells were in fact precursors that required co-administration of epigenetic regulators or other signalling molecules to fully mature [155, 158]. In addition, direct conversion requires the identification of specific reprogramming factors for each particular cell-to-cell conversion, contrary to the versatility of the Yamanaka factors that are able to induce pluripotency in several starting cell types [51, 57-65] .

Beyond the extra efforts in the search for specific reprogramming cues, poor conversion efficiency acted as limiting factor in most of the studies and can compromise the therapeutic outcomes of the strategy [148]. Such obstacle is sometimes exacerbated by immune clearance of viral vectors and virally transduced cells [148, 153]. Indeed, *in vivo* transdifferentiation has so far relied heavily on the use of viral vectors for the delivery and expression of reprogramming factors, which also complicates to a certain extent the cruise towards the clinic. Various studies have used retrovirus in order to exclusively

restrict the infection to dividing cells [147-149]. However, engineering safer non-viral vectors that can more sophisticatedly target specific cell types is desirable.

Finally, in those studies with therapeutic aims, there is a need to investigate the effects and outcomes of *in vivo* transdifferentiation when reprogramming factors are administered at different time points after the onset of injury. All the studies published to date, with the exception of Murry et al. [146], induced the cell fate conversion at the time of injury. Such experimental design not only questions clinical relevance; it might also underestimate the therapeutic potential of those strategies that rely on the injury-triggered proliferation of particular cell types (e.g. cardiac fibroblasts, astrocytes) to be available for transdifferentiation.

Overall, *in vivo* transdifferentiation has the potential to become a very powerful tool in tissue repair and regeneration but the results of the studies presented here should be considered with caution before overenthusiastic promises are conveyed.

1.5. The third way: generating pluripotent cells *in situ*.

1.5.1. *In vivo* reprogramming to pluripotency: proof-of-concept.

Recent studies have suggested that induced reprogramming of differentiated cells to pluripotency could also be feasible within the living organism [161-163]. Should these initial findings be fully confirmed, they could constitute a third therapeutic alternative by which cell reprogramming could contribute to tissue regeneration (i.e. in addition to *in vitro* iPS cell generation and transplantation and *in vivo* transdifferentiation).

In 2012, Vivien et al. were first to report *in vivo* somatic cell reprogramming to pluripotency in a non-mammalian model. Their work was conducted on pre-metamorphic tadpoles, therefore not fully developed organisms. However, that study offered an important contribution to the field, by confirming that ectopic expression of Yamanaka factors (excluding *c-Myc*) induces pluripotency against the pro-differentiation signals present in the *in vivo* microenvironment. Forced expression of OKS factors in the tadpole tail muscle triggered the expression of pluripotency genes, silenced at such developmental stage under normal circumstances. In addition, cell clusters expressing such

markers were found within the muscle tissue, which were able to differentiate *in vitro* towards all three lineages when exposed to different conditions [161].

Our laboratory performed simultaneously studies with mammalian models (BALB/c mouse) that were reported by Yilmazer et al. This initial work evidenced that the adult mouse liver microenvironment is also permissive to OKSM-mediated induction of pluripotency. Forced expression of OKSM factors in mouse hepatocytes resulted in rapid and transient upregulation of pluripotency markers at the mRNA level and downregulation of hepatocyte-specific genes. Protein expression also suggested a shift of the differentiated status of the cells towards pluripotency, but no confirmation was provided of the generation of fully functionally pluripotent cells within the liver tissue [162, 163].

1.5.2. Hypotheses, promises and challenges of *in vivo* reprogramming to pluripotency.

Importantly, the studies by Vivien et al. and Yilmazer et al. did not report complications associated to teratoma formation or other aberrations in the tissue. In addition, the pluripotent conversion was not sustained for extended periods of time [161-163]. These observations suggest that *in vivo* reprogramming to pluripotency might also have a space in the regenerative medicine toolbox. Given that the cell fate conversion takes place *in vivo* but making use of the very versatile Yamanaka factors, *in vivo* reprogramming to pluripotency might even overcome some of the limitations associated to *in vitro* iPS cell generation and *in vivo* transdifferentiation. However, at the time of initiation of this thesis there was only one report of this kind in mammalian (mouse) organisms, confirmation of complete reprogramming to functional pluripotency was yet to be obtained and, more importantly, the potential of this strategy to contribute to regeneration had not yet been challenged in disease models. Therefore, the early stage of this technology makes it challenging to predict the specific opportunities and limitations that will be involved. In this thesis, we aimed to fill some of such gaps in order to better understand the possible role of *in vivo* reprogramming to pluripotency in regenerative medicine.

Chapter II.
Aims and hypotheses.

The capacity to induce changes in cell fate that generate patient-specific, customised, replacement cells for the tissue where they are needed – via *in vitro* iPS cell generation or *in vivo* transdifferentiation - suggests new and exciting ways to tackle disease and may develop into a very powerful tool in regenerative medicine [164]. The first clinical study using iPS cell derivatives is currently taking place in Japan [165, 166] and, although still at their infancy, these strategies have the chance to become a clinical reality in the near future. However, they are not devoid of limitations. The generation of iPS cells suffers from the risks associated with long *in vitro* culture protocols and the challenges of cell delivery and transplantation [120]. Although transdifferentiation to specific cell types can be directly achieved *in vivo*, this strategy is complicated by the need to identify specific reprogramming factors for each particular cell fate conversion and its poor efficiency [144, 148, 155].

In vivo cell reprogramming to pluripotency could combine the opportunities offered by *in vitro* iPS cell generation and *in vivo* transdifferentiation, as well as circumvent some of the limitations faced by each of such approaches. However, it is yet largely unexplored. The overall aim of this thesis was to explore *in vivo* cell reprogramming to pluripotency as a novel strategy to enhance regeneration of injured tissues.

Based on Yilmazer et al.'s first-ever report suggesting *in vivo* reprogramming towards pluripotency in a mammalian tissue [162], we hypothetised that adult, fully differentiated cells from different tissues could be reversed *in vivo* to a functionally pluripotent state via ectopic expression of Yamanaka factors. We speculate that reprogrammed cells would only exist transiently in the pluripotent state in such scenario, given the pro-differentiation cues present in the tissue microenvironment; and that such signals would assist the re-differentiation of the pluripotent intermediates towards the appropriate phenotype. This hypothesis is represented in **Figure 2.1** using the mouse liver as an illustrative example. Thus, the generation of transiently pluripotent cells *in situ* could contribute to the replenishment and regeneration of injured tissues.

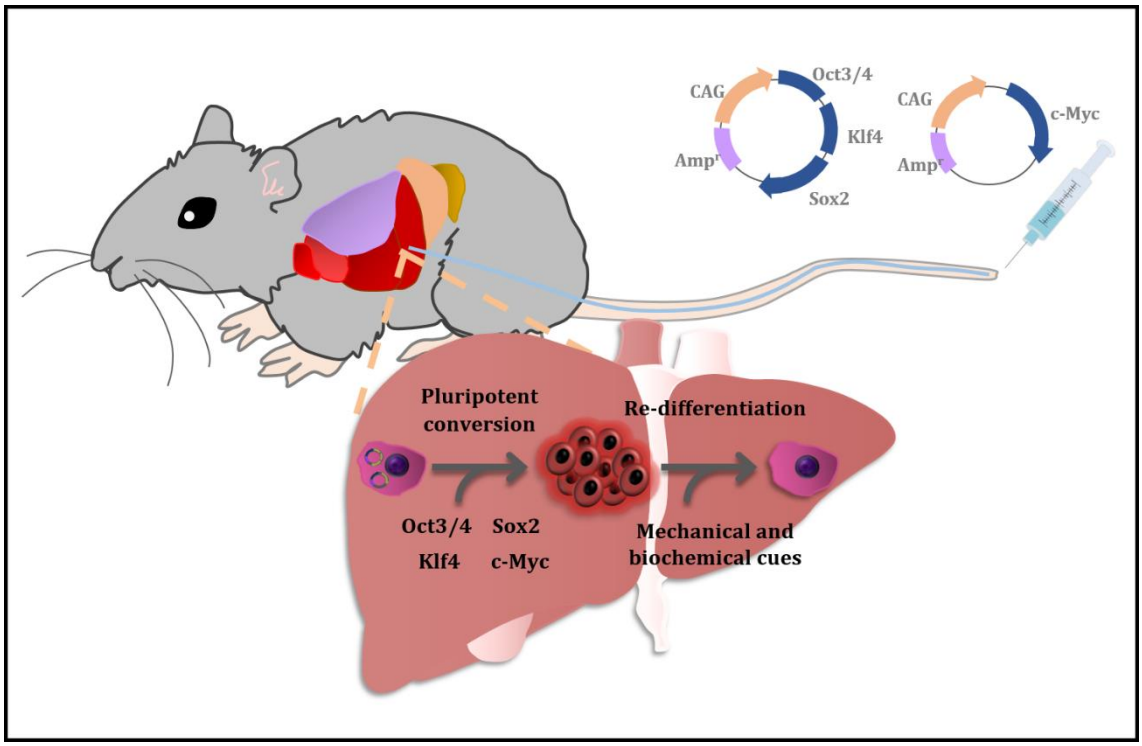

Figure 2. 1. Hypothesis: in vivo induced reprogramming to pluripotency and re-differentiation within the native microenvironment.

In order to prove the hypotheses above, the particular aims of this thesis were:

- **To further investigate the induction of pluripotency in mouse liver,** reassuring the safety of the approach and exploring modifications to the Yilmazer et al.'s protocol.

- **To determine the differentiation potential of *in vivo* reprogrammed cells.** *In vivo* reprogrammed cells could share the differentiation potential of iPS and ES cells. However, it is known that incomplete reprogramming can lead to an intermediate state that shares morphological and molecular similarities with pluripotent stem cells [119] but is not functionally pluripotent (i.e. fails to differentiate into representatives of all three lineages). In order to confirm the pluripotency of *in vivo* reprogrammed cells, we aimed to isolate them from the tissue and establish them as a stable cell line *in vitro* for comparison to a standard ES cell line, the gold standard of pluripotency.

- **To challenge the capacity of Yamanaka factors to induce pluripotency in tissues of different developmental origin.** One of the anticipated benefits of *in vivo* reprogramming to pluripotency over *in vivo* transdifferentiation relies on the versatility of the Yamanaka cocktail. This combination of transcription factors has proven able to reverse a variety of differentiated cell types to pluripotency *in vitro* and therefore is considered a universal tool to induce such fate switch [164]. It was thus among our objectives to verify that such observation holds in the *in vivo* scenario by attempting the induction of pluripotency with such cocktail in tissues of different developmental origin.

- **To follow the fate of the *in vivo* reprogrammed cells in the tissue.** *In vivo* reprogrammed cells were expected to proliferate, based on the fact that active cell division has been identified as a mandatory step in the pluripotent conversion [167]. Hence, we aimed to confirm the occurrence of cell proliferation and intended to confirm the re-integration of the *in vivo* reprogrammed cells into the tissue after such phase.

- **To investigate whether the generation of pluripotent cells *in vivo* would enhance regeneration and functional recovery of injured tissue.** The ultimate aim of this thesis was to explore the therapeutic potential of *in vivo* reprogramming to pluripotency in the event of tissue injury. For this, we aimed to establish a reproducible injury model and subsequently test different therapeutic interventions involving the administration of reprogramming pDNA and induction of pluripotency in the injured tissue.

Chapter III.

In vivo reprogramming to pluripotency in mouse liver:

Generation and characterisation of *in vivo* induced pluripotent stem (i^2PS) cells

3.1. Scope of Chapter III.

Reprogramming of somatic cells to pluripotency via forced expression of transcription factors *in vitro* has been intensively explored for the last 9 years. However, very little has been reported about the possibility to induce this particular cell fate conversion *in vivo*. The first account of *in vivo* cell reprogramming to pluripotency dates to 2012, when Vivien and colleagues induced the generation of pluripotent cells within tadpole tail muscle tissue [161]. A recent report by Yilmazer et al. suggested that a similar effect could be achieved in an adult, fully differentiated, mammalian tissue - the mouse liver. In this work, a shift towards pluripotency in gene and protein expression of liver cells was evidenced, but a definite proof of the generation of *bona fide* pluripotent cells within the tissue remained to be obtained [162, 163].

In this Chapter, we sought to further explore the induction of pluripotency in mouse liver following on Yilmazer's studies but, more importantly, we aimed to characterise the resulting *in vivo* reprogrammed cells and their differentiation potential in order to confirm, or not, functional pluripotency.

3.2. Introduction.

Although the forced expression of reprogramming factors is not free of impediments when it is performed in the culture dish [120], even more challenging is to deliver such factors and induce the pluripotent conversion *in vivo*. Specificity for a particular cell population (to avoid off-target effects or widespread reprogramming), efficiency and safety are requirements of particular relevance. In Yilmazer's report, hydrodynamic tail vein (HTV) injection was the administration method of choice to specifically and efficiently transfect mouse hepatocytes with naked pDNA and avoid the risks inherent to the use of viral delivery vectors [162, 163]. HTV injection is a well-established technique for the expression of foreign genes *in vivo* via systemic administration of naked pDNA, first described by Liu et al. [168] in the late 1990s. It results in high levels of gene expression in the liver, especially in hepatocytes, whereas transgene expression is minor in other organs. Importantly, this approach has not only achieved satisfactory results in small

rodents, but has also been escalated to larger animal models such as rabbits [169] and pigs [170-172] and translated into human clinical trials [172].

The procedure involves the injection of a large volume of pDNA solution (8-12% of the total body weight) in a short time interval (no more than 5 s for a 20 g mouse) via the tail vein, being these the two most crucial parameters to achieve high expression of the exogenous genes [168, 173]. A single mechanism has not yet been identified to explain the preferential uptake of pDNA by hepatocytes after HTV injection and it may be possible that different processes contribute to this end-effect. The rapid injection of such a large volume exceeds cardiac output, increasing the pressure in the inferior vena cava and driving the injected solution to backfill the liver circulation. In addition, the rise in hydrostatic pressure in the liver opens the sinusoids fenestrae, thus assisting the extravasation of pDNA solution, and may lead to pore formation in the hepatocyte membrane [174]. The rapid entrance of pDNA in the hepatocytes acts as a protective mechanism against its degradation by nucleases present in the blood stream, contributing as well to high levels of transgene expression [168]. Finally, some studies have suggested contribution of a receptor-mediated mechanism [175].

Following this strategy to express Yamanaka factors in mouse hepatocytes, Yilmazer and collaborators reported a rapid and transient upregulation of pluripotency markers and downregulation of hepatocyte-specific genes in the BALB/c mouse liver, which was interpreted as the de-differentiation of a subset of cells towards pluripotency in the tissue. Hepatocytes are parenchymal cells that derive from the anterior portion of the endoderm, one of the three germ layers formed in the embryo during gastrulation. This process has been extensively reviewed by others [176, 177], which has allowed the identification of key hepatocyte-lineage marker genes. Such markers have been classified in four groups according to the stage in hepatocyte development in which their role is more relevant. Endodermal markers such as *Afp* and *Foxa2* are expressed from the establishment of the endoderm layer, while genes whose role commences at later developmental stages include *Alb* (fetal hepatocyte marker), *G6pc* and *Tat* (perinatal expression) and *Cyp3a*, *Pc1k*, *Tdo*, *Aat* and *Trf* (characteristic of mature hepatocytes only) [178]. The knowledge built around these markers has been used by Yilmazer et al. and in this Chapter to assess the potential loss of hepatocyte identity upon *in vivo* reprogramming.

In Yilmazer's report, the induction of pluripotency happened faster (as early as 2 days after HTV injection) and was more efficient (estimated in 5 to 15% of the total hepatocyte population) than the vast majority of *in vitro* reprogramming protocols described to date. In addition, such effect was not sustained over time. Hepatocyte gene expression returned to baseline levels after 8 days and cells expressing pluripotency markers at the protein level were only found within the liver tissue until day 4 after HTV injection [162, 163]. Equally encouraging was the fact that no teratoma formation or other abnormalities were detected in the tissues after the procedure. However, no further information regarding the nature of such *in vivo* reprogrammed cells was gathered and hence complete reprogramming to functional pluripotency could not be confirmed.

In this chapter we used different reprogramming pDNA and administration schemes, based on those utilised by Yilmazer et al., to further investigate *in vivo* reprogramming to pluripotency in mouse liver. We also isolated the *in vivo* reprogrammed cells from the tissue and cultured them as a stable cell line *in vitro* in order to investigate their molecular signature and differentiation potential in comparison to a standard pluripotent stem cell line.

3.3. Materials and Methods.

3.3.1. Materials used in Chapter III.

3.3.1.1. pDNA vectors.

Three different reprogramming pDNA were used in this work. pLenti-III-EF1α-mYamanaka (referred to as **OKSM**) encodes the reprogramming factors Oct3/4, Klf4, Sox2 and c-Myc and the reporter eGFP under the control of the EF1α promoter. pCX-OKS-2A (referred to as **OKS**) encodes Oct3/4, Klf4 and Sox2 and pCX-c-Myc (referred to as **M**) encodes c-Myc, both under the control of the CAG promoter. **OKS** and **M** have been used in previous publications for iPS cell generation [107, 108]. When these two pDNA were administered together, we referred to the combination as **OKS+M**.

OKS and **M** were obtained from Addgene (USA) and **OKSM** was purchased from Applied Biological Materials (USA), in all cases as bacterial stabs. pDNA

production was performed by Plasmid Factory (Germany). Relevant pDNA maps are represented in **Figure S1**.

3.3.1.2. Mouse strains.

Female mice were used in this work that entered the procedures at 7 weeks of age, unless otherwise specified. BALB/c mice were purchased from Harlan, UK. E12.5-14.5 pregnant CD1 mice for MEF isolation, CD1 nude mice for teratoma studies and C57BL/6 and BDF1 mice for chimerism experiments were obtained from Charles-River, UK. BDF1 mice (B6D2F1) are a cross between female C57BL/6 and male DBA/2.

All experiments were performed with previous approval from the UK Home Office under a project license PPL 70/7763 and after allowing the mice to acclimatise to the facilities for one week.

3.3.1.3. Cell lines.

E14TG2a, a mouse ES (mES) cell line isolated from 129/Ola mice blastocysts, was purchased from the American Type Culture Collection (ATCC). Cells were maintained in an incubator at 37°C and 5% CO_2 pressure. Culture medium was changed daily and cells were passaged every other day.

The composition of the various cell culture media used in different studies in this chapter are listed in **Table S4**.

3.3.2. Methodology involved in Chapter III.

3.3.2.1. Hydrodynamic tail vein (HTV) injection of pDNA.

BALB/c mice (n=3) were warmed at 37°C in a heating chamber, anesthetised with isoflurane and administered 1.5 ml of pDNA solution prepared in 0.9% saline via the tail vein. Injection time was fixed to 5 s. For the different groups, the pDNA solution included: 75 μg **OKS** and 75 μg **M**, 75 μg **OKS** alone or 150 μg **OKSM**. Control groups were administered the same volume of 0.9% saline alone. Mice were culled at different time points specified for each study, including 2, 4, 8, 12 and 24 days after HTV injection, and livers were processed for investigation.

3.3.2.2. Repeated HTV injection of pDNA.

BALB/c mice (n=3) were HTV injected with 75 μg **OKS** and 75μg **M** in 1.5 ml 0.9% saline, as described before. The control group was administered the same volume of 0.9% saline alone. 3 days after the injection, animals were either culled or administered a second dose of the corresponding treatment. Animals that received two doses of pDNA or saline solution were sacrificed at days 4 and 8 after the first administration (1 and 5 days after the second HTV injection, respectively). Livers were processed for gene expression studies.

3.3.2.3. Characterisation of *in vivo* reprogrammed liver tissue.

Isolation of hepatocyte population. Mouse livers were perfused and digested as previously described [179] with some modifications. In brief, under terminal anaesthesia, mice were first perfused from the inferior cava vein with 10 ml of Ca^{2+} and Mg^{2+} free Hank's Buffered Salt Solution (HBSS, Sigma-Aldrich, UK), pre-warmed at 37°C, for approximately 3 min, until the liver whitened. Perfusion was then continued with Liver Digest Medium containing collagenase (LDG, Gibco, UK), pre-warmed also at 37°C, and at a flow rate of 0.6 ml/min for 10-15 min, until the liver became swollen and loose. Digested livers were washed with Hepatocyte Wash Medium (HWM, Gibco, UK) at 4°C and disrupted through a 100 μm cell strainer (BD Biosciences, UK) to obtain a cell suspension. 5 min centrifugation at 50 g was used to separate parenchymal cells (including hepatocytes), which were collected in the pellet, and non-parenchymal cells (including Kupffer cells and epithelial cells), which stayed in the supernatant. The cell pellet was re-suspended in HWM and the hepatocyte fraction was collected after 4 repeats of the centrifugation procedure.

RNA isolation and real-time Reverse Transcription-quantitative Polymerase Chain Reaction (real-time RT-qPCR) analysis. Nucleospin RNA II kit (Macherey-Nagel, UK) was used to extract total RNA from isolated hepatocytes. RNA concentration and quality were analysed by UV spectrophotometry (BioPhotometer, Eppendorf, UK). cDNA synthesis was performed from 1 μg RNA sample with iScript cDNA synthesis kit (Bio-Rad, UK) according to manufacturer's instructions. The protocol for reverse transcription was as follows: 25°C for 5 min, 42°C for 30 min, 85°C for 5 min and 4°C for 5 min. 2 μl of cDNA sample were used

for each real-time qPCR reaction performed with iQ SYBR Green Supermix (Bio-Rad, UK). Experimental duplicates of each sample were run on CFX-96 Real Time System (Bio-Rad, UK) with the following protocol: 95°C for 3 min, 1 cycle; 95°C for 10 s, 60°C for 30 s, – repeated for 40 cycles. Melt curve analysis was conducted at the end of the protocol to confirm amplification of a single product. *β-actin* was used as housekeeping gene and gene expression levels were normalised to saline-injected control groups, unless otherwise specified. Livak's method was followed to analyse the data and dCt values were utilized for statistical analysis. The primer sequences used are listed in **Table S5**.

Immunohistochemistry (IHC) of mouse livers. Livers were perfused with 10 ml HBSS, as described before, but then immediately immersed in isopentane, pre-cooled in liquid nitrogen, for fixation. Frozen livers (n=3) were stored at -80°C until further processing. 14 µm thick sections were prepared on a cryostat (Leica Microsystems, CM3050S) and air-dried for 1 h at room temperature (RT) before storage at -20°C. Before staining, liver sections were post-fixed with methanol, pre-cooled at -20°C, for 10 min and then air-dried for 15 min and washed twice with Phosphate Buffered Saline (PBS, 5 min each, RT). 1 h incubation in blocking buffer (5% goat serum-0.1% Triton in PBS, pH 7.3) at RT was followed by two washing steps with washing buffer (1 %BSA- 0.1% Triton in PBS, pH 7.3). Tissue sections were incubated overnight at 4°C with the corresponding primary antibody: rabbit pAb anti-OCT4 (ab19857, 3 µg/ml, Abcam, UK), rabbit pAb anti-SOX2 (ab97959, 1 µg/ml, Abcam, UK), rabbit pAb anti-NANOG (ab80892, 1 µg/ml, Abcam, UK) or mouse mAb anti-SSEA1 (ab16285, 20 µg/ml, Abcam,UK). The next day, 3 washing steps (5 min each) with washing buffer were followed by 1.5 h incubation at RT with the corresponding secondary antibody: goat pAb anti-rabbit IgG labeled with Cy3, 1/250 or goat pAb anti-mouse IgG labeled with Cy3, 1/250, both purchased from Jackson ImmunoResearch Laboratories, UK. Finally, sections were washed with PBS and mounted with DAPI and antifade containing medium (Vectashield, Vector Laboratories, UK). Slides were visualised under an epi-fluorescence microscope (Zeiss Axio Observer). 40X images were obtained with Axiovision Software. . At least 3 random fields/liver were included for quantification of positive cells.

3.3.2.4. Generation and *in vitro* culture of i²PS cell colonies.

Isolation of primary mouse embryonic fibroblasts (MEFs). Mouse embryonic fibroblasts (MEFs) were isolated as previously described [180], with some modifications. In brief, an E12.5-14.5 pregnant CD1 mouse was sacrificed by CO_2 suffocation and the developing embryos were released from the uterine horns. After removal of the placenta and surrounding membranes, internal organs including heart, liver and brain were excised. The remaining material of each embryo was finely minced, suspended in 2 ml of 0.25% trypsin solution with 100 µl DNAse and incubated at 37˚C for 30 min with frequent homogenization. After incubation, 6 ml of fresh MEF medium **(Table S4)** were added and vigorous pipetting was used to enhance tissue dissociation. Big pieces of tissue were let to settle down to the bottom of the tube for a few minutes and the supernatant was then centrifuged at 200g for 5 min. The cell pellet was re-suspended in 8 ml of pre-warmed MEF medium and then plated at a density of 1 embryo/T75 tissue culture vessel, which constituted passage 0 of the primary MEF culture. The cells were maintained at 37ºC and 5% CO_2 pressure and MEF medium was changed daily until the cells became confluent and were either split of frozen. A maximum of 3 passages were done before the cells were mitotically arrested to be used as feeder layers.

Mitotic inactivation and preparation of MEF feeder layers. Primary MEFs were treated as described in a previous report [180], with some modifications, to prepare feeder layers for the culture of pluripotent stem cells. MEF medium was removed from a confluent T75 tissue culture vessel and 10 ml of inactivation medium (containing 10 µg/ml mitomycin C, **Table S4**) were added. Cells were incubated at 37˚C and 5% CO_2 pressure for 3 h. Following 3 washes with PBS, the cells were trypsinised and plated in new tissue culture vessels with fresh MEF medium. A density from 1.0 to 1.5 x 10^5 inactivated MEFs/cm^2 was appropriate to produce feeder layers. Inactivated MEFs were ready to be used as feeder layers or frozen as inactivated stocks one day after the treatment with mitomycin C.

Generation of i²PS cell colonies. BALB/c mice (n=3) were HTV injected with 75 µg **OKS** and 75µg **M** in 1.5 ml of 0.9% saline or 1.5 ml of 0.9% saline alone (control) and the hepatocyte fraction was isolated 2 days after injection as described above. 2 x 10^6 cells were seeded on each well of a 6-well plate where MEF feeder layers

had been previously prepared. Cultures were maintained in DMEM/LIF medium **(Table S4)**, which was changed daily. Cells were passaged 1:2 on fresh MEF feeders after 10 days in culture and 2 days later compact cell colonies started to appear in the cultures from **OKS+M** group. No colonies were formed from saline-injected control mice. i^2PS cell colonies were established as a stable cell line *in vitro*, culture medium was changed daily and cells were passaged every other day. Specific culture conditions are indicated for each particular study.

3.3.2.5. Pluripotency assays at the molecular level.

Real-time RT-qPCR gene expression analysis of E14TG2a and i^2PS cells. E14TG2a and i^2PS cells (n=3) were cultured on 0.1% gelatin coated tissue culture vessels and DMEM/LIF conditions for 3 passages until complete removal of feeder cells was achieved. Total RNA was extracted from 2 x 10^6 cells with Nucleospin RNA II kit (Macherey-Nagel, UK) and used for real-time RT-qPCR analysis as described in **Section 3.3.2.3**. The expression of pluripotency and early differentiation markers in i^2PS cells was normalised to that in E14TG2a cells. Livak's method was followed to analyse the data and dCt values were utilized for statistical analysis. Primer sequences are listed in **Table S5**.

Whole-genome expression profiling by DNA Microarray. 1 μg RNA extracted from feeder-free E14TG2a and i^2PS cells (n=3) as described above was used for DNA microarray analysis. Mouse WG-6 v2.0 Expression BeadChip array (Illumina) was used, which allowed the profiling of 45,200 transcripts. The array was performed by the staff at the Genome Centre, Queen Mary University of London (UK), which also assisted in data analysis. GenomeStudio software and the National Center for Biotechnology Information (NCBI) database were used to interpret the results by gene clustering and pathway analysis. The data obtained from this study is deposited in the NCBI Gene Expression Omnibus (GEO), with accession number: GSE55996.

http://www.ncbi.nlm.nih.gov/geo/query/acc.cgi?acc=GSE55996

Response to 2i conditions. E14TG2a and i^2PS cells (n=3) were cultured on 0.1% gelatin-coated vessels and maintained under standard ES conditions (DMEM/LIF medium) or on a dual-inhibition medium (KODMEM/LIF/2i), described elsewhere [119]. The detailed composition is listed in **Table S4**. In both conditions, medium

was changed daily and cells were passaged every other day. The effects of culture conditions on the expression of the pluripotency genes *Nanog* and *Rex1* were studied by real-time RT-qPCR for up to 40 days after the start of the culture. Primer sequences are listed in **Table S5.**

Immunocytochemistry (ICC) of i²PS cell colonies. i²PS cell colonies cultured on MEF feeder layers and DMEM/LIF conditions were fixed with methanol, pre-cooled at -20°C, for 10 min and processed for ICC using the same antibodies and protocol described in **Section 3.3.2.3**.

CDy1 live staining. The compound of designation yellow 1(CDy1) that selectively stains live ES and iPS cells [181] was kindly provided by Dr. Young-Tae Chang (National University of Singapore and A*STAR Singapore), and used according to instructions provided. Briefly, i²PS cell colonies were cultured on MEF feeder layers and DMEM/LIF conditions. CDy1 dye was diluted to 0.1μM in the culture medium and the cells were incubated at 37°C and 5% CO_2 for 1 h. After 3 washes and 2 h incubation (37°C, 5% CO_2) with full medium free of the compound, live imaging was perfomed with an epi-fluorescence microscope (Zeiss Axio Observer).

3.3.2.6. Pluripotency assays at the functional level.

Generation and differentiation of embryoid bodies (EBs). Feeder-free i²PS cultures (DMEM/LIF conditions) were used to generate embryoid bodies (EBs) following a previous report [182]. In brief, i²PS cells were detached from the tissue culture vessel with 0.05% trypsin-EDTA and dissociated into a single cell suspension in EB medium **(Table S4)**. 10,000 cells were seeded in each well of a 1% agar-coated 96-well plate, maintained in EB medium culture conditions, which is free from LIF, and left to form EBs. After 3 days, the cell aggregates were transferred to 0.1% gelatin-coated culture dishes and left to differentiate spontaneously for 7 or 15 days when they were used for ICC and gene expression analysis, respectively.

ICC of cells differentiated from EBs. After 7 days of spontaneous differentiation from EBs, cell cultures were processed for ICC following the protocol described in **Section 3.3.2.3**. As primary antibodies, rabbit pAb anti-beta-III-tubulin (ab76287, 1/200, Abcam, UK), rabbit pAb anti-alpha 1-fetoprotein (N1501, ready to use, DAKO, UK) and mouse mAb anti-alpha smooth muscle actin (N1584, ready to use,

DAKO, UK)] were used. As secondary antibodies, goat pAb anti-rabbit IgG labeled with Cy3 and goat pAb anti-mouse IgG labeled with Cy3 (1/250, Jackson ImmunoResearch Laboratories) were used.

Real-time RT-qPCR gene expression analysis of cells differentiated from EBs. Total RNA was extracted from cultures left to differentiate for 15 days from the EBs (n=3). The starting i^{2}PS cells used to generate the EBs and MEFs we included in the study as controls of pluripotent and differentiated cells, respectively. Real-time RT-qPCR was performed as described in **Section 3.3.2.3** and the expression of pluripotency (*Oct3/4*, *Nanog*) and early differentiation markers (*Afp*, *Fgf-5*, *T*) was normalised to that of the starting of i^{2}PS cells. Primer sequences are listed in **Table S5.**

Teratoma assay. Primary hepatocytes were isolated 2 days after HTV injection with 75 μg **OKS** and 75 μg **M** in 1.5 ml 0.9% saline or 1.5 ml 0.9% saline alone, as previously described. Feeder-free i^{2}PS and E14TG2a cultures (DMEM/LIF conditions) were obtained as described before. Female CD1 nude mice (n=5) were anaesthetised with isoflurane and implanted with 2 x 10^6 cells of the groups above suspended in DMEM medium. Primary hepatocytes were obtained from 3 mice and pooled prior to implantation. When i^{2}PS or E14TG2a cells were implanted, a single independent line of each type was tested. The administration was subcutaneous (sc) in the dorsal flank and was done bifocally. Tumours were left to develop for 5 weeks and then dissected and fixed in 4% paraformaldehyde (PFA). Paraffin-embedded tumour sections were stained with H&E and images were captured by light microscopy (10X).

Chimera generation and genotyping. i^{2}PS cells were cultured on MEF feeder layers and DMEM/LIF medium, or on 0.1% gelatin and KO-DMEM/2i/LIF conditions. At passage 13 (P13), i^{2}PS cells were microinjected in embryos that were then surgically transferred to synchronized pseudopregnant CD1 surrogate mothers. 3.5 days post coitum (dpc) blastocysts from C57BL/6 background, 2.5 dpc morulas from the same origin and 2.5 dpc morulas from BDF1 hybrids were used for different studies. The detailed conditions of each study including the number of i^{2}PS cells injected per embryo and number of embryos injected are compiled in **Table 3.1**. Genotyping for the Major Histocompatibility Complex (MHC) Class I antigen was performed to assess the contribution of each

background when C57BL/6 embryos were used. Primer sequences were designed to differentiate between H2-Kb (C57BL/6) and H2-Kd (BALB/c). When BDF1 morulas were used, chimerism assessment relied on the differences in D19Mit59 satellite DNA. Relevant primer sequences are listed in **Table S5** and PCR conditions were as follows: 94°C for 3 min, 1 cycle; 94°C for 30sec, 58°C for 30sec, 72°C for 30sec– repeated for 32 cycles, 72°C for 10 min. To visualize the differences in amplicon size, PCR products were resolved by agarose gel electrophoresis (1.2% agarose, 1X TBE, 70V).

3.3.2.7. Investigation of transgene integration.

PCR-based screening for genomic integration. Potential transgene integration in the i^{2}PS cell genome was studied by a PCR-based method, modified from previous studies [107, 108]. In brief, genomic DNA (gDNA) was isolated from 2 x 10^6 feeder-free i^{2}PS (n=4) or E14TG2a cells (n=2), cultured in DMEM/LIF conditions, with PureLink Genomic DNA Kit (Life Technologies, UK). 0.2 μg gDNA were used for each PCR reaction. 11 sets of primers were used to amplify specific regions of **OKS** and **M** pDNA used to generate i^{2}PS cells. Relevant sequences are listed in **Table S6.** Samples were run on CFX-96 Real Time System (Bio-Rad, UK) with the following protocol: 92°C for 2 min- 1 cycle; 92°C for 20 s, 64°C for 20 s, 72ºC for 40 s– repeated for 40 cycles, 72ºC for 3 min – 1 cycle. The PCR products were separated by agarose gel electrophoresis (0.7% agarose, 1X TBE, 90 V). **OKS** and **M** pDNA were included as positive controls for the presence of the transgenes and E14TG2a cells were used as positive control for the endogenous locus and negative for the transgene.

Southern-blot based assessment of transgene integration. A Southern Blot protocol, modified from a previous study [183], was used to detect integration of **OKS** and **M** pDNA in the genome of i^{2}PS cells. All Southern Blot related reagents were purchased from Roche, UK. Digoxigenin (DIG)-labelled probes against *Oct4*, *Sox2*, *Klf4* and *c-Myc* were synthesized using PCR DIG Probe Synthesis Kit, by which DIG-11-dUTP was incorporated every 10–20 nucleotides. gDNA was obtained as described above and from the same samples (i^{2}PS cells, n=4; E14TG2a, n=2). 15μg gDNA were digested using EcoRI and BamHl restriction enzymes (2 h, 37°C), followed by deactivation of the restriction enzyme at 60°C for 15 min. Digested gDNA was separated in 0.8% agarose gel (1X TBE, 30V, 4 h), depurinated and

denatured prior to overnight transfer to a positively charged nylon membrane in high salt concentration solution (20X SSC). After transfer, gDNA bands were fixed to the membrane by UV light exposure for 3 min. The blot was pre-hybridised in DIG Easy Hyb buffer at 40°C for 30 min. The same buffer, pre-warmed at 40°C, was also used to prepare the hybridization solution containing 50 µl of DIG-labelled denatured probe in 25 ml buffer. After 12 h hybridisation at 40°C with continuous shaking, the membrane was washed first with low stringency buffer at RT, followed by high stringency buffer at 65°C. Finally, hybridised probes were detected via incubation with an anti-Digoxigenin-AP antibody (1 h, RT) and a colour substrate solution (NBT/BCIP in 1X detection buffer), overnight with shaking.

3.3.3. Statistical analysis.

N numbers were specified for each particular study. Statistical analysis was performed first by Levene's test to assess homogeneity of variance. When no significant differences were found in the variances of the different groups, statistical analysis was continued by one-way ANOVA and Tukey's post-hoc test. When variances were unequal, the analysis was followed with Welch ANOVA and Games-Howell's post-hoc test. Probability values <0.05 were regarded as significant. SPSS software, version 20.0 was used to perform this analysis.

3.3. Results.

3.3.1. *In vivo* reprogramming to pluripotency in mouse liver with different reprogramming pDNA vectors.

Yilmazer et al. demonstrated rapid and transient induction of pluripotency and downregulation of hepatocyte-specific genes in BALB/c mouse liver via HTV administration of a combination of two reprogramming pDNA, **OKS** (encoding Oct3/4, Sox2, and Klf4) and **M** (encoding c-Myc) [162, 163]. Here, we aimed to confirm whether the same effect would be achieved with a different pDNA vector encoding all such factors in a single cassette. We also investigated if the exclusion of c-Myc from the reprogramming cocktail or the repeated administration of reprogramming pDNA would affect the changes observed in the tissue. Relevant pDNA maps are represented in **Figure S1**.

3.3.1.1. Gene expression in mouse liver after HTV administration of different reprogramming pDNA.

We first tested a polycistronic pLenti-III-EF1α-mYamanaka vector, referred to as **OKSM**, which encoded the four Yamanaka factors (Oct3/4, Sox2, Klf4 and c-Myc) and a reporter eGFP under the control of the EF1α promoter. Transgenes were separated by 2A peptides to allow the expression of multiple products from a single cassette. We selected this pDNA because the presence of the eGFP reporter could facilitate the identification and isolation of the transfected cells. In addition, the use of a single cassette could reduce the chances of insertional mutagenesis in the host genome, since equivalent copy numbers of the transgenes are delivered in half the number of pDNA constructs. A dose escalation study in Yilmazer's work identified the combination of 75 μg **OKS** and 75 μg **M** (equivalent to 8.17×10^{12} and 1.14×10^{13} copies of each pDNA, respectively) as the lowest pDNA dose that triggered the highest reprogramming effect before a plateau was reached [162]. We compared the performance of an **OKSM** dose equivalent to the above **OKS+M** combination in transgene copies (150 μg **OKSM**, 9.58×10^{12} pDNA copies). BALB/c mice were injected with 75 μg **OKS** and 75 μg **M**, 150 μg **OKSM** or 0.9% saline alone as control. Injection volume was adjusted to 1.5 ml (10% of the body weight, approximately) and administered in 5 s in all the studies involving HTV injection, in order to achieve optimal transgene expression.

Real-time RT-qPCR data of the isolated hepatocyte fraction evidenced that the administration of similar transgene copy numbers, delivered in **OKS+M** or **OKSM** pDNA cassettes, resulted in similar expression of reprogramming factors. Such observation was made both 2 and 4 days after injection **(Figure 3.1a)** and a similar finding was obtained when comparing the expression of endogenous pluripotency genes **(Figure 3.1b)**. Administration of the different cassettes led to very similar *Nanog* and *Rex1* expression levels.

In order to elucidate the longer-term changes in gene expression triggered by a single HTV administration of 150 μg **OKSM**, BALB/c mice were culled 2, 4, 8, 12 and 24 days after injection. The expression of reprogramming, reporter, pluripotency and hepatocyte-specific genes was studied by real-time RT-qPCR in the isolated hepatocyte population. In agreement with the findings by Yilmazer et al. [162], the expression of reprogramming factors was at its highest 2 days after HTV injection and decreased over time. *Sox2* and *c-Myc* levels were very low by day 8 after injection when compared to saline-injected controls and c-Myc expression decreased to baseline levels by day 24, both when saline-injected or uninjected mice were included as control group **(Figure 3.2a)**. The reporter *eGFP* followed a similar trend, with a peak on day 2 that rapidly plummeted by day 4 and negligible expression 12 days after HTV injection **(Figure 3.2b)**. Regarding the expression of endogenous pluripotency markers, *Nanog* and *Rex1* were upregulated compared to the saline-injected group as early as 2 days after *in vivo* transfection **(Figure 3.2c, top panel)**, indicating the fast kinetics of the pluripotent conversion. Notably, such upregulation was even more prominent when gene expression levels were compared to those of uninjected animals **(Figure 3.2c, bottom panel)**. Finally, the study of hepatocyte-specific genes indicated a transient downregulation in the pDNA-injected group compared to saline-injected control on days 2 and 4 after injection, which was not observed at later time points **(Figure 3.2d)**.

Next, we investigated whether the exclusion of c-Myc from the reprogramming cocktail would affect the induction of pluripotency. *c-Myc* is a known oncogene and therefore its use *in vivo* may question the safety of this approach. Although reprogramming to pluripotency with Oct3/4, Sox2 and Klf4 and without c-Myc has been achieved *in vitro*, decreased reprogramming efficiencies have been reported in the absence of this factor [56]. BALB/c mice were HTV injected with 75 μg **OKS** and 75 μg **M**, 75 μg **OKS** alone or 0.9% saline as

control. At day 4 after injection, the c-Myc-free reprogramming cocktail failed to achieve the same levels of *Nanog* and *Rex1* upregulation triggered by the four-factor combination **(Figure 3.3b)**. The downregulation of hepatocyte-specific genes was only clearly achieved when all four factors were present. In the absence of c-Myc, only *Aat* showed minor downregulation 4 days after the injection, however significantly less prominent compared to the result in the **OKS+M** group. **(Figure 3.3c)**.

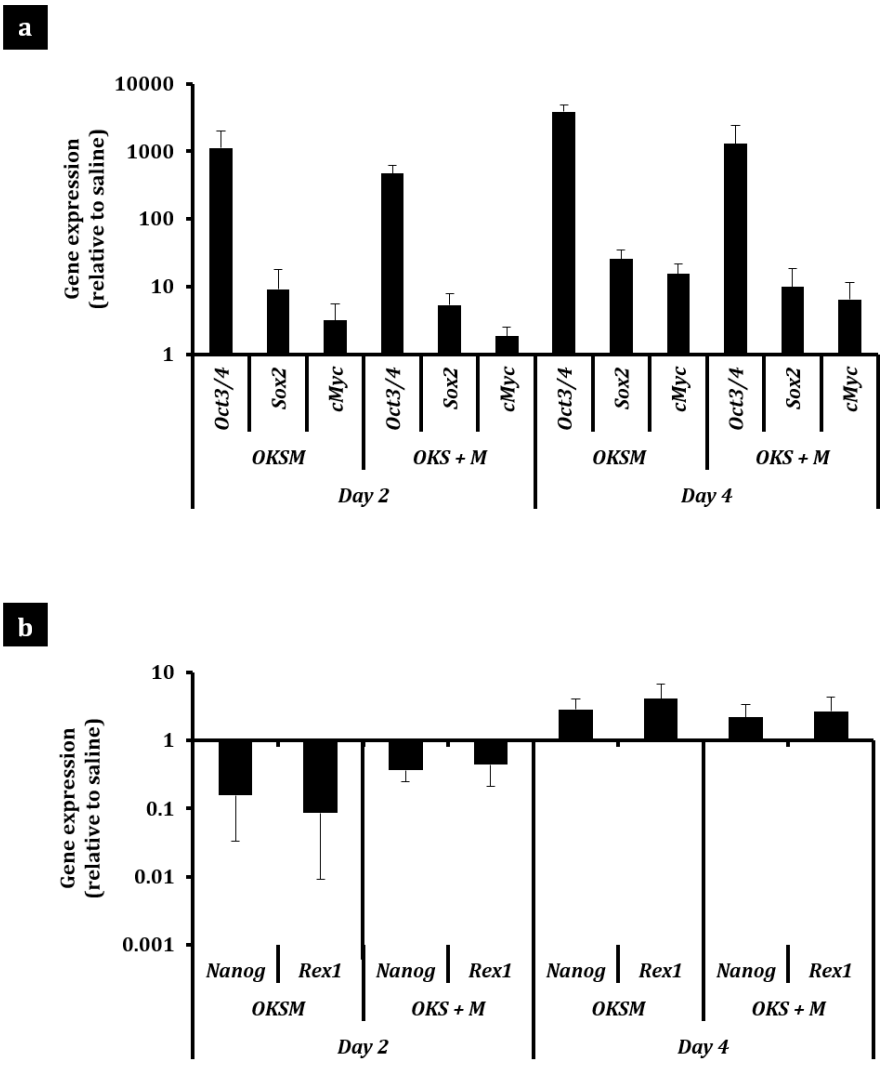

Figure 3. 1. Gene expression in mouse liver upon HTV administration of different reprogramming pDNA. *BALB/c mice were HTV injected with 150 µg OKSM or 75 µg OKS and 75 µg M in 0.9% saline. A control group was injected with 0.9% saline alone. Primary hepatocytes were isolated on days 2 and 4 after injection and real-time RT-qPCR was conducted to determine the relative gene expression of* ***(a)*** *transfected reprogramming factors and* ***(b)*** *endogenous pluripotency genes. Gene expression was normalised to the saline-injected group. No statistically significant differences in gene expression were found between the groups injected with different reprogramming pDNA, assessed by one-way ANOVA. Data are presented as mean ± SD, n=3.*

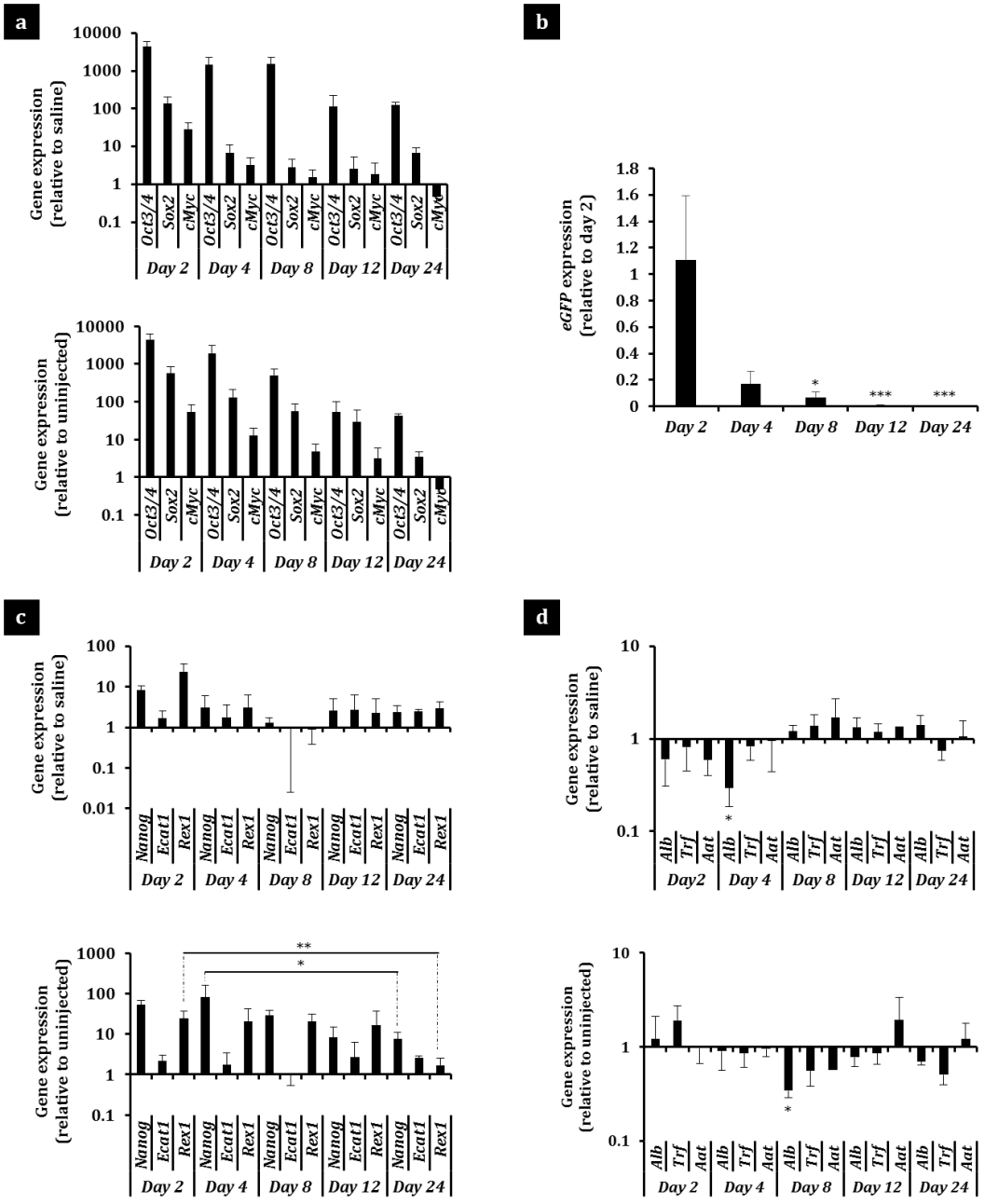

Figure 3. 2. Long-term gene expression changes in mouse liver after HTV administration of OKSM reprogramming pDNA. *BALB/c mice were HTV injected with 0.9% saline alone,150 µg OKSM in 0.9% saline or left uninjected. Primary hepatocytes were isolated on days 2, 4, 8, 12 and 24 after injection and real-time RT-qPCR was performed to determine the relative gene expression of* ***(a)*** *transfected reprogramming factors,* ***(b)*** *eGFP reporter,* ***(c)*** *endogenous pluripotency genes and* ***(d)*** *hepatocyte-specific markers. Gene expression levels were normalised to the saline-injected group (top panels) or the uninjected control (bottom panels) with the exception of eGFP values, which were normalised to the expression 2 days after injection in the pDNA-injected group. *p<0.05 and ***p<0.001 indicate statistically significant difference in eGFP expression compared to that of day 2 after administration, assessed by one-way ANOVA and Tukey's test. *p<0.05 and **p<0.01 indicate statistically significant differences in the upregulation of pluripotency markers and downregulation of hepatocyte-specific genes among treatment groups and time points, assessed by Welch ANOVA and Games-Howell's test. All data are presented as mean ± SD, n=3.*

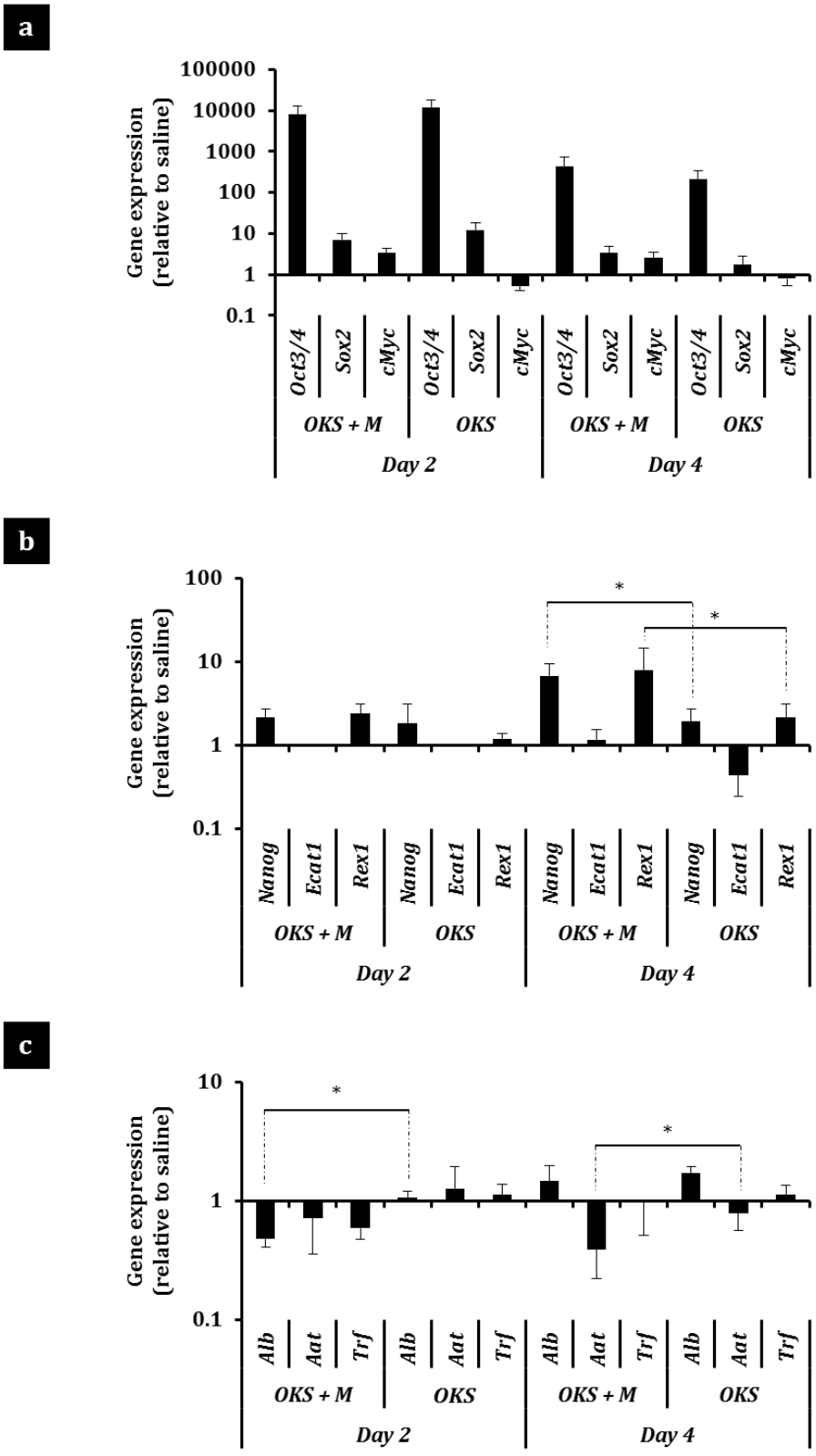

Figure 3. 3. Contribution of the reprogramming factor c-Myc to the induction of pluripotency. *BALB/c mice were HTV injected with 75 µg OKS and 75 µg M or 75 µg OKS alone in 0.9% saline. A control group was injected with 0.9% saline alone. Primary hepatocytes were isolated on days 2 and 4 after injection and real-time RT-qPCR was performed to investigate the relative gene expression of* ***(a)*** *the transfected reprogramming factors,* ***(b)*** *endogenous pluripotency genes and* ***(c)*** *hepatocyte markers. Gene expression levels were normalised to the saline-injected group. *p<0.05 indicates statistically significant differences in the expression of pluripotency and hepatocyte markers in the presence or absence of c-Myc, assessed by one-way ANOVA. Data are presented as mean ± SD, n=3.*

3.3.1.2. Protein expression in mouse liver upon HTV administration of different reprogramming pDNA.

The expression of markers characteristic of the pluripotent state after HTV injection with different combinations of reprogramming pDNA, including **OKSM**, **OKS+M**, and **OKS** alone, was further investigated at the protein level. Immunostaining for different pluripotency markers (NANOG, SOX2, OCT4) and an ES cell-specific surface antigen (SSEA1) was performed on liver tissue sections collected 2 days after HTV injection. All markers investigated were reproducibly observed in several tissue sections from all pDNA-injected groups, indicating the presence of cells expressing proteins characteristic of the pluripotent state throughout the liver tissue **(Figure 3.4)**. No immunoreactivity was detected in the saline-injected group. and no statistically significant differences in the number of positive cells were observed among the groups HTV-administered with different reprogramming pDNA

Overall, these results showed that cells expressing pluripotency markers at the protein level appeared within the liver tissue when the single cassette **OKSM**, the combination **OKS+M** and even **OKS** alone were administered, without significant differences among the groups. However, since gene expression results were optimal when c-Myc was administered, we decided not to exclude this factor for the rest of the studies in this Chapter.

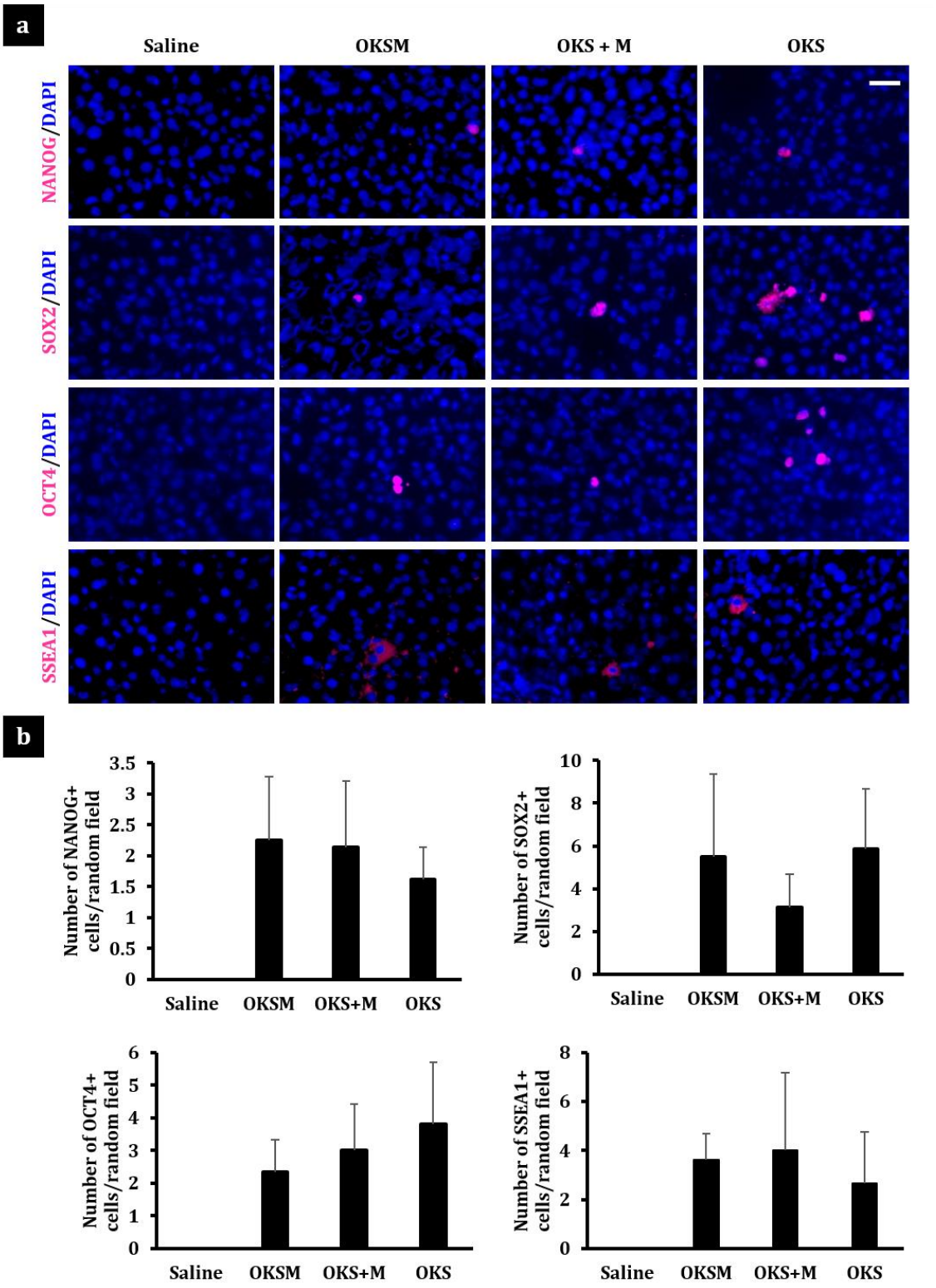

Figure 3. 4. Protein expression of pluripotency markers in mouse liver tissue upon HTV administration of different reprogramming pDNA. *BALB/c mice (n=3) were HTV injected with 150 µg OKSM, 75 µg OKS and 75 µg M or 75 µg OKS pDNA alone in 0.9% saline. A control group was administered with 0.9% saline alone.* ***(a)*** *Livers were collected 2 days after injection and 14 µm thick frozen tissue sections were stained with anti-NANOG, anti-SOX2, anti-OCT4 and anti-SSEA1 antibodies. The pattern was faithfully recapitulated in pDNA-injected mice compared to saline controls. Representative images were images were captured with an epi-fluorescence microscope (40X). Scale bar represents 50 µm.* ***(b)*** *Quantification of positive cells for each marker under investigation. No statistically significant differences in the number of positive cells were found across groups HTV-administered with different reprogramming pDNA (one-way ANOVA, n=3 mice per condition, at least 3 random fields/mouse). Data are presented as mean ± SD.*

3.3.1.4. Repeated HTV administration of reprogramming pDNA: effects on the expression of reprogramming, pluripotency and hepatocyte-specific genes.

The expression of the transfected reprogramming factors was consistently found at its highest levels on day 2 after HTV injection, regardless of the combination of pDNA used, to gradually decrease over time after this time point. Repeated HTV injection of pDNA has been shown to restore transgene expression back to peak levels in a previous study [168]. We investigated how repeated HTV administration of reprogramming pDNA would affect not only the expression of reprogramming factors but also the up- and downregulation of pluripotency and hepatocyte-specific markers, respectively. BALB/c mice were HTV injected with 75 μg **OKS** and 75 μg **M** or 0.9% saline as control. A cohort of animals from each group was culled 3 days after injection while the rest were administered a second dose of the same treatment and sacrificed 1 or 5 days after the second administration (i.e. 4 or 8 days after the first injection, respectively). A diagram representing such administration schemes is provided in **Figure 3.5a**.

One day after the second dose, the expression of the administered reprogramming factors experienced a significant rise (ca. 10-fold increase compared to the levels observed on day 3, just before the second injection). On day 5 after the second administration (i.e. day 8 after the first dose) the expression levels decreased. However, they were still comparable to those reported on day 3 after the first injection **(Figure 3.5b)**. This confirmed that a second dose was able to restore transgene expression levels momentarily, however it failed to increase the expression of pluripotency markers **(Figure 3.5c)**. In addition, no significant differences in the expression of hepatocyte-specific genes were observed throughout the course of the study **(Figure 3.5d)**. These data suggested that no enhancement of the *in vivo* reprogramming outcomes at the mRNA level was obtained by repeated administration of reprogramming pDNA.

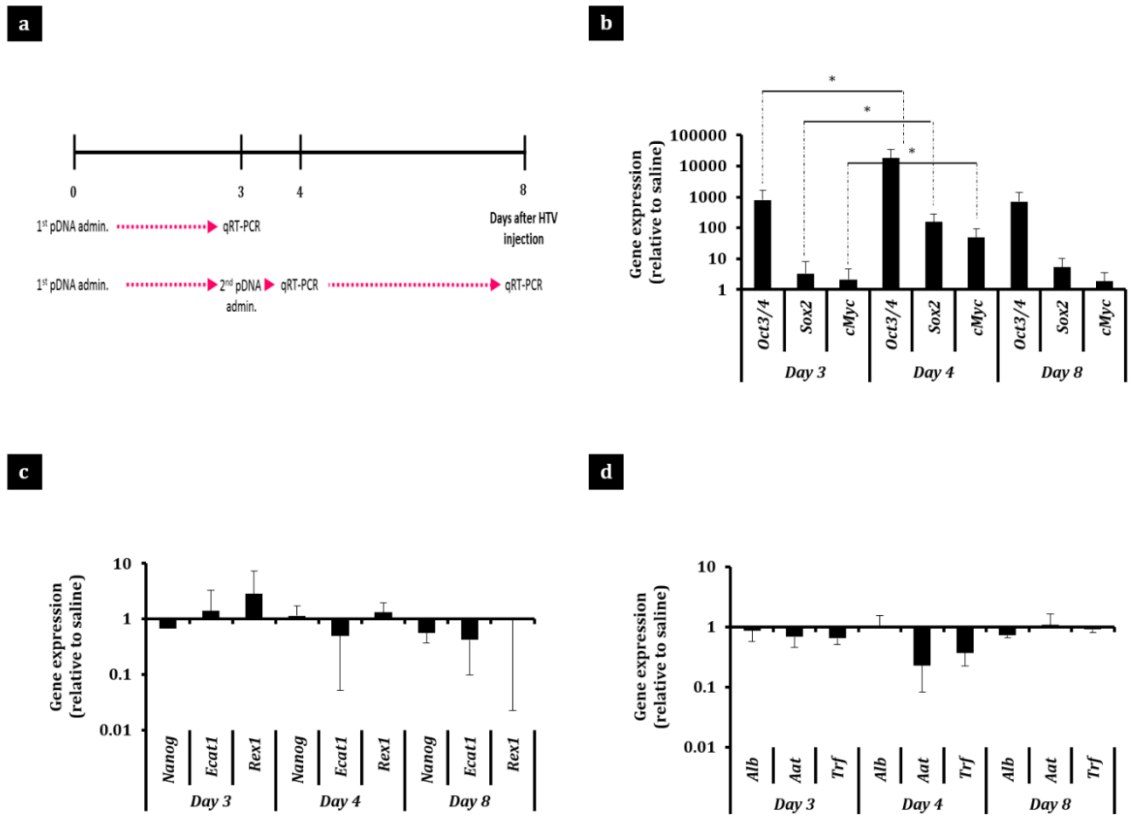

Figure 3. 5. Gene expression in mouse liver after repeated HTV administration of reprogramming pDNA. (a) *BALB/c mice were HTV injected with 75 µg OKS and 75µg M in 0.9% saline. A control group was injected with 0.9% saline alone. A cohort of animals from each group was culled on day 3 after injection while the remaining were administered a second dose of the corresponding treatment and culled 1 or 5 days after the second injection (4 or 8 days after the first dose). Real-time RT-qPCR analysis was performed to determine the relative gene expression of* ***(b)*** *transfected reprogramming factors,* ***(c)*** *endogenous pluripotency genes and* ***(d)*** *hepatocyte markers. Gene expression was normalised to the saline-injected group. *p<0.05 designates statistically significant differences in the expression of reprogramming factors between the first and second injection assessed by one-way ANOVA and Tukey's test. Data are presented as mean ± SD, n=3.*

3.3.1.5. Effects of liver damage on the expression of reprogramming, pluripotency and hepatocyte-specific genes.

Certain pluripotency-related genes are also involved in the process of hepatocyte regeneration, thus any liver insult can alter their expression [184]. Yilmazer et al. reported minor liver damage as a consequence of the HTV injection procedure, albeit only detected at the earliest time point (day 2) after injection and resolved immediately after [162]. We evaluated the effect of this transient damage in the expression of genes of interest for our study. These included the administered reprogramming factors (*Oct3/4*, *Sox2* and *c-Myc*), since the corresponding endogenous loci are involved in pluripotency pathways, other pluripotency-related genes (*Nanog*, *Ecat1*, *Rex1*) and hepatocyte-specific genes

(*Alb*, *Aat* and *Trf*). BALB/c mice were HTV administered with 0.9% saline, without reprogramming pDNA. 2 days after injection, gene expression in the hepatocyte fraction was compared to that of uninjected animals.

All pluripotency-related genes investigated were upregulated in the group that received the injection. For *Oct3/4*, *Sox2*, *c-Myc*, *Nanog* and *Rex1* the differences were statistically significant. On the other hand, hepatocyte-specific genes such as *Alb*, *Aat* and *Trf* were significantly upregulated in the saline-injected group **(Figure 3.6)**. These changes in the gene expression profile of the hepatocytes are attributed to the minor damage inherent to HTV administration and the subsequent regeneration and proliferation of the liver cells and should be taken into account when interpreting the gene expression data in this study.

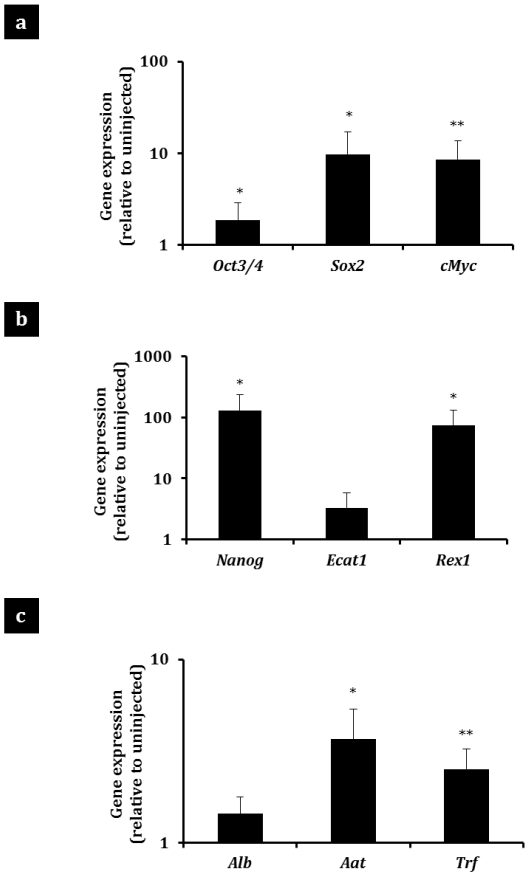

Figure 3. 6. Effects of HTV injection on the expression of pluripotency and hepatocyte-specific genes. *BALB/c mice were HTV injected with 0.9% saline and hepatocytes were isolated 2 days after injection. Real-time RT-qPCR was performed to determine the relative gene expression of* ***(a)*** *endogenous pluripotency genes that are also encoded in the reprogramming pDNA used in this study,* ***(b)*** *endogenous pluripotency genes not encoded in reprogramming pDNA and* ***(c)*** *hepatocyte-specific markers. Gene expression was normalised to a control uninjected group. *p<0.05 and **p<0.01 indicate statistically significant differences in the expression of pluripotency and hepatocyte-specific genes between the injected and uninjected groups, assessed by one-way ANOVA. Data are presented as mean ± SD, n=3.*

3.3.2. *In vitro* culture of *in vivo* reprogrammed liver cells: generation of i²PS cells, confirmation of pluripotency and study of genomic integrity.

Once the changes in gene and protein expression in mouse liver were reproduced with various combinations of reprogramming pDNA, it was of our interest to confirm whether the cells enduring those changes were fully reprogrammed and functionally pluripotent. For this, we aimed to establish them as a stable cell line *in vitro* and used a mES cell line, E14TG2a, as benchmark of pluripotency for comparison.

3.3.2.1. Generation of *in vivo* induced pluripotent stem (i²PS) cell colonies.

Mouse embryonic fibroblasts (MEFs) secrete factors that help to maintain the pluripotency and undifferentiated state of stem cells. For this reason, mitotically inactivated MEFs are commonly used as feeder layers to support the growth of a variety of pluripotent stem cells, including ES and iPS cells [180]. Here, MEFs were isolated from E12.5-14.5 CD1 embryos, mitotically inactivated with mitomycin C after three passages **(Figure S2a),** and used as feeder layers for the culture of E14TG2a cells and for the generation and culture of pluripotent cell colonies from *in vivo* reprogrammed cells. **Figure S2b** shows the characteristic morphology of E14TG2a cells when cultured on feeder layers, i.e. domed-shaped colonies with well-defined and refractive edges. Conversely, colonies of the same cell line cultured on 0.1% gelatin-coated culture vessels without the support of feeder cells exhibited a flatter shape, together with less clearly defined edges and the differentiation of some cells from their margins **(Figure S2c)**.

We took advantage of the eGFP reporter in the **OKSM** cassette to endeavour the sorting of cells transfected with reprogramming pDNA, candidate *in vivo* reprogrammed cells, by Fluorescence Activated Cell Sorting (FACS). However, due to the low cell numbers recovered from the sorting and the detrimental impact of the procedure in their viability, we were not able to maintain such cells in culture (data not shown). We next decided to culture the whole hepatocyte extract, which contains the *in vivo* reprogrammed cells, in an attempt to generate pluripotent stem cell colonies *in vitro*.

Figure 3.7 illustrates the timeline for the generation of i²PS cell colonies from *in vivo* reprogrammed liver cells. BALB/c mice were HTV injected with 75 μg **OKS** and 75 μg **M** or 0.9% saline as control. 2 days later, the hepatocyte fraction

was isolated as previously described, seeded on MEF feeder layers and cultured under standard mES cell conditions (DMEM/LIF medium). Cells were passaged 1:2 on fresh feeders after 10 days in culture and 2 days later colonies began to form that shared morphological features with mES cells (i.e. large nucleus and reduced cytoplasmic space, domed shape and refractive edges). Such colonies, which were only found in cultures originated from pDNA-injected mice but not from the saline control, were named ***i**n vivo* **i**nduced **p**luripotent **s**tem (i²PS) cells in reference to their origin [185]. Nonetheless, complete reprogramming to functional pluripotency had to be confirmed with further studies. In addition, the derivation of i²PS cells from *in vivo* reprogrammed livers proved very challenging. Only one out of approximately 20 pDNA-injected livers, processed in different experiments, gave rise to i²PS cell colonies when cultured under these conditions.

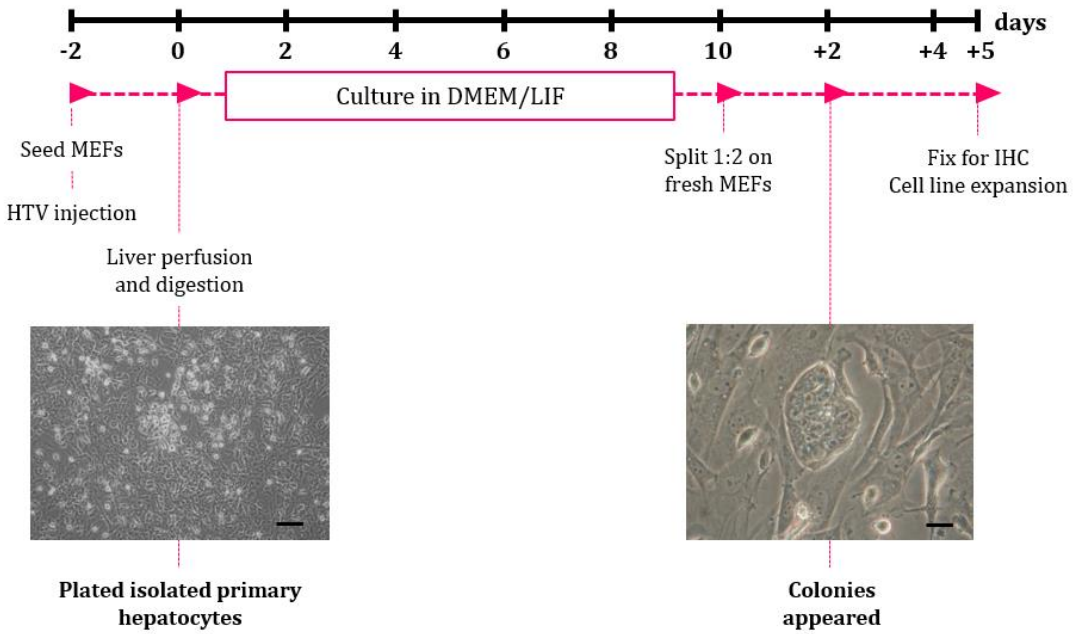

Figure 3. 7. Generation of i²PS cell colonies from in vivo reprogrammed liver cells. *BALB/c mice were HTV administered with 75 µg OKS and 75 µg M pDNA in 0.9% saline. Mice in the control group were injected with 0.9% saline alone. The hepatocyte fraction was isolated 2 days after injection, seeded on MEF feeder layers and cultured in DMEM/LIF medium. Cells were passaged (1:2) 10 days after the start of the culture and i²PS cell colonies were visible 2 days after passaging. Images of the cultures were taken with an optical microscope. Scale bars represent 100 µm (left picture, 10X) and 25 µm (40X, right). This experiment was performed by Dr. Cyrill Bussy.*

3.3.2.2. Assessment of pluripotency at the molecular level.

When a new iPS cell line is generated, pluripotency cannot be confirmed by their ES-like morphological appearance but has to be verified through exhaustive examination [119, 186]. Such confirmation was of special relevance in the case of

i²PS cells, being the first-ever reported iPS cell line generated *in vivo*. Our initial objective was to challenge the pluripotency of i²PS cells at the molecular level.

Gene expression profile of i²PS cells in comparison to a standard mES cell line

The gene expression signature of i²PS cells was compared to that of E14TG2a cells. Prior to RNA extraction, both cell lines were passaged 3 times on 0.1% gelatin-coated tissue culture vessels in order to remove any remaining feeder cells that could interfere in the results **(Figures 3.8a and b)**.

Real-time RT-qPCR data evidenced the upregulation of a series of pluripotency genes in i²PS cells, compared to E14TG2a cells. For *Nanog*, *Ecat1*, *Rex1*, *Cripto*, *endo-Sox2* and *endo-Klf4* the difference was significant **(Figure 3.8c)** although in none of the cases was it higher than a 3-fold increase. Regarding the expression of early differentiation markers, *Afp* (endoderm) was 10-fold upregulated in i²PS cells, while *Fgf-5* (ectoderm) and *T* (mesoderm) were downregulated compared to E14TG2a cells **(Figure 3.8d)**.

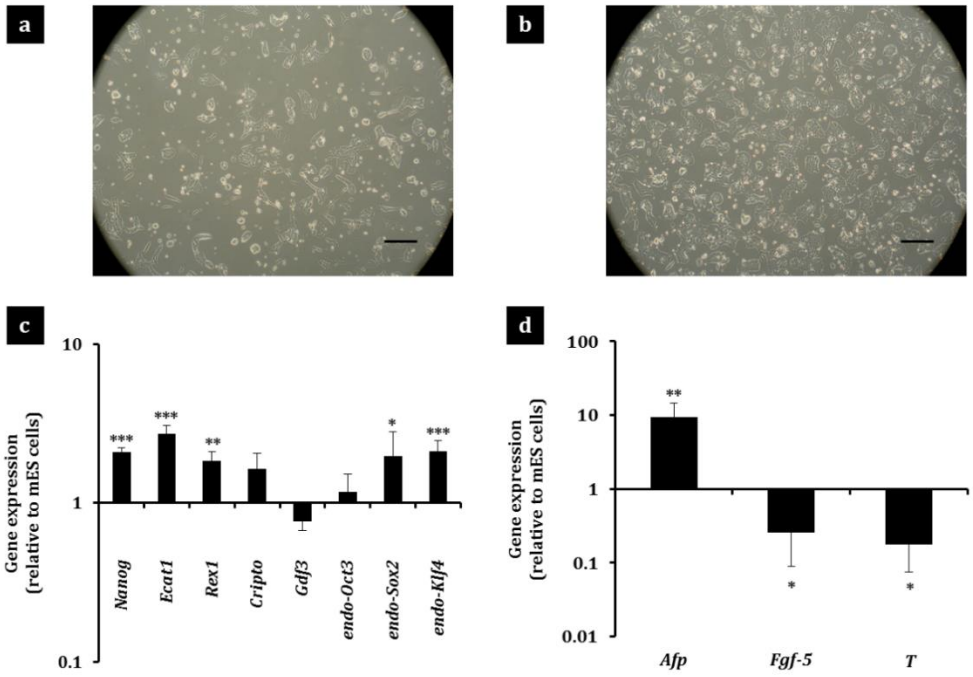

Figure 3. 8. Gene expression of key pluripotency and early differentiation markers in i²PS cells and a standard mES cell line. (a) *E14TG2a mES and* ***(b)*** *i²PS cells were cultured on gelatin-coated tissue culture vessels (scale bars represent 100 μm). Total RNA was extracted from 2 x 10⁶ cells and real-time RT-qPCR was performed to determine the relative gene expression of* ***(c)*** *pluripotency markers and* ***(d)*** *an early differentiation marker representing each of the three germ layers. Gene expression in i²PS cells was normalised to that of E14TG2a cells. *p<0.05, **p<0.01 and ***p<0.001 indicate statistically significant differences in the expression of pluripotency and differentiation markers between both cell lines, assessed by one-way ANOVA. Data are presented as mean ± SD, n=3.*

In order to further confirm the results obtained by real-time RT-qPCR and to build a whole-genome expression profile of the generated i²PS cells, a DNA microarray study was conducted. Out of the 45,200 probes analysed in the array, 2,327 were differently expressed in i²PS compared to E14TG2a cells, however the expression of key genes related to pluripotency such as *Nanog*, *Ecat1* and *Rex1* was very similar in both cell lines **(Figure 3.9a)**. In agreement with these observations, hierarchical clustering analysis of the different cell samples showed that i²PS and E14TG2a cells clustered relatively close to each other when the whole transcriptome was considered **(Figure 3.9b)**.

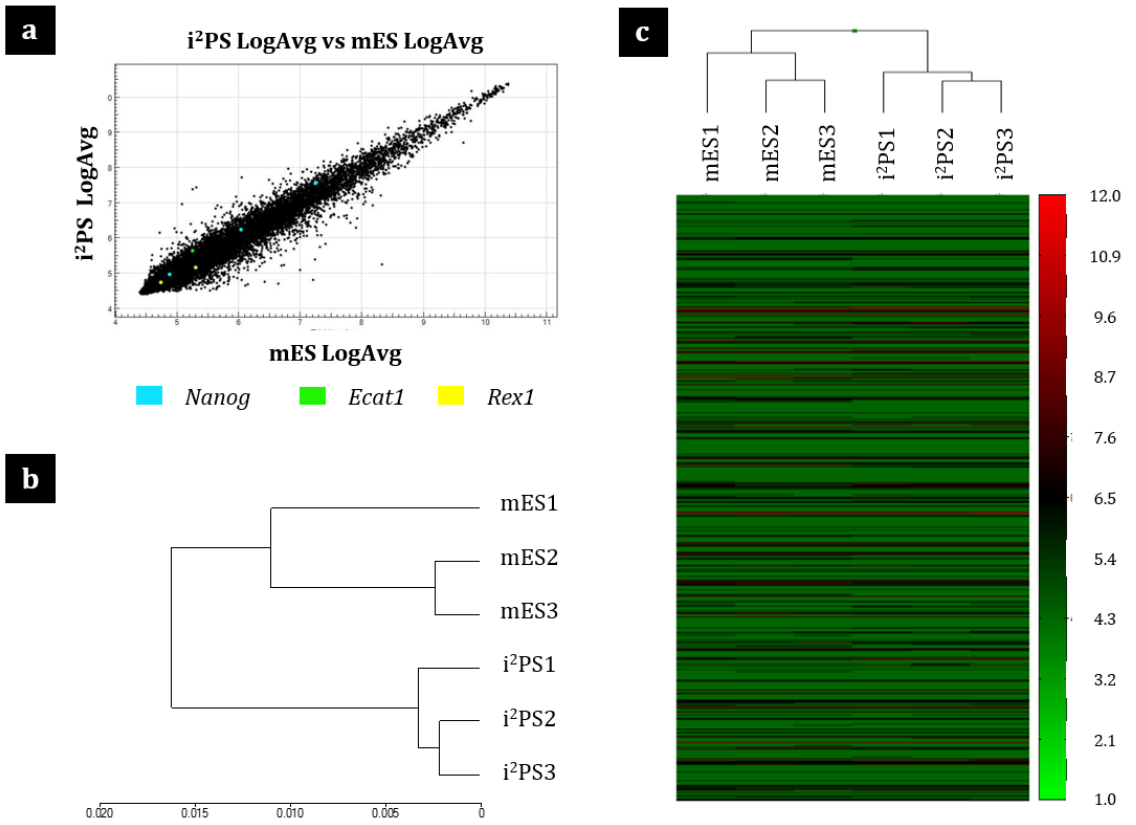

Figure 3. 9. Whole-genome expression profile of i²PS and E14TG2a mES cells. *1 µg RNA was extracted from feeder-free i²PS and E14TG2a cell cultures (n=3) and the global gene expression profiles of both cell types were compared by DNA microarray. Biological replicates of each cell type are numbered 1-3.* ***(a)*** *The scatter plot represents the expression of 45,200 probes in i²PS (Y axis) and E14TG2a cells (X axis). Each dot represents the logarithm of the average signal intensity of a probe.* ***(b)*** *Dendrogram representing the hierarchical clustering of the different cell samples.* ***(c)*** *Heatmap comparing the expression of 274 genes involved in the induction, maintenance, amelioration or loss of pluripotency. The array was performed by the staff at the Genome Centre, Queen Mary University of London (UK), who also assisted with the analysis of the data.*

Microarray data can be accessed at http://www.ncbi.nlm.nih.gov/geo/query/acc.cgi?acc=GSE55996.

Once the global gene expression profile of both cell lines was compared, the focus of the study shifted to different sets of genes involved in specific pathways and developmental processes. In a comprehensive study, Som *et al.* unveiled a network of 574 molecular interactions, including activations and inhibitions, which are involved in the pluripotency pathway in the mouse. 274 genes were found to participate in the induction, maintenance, amelioration or loss of pluripotency [187]. The expression of these genes was found to be very similar in i²PS and E14TG2a cells, as illustrated in **Figure 3.9c.**

Next, in order to identify whether the differentiation potential of i²PS cells was favoured towards a particular lineage, the expression of genes related to the early development of the endoderm **(Figure 3.10a)**, mesoderm **(Figure 3.10b)** and ectoderm **(Figure 3.10c)** was investigated. These genes were clustered using the NCBI Biosystems Database and no remarkable differences in their expression were observed between cell lines.

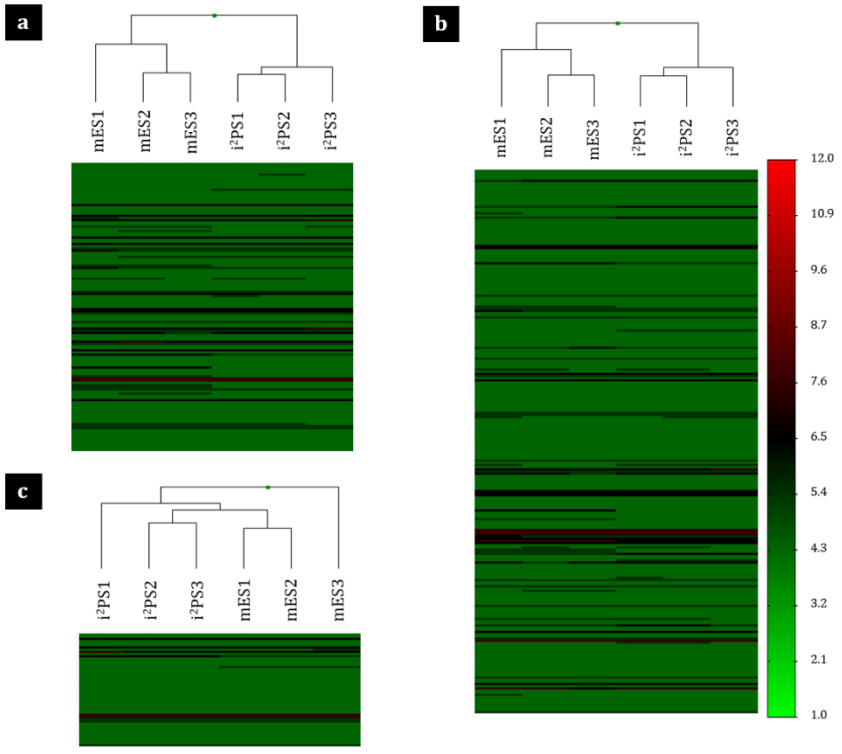

Figure 3. 10. Expression of genes involved in the early differentiation of the three germ layers. *The expression of early differentiation markers was investigated in i²PS and E14TG2a mES cells (n=3) by DNA microarray. Biological replicates of each cell type are numbered 1-3. Heatmaps show clusters of* ***(a)*** *123 genes involved in endoderm development,* ***(b)*** *228 genes participating in mesoderm development and* ***(c)*** *60 genes related to the ectoderm lineage. The array was performed by the staff at the Genome Centre, Queen Mary University of London (UK), who also assisted with the analysis of the data.*

Microarray data can be accessed at http://www.ncbi.nlm.nih.gov/geo/query/acc.cgi?acc=GSE55996.

Finally, the possibility that a gene expression signature characteristic to the tissue of origin remained in i²PS cells was investigated. A set of 10 genes highly expressed at different stages of hepatocyte differentiation within the endoderm lineage were analysed. *Afp* and *Foxa2* were selected as representatives of early endoderm, *Alb* and *Cyp3a16* for fetal hepatocytes, *Tat* and *G6pc* for perinatal hepatocytes and *Cyp3a11*, *Cyp3a25*, *Pck1* and *Tdo2* for postnatal hepatocytes, as described in a previous work [178]. As shown in **Figure 3.11**, none of those genes were highly expressed in the E14TG2a control, nor in i²PS cells.

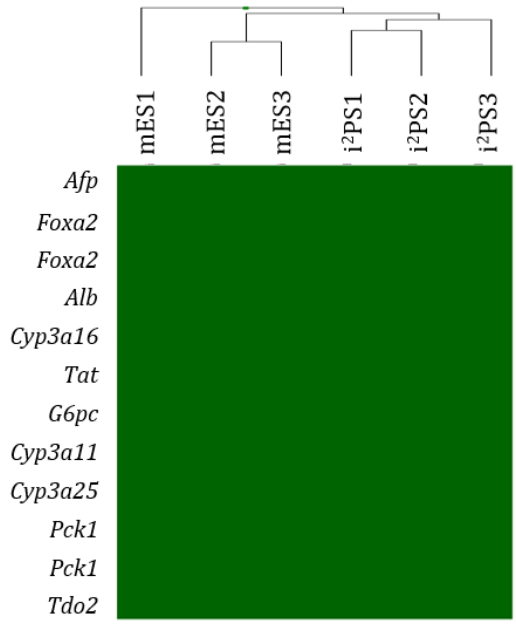

Figure 3. 11. Expression of genes upregulated at different stages during hepatocyte differentiation. *The heatmap represents the expression of markers characteristic of early endoderm development (Afp, Foxa2); fetal hepatocyte (Alb, Cyp3a16); perinatal hepatocyte (Tat, G6pc) and postnatal hepatocyte (Cyp3a11, Cyp3a25, Pck1, Tdo2) in E14TG2a mES and i²PS cells (n=3), analysed via DNA microarray. Biological replicates of each cell type are numbered 1-3. The array was performed by the staff at the Genome Centre, Queen Mary University of London (UK), who also assisted with the analysis of the data.*

(Microarray data can be accessed at http://www.ncbi.nlm.nih.gov/geo/query/acc.cgi?acc=GSE55996)

Overall, the results of the array suggested that the gene expression program of the reprogrammed hepatocytes had been shifted to recapitulate very closely that of pluripotent cells. However, the remaining of particular signatures of the tissue of origin upon reprogramming cannot be completely ruled out in the absence of *ad hoc* epigenetic studies and taking into account the 10-fold upregulation of *Afp* found via RT-qPCR **(Figure 3.8)**.

Response of i²PS and mES cells to dual inhibition (2i) conditions

The behaviour of reprogrammed cells upon exposure to defined molecular conditions present in the embryonic stages in natural development has been previously studied. The inhibitors GSK3 and Mek1/2 are known to neutralise differentiation signals and maintain the pluripotency and self-renewal capacity of ES cells. The presence of such molecules in the culture medium (known as dual inhibition or 2i conditions) can induce partially reprogrammed cells (i.e. not fully pluripotent) to a state of ground pluripotency. Upon exposure to 2i conditions, mRNA levels of key pluripotency genes such as *Nanog* and *Rex1*, barely detectable in the starting partially reprogrammed cells, were comparable to those of ES cells [119].

We aimed to explore the response of i²PS cells to 2i conditions compared to that of E14TG2a cells and to elucidate whether the expression of pluripotency markers had reached a plateau or could be upregulated any further. The cells were maintained on 0.1% gelatin-coated culture vessels and either standard mES cell culture conditions (DMEM/LIF) or 2i supplemented medium (KODMEM/2i/LIF). *Nanog* and *Rex1* expression at different time points post-culture (pc) was compared to that of the starting cells by real-time RT-qPCR.

Figure 3.12a shows the evolution of *Nanog* and *Rex1* mRNA levels over time in i²PS cells cultured under DMEM/LIF conditions. 3 days after the start of the culture, a slight decrease in *Nanog* - but not *Rex1*- expression was detected compared to the starting cells. The expression of both genes increased significantly with the increased passaging of the cells, reaching baseline levels for *Nanog* and an approximate 10-fold upregulation over the starting cells' levels for *Rex1* by day 30 pc. When i²PS cells were maintained under KODMEM/2i/LIF conditions **(Figure 3.12b)** *Nanog* and *Rex1* were upregulated from the earliest time point after the start of the culture (day 3). By the end of the culture (day 40) the upregulation of both genes did not surpass the 10-fold increase.

No difficulties were found in maintaining the initial expression levels of pluripotency markers in E14TG2a cells, even at the earliest time points in DMEM/LIF cultures **(Figure 3.12c)**. In fact, *Nanog* and *Rex1* were significantly upregulated from day 5 pc, compared to the starting cells. Similarly to the response of i²PS cells in this medium, the expression of pluripotency markers increased with

passaging, showing significant differences between day 5 and day 10 pc. When exposed to 2i conditions, a remarkable 10-fold upregulation - for both *Nanog* and *Rex1* -was found in E14TG2a cells as early as 2 days after the start of the cultures **(Figure 3.12d)**. Once again, gene expression of the pluripotency markers continue to increase with increased passaging, this time reaching almost a 100-fold upregulation. Overall, these results indicated minor problems to maintain the expression of *Nanog* in i²PS cells cultured in DMEM/LIF, which were resolved with extended passaging. These data suggested as well that the expression of pluripotency markers could be further upregulated in both cell lines not only with increased passaging but also soon after the start of the cultures when exposed to 2i. The pluripotency upregulation triggered by 2i exposure was more apparent in E14TG2a cells, which might be explained by the slightly but significantly lower expression of pluripotency genes in such cells compared to i²PS cells **(Figure 3.8c)**.

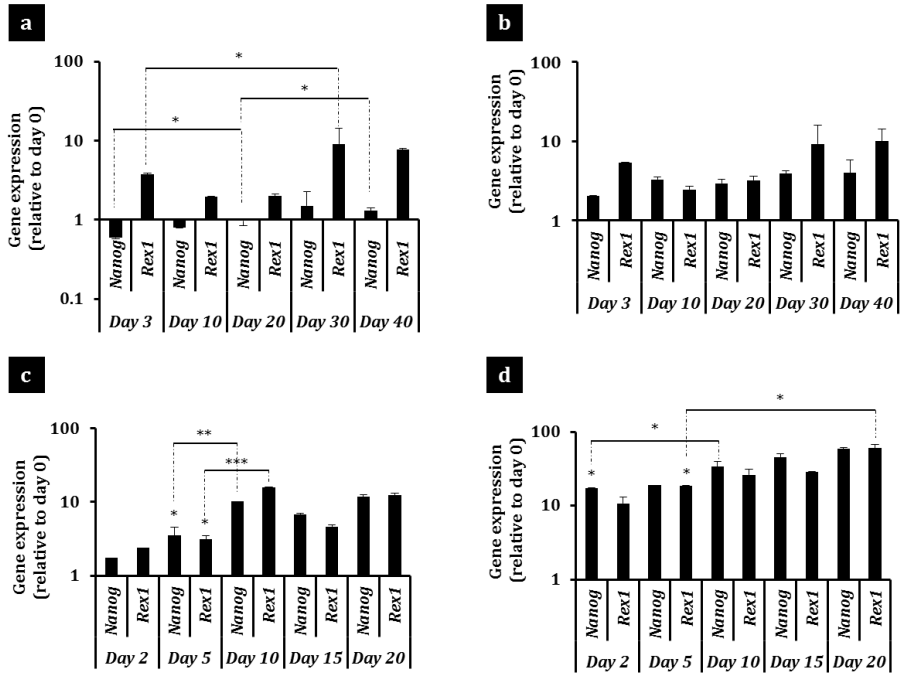

Figure 3. 12. Response of i²PS and E14TG2a cells to 2i culture conditions. *i²PS and E14TG2a cell colonies were cultured in DMEM/LIF or KODMEM/2i/LIF medium and the expression of pluripotency-related genes was analysed by real-time RT-qPCR to evaluate the changes triggered by dual inhibition.* ***(a)*** *i²PS cells in DMEM/LIF,* ***(b)*** *i²PS cells in KODMEM/2i/LIF,* ***(c)*** *E14TG2a cells in DMEM/LIF,* ***(d)*** *E14TG2a cells in KODMEM/2i/LIF. Gene expression levels were normalised to those at the start of the culture (day 0). *p<0.05, **p<0.01 and ***p<0.001 indicate statistically significant differences in Nanog and Rex1 mRNA levels among the different time points, assessed by one-way ANOVA and Tukey's test. Data are presented as mean ± SD, n=3.*

Protein expression

Next, we investigated whether i²PS cell colonies expressed pluripotency markers at the protein level. Live staining with a pluripotency-specific dye, CDy1, was positive in colonies that also exhibited high AP activity **(Figure 3.13a)**. Immunoreactivity for the pluripotency markers OCT3/4, SOX2 and NANOG and the ES cell marker SSEA1 was also observed **(Figure 3.13b)**. Identical results were obtained in the stainings of E14TG2a cell colonies [185].

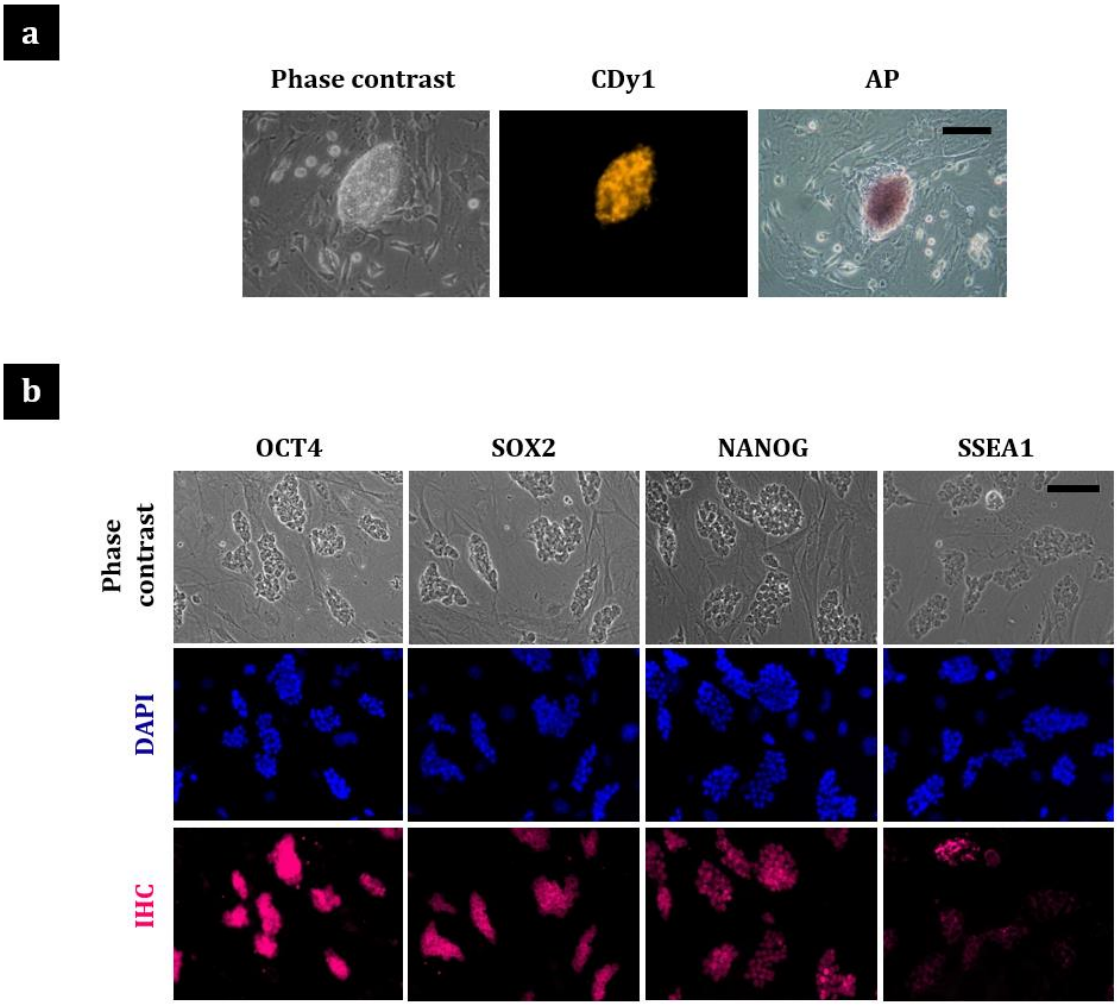

Figure 3. 13. Expression of pluripotency markers at the protein level in i²PS cell colonies. (a) *Live i²PS cell colonies cultured on MEFs feeder layers were stained with the pluripotency-specific fluorescent dye CDy1 and later fixed and stained with the BCIP/NBT substrate to detect AP activity.* ***(b)*** *Fixed i²PS cell colonies were stained with anti-OCT4, anti-SOX2, anti-NANOG and anti-SSEA1antibodies. Images were acquired with optical (AP) and epi-fluorescence (CDy1, IHC) microscopes. Scale bars represent 200 μm. This experiment was performed by Dr. Cyrill Bussy.*

3.3.2.3. Assessment of pluripotency at the functional level.

Once we confirmed that i²PS cells showed a gene and protein expression profile characteristic of the pluripotent state, there was a need to prove that such cells were functionally pluripotent and thus able to differentiate into cells from all three germ layers (endoderm, mesoderm and ectoderm). The differentiation potential of i²PS cells was tested *in vitro* and *in vivo*.

In vitro study of functional pluripotency: embryoid bodies (EBs)

When cultured on non-adherent surfaces, pluripotent cells form spherical aggregates in which cells start to differentiate. Given the resemblance with the gastrulating embryo, they are known as embryoid bodies (EBs). The presence in these aggregates of representatives of all three germ layers is considered an *in vitro* proof of functional pluripotency [182, 188, 189].

Feeder-free i²PS cells cultured on DMEM/LIF conditions were dissociated and seeded on non-adherent surfaces (agar-coated 96-well plates). LIF was removed from the culture medium to allow the cells to differentiate spontaneously and form EBs. Loose aggregates formed as early as 1 day after seeding **(Figure 3.14a)** and evolved into more compact spheroids after 3 days. The floating EBs were then transferred and left to attach onto gelatin-coated dishes in order to culture the cells differentiating and spreading out from their outer layers **(Figure 3.14b)**.

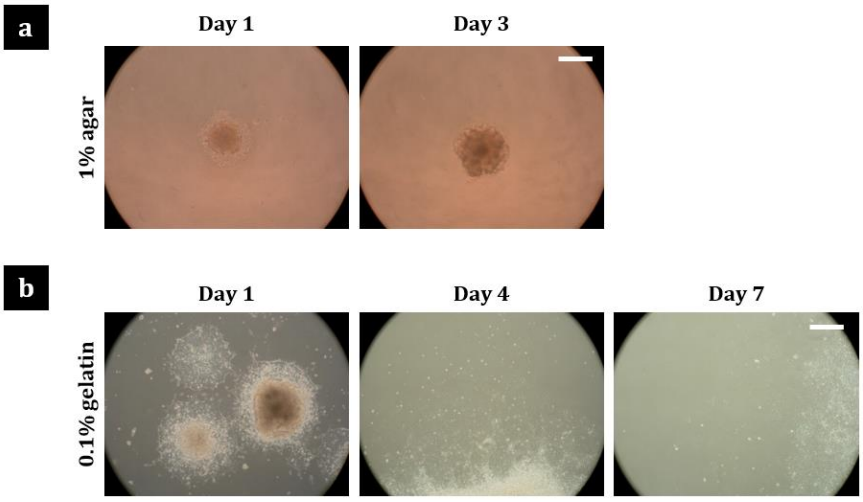

Figure 3. 5. Generation of EBs from i²PS cells and spontaneous differentiation in vitro. (a) *i²PS cells formed compact EBs after 3 days culture on agar–coated surfaces and in the absence of LIF.* ***(b)*** *The aggregates were transferred to 0.1% gelatin-coated tissue culture dishes where cells differentiated spontaneously. Images were acquired with an optical microscope. Scale bars represent 100 μm.*

mRNA levels of pluripotency and early differentiation markers were assessed by real-time RT-qPCR in cells left to differentiate for 15 days on the gelatin support. The levels were compared to that of the starting i^{2}PS cells used to generate the EBs. Fibroblasts (MEFs) were also included in the study as a control for fully differentiated cells (ectoderm lineage). **Figure 3.15a** shows the expression levels of *Afp* (endoderm), *T* (mesoderm) and *Fgf-5* (ectoderm). As expected, the ectodermal marker *Fgf-5* was 100-fold upregulated in the control fibroblast compared to i^{2}PS cells, whereas *Afp* and *T* were downregulated. The three markers were significantly upregulated in the cells originated from EBs, suggesting their differentiation towards all three lineages. Regarding the expression of two key pluripotency genes, MEFs showed a remarkable downregulation in both *Nanog* (10^4-fold) and *Oct3/4* (ca. 10^6-fold), as predicted for terminally differentiated cells **(Figure 3.15b)**. These markers were also significantly downregulated in the cells differentiated from EBs when compared to the starting i^{2}PS cells; however the difference in gene expression was not as prominent (10-fold downregulation). This result was expected given that EBs consist of cells in the early stages of differentiation together with cells that still retain some degree of pluripotency. These findings were supported by findings in protein expression. IHC for early differentiation markers confirmed the presence among the cells originated from EBs, of representatives of endoderm (AFP), mesoderm (α-SMA) and ectoderm (β-III TUBULIN) lineages **(Figure 3.15c)**. All together, these results confirmed that i^{2}PS cells behaved as pluripotent cells in the culture dish.

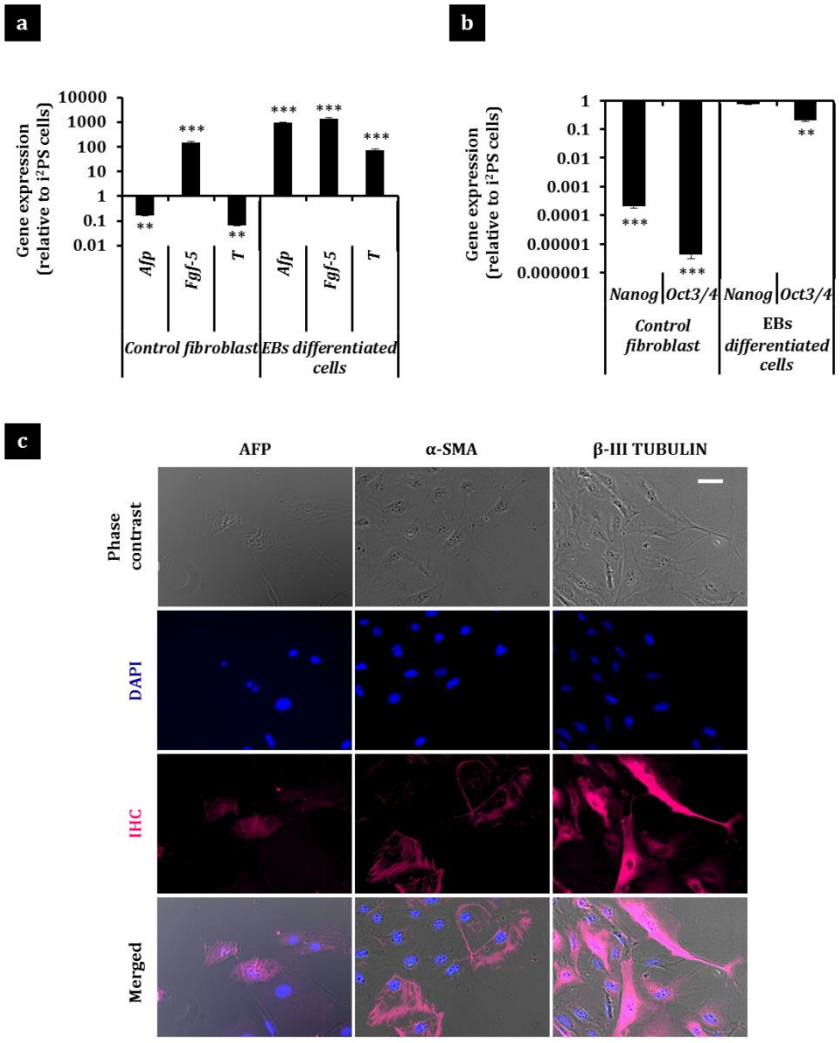

Figure 3. 15. In vitro assessment of pluripotency. *mRNA levels of* ***(a)*** *early differentiation markers and* ***(b)*** *pluripotency genes were assessed by real-time RT-qPCR in cells left to differentiate spontaneously for 15 days from the EBs and in MEFs. Gene expression was normalised to the starting i²PS cells used to generate the EBs. **p<0.01 and ***p<0.001 indicate statistically significant differences in gene expression between the starting i²PS cells and the cells differentiated from EBs or the control fibroblasts (MEFs), assessed by one-way ANOVA. Data are presented as mean ± SD, n=3.* ***(c)*** *AFP (endoderm), α-SMA (mesoderm) and β-III TUBULIN (ectoderm) immunostaining on cells differentiated from EBs. Images were obtained with an epi-fluorescence microscope. Scale bar represents 50 µm.*

In vivo study of functional pluripotency: teratoma assay

When subcutaneously (s.c.) injected in immunodeficient mice, fully pluripotent cells form teratomas containing tissues from all developmental origins. This is often used to validate the differentiation potential of candidate pluripotent cells in the *in vivo* scenario [186, 190]. 2x10^6 feeder-free *i²*PS cells were s.c. injected in the dorsal flank of CD1 nude mice. Equal numbers of E14TG2a cells were administered following the same procedure, as positive control for the generation of teratomas. Primary hepatocytes isolated 2 days after HTV injection

with 75 µg **OKS** and 75 µg **M** were also included in the study. This was aimed to test the differentiation potential held by the *in vivo* reprogrammed cells prior to any culturing procedure.

Finally, hepatocytes isolated 2 days after HTV injection with 0.9% saline alone were included as negative control. After 5 weeks, all the animals (n=5) injected with *i*²PS or E14TG2a cells developed teratomas with the presence of tissues from all three germ layers **(Figure 3.16)**. Most importantly, teratomas were also generated with a 100% efficiency upon implantation of primary cells directly extracted from mice administered with **OKS+M** (without any culturing), although their growth was generally slower than that of the i²PS and E14TG2a groups and the various tissue types present did not seem as differentiated. Primary hepatocytes from saline-injected animals failed to form tumours. This result not only reaffirmed the functional pluripotency of the i²PS cell line but also demonstrated that the conversion to such state took place in the mouse liver and not as a result of the culture conditions, favourable to maintain pluripotent cells that were used to generate i²PS cell colonies.

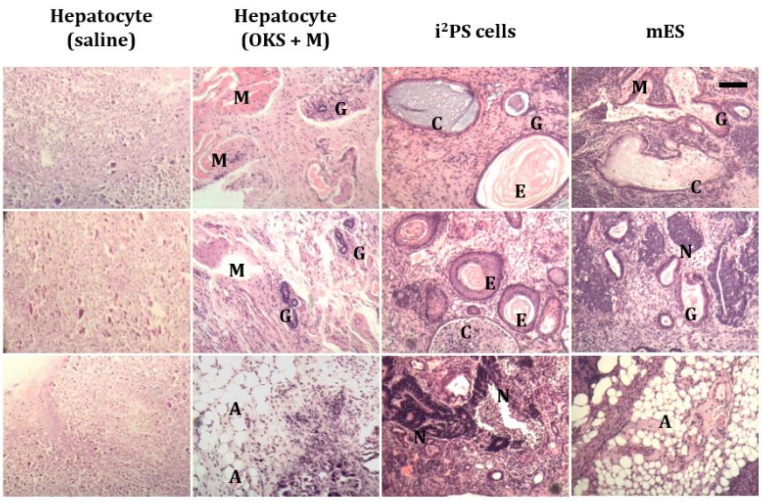

Figure 3. 16. In vivo assessment of pluripotency via teratoma formation in nude mice. *2 x 10⁶ hepatocytes extracted from n=3 mice 2 days after HTV injection with 0.9% saline or 75 µg OKS and 75 µg M were pooled together and s.c. implanted in CD1 nude mice (n=5) to investigate their differentiation potential in vivo. The same number of i²PS and E14TG2a mES cells (from a single independent cell line of each type) were also injected following the same procedure. Tumours were dissected 5 weeks after injection and the presence of different tissue types was observed in H&E stained sections. All animals (n=5) injected with primary hepatocytes extracted upon pDNA administration, i²PS or E14TG2a cells developed tumours. No teratomas were formed in the animals injected with hepatocytes from saline-injected mice, but the site of implantation was also sectioned and analysed. Representative images were obtained with an optical microscope (10X). n=5 mice per condition. M, G, N, C, E and A indicate muscle, gland, neural, cartilage, epidermis and adipose tissue respectively. This experiment was performed with Dr. Acelya Yilmazer.*

In vivo study of functional pluripotency: chimerism experiment

Contribution to the adult tissues of chimeric mice is considered as one of the most stringent requisites for the confirmation of functional pluripotency [191]. Passage 13 (P13) i^{2}PS cells were selected for embryo injections since we previously observed a significant increase in the upregulation of pluripotency markers with increased passaging, regardless of the culture conditions **(Figure 3.12)**. This agreed with previous studies in which extended passaging was reported to erase epigenetic memory and improve the overall differentiation potential of iPS cells [192].

We first attempted to generate chimeric mice with i^{2}PS cell contribution by injecting these cells - originated from BALB/c liver cells - in 3.5 dpc blastocysts from C57BL/6 background. i^{2}PS cells were either cultured on MEF feeder layers and DMEM/LIF conditions or on 0.1% gelatin-coated tissue culture vessels under 2i conditions (KODMEM/2i/LIF) **(Figure 3.17a)**. Upon fibroblast removal if required, i^{2}PS cells were microinjected in C57BL/6 blastocysts, which were then surgically transferred to synchronized pseudopregnant CD1 surrogate mothers. **Figure 3.17b** illustrates the sequence of i^{2}PS cell inoculation into the embryos with a microinjector.

Blastocyst injection of i^{2}PS cells cultured under 2i conditions failed to generate viable offspring. In contrast, 11 viable mice were obtained from i^{2}PS cells cultured in DMEM/LIF-MEFs, although i^{2}PS cell contribution could not be confirmed by the fur coat colour – as evidenced from the lack of white patches **(Figure 3.17d).** We then took advantage of the differences in the Major Histocompatibility Complex (MHC) Class I haplotype between mice strains (H2-Kb for C57BL/6 and H2-Kd for BALB/c mice) to genotype the adult offspring. Two of the mice – identified as no. 7 and 8 - were positive for both haplotypes, which confirmed the co-existence of C57BL/6 and BALB/c derived cells **(Figure 3.17c)**. Next, i^{2}PS cell contribution to various tissues of different developmental origin was investigated **(Figure 3.17e)**. As expected, no i^{2}PS cell contribution was observed in mice no. 5 and 6, which had shown pure C57BL/6 genotype in the previous study. Interestingly, chimerism was widespread in all tissues examined in mice no. 7 and 8. Very importantly, these mice reached adulthood, were sacrificed at 6 months of age and no teratomas were observed in any of the organs upon necropsy.

The next step was to test the contribution of i²PS cells to the germline. Mice no. 7 and 8 were mated with pure BALB/c background partners. Although we had confirmed i²PS cell contribution to the gonads **(Figure 3.17e)**, no pure BALB/c genotypes were obtained in the first generation (F1, data not shown) and thus germline transmission remained to be demonstrated.

Driven by the low chimera generation efficiency achieved via blastocyst injection, we repeated the experiment injecting i²PS cells in embryos at the morula stage (2.5 dpc). Given the lower number of host's cells present in the morula as compared to the blastocyst, we hypothesised that i²PS cell contribution to the adult organism would be favoured. In spite of the larger number of surrogate mothers implanted **(Table 3.1)**, a first round of injections of i²PS cells (DMEM/LIF-MEFs) in C57BL/6 morulas yielded only 2 viable mice. None of them showed *H2-Kd* genotype that confirmed i²PS cell contribution **(Figure 3.18a)**. The same procedure was repeated with i²PS cells (KODMEM/2i/LIF-gelatin) in BDF1 morulas. Genotyping for the MHC Class I antigen could not be used since this strain shares the *H2-Kd* haplotype with BALB/c mice. The satellite DNA *D19Mit59* was therefore selected given its different size in the two strains [193]. As in the previous attempt, the viable offspring was very limited in numbers and the presence of i²PS derived cells could not be verified **(Figure 3.18b)**.

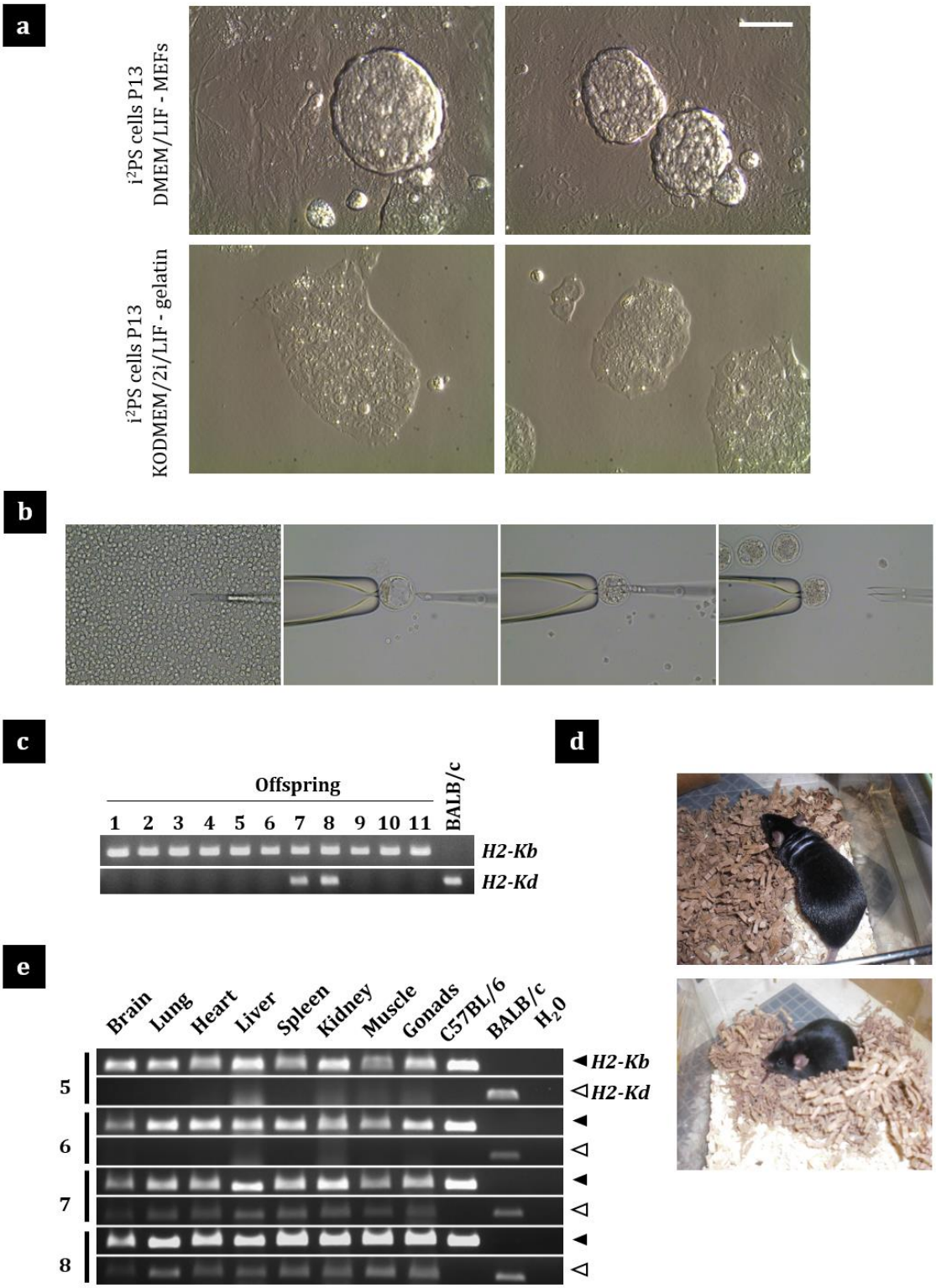

Figure 3. 17. i²PS cell contribution to adult tissues of mice generated via blastocyst injection. ***(a)*** *i²PS cell colonies were cultured under DMEM/LIF-MEFs or KODMEM/2i/LIF-gelatin conditions. Scale bar represents 50 µm.* ***(b)*** *i²PS cells were microinjected in C57BL/6 embryos at the blastocyst stage (3.5 dpc).* ***(c)*** *Genotype of the MHC Class I antigen in mice generated from the injection of i²PS cells cultured under DMEM/LIF-MEFs conditions (H2-Kb – C57BL/6 and H2-Kd – BALB/c).* ***(d)*** *Images of mouse 7 and 8, which showed i²PS cell contribution as indicated by the presence of the H2-Kd gene, but not evidenced in the fur coat colour.* ***(e)*** *Contribution of i²PS cells to adult tissues of different developmental origins investigated by MHC Class I haplotype genotyping. Embryo injections and surrogate mother implantation were performed by the staff at the Transgenic Facility, University of Manchester (UK).*

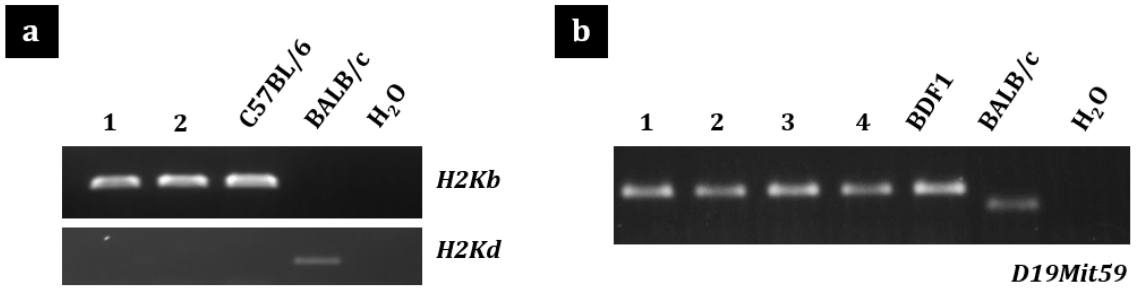

Figure 3. 18. i²PS cell contribution in adult mice obtained via morula injection. (a) *i²PS cells cultured under DMEM/LIF-MEFs conditions were microinjected in C57BL/6 morulas (2.5 dpc) and transplanted to surrogate mothers. i²PS contribution to the offspring was assessed via MHC Class I antigen genotype.* ***(b)*** *i²PS cells cultured under KODMEM/2i/LIF-gelatin conditions were microinjected in BDF1 morulas (2.5 dpc) and transplanted to surrogate mothers. i²PS contribution to the offspring was assessed via D19Mit59 satellite DNA genotype. Embryo injections and surrogate mother implantation were performed by the staff at the Transgenic Facility, University of Manchester (UK).*

A summary of the conditions and results obtained in the various chimerism experiments described here can be found on **Table 3.1**. In spite of the low efficiency and poor offspring viability in the generation of chimeras, this study proved that i²PS cells are fully functionally pluripotent in the *in vivo* scenario that most closely resembles natural development.

Condition	*Passage No.*	*No. cells/embryo*	*No. embryos injected*	*No. mothers implanted*	*No. viable adults*	*No. chimeric adult mice*
DMEM/LIF MEFs	P13	5-8	22 (blastocyst) C57BL/6	2	11	2
KODMEM/2i/LIF Gelatin	P13	15-20	46 (blastocyst) C57BL/6	3	0	0
DMEM/LIF MEFs	P13	5-8	65 (morula) C57BL/6	4	2	0
KODMEM/2i/LIF Gelatin	P13	5-8	135 (morula) BDF1	7	4	0

Table 3. 1. Conditions, injections and outcomes in chimerism experiments.

3.3.2.4. Investigation of transgene integration.

Transgene integration in the genome is one of the main concerns surrounding the generation of iPS cells, since disruptions in the host's genome (insertional mutagenesis) or the permanent integration of oncogenic reprogramming factors can trigger tumourigenesis [194]. The use of naked pDNA does not involve as high a risk of genomic integration as other reprogramming technologies, one of the most problematic being the use of retroviral vectors [120]. However, occasional integration of the pDNA cassette or regions of it may still occur and has indeed been reported by others [107, 108, 183]. It was therefore our aim to investigate the integrity of the genome of i^{2}PS cells with a focus on pDNA integration.

PCR-based study of genomic integration

Genomic DNA (gDNA) was extracted from i^{2}PS cells and a set of specific primers was used to amplify 11 distinct regions of the reprogramming pDNA used in their generation **(OKS+M)**. The location of such regions in the pDNA cassettes is shown in **Figure 3.19a**. A mixture of **OKS+M** pDNA was included as positive control to detect the presence of the transgenes, while gDNA extracted from E14TG2a cells was used as positive control for the amplification of the endogenous loci and negative control for the transgenes. PCR products were run in an agarose gel and differences in size were used to discern between transgenes and endogenous loci, when these existed. Signs of genomic integration were only found for c-Myc transgene in one out of four i^{2}PS samples screened, as deduced from the appearance of a band the same size as that of the pDNA control **(Figure 3.19b)**. Integration of other pDNA regions investigated in this study was not suggested from these data.

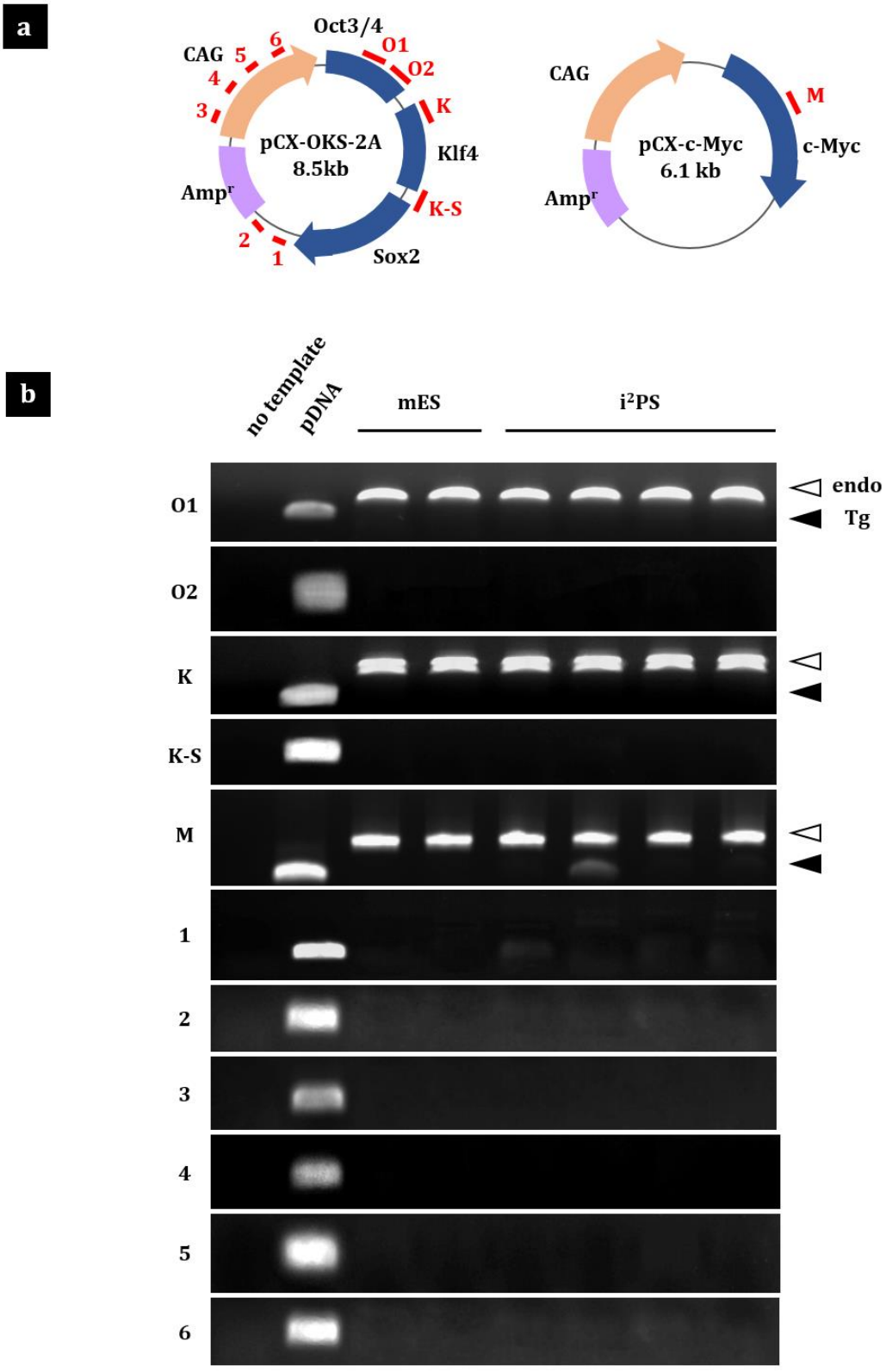

Figure 3. 19. PCR screening of pDNA integration in the genome. ***(a)*** *Location of the 11 regions amplified in OKS and M pDNA cassettes to assess their integration in the genome;* ***(b)*** *A mixture of OKS+M was included as positive control for the presence of the transgenes, while gDNA from E14TG2a mES cells (n=2) was included as negative control for the transgene and positive for the endogenous loci. i²PS cell gDNA (n=4) was amplified in independent PCR reactions for the specified regions and the products were separated by agarose gel electrophoresis. When primers amplified both the endogenous locus and the transgene, open arrowheads indicate bands corresponding to the endogenous locus while closed arrowheads indicate bands derived from the transgene. Biological replicates are numbered 1-2 for E14TG2a and 1-4 for i²PS cells.*

Southern Blot study of genomic integration

To confirm the above observations, gDNA from i²PS cells was analysed by Southern Blot using digoxigenin (DIG)-labelled probes against Oct3/4, Sox2, Klf4 and c-Myc. As in the previous study, gDNA from E14TG2a cells was used to identify the hybridisation with the endogenous genes while a mixture of **OKS+M** pDNA served to detect the bands corresponding to the transgenes. As expected, endogenous genes were detected in all i²PS cell clones screened. No signs of integration were detected when Oct3/4 and Sox2 probes were investigated **(Figure 3.20a and b)**, but bands corresponding to the Klf4 transgene were found in 2 of the samples tested **(Figure 3.20c)**. In agreement with the PCR study, one of the i²PS cell samples suggested c-Myc integration **(Figure 3.20d)**.

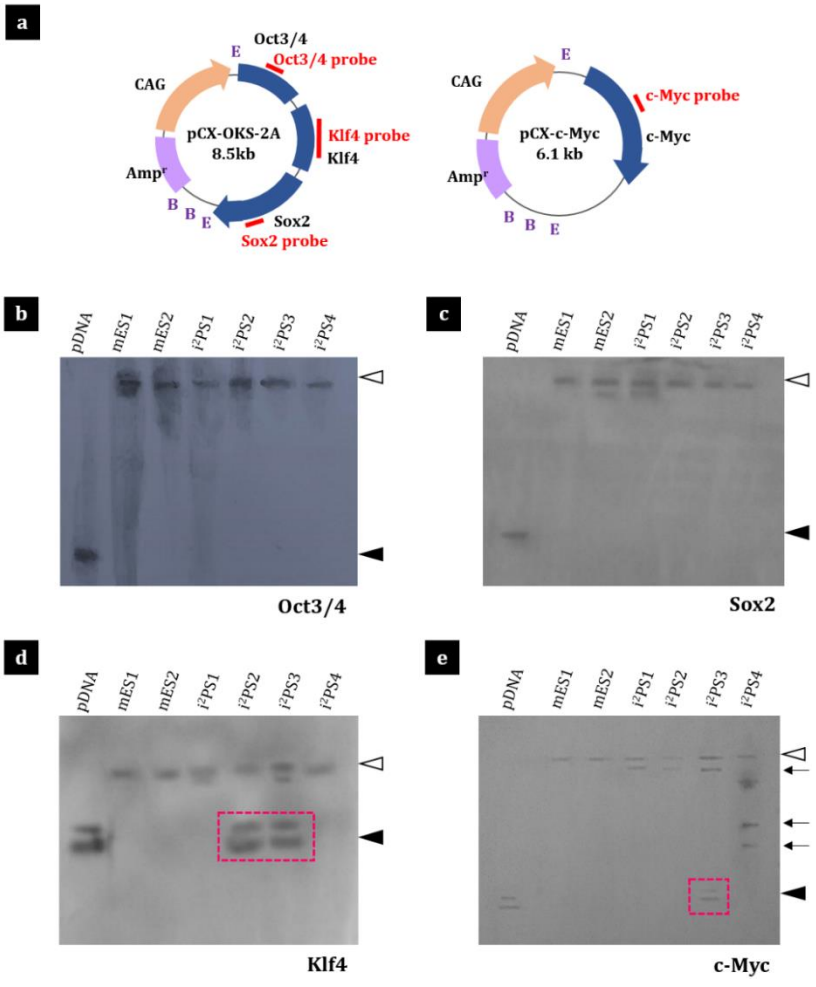

Figure 3. 20. Southern blot investigation of pDNA integration. *gDNA extracted from E14TG2a (n=2) and i²PS (n=4) cells was digested with EcoRI and BamHI restriction enzymes. A mixture of OKS and M pDNA was used as control.* ***(a)*** *Location of probes and restriction sites in the pDNA cassettes. (E, EcoRI; B, BamHI). DIG-labelled probes were used to detect the integration of* ***(b)*** *Oct3/4,* ***(c)*** *Sox2,* ***(d)*** *Klf4 and* ***(e)*** *c-Myc. Closed arrowheads indicate bands derived from the transgenes, while open arrowheads indicate bands corresponding to the endogenous genes. Arrows indicate non-specific bands integrated in the genome. Biological replicates are numbered 1-2 for E14TG2a and 1-4 for i²PS cells.*

3.4. Discussion.

In spite of the numerous laboratories now dedicated to the cell reprogramming field, the vast majority of research has focused on reprogramming cells in the culture dish. It was not until 2012 that the first report of somatic cells reprogrammed to pluripotency *in vivo* was published by Vivien et al. using an amphibian model (pre-metamorphic tadpoles) [161]. The only report to date of *in vivo* reprogramming to pluripotency in an adult, mammalian, non-genetically modified organism (WT BALB/c mice) was published by Yilmazer et al. one year later [162, 163]. These two studies utilised the same reprogramming technology (naked pDNA) and, even if in very different organisms, obtained very similar findings. These included the efficient expression of reprogramming factors in the tissue upon administration of the reprogramming pDNA, which decreased over time, and the upregulation of otherwise repressed pluripotency genes while in the absence of teratoma formation. The greatest significance of both reports lays not only in the demonstration that somatic cells can be reprogrammed to pluripotency within live tissues - in spite of the pro-differentiation signals present in the *in vivo* microenvironment - but also in the fact that the pluripotent conversion was transient. These very relevant observations were confirmed in the present chapter.

In Yilmazer's work, liver cell reprogramming towards pluripotency was not only evidenced by the upregulation of pluripotency-related genes but also by the downregulation of hepatocyte-specific markers. Both changes occurred fast and transiently after injection and were induced via HTV administration of a combination of two reprogramming pDNA, **OKS**+**M**, encoding all four Yamanaka factors but with c-Myc in a separate cassette. We demonstrated here that the same gene expression changes were induced by the administration of similar transgene copy numbers in a single polycystronic vector encoding all factors in the same cassette, **OKSM (Figure 3.1).** A 24-day long gene expression study following HTV administration of this pDNA confirmed Yilmazer's previous observations that the shift of the gene expression profile towards pluripotency was sustained for less than a week after injection **(Figure 3.2)**. The observations at the mRNA level agreed with the expression of the protein. Cells expressing pluripotency markers were detected within the liver tissue 2 days after injection, regardless of the pDNA

vector used **(Figure 3.4),** but could not be observed any later than day 4 (data not shown).

In fact, all the studies presented in this chapter, involving different combinations of reprogramming pDNA and administration schemes, came to reaffirm the fast kinetics and short duration of the pluripotency induction **(Figures 3.2, 3.4 and 3.5)**. We attribute this finding to the non-sustained expression of reprogramming factors provided by the use of a minimally integrative vector (pDNA) **(Figures 3.2, 3.19 and 3.20)** and the fact that the reprogrammed cells reside within the liver microenvironment, where they are exposed to pro-differentiation signals. We also propose that the transient duration of the pluripotency induction together with the fact that only a small percentage of cells are reprogrammed to pluripotency (5-15% of the total hepatocyte population [162]), account for the absence of tumourigenesis in the reprogrammed tissues in both Vivien's and Yilmazer's reports [161, 162]. Although we did not perform here a systematic histological study to assess the appearance of teratomas, none of the mice included in the long term study in this chapter **(Figure 3.2)** showed signs of disease or weight loss, nor did we find any visible tumour mass or dysplastic lesion when the liver tissues were dissected and processed for the different studies. We recorded no deaths prior to the conclusion of the study.

Two more recent reports by Abad et al. [195] and Ohnishi et al. [196] have not only confirmed the feasibility to reprogram cells to pluripotency *in vivo*, but also reinforced the hypotheses above. Unlike Vivien's, and Yilmazer's studies (and its continuation, presented here), which relied on a single administration of naked pDNA targeted to a particular tissue, Abad and Ohnishi used a genetically modified (GM) "reprogrammable" mouse strain in which the Yamanaka factors were inserted in the genome and their expression was induced upon the administration of doxycycline [195, 196]. While the use of naked pDNA that minimally integrated in the genome **(Figures 3.19 and 3.20)** resulted in expression of reprogramming factors that decreased over time **(Figures 3.2 and 3.5)**, this GM model allowed to sustain the expression of Yamanaka factors for as long as the drug was administered. In addition, the expression of such factors was widespread in the organism of the mice, due to the ubiquitous presence of the genetic modification. Like ours, both studies using the reprogrammable mouse confirmed the correlation of the expression of pluripotency markers with the loss of cell-type

specific markers in the reprogrammed tissues. However, this event resulted, in their studies, in the emergence of teratomas. Prolonged administration of doxycycline triggered widespread tumourigenesis and high mortality among *in vivo* reprogrammed mice in both reports. Importantly, Abad *et al* observed that higher doses of the drug administered for shorter periods of time generated significantly less teratomas than the administration of lower doses for longer periods, indicating that the duration of the OKSM expression might be more relevant for the fate of the reprogrammed cells than the expression levels themselves [195]. In agreement with this observation, Ohnishi *et al* reported that when the expression of reprogramming factors was switched off via doxycycline withdrawal after 5 days, no dysplastic lesions were observed in many of the mice. When doxycycline was withdrawn at even slightly later time points (day 7), the dysplastic lesions reverted to normal phenotype - the cells entered proliferation but did not progress to carcinogenesis – and were integrated in the tissue preserving their normal function [196].

The most relevant conclusion inferred from all *in vivo* reprogramming to pluripotency studies reported so far is thus the correlation between the duration of the expression of reprogramming factors (and hence the pluripotent conversion) with the appearance of teratomas [161, 162, 195, 196]. We have proposed that opposite de-differentiation signals (from the expression of reprogramming factors) and pro-differentiation signals (provided by the microenvironment) coexist *in vivo*. When the expression of reprogramming factors is not sustained over time, the tissue microenvironment might rapidly drive the re-differentiation of the pluripotent intermediates preventing teratoma formation [164]. Whatever the mechanisms behind, the above observations position the transient pluripotent conversion achieved by administration of naked reprogramming pDNA in a favoured position to progress towards clinical translation.

We have provided here other valuable information regarding the induction of pluripotency in mouse liver via HTV administration of reprogramming pDNA. The capacity to induce such cell fate conversion without the oncogenic c-Myc could facilitate its clinical translation [53]. Previous *in vitro* studies reported slower and less efficient iPS cell generation when c-Myc was not present [56]. In agreement with those reports, our results showed that lower expression of pluripotency

markers **(Figure 3.3b)** and higher mRNA levels of hepatocyte-specific genes were obtained when reprogramming was induced in the absence of c-Myc **(Figure 3.3c)**. However, this did not prevent the expression of proteins characteristic of the pluripotent state in cells within the liver tissue **(Figure 3.4)**. Especially because we lacked a quantitative study of protein expression, we preferred to maintain all factors in the reprogramming cocktail for the rest of the studies, based on the better gene expression results and to ensure maximum reprogramming effect. Nevertheless, the induction of pluripotency *in vivo* without c-Myc should be explored further as this technology advances towards the clinical scenario. Repeated HTV administration of reprogramming pDNA was also tested to confirm whether a higher upregulation of pluripotency markers and downregulation of tissue specific genes could be achieved in the mouse liver. As anticipated from a previous study [168], a second HTV administration of pDNA was able to restore the decreasing expression of reprogramming factors **(Figure 3.5a)**. However, this did not trigger any differences in the expression of pluripotency and hepatocyte-specific genes compared to the single injection protocol **(Figures 3.5b and 3.5c)**. We decided to administer the second pDNA dose 3 days after the first injection, since at this point the liver has started to recover from the damage derived from the first administration (according to the observations by Yilmazer et al. [162] and others [168]) and transgene expression has started to decrease but not yet plummeted. Considering our lack of success in enhancing the reprogramming effect with this protocol, other time frames for the second HTV injection could be considered in the future.

We noticed that the mRNA values of the pluripotency markers *Nanog* and *Rex1* were - in some, but not all experiments - relatively elevated in the saline-injected controls when analysed 2 days after injection. This masked the upregulation of such genes in the pDNA-injected groups after normalisation (for examples of this see, **Figure 3.1b,** day 2 data). *Nanog* and *Rex1* were in fact significantly upregulated when we compared hepatocyte gene expression in saline-injected animals to uninjected controls **(Figure 3.6b)**. Other pluripotency-related genes, including those encoded in the reprogramming pDNA, were also upregulated **(Figure 3.6a)**. However, the mRNA values detected in the saline group were not as high as those of *Nanog* and *Rex1,* which can explain why their expression in pDNA-injected groups was never masked. We attributed these effects

to the mild liver damage inherent to HTV administration, which is known to peak on day 2 after injection, precisely the time point when we found expression of pluripotency-related genes in the controls, and is resolved rapidly afterwards [162, 168]. In fact, increased expression of several pluripotency markers, including *Nanog* and *Rex1,* as a result of liver insult had been reported by others and attributed to their roles in hepatocyte proliferation and regeneration after injury [184]. On the other hand, we found no downregulation of hepatocyte-specific markers – a characteristic finding reproducibly observed upon *in vivo* reprogramming to pluripotency - as a consequence of the injection **(Figure 3.6c)**. *Aat* and *Trf* were in fact significantly upregulated compared to the uninjected controls, which might be a consequence of the hepatocyte proliferation after the mild injury. Importantly, these results confirmed that the expression of pluripotency genes triggered by the HTV injection procedure is most likely linked to regeneration mechanisms and definitely not to genuine reprogramming, and did not lead to de-differentiation of the cells. The variability in the expression of pluripotency genes in the saline controls in different experiments might be due to technical differences in the execution of the HTV injection, even though volume and time of injection were kept constant precisely to minimise such problem. These results were very relevant to confirm that the reprogramming effect observed in the tissue upon HTV administration of reprogramming pDNA was genuinely credited to the transfected Yamanaka factors.

Changes in the gene expression profile of the tissue, together with the identification of cells expressing pluripotency markers **(Figure 3.4),** suggested the presence of *in vivo* reprogrammed cells within the liver tissue in the pDNA-injected groups. However, those findings were not enough to proof whether such cells had been fully reprogrammed into *bona fide* pluripotent cells. We demonstrated here that *in vivo* reprogrammed cells are functionally pluripotent and able to differentiate into representatives of all three lineages in different scenarios.

The pluripotency of i^{2}PS cells, generated from the culture of whole hepatocyte extracts from **OKS**+**M**-injected mice, was anticipated by their capacity to self-renew and proliferate in colonies morphologically very similar to those of E14TG2a mES cells **(Figures 3.8a and 3.8b)**. Importantly, we have provided here several pieces of evidence, generated in different studies, which prove that such cells originated from genuine reprogramming and not as a result of cross-

contamination with the mES cells handled in our laboratory (E14TG2A). First, their genome-wide gene expression profile was clearly distinguishable when hierarchical cluster analysis was performed **(Figure 3.9b)**. Secondly, the BALB/c origin of i²PS cells was confirmed by the presence of the H2-Kd haplotype in the chimeric mice obtained via blastocyst injection **(Figure 3.17)**, which differed from that of E14TG2A cells (129/Ola mice background, H2-Kb haplotype). Finally, the fact that Klf4 and c-Myc transgenes were integrated in some of the i²PS cell samples analysed also confirmed their reprogrammed cell origin **(Figures 3.19 and 3.20)**. In addition, since such colonies did not appear in the cultures from saline-injected mice, their generation was attributed to the presence of *in vivo* reprogrammed cells in the hepatocyte extract of the pDNA-injected animals and not to the effects of the *in vitro* culture conditions (i.e. presence of LIF to sustain pluripotency) **(Figure 3.7)**. It was also confirmed that i²PS cells share numerous similarities at the molecular level with other pluripotent cells. Similar expression of pluripotency markers to that of E14TG2a cells was evidenced at the mRNA level by real-time RT-qPCR **(Figure 3.8)** and DNA microarray **(Figure 3.9c),** and at the protein level by IHC **(Figure 3.13)**. Even the whole transcriptome of the two cell lines was considerably similar **(Figure 3.9a-b)**, in spite of their very different origin: i²PS cells were generated from *in vivo* reprogrammed BALB/c mice hepatocytes, whereas E14TG12a cells were derived from the ICM of 129/Ola mouse blastocysts. Microarray analysis of the expression of 123 genes involved in endoderm development and 10 genes specific to hepatocyte differentiation did not suggest any significant differences between the two cell lines **(Figures 3.10 and 3.11)**, although real-time RT-qPCR analysis did determined a 10-fold upregulation of the endoderm-specific marker *Afp* in i²PS compared to E14TG2a cells **(Figure 3.8d)**. These findings suggested that in parallel with the acquisition of a gene expression profile characteristic of the undifferentiated pluripotent state, the gene expression signature of the hepatocyte had been lost to a certain extent. Together with the fact that genes involved in ectoderm and mesoderm development showed also very similar expression to that found E14TG2a cells **(Figure 3.10)**, these observations suggested that i²PS cells would have the potential to differentiate towards any of the three developmental lineages. However, whether such cells still retain epigenetic memory from the tissue of origin which could drive preferential differentiation towards endoderm lineages remains to be determined.

Nevertheless, the tri-lineage potential of i²PS cells was confirmed at the functional level when such cells were left to differentiate spontaneously- without the aid of any growth factor – and generated cells and tissues from all three germ layers. Such finding held both in the *in vitro* – embryoid bodies assay **(Figure 3.15)** - and *in vivo* setting – teratoma assay **(Figure 3.16)** and generation of chimeras **(Figure 3.17)**.

Of particular relevance was the observation that *in vivo* reprogrammed cells generated teratomas containing tissues from all three germ layers, not only when cultured as i²PS cells but also when directly isolated from the liver and without undergoing any *in vitro* culturing. On the one hand, this ruled out the possibility that the cells had been partially reprogrammed *in vivo* but only acquired functional pluripotency features thanks to the components of the culture medium, which were tailored to support pluripotency (i.e. presence of LIF). In addition, the fact that *in vivo* reprogrammed cells were able to form teratomas when transplanted to a different host contrasted with Yilmazer's findings related to the absence of tumourigenesis when such cells were left to reside in their native microenvironment (i.e. liver), even for prolonged periods of time (120 days). This different behaviour might be explained by the pro-differentiation signals in the tissue microenvironment that, as we have hypothetised before [164], would be able to drive the re-differentiation of the cells to an appropriate phenotype. More studies will however be necessary to further elucidate the prevailing mechanisms, interactions and cues present in the *in vivo* microenvironment that might govern this process. In addition, it should be noted that nude mice were used for the teratoma assay. Future work will have to address the role of the immune system towards the *in vivo* reprogrammed cells.

The modest results in the generation of chimeric mice from BALB/c i²PS cells **(Table 3.1)** agreed with previous studies reporting the many challenges to first derive mES cells from BALB/c blastocysts and then generate chimeric mice with them. The efficiency of chimera generation achieved with this background was significantly lower as compared to that from other mice strains and BALB/c contribution to the fur coat and germline of such chimeras was also very poor [197-199]. Many factors other than the genetic background of the mice can also dramatically influence the generation of chimeras and might have posed an effect in our experiments. Among them, technical aspects of the microinjection [200],

culturing conditions[201], chromosomal abnormalities [202, 203], length of the telomeres [204] and epigenetic signatures present in the injected cells [199] play a crucial role and should be thoroughly investigated for i²PS cells if higher efficiency and BALB/c contribution were sought. Nevertheless, and although transmission to the germline remains to be demonstrated, the widespread contribution of i²PS cells to numerous tissues of diverse developmental origin in the adult chimeric mice **(Figure 3.17e)** further proved the functional pluripotency of i²PS cells and the lack of predisposition to differentiate into a particular lineage in detriment of the others.

Further relevant observations related to the full pluripotent character of i²PS cells were that (a) they did not need to be exposed to 2i conditions in order to generate chimeras and (b) the expression of pluripotency genes such as *Nanog* and *Rex1* was comparable – even slightly upregulated – to that of mES cells and did not increase dramatically upon exposure to such dual inhibition **(Figures 3.8c and 3.15-a-b)**. In the opposite scenario, other reports have shown that partially reprogrammed cells expressed very low mRNA levels of *Nanog* and *Rex1* and had to be exposed to 2i conditions for at least 10 days before the expression of such genes reached levels comparable to mES and the cells acquired the differentiation potential required to participate in the adult tissues of murine chimeras [119]. In spite of this very positive indications, more specific studies such as the investigation of the re-activation of the X-chromosome and the mono- or bi-allelic expression of *Nanog* should be carried out to fully confirm that i²PS cells have reach what has been denominated as "ground-state pluripotency" [205], which falls beyond the scope of this thesis.

None of the two chimeric mice or their progeny obtained in this study suffered from the development of tumours, as opposed to what has been described by others and attributed to the occurrence of insertional mutagenesis or the reactivation of *c-Myc* [53]. This outcome was therefore interpreted as a sign that not major genomic integration of the transgenes occurred in i²PS cells. However, and especially taking into account the very limited number of chimeric mice obtained, this was not enough proof of the genomic integrity of i²PS cells. Transfection with pDNA does not present as high a risk of insertional mutagenesis as other technologies such as the use of retroviral vectors, but there is still a possibility of genomic integration of the transgenes or regions of the pDNA

cassettes and hence we planned specific experiments to investigate this possibility [206]. We confirmed minor integration of two of the transgenes (Klf4 and c-Myc) by two different techniques (PCR and Southern Blot) **(Figures 3.19 and 3.20)**, although 2 out of 4 i^{2}PS cell samples screened were absolutely free from transgenes. Other studies employing the same pDNA cassettes to reprogram somatic cells *in vitro* have however shown a much higher degree of integration. Okita *et al* reported variable occurrence of such event depending on the transfection protocol used [107], the most efficient providing only 3 out of 15 integration-free clones. Remarkably, this protocol relied in the repeated transfection (4 times) of somatic cells with reprogramming pDNA [108]. Another study involving liposomal magnetofection with the same pDNA vectors accelerated and increased the efficiency of the pluripotent conversion, even reducing the number of transfection rounds required (2 transfections). However, only 2 out of the 7 iPS cell lines investigated were integration-free [183]. The lower degree of pDNA integration reported in our study might be due to the fact that a single *in vivo* transfection was needed to generate i^{2}PS cells. Although, this data should still be taken into consideration and non-integrating vectors should be designed if therapeutic interventions based in this approach are to be sought, it is also to mention that the culture protocol used to generate i^{2}PS cell might have selected and expanded the *in vivo* reprogrammed bearing higher degrees of integration. We have not investigated the genomic integrity of *in vivo* reprogrammed cells directly extracted from the tissue, mainly due to the challenges to sort this population from the rest of the cells in the liver. However, it could be possible that the proportion of cells showing integration of the pDNA in their genome was lower than among i^{2}PS cells. Yilmazer's observations regarding the absence of teratoma formation in the liver upon *in vivo* reprogramming [162] and our findings in the decrease of the expression of reprogramming factors over time after injection **(Figure 3.2)** support the hypothesis that the integration of the transgenes *in vivo* was marginal.

Overall, the studies presented in this Chapter confirmed that somatic cells can be reprogrammed to functional pluripotency *in vivo*, in spite of the pro-differentiation signals present in the tissue, and that transient expression of reprogramming factors is crucial to prevent the pluripotent conversion from generating teratomas. Functional pluripotency was acquired *in vivo*, and not as a result of favourable culture conditions. Finally, the establishment of the *in vivo*

reprogrammed cells as a cell line *in vitro* allowed their direct comparison to a standard mES cell line, hence providing further information on their molecular signature and differentiation potential, as well as genomic integrity.

Chapter IV.

In vivo reprogramming to pluripotency in mouse skeletal muscle.

4.1. Scope of Chapter IV.

In the previous Chapter, we explored the reprogramming of mouse liver cells to pluripotency *in vivo* via forced expression of Yamanaka factors. Following from a previous work [162], we confirmed that the pluripotent conversion happened rapidly and transiently - which precluded the generation of teratomas – and was manifested in the tissue by the upregulation of pluripotency markers and downregulation of tissue-specific genes. We confirmed that the reprogrammed cells formed colonies of self-renewing pluripotent cells (i^2PS cells) when cultured *in vitro* although, more importantly, functional pluripotency was already acquired in the *in vivo* microenvironment.

The combination of the four Yamanaka factors has been postulated as a virtually universal reprogramming cocktail, able to return a diverse range of differentiated cell types to the pluripotent state when transfected *in vitro* [60, 62, 207]. In this Chapter, we first sought to confirm whether such findings also hold when the pluripotent conversion takes place *in vivo.* With this aim, we tried to reproduce *in vivo* reprogramming to pluripotency in a tissue originated from a developmental lineage (mesoderm) entirely different from that of liver (endoderm), and in which pDNA can be efficiently expressed, such as the skeletal muscle. Secondly, we aimed to further investigate the fate of the reprogrammed cells *in vivo* in order to understand whether they would be able to reintegrate into the tissue or on the contrary, would not survive in a microenvironment which is not designed to support pluripotent cells.

4.2. Introduction.

We have previously hypothesised that reprogramming any somatic cell to pluripotency *in vivo* might be achievable provided that we are able to efficiently deliver the Yamanaka reprograming factors to the target tissue and cells [164]. The myofibers populating the skeletal muscle constitute a convenient target for gene delivery and its applications for a number of reasons. First, myofibers have been shown to spontaneously uptake naked pDNA [208]. In this particular tissue, such process has proven more efficient than the use of viral vectors to deliver nucleic acid cargos, with the added benefit of a significantly safer profile [209]. The exact

mechanism by which naked pDNA can enter myofibers has not yet been fully disclosed, however suggested hypotheses include an active uptake mechanism [210] and the use of the T tubule system [211]. Whatever the mechanism of uptake, the work led by John Wolff and colleagues in the early 90s showed that moderately high - albeit variable - levels of foreign gene expression can be achieved in muscle cells after intramuscular (i.m.) administration of pDNA [208]. In addition, the post-mitotic status of the myofibers provides a platform for stable transgene expression, even when a minimally integrating method such as naked pDNA is employed [212]. This has prompted the i.m. administration of pDNA in gene therapy strategies against muscle-related ailments and in DNA vaccinations. Overall, such tissue peculiarities make the skeletal muscle a favorable target to be transfected with reprogramming pDNA *in vivo*.

On the other hand and from the developmental and architectural point of view, the skeletal muscle is a very distinct tissue in the mammalian organism. The process of myogenesis is finely orchestrated by a series of changes in the expression of defined regulatory factors, as illustrated in **Figure 4.1**. In prenatal development, myogenesis starts when *Pax3*$^{+}$*Pax7*$^{+}$ myogenic progenitor cells initiate the expression of muscle determination factors (*Myf5*, *MyoD*, *Mrf4*, *Mef2c*) and commit to the myogenic lineage. The resulting cells, still undifferentiated, are known as myoblasts and eventually exit the cell cycle and fuse to each other forming syncytial myotubes. In such cells, which express *Mhy1* and *Myog*, the multiple nuclei are aligned in the centralised position. Finally, the mature myofiber is characterised by the migration of the nuclei to the periphery of the cells [213-215]. A very similar series of events takes place during postnatal growth and muscle regeneration after injury. In such scenarios, satellite cells – muscle specific stem cells that reside underneath the basal lamina adjacent to the myofiber and are normally quiescent – proliferate and differentiate into myoblasts which eventually fuse to and enlarge the existing myofibers in postnatal growth and are also able to form *de novo* fibers after injury [216, 217].

Precisely the lack of cell division and the presence of various nuclei in a single cell, position the myofibers as a more challenging cell type to reprogram in comparison to the more commonly used fibroblasts or the primary hepatocytes discussed in Chapter III. While myoblasts have been reprogrammed to pluripotency *in vitro* by forced expression of Yamanaka factors, generating iPS cells

[218], there is to our knowledge no proof that such cell fate conversion can be achieved in fully differentiated myofibers.

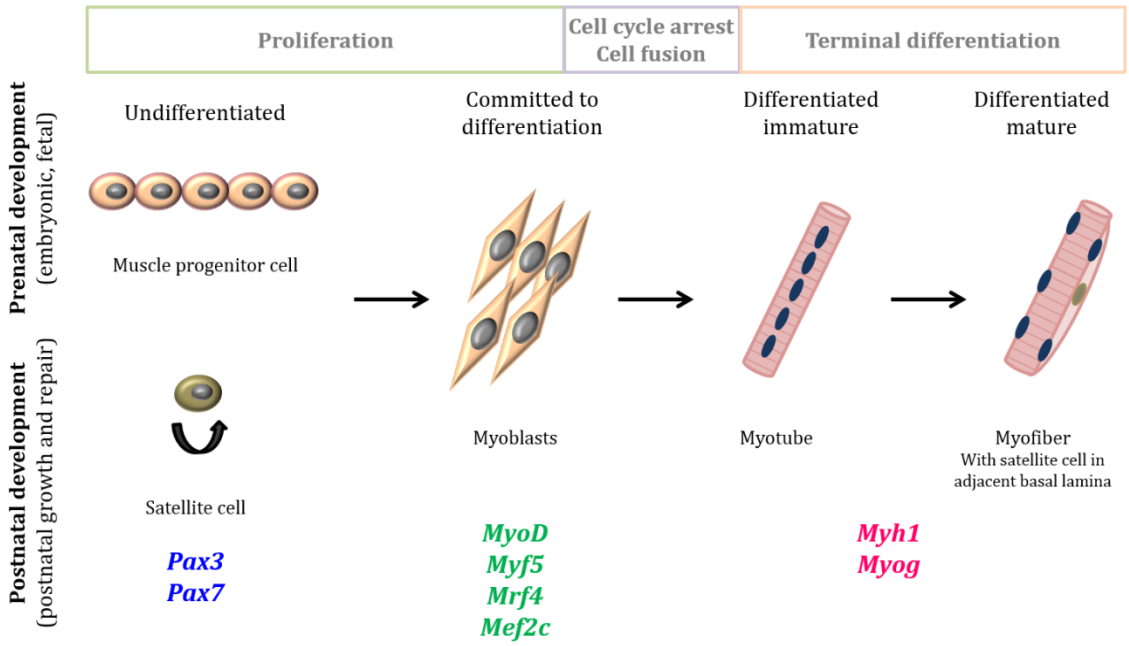

Figure 4. 1. Main cellular and gene expression events involved in myogenesis. *During normal development (pre- or postnatal) or as a part of a regenerative response to injury in the adult, muscle progenitors proliferate to then commit to the myogenic lineage as myoblasts, which exit the cell cycle and fuse into multinucleated myotubes. In fully differentiated mature myofibers, nuclei migrate to the periphery of the cell, while the satellite cells relocate underneath the adjacent basal lamina. This process is finely orchestrated by changes in gene expression illustrated here.*

Overall, we attempted here to achieve *in vivo* reprogramming to pluripotency in a different tissue that, although favorable in terms of exogenous gene expression, may be biologically more challenging to induce to the pluripotent state.

4.3. Materials and methods.

4.3.1. Materials used in Chapter IV.

4.3.1.1. Plasmid (pDNA) vectors.

Reprogramming pDNA pCX-OKS-2A (**OKS**, encoding Oct3/4, Klf4, Sox2), pCX-cMyc (**M**, encoding cMyc) and pLenti-lll-EF1α-mYamanaka (**OKSM**, encoding Oct3/4, Klf4, Sox2, cMyc and eGFP) were used in this study. A more detailed description of

the cassettes is provided in **Chapter III**, **Section 3.3.1.1**. pDNA maps are illustrated in **Figure S1.**

4.3.1.2. Mouse strains.

Female mice were used in this work that entered the procedures at 7 weeks of age, unless otherwise specified. BALB/c mice were purchased from Harlan, UK. C57BL/6 mice were obtained from Charles-River, UK. For the muscle reprogramming experiments in juvenile mice, a pregnant C57BL/6 mouse was obtained from the in house breeding facility at the University of Manchester. Juvenile mice entered the procedure 2 weeks after birth.

Sv129-Tg(Nanog-GFP) mice, which carry the *eGFP* reporter inserted into the *Nanog* locus [219], were a kind gift from the Wellcome Trust Centre for Stem Cell Research, University of Cambridge (UK) and bred and genotyped at the University of Manchester. This strain is also reported in the literature as TNG-A (Targeted Nanog GFP clone A), however for simplicity it will be referred to as Nanog-GFP in this thesis.

CBA-Tg(Pax3-GFP), in which *eGFP* replaces the *Pax3* coding sequence of exon 1[220], were kindly provided by Professor Giulio Cossu at the Faculty of Medical and Human Sciences, University of Manchester (UK). They will be referred to as Pax3-GFP for simplicity.

All experiments were performed with previous approval from the UK Home Office under a project license PPL 70/7763 and after allowing the mice to acclimatise to the facilities for one week.

4.3.2. Methodology involved in Chapter IV.

4.3.2.1. Intramuscular (i.m.) administration of reprogramming pDNA vectors.

Mice were anesthetised with isofluorane and the left gastrocnemius (GA) muscle was i.m. injected with 50 μg **OKSM**, 50 μg **OKS** and 50 μg **M**, or 50 μg **OKS** alone in 0.9% saline. Since it has been reported that larger volumes of injection favour higher and less variable gene expression levels upon i.m. administration of pDNA [221], injection volume was fixed to 50 μl, which corresponds to the maximum recommended for i.m. administration in mice. The contralateral (right) GA muscle

was injected with 50 µl 0.9% saline solution alone and used as internal control. In the studies were the internal control received no injection (intact muscle), this has been clearly stated. Mice were culled at different time points, including 2, 4, 8, 12, 24, 50 and 120 days after i.m. injection, as specified in each particular study.

4.3.2.2. RNA extraction and real-time Reverse-Transcription quantitative Polymerase Chain Reaction (RT-qPCR) analysis.

Aurum Fatty and Fibrous Kit (Bio-rad, UK) was used to isolate total RNA from whole GA muscles. RNA quantity and quality was assessed by UV spectrophotometry (BioPhotometer, Eppendorf, UK). cDNA synthesis from 1 µg of RNA sample was performed with iScript cDNA synthesis kit (Bio-Rad, UK) according to manufacturer's instructions. 2 µl of cDNA sample were used for each real-time qPCR reaction, performed with iQ SYBR Green Supermix (Bio-Rad, UK). Experimental duplicates of each sample were included and run on CFX-96 Real Time System (Bio-Rad, UK) with the following protocol: 95°C for 3 min, 1 cycle; 95°C for 10 sec, 60°C for 30 sec, – repeated for 40 cycles. *β-actin* was used as housekeeping gene and gene expression levels were normalised to saline-injected controls, unless otherwise specified. Livak's method was followed to analyse the data and dCt values were utilized for statistical analysis. Primer sequences used in this Chapter are listed in **Table S7**.

4.3.2.3. Preparation of muscle frozen sections for histological examinations.

GA muscles were dissected from the hind limb and immediately immersed into isopentane, pre-cooled in liquid nitrogen, for 20 s. Frozen muscles were stored at -80°C until further processing. 10 µm thick transverse sections were prepared on a Cryostat (Leica Microsystems, CM3050S) with the chamber temperature set at -24°C. Muscle tissue sections were air-dried for 1 h at RT and stored at -80°C until H&E, IHC or Tunel staining were performed.

4.3.2.4. Haematoxylin and Eosin (H&E) staining.

10 µm thick frozen sections obtained as described in **Section 4.3.2.3** were warmed at RT and H&E staining was performed following a standard protocol in an automated tissue stainer (Shandon Varistain 24-4).

4.3.2.5. Characterisation (IHC) of GFP$^+$ cell clusters in Nanog-GFP and Pax3-GFP muscle tissue sections.

Nanog-GFP (n=3) and Pax3-GFP (n=2) mice were i.m. administered in the left GA with 50 µl **OKS** and 50 µl **M** in 50 µl 0.9% saline. The right GA muscle was administered with the same volume of 0.9% saline, as control. Mice were sacrificed 2 or 4 days after injection and their GA muscles were processed as detailed in **Section 4.3.2.3**. To observe the GFP signal generated by *Nanog* or *Pax3* expression, tissue sections were mounted with ProLong® Gold anti-fade DAPI containing mountant (Life Technologies, UK) after fixation with methanol (pre-cooled at -20°C, 10 min) and imaged with 3D Histech Pannoramic 250 Flash slide scanner and Panoramic Viewer Software (100X). To investigate co-localisation of the GFP signal with the expression of different markers, tissue sections were processed for IHC. In brief, muscle sections were post-fixed with methanol (pre-cooled at -20°C, 10 min), air-dried for 15 min and finally washed twice with PBS for 5 min. Sections were then incubated for 1 h in blocking buffer (5% goat serum-0.1% Triton in PBS pH 7.3) at RT, followed by two washing steps with PBS (1 %BSA- 0.1% Triton, pH 7.3) and overnight incubation at +4°C with the primary antibody: Rabbit pAb anti-OCT4 (ab19857,3 µg/ml, Abcam, UK), rabbit pAb anti-NANOG (ab80892, 1 µg/ml, Abcam, UK), rabbit pAb anti-AP (ab95462, 1:200, Abcam, UK), mouse mAb anti-SSEA1 (ab16285, 20 µg/ml, Abcam, UK), rabbit pAb anti-Pax7 (pab0435, 1:200, Covalab, France), and rabbit mAb anti-PDGFrβ (#3169, 1:100, Cell Signalling). Anti-PDGFrβ were a kind gift from Prof. Cossu's lab (University of Manchester). The next day, sections were washed (2 min each) with PBS and incubated (1.5 h, RT) with the secondary antibody: goat pAb anti-rabbit IgG labeled with Cy3 or goat pAb anti-mouse IgG labeled with Cy5 (1/250, Jackson ImmunoResearch Laboratories). After two washes in PBS (5 min each), sections were mounted with ProLong® Gold anti-fade DAPI containing mountant (Life Technologies, UK). 100X images were obtained with a Leica TCS SP5 AOBS inverted confocal microscope.

4.3.2.6. BrdU labelling and detection of proliferating cells.

5-Bromo-2'-deoxyuridine (BrdU) assay was used to label proliferating cells *in vivo*, as previously described[222]. BALB/c mice (n=3) were intraperitoneally (i.p.) administered with 500mg/kg BrdU (B5002, Sigma, UK) in 1 ml 0.9% saline 18 h after i.m. injection with 50 µg **OKSM** or saline control. 6 h later, GA muscles were

dissected and processed for IHC as described in **Section 4.3.2.5**. Treatment with 2 N HCl (10 min at 37°C) after fixation of the sections was included to denature the DNA. Mouse mAb anti-BrdU (B8434, 1:100, Sigma, UK) and goat pAb anti-mouse IgG labeled with Cy5 (1/250, Jackson ImmunoResearch Laboratories) were used. 100X images were captured with a Leica TCS SP5 AOBS inverted confocal microscope.

4.3.2.7. Histological and morphometric evaluation of muscle tissue after i.m. administration of reprogramming pDNA.

The GA muscles of BALB/c mice (n=3) were dissected on days 2, 4, 8, 15, 50 and 120 after i.m. injection with 50 µg **OKSM** or 50 µl 0.9% saline (control) and processed for H&E staining following the procedures in **Sections 4.3.2.3** and **4.3.2.4**. Tissue sections were imaged with a 3D Histech Pannoramic 250 Flash slide scanner and representative images at 40X and 100X magnification were taken with Pannoramic Viewer software. The number of nuclei/mm^2 was counted with Histoquant Software in 12 sections per muscle and we observed 3 muscles per condition and time point. The minimum myofiber diameter and number of myofibers/cross-sectional area were analysed from 5 sections per muscle (3 muscles per condition and time point), with ImageJ 1.48 software.

4.3.2.8. TUNEL staining.

The GA muscles of BALB/c mice (n=3) were i.m. administered with 50 µg **OKSM** or 50 µl 0.9% saline (control) and dissected 2, 4 and 8 days after injection. 10 µm thick frozen tissue sections were obtained as detailed in **Section 4.3.2.3** and stained with DeadEnd Colorimetric TUNEL Assay kit (Promega, G7130, UK) according to manufacturer's specifications. In brief, sections were fixed with 4% PFA for 15 min at RT and permeabilised with Proteinase K (20µg/ml, 15 min, 37°C). Tissue sections were then incubated with TUNEL reaction mixture containing recombinant terminal deoxynucleotidyl transferase (rTdT) and biotinylated nucleotide (1 h, 37°C). After several washes in 20X SSC and PBS, slides were blocked with 0.3% hydrogen peroxide in PBS for 5 min and incubated with horseradish peroxidise-labelled streptavidin (Streptavidin-HRP) antibody diluted 1:500 in PBS. Reaction with diaminobenzidine (DAB) was observed by light

microscopy (Leica, UK) and representative images were taken at 40X magnification.

4.3.2.9. Desmin/laminin/DAPI staining.

The GA muscles of BALB/c mice (n=3) were dissected on days 2, 4, 8, 15, 50 and 120 after i.m. injection with 50 μg **OKSM** or 50 μl 0.9% saline (control) and processed for IHC staining following the procedures in **Sections 4.3.2.3** and **4.3.2.5**. Rabbit pAb anti-laminin (ab11575, 1:200, Abcam, UK) and mouse mAb anti-desmin (ab6322, 1:200, Abcam, UK) were used as primary antibodies. Goat pAb anti-rabbit IgG labeled with Cy3 and goat pAb anti-mouse IgG labeled with Cy5 (1/250, Jackson ImmunoResearch Laboratories Inc) were used as secondary antibodies. 40X images were obtained with a Zeiss Axio Observer epi-Fluorescence microscope.

4.3.3. Statistical analysis.

N numbers were specified for each particular study. Statistical analysis was performed first by Levene's test to assess homogeneity of variance. When no significant differences were found in the variances of the different groups, statistical analysis was continued by one-way ANOVA and Tukey's post-hoc test. When variances were unequal, the analysis was followed with Welch ANOVA and Games-Howell's post-hoc test. Probability values <0.05 were regarded as significant. SPSS software version 20.0 was used to perform this analysis.

4.4. Results.

4.4.1. Gene expression in mouse skeletal muscle after i.m. administration of reprogramming pDNA.

C57BL/6 mice were i.m. administered in the left GA muscle with either 50 μg **OKSM (Figure 4.2a)** or 50 μg **OKS** and 50 μg **M (Figure 4.3a)** reprogramming pDNA. The contralateral GA muscle was injected with 0.9% saline alone, as internal control. It has been reported that larger volumes of injection favour higher and less variable transgene expression levels upon i.m. administration of pDNA [221]. Hence, injection volume was fixed to 50 μl in all the studies on adult mice in this Chapter, which corresponds to the maximum recommended for i.m. administration in mice. Gene expression was studied in GA muscles dissected 2 days after injection and similar results were obtained, regardless of the combination of reprogramming pDNA used. In brief, successful expression of the transgenes encoded in the reprogramming pDNA **(Figures 4.2b and 4.3b)** was accompanied by the upregulation of endogenous pluripotency markers **(Figures 4.2c and 4.3c)**. Next, the expression of three markers, each of them related to a different stage during myogenesis, was investigated **(Figures 4.2d and 4.3d)**. A 10-fold upregulation of *Pax3* - which is distinctly expressed in myogenic progenitors but downregulated with differentiation [223] - was found in the groups i.m. administered with reprogramming pDNA, compared to the saline controls. On the contrary, the committed myoblast marker *MyoD* was downregulated upon injection of any of the reprogramming pDNA combinations. Finally, mRNA levels of *Myh1*, a marker of differentiated myofibers [213], did not show significant differences between saline and pDNA injected animals.

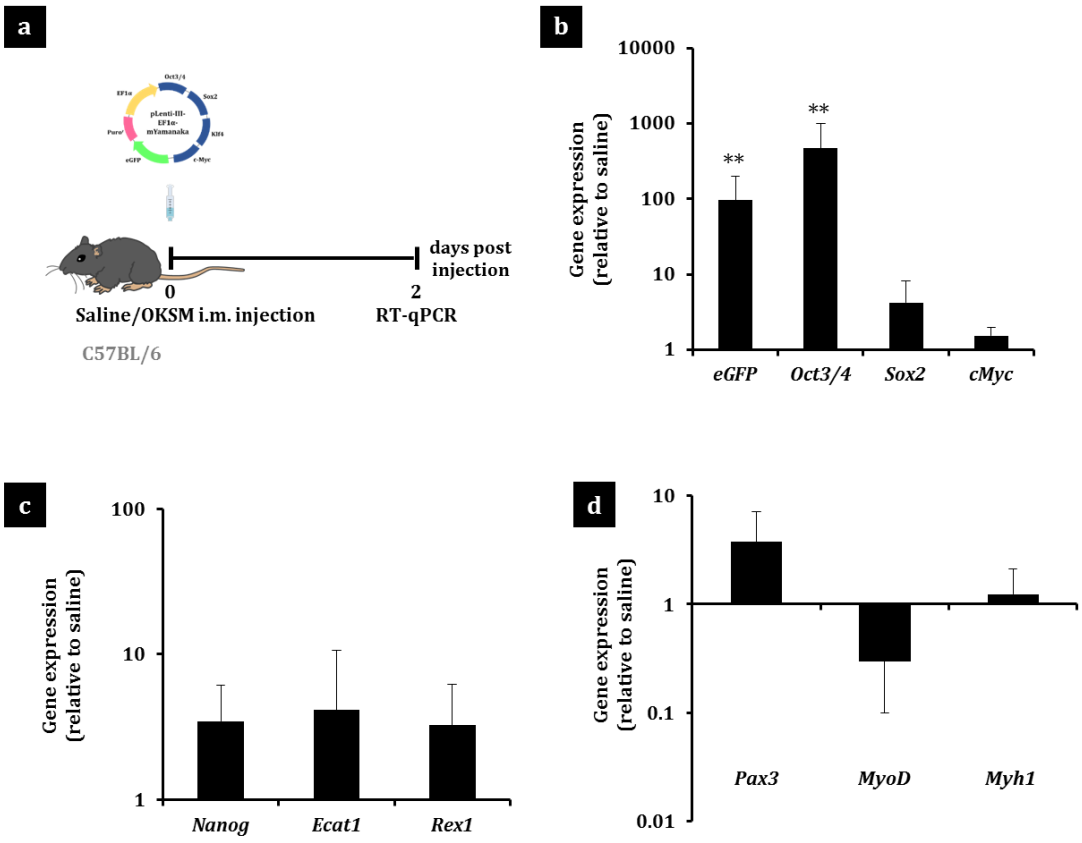

Figure 4. 2. Gene expression in C57BL/6 mouse skeletal muscle after i.m. administration of OKSM reprogramming pDNA. ***(a)*** *C57BL/6 mice were i.m. injected in the GA muscle with 50µg OKSM in 50 µl 0.9% saline or 50 µl 0.9% saline alone. GA muscles were dissected 2 days after injection and real-time RT-qPCR was performed to determine the relative gene expression of* ***(b)*** *reprogramming factors,* ***(c)*** *endogenous pluripotency markers and* ***(d)*** *genes involved in myogenesis. Gene expression levels were normalised to the saline-injected controls. **p<0.01 indicates statistically significant differences in gene expression between pDNA and saline-injected groups, assessed by one-way ANOVA. Data are presented as mean ± SD, n=3.*

Overall - and similar to our observations in liver tissue - the expression of otherwise repressed pluripotency genes (*Nanog*, *Ecat1*, *Rex1*) and of a muscle early progenitor marker (*Pax3*), together with the downregulation of a marker characteristic of a later stage in myogenesis (*MyoD*), suggested the de-differentiation of a subset of cells in the injected GA muscle. Interestingly, the same changes in gene expression were observed when the study was reproduced on a different WT mouse strain (BALB/c mice, **Figure S3**) confirming the reproducibility of this effect across mouse strains.

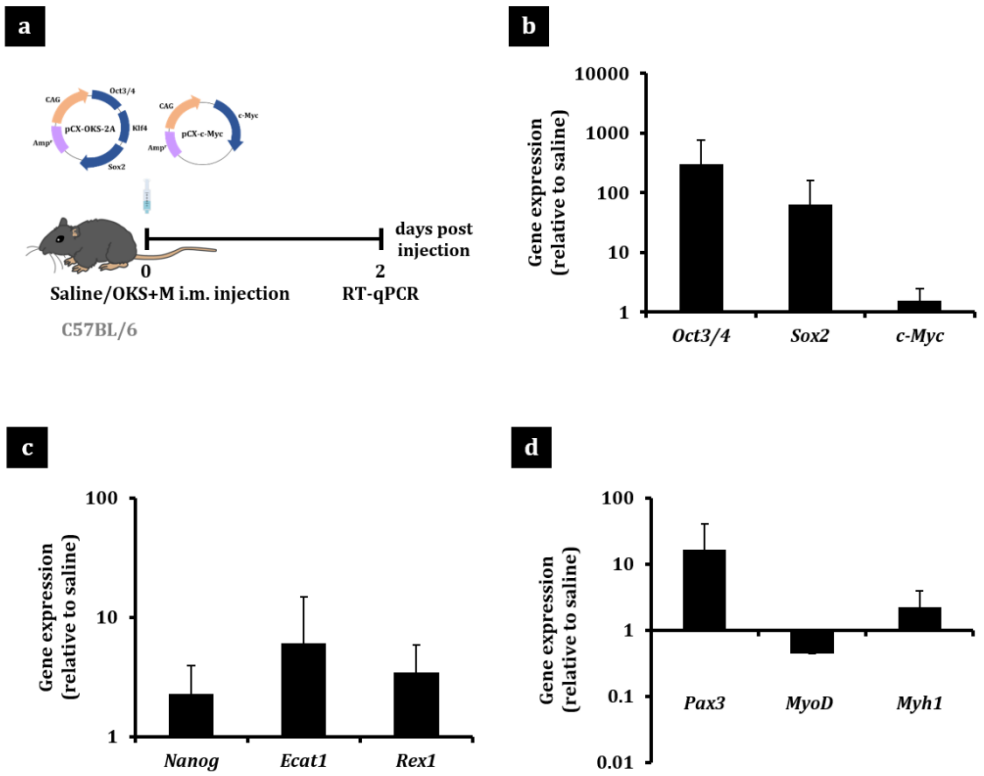

Figure 4. 3. Gene expression in C57BL/6 mouse skeletal muscle after i.m. administration of OKS and M reprogramming pDNA. (a) *C57BL/6 mice were i.m. injected with 50μg OKS and 50 μg M in 50 μl 0.9% saline or 50 μl 0.9% saline alone. GA muscles were dissected 2 days after injection and real-time RT-qPCR was performed to determine the relative gene expression of* ***(b)*** *reprogramming factors,* ***(c)*** *endogenous pluripotency markers and* ***(d)*** *genes involved in myogenesis. Gene expression levels were normalised to the saline-injected group. Data are presented as mean ± SD, n=3.*

Next, in order to interrogate whether the minor trauma provoked by the i.m. injection itself had any effect on the expression of the genes of interest, mRNA levels of pluripotency and myogenesis-related genes were compared in saline-injected and uninjected GA muscles. Expression of the reprogramming factors encoded in the pDNA used in the study, *Oct3/4*, *Sox2* and *c-Myc,* was also investigated because the endogenous genes have roles in pluripotency. **Figure 4.4** shows that no significant differences in the expression of such genes were observed between the two groups. This diverged from what we observed in the hepatocyte gene expression profile after HTV administration with saline solution, where both pluripotency and hepatocyte-specific markers appeared upregulated **(Chapter III, Figure 3.7)**. These differences are most probably due to the fact that the injury caused upon HTV injection, albeit still mild, is more severe than that produced by i.m. administration; thus expected to trigger a more apparent activation of regenerative mechanisms, which involve the genes investigated in our study.

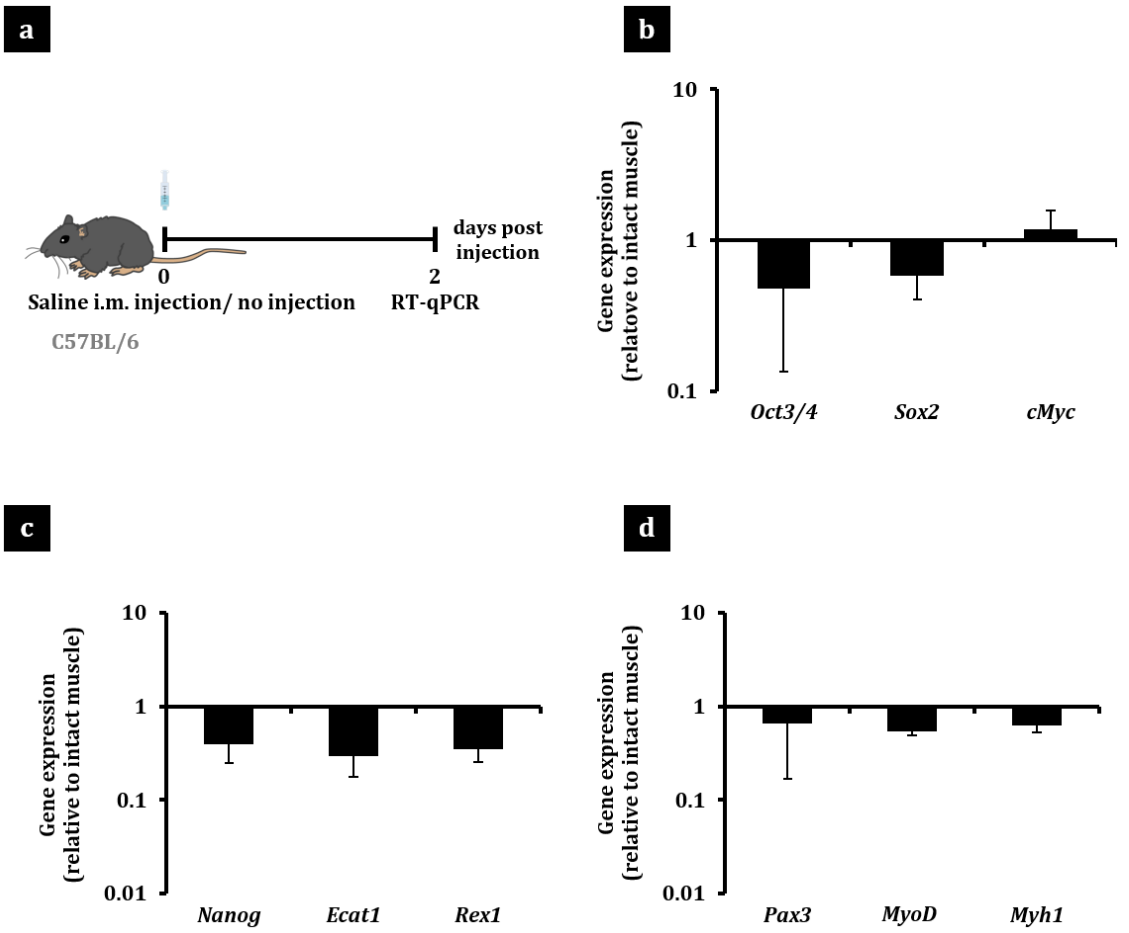

Figure 4. 4. Effects of i.m. injection on the expression of reprogramming, pluripotency and myogenesis-related genes. (a) *C57BL/6 mice were i.m. injected in the GA muscle with 50 µl 0.9% saline or left uninjected. GA muscles were dissected 2 days after injection and real-time RT-qPCR was performed to determine the relative gene expression of* ***(b)*** *reprogramming factors,* ***(c)*** *endogenous pluripotency genes and* ***(d)*** *genes involved in myogenesis. Gene expression levels were normalised to the uninjected (intact) group. Data are presented as mean ± SD, n=3.*

4.4.2. Gene expression in juvenile mouse skeletal muscle after i.m. administration of reprogramming pDNA.

It was also of our interest to determine whether i.m. injection of reprogramming pDNA in younger animals would provide different outcomes at the gene expression level. We chose to repeat the study in 2-week-old C57BL/6 mice since at this post-natal stage highest levels of transgene expression after i.m. administration of naked pDNA have previously been achieved [224]. In addition, the observation that progenitor cells are more amenable to reprogramming than their differentiated counterparts – shown for several cell types [225-227], including muscle cells [228] - together with the fact that the percentage of such cells is significantly larger soon after birth [229], suggested that a higher reprogramming effect could be achieved in juvenile mice. We administered the

same doses as in previous experiments (50 µg) of either **OKSM** or **OKS+M** in the GA muscle of 2-week-old C57BL/6 mice, although injection volume was reduced in accordance to the smaller size of the hind limb muscles, and studied gene expression 2 days after injection.

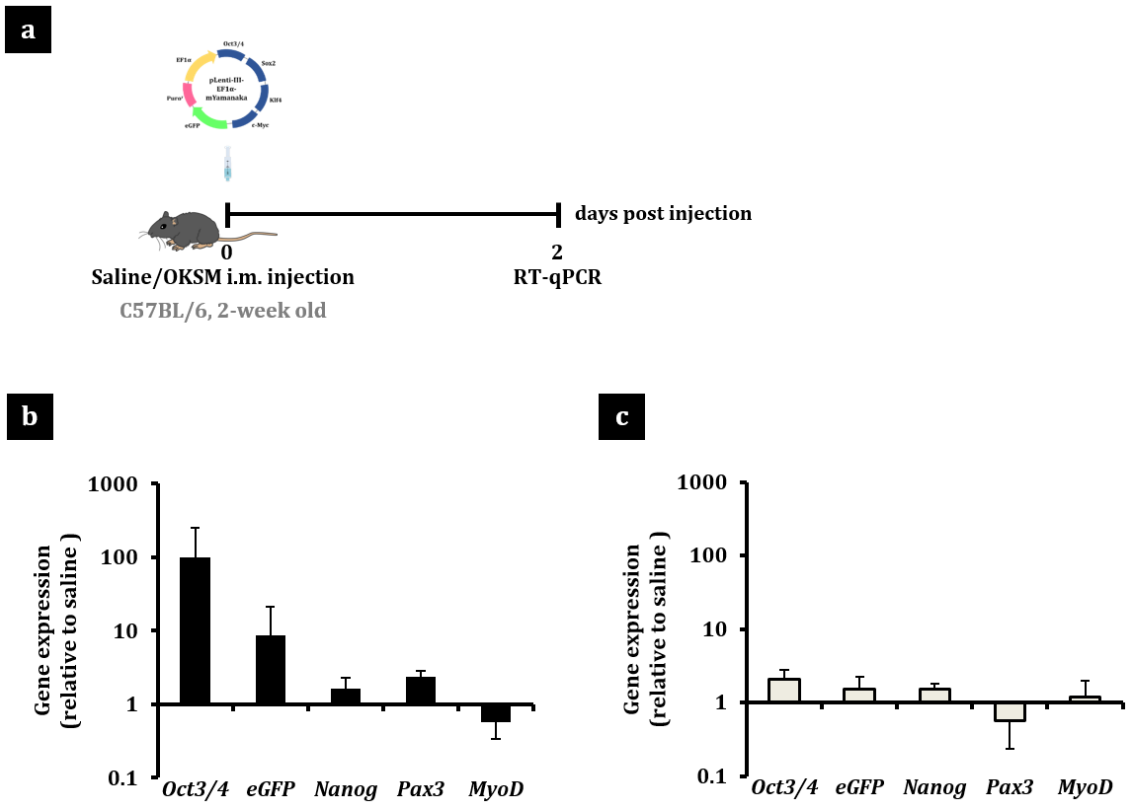

Figure 4. 5. Gene expression in juvenile mouse skeletal muscle after i.m. administration of OKSM reprogramming pDNA. ***(a)*** *2-week-old C57BL/6 mice were i.m. injected in the GA muscle with 50µg OKSM in 20 µl 0.9% saline or 20 µl 0.9% saline alone. 2 days after injection, real-time RT-qPCR was performed to determine the relative gene expression of reprogramming factors, pluripotency markers and genes involved in myogenesis in* ***(b)*** *GA and* ***(c)*** *biceps muscles. Gene expression levels were normalised to saline-injected controls. Data are presented as mean ± SD, n=3.*

When **OKSM** was administered, Oct3/4 and eGFP transgenes encoded in the vector were successfully expressed in the GA muscle **(Figure 4.5b)**, however the mRNA levels were ca. 10-fold lower than those achieved in adult mice **(Figure 4.2b)**. In addition, although the same trend was observed in the expression of pluripotency and muscle-specific genes, we did not observe any enhancement in the upregulation of *Nanog* and *Pax3*, nor in the downregulation of *MyoD* compared to the adult counterparts. Similar results were obtained with the administration of **OKS** and **M**, although in this case we could not even confirm the upregulation of *Pax3* compared to saline-injected controls **(Figure 4.6b)**.

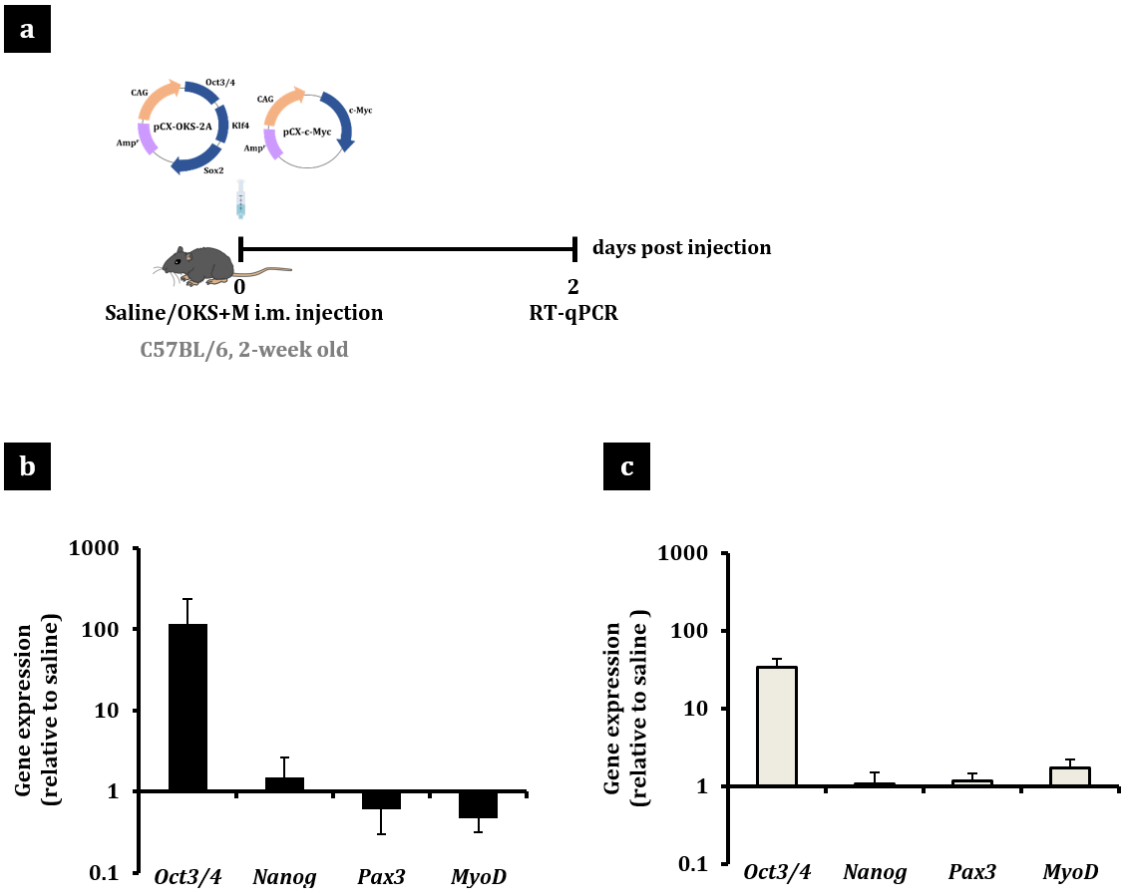

Figure 4. 6. Gene expression in juvenile mouse skeletal muscle after i.m. administration of OKS and M reprogramming pDNA. ***(a)*** *2-week-old C57BL/6 mice were i.m. injected in the GA muscle with 50µg OKS and 50 µg M in 40 µl 0.9% saline or 40 µl 0.9% saline alone. 2 days after injection, real-time RT-qPCR was performed to determine the relative gene expression of reprogramming factors, pluripotency markers and genes involved in myogenesis in* ***(b)*** *GA and* ***(c)*** *biceps muscles. Gene expression levels were normalised to saline-injected controls. Data are presented as mean ± SD, n=3.*

We then decided to analyse the expression of the same genes in the biceps muscle. We hypothesised that given the large injection volume for the small GA muscle of the juveniles, albeit reduced compared to that of our studies on adult mice, a significant part of the dose could have infused the biceps muscle instead. However, the expression of the transgenes encoded in the pDNA was even lower than that achieved in the GA muscle, especially 20µl **OKSM** were administered, and the levels of *Nanog*, *Pax3* and *MyoD* did not show any significant differences with the saline injected-controls that resembled our previous observations in adult mice **(Figures 4.5c and 4.6c)**. In conclusion and due to causes yet unidentified, our studies did not support previously published work that pointed at higher pDNA expression efficiencies in juvenile mice [224]. Consequently, we did not observe an enhancement in the efficiency of reprogramming. These observations

will merit *ad hoc* studies to determine the effects of age in the efficiency of pDNA expression and *in vivo* reprogramming.

4.4.3. Gene expression in mouse skeletal muscle after i.m. administration of reprogramming pDNA in the absence of c-Myc.

Given the oncogenic nature of c-Myc, we next investigated whether this reprogramming factor was strictly necessary to induce comparable changes in gene expression to those obtained with all four Yamanaka factors. To gather more information regarding the effects on myogenesis-related genes, expression of the myoblast marker *Myf5* and of *Myog*, expressed by myotubes and mature myofibers, was also studied. BALB/c mice were i.m. injected in the GA muscle with 50 μg **OKS** in 50 μl 0.9% saline or the same volume of 0.9% saline alone, as control **(Figure 4.7a)**. When the expression of endogenous pluripotency markers *Nanog*, *Ecat1* and *Rex1* was investigated 2 days after injection, ca. 10-fold upregulation was observed in the tissues administered with reprogramming pDNA compared to saline-injected controls **(Figure 4.7c).** Regarding the expression of muscle-specific genes, *Pax3* was also 10-fold upregulated, while the myoblast markers *MyoD* and *Myf5* appeared downregulated **(Figure 4.7d)**. The expression of all such genes was therefore in the same order of magnitude as that observed when all four factors were administered, both in this (BALB/c, **Figure S3**) and a different mouse strain (C57BL/6, **Figures 4.2 and 4.3**). Only the markers associated to the myotube and mature myofiber – *Myog* and *Myh1* - showed a marginal increase in their mRNA levels compared to the studies with the complete reprogramming cocktail. We did not find this result relevant, considering the expression of the rest of the genes investigated.

These findings were even more encouraging than what we observed in liver tissue where, although we detected protein expression of pluripotency markers, we could not reproduce the same mRNA levels of pluripotency and hepatocyte-specific genes in the absence of c-Myc **(Figures 3.3 and 3.4)**. Although this might mean that such factor is dispensable to induce pluripotency in the skeletal muscle *in vivo*, we decided to maintain the complete reprogramming cocktail for the rest of our studies to ensure maximum reprogramming efficiency. However, the effects of Oct3/4, Sox2 and Klf4 alone should be further explored if *in vivo* reprogramming to pluripotency is to be translated to the clinical setting.

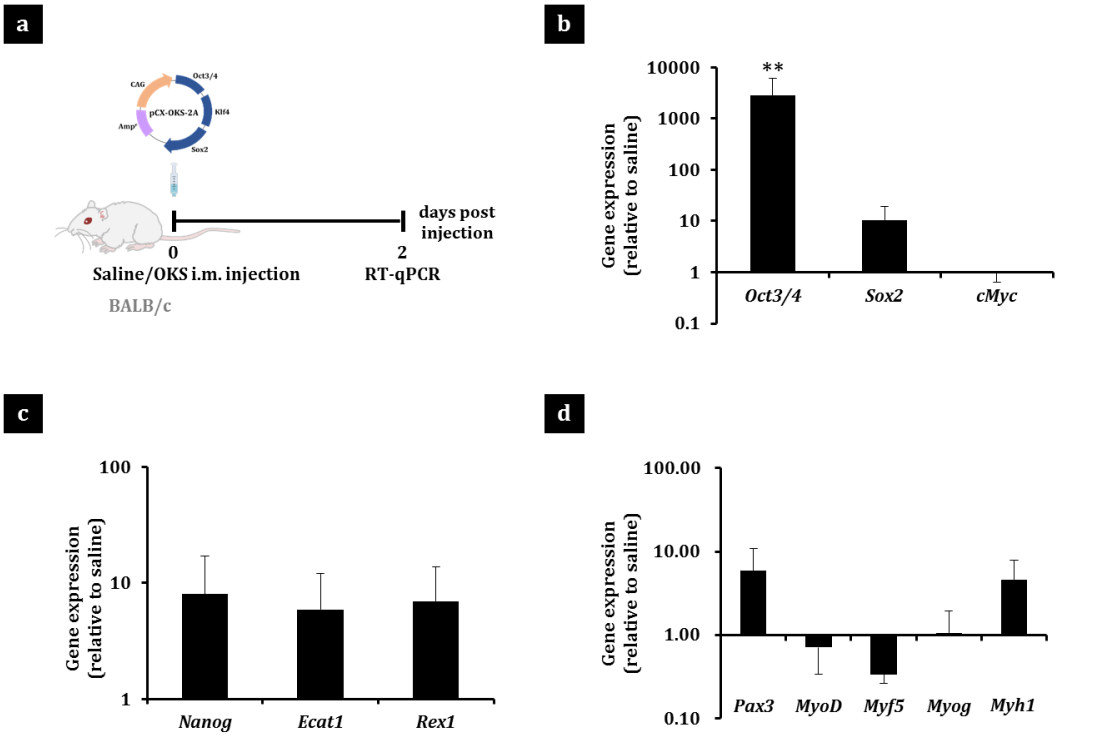

Figure 4. 7. Gene expression in mouse skeletal muscle after i.m. administration of OKS reprogramming pDNA (in the absence of c-Myc). ***(a)*** *BALB/c mice were i.m. injected in the GA muscle with 50μg* ***OKS*** *in 50 μl 0.9% saline or 50 μl 0.9% saline alone. GA muscles were dissected 2 days after injection and real-time RT-qPCR was performed to determine the relative gene expression of* ***(b)*** *reprogramming factors,* ***(c)*** *endogenous pluripotency markers and* ***(d)*** *genes involved in myogenesis. Gene expression levels were normalised to saline-injected controls. **p<0.01 indicates statistically significant differences in Oct3/4 gene expression between pDNA and saline-injected groups, assessed by one-way ANOVA. Data are presented as mean ± SD, n=3.*

4.4.4. Gene and protein expression in Nanog-GFP and Pax3-GFP transgenic mice skeletal muscle after i.m. administration of reprogramming pDNA.

Once the upregulation of genes characteristic of pluripotent and myogenic progenitor cells was confirmed in the skeletal muscle soon after the administration of reprogramming pDNA, we moved on to monitor changes in the mRNA levels of such markers at later time points, as well as their expression at the protein level. We performed this study on a Nanog-GFP transgenic mouse strain, which contains a *GFP* reporter inserted in the *Nanog* locus [230], under the hypothesis that the green fluorescence emitted by *Nanog*$^{+}$ cells would facilitate the identification of the reprogrammed cells within the tissue.

Gene expression

Nanog-GFP mice were i.m. administered with 50 μg **OKS** and 50 μg **M** in 50 μl 0.9% saline or the same volume of saline solution alone in the GA muscle. Gene expression was analysed 2, 4 and 8 days after injection **(Figure 4.8a)**. The expression of the reprogramming factors *Oct3/4*, *Sox2* and *c-Myc* was at its highest on day 2 and gradually diminished over time **(Figure 4.8b)**. The expression of endogenous pluripotency markers - including the *GFP* reporter controlled by the *Nanog* promoter – was also high 2 days after injection, but decreased to baseline levels after this time point **(Figure 4.8c)**. These observations confirmed that the induction of pluripotency in skeletal muscle was fast and transient, as observed in liver tissue. The investigation of myogenesis-related genes reaffirmed the upregulation of the myogenic progenitor marker *Pax3* in the mice treated with reprogramming pDNA, juxtaposed to the downregulation of markers relevant to any later stages in myogenesis. Particularly strong was the downregulation of *MyoD* 2 days after injection **(Figure 4.8d).**

We also examined the mRNA levels of genes characteristically expressed in other cell types resident in the skeletal muscle. We chose to focus on satellite cells and pericytes given that they possess myogenic potential [217, 231]. *Pax3* is mainly expressed by muscle progenitors during embryonic development but also by a subset of satellite cells in the adult organism [223, 232, 233]. Therefore, the study of other markers characteristic of such cell population was necessary to identify whether the increase in *Pax3* mRNA levels was due to satellite cell proliferation or to genuine reprogramming to an embryonic-like phenotype. The analysis of markers specifically expressed in quiescent and/or activated satellite cells, identified in a previous work [234], evidenced a moderate but significant downregulation of all such transcripts in the pDNA treated group **(Figure 4.8e)**, dismissing the hypothesis of satellite cell proliferation. Likewise, the investigation of pericyte-specific genes manifested the downregulation of such markers upon i.m. administration of reprogramming pDNA **(Figure 4.8f)**. Overall, this data did not suggest the involvement of satellite cell and/or pericyte proliferation in the processes taking place in the tissue after the administration of reprogramming factors.

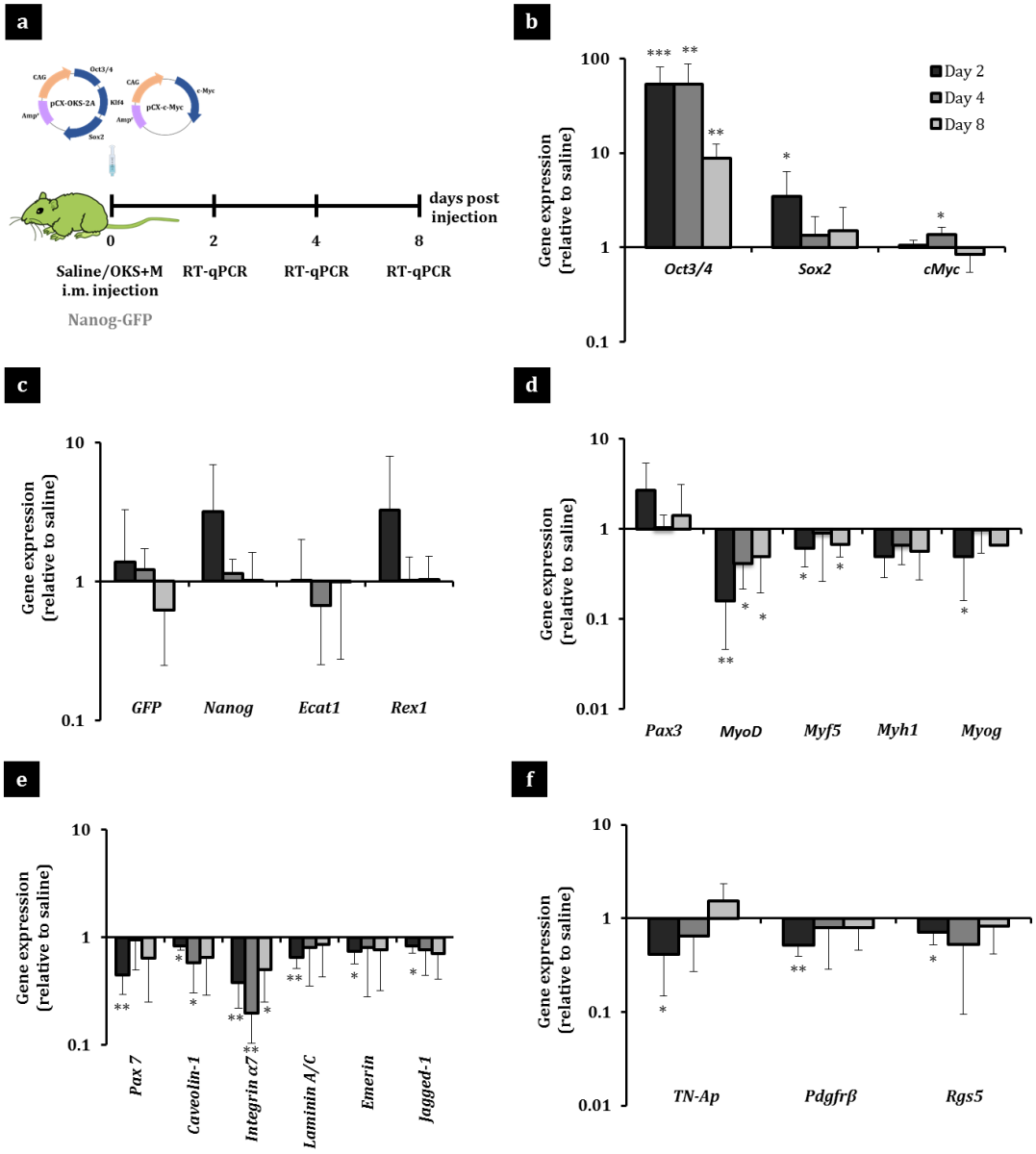

Figure 4. 8. Gene expression in Nanog-GFP transgenic mouse skeletal muscle after i.m. administration of reprogramming pDNA. ***(a)*** *Nanog-GFP transgenic mice were i.m. injected in the GA muscle with 50µg OKS and 50 µg M in 50 µl 0.9% saline or 50 µl 0.9% saline alone. GA muscles were dissected 2, 4 and 8 days after injection and real-time RT-qPCR was performed to determine the relative gene expression of* ***(b)*** *reprogramming factors,* ***(c)*** *endogenous pluripotency markers,* ***(d)*** *genes involved in myogenesis,* ***(e)*** *satellite cell markers and* ***(f)*** *pericyte markers. Gene expression was normalised to saline-injected controls. *p<0.05, **p<0.01 and ***p<0.001 indicate statistically significant differences in gene expression between pDNA and saline-injected groups, assessed by one-way ANOVA when p≥0.05 in Levene's test and by Welch ANOVA when p<0.05 in Levene's test. Data are presented as mean ± SD, n=4.*

Protein expression - characterisation of clusters of *in vivo* reprogrammed cells

Histological analysis of GA muscle tissue sections from the same study revealed the presence of clusters of GFP^+ mononucleated cells**.** Such clusters were only found in tissues from mice administered with reprogramming pDNA, hence we identified them as *Nanog* expressing *in vivo* reprogrammed cells **(Figure 4.9b)**. Green fluorescence was not detected any later than day 2 after injection **(Figure S4)**, which again highlighted the transiency of the induction of pluripotency.

The GFP signal triggered by *Nanog* upregulation co-localised with the expression of other pluripotency and ES cell specific markers - NANOG, OCT4, AP and SSEA1 - identified by IHC **(Figure 4.9c)**. Positive cells for such markers that did not seem to express GFP – or exhibited very faint green fluorescence - were rarely but sometimes found within the clusters. This might be explained by the substitution strategy utilised to generate the transgenic strain, which involves that only heterozygous mice are viable and therefore GFP expression is monoallelic [219], but it might also be possible that a heterogeneous population of cells forms the clusters. No immunoreactivity for any of the pluripotency markers tested was found in saline-injected controls, excluding AP, which is also expressed by pericytes **(Figure S5c)**. We also found cells staining positively for satellite cell and other pericyte markers (PAX7 and PDGFrβ, respectively) in the tissues from pDNA-injected mice **(Figure S5b).** However, such cells were found in similar numbers as in saline-injected controls **(Figure S5c)** and were located in the vicinity of the clusters but not co-localising with the GFP^+ cells within them. This finding reaffirmed our observations at the mRNA level **(Figure 4.8)** and indicated that the events triggered in the skeletal muscle upon *in vivo* reprogramming to pluripotency were different from a proliferative response of resident cells.

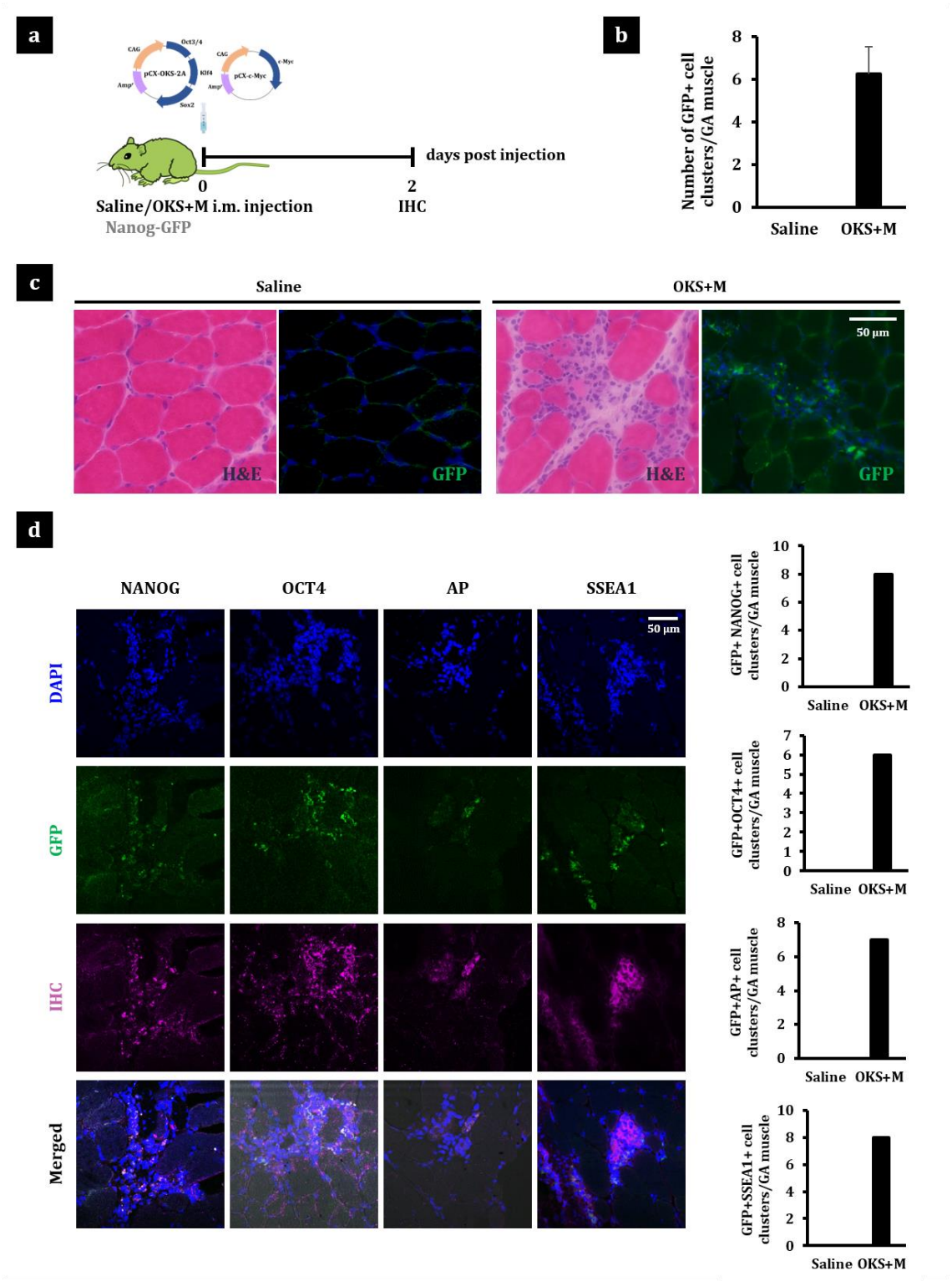

Figure 4. 9. Characterisation of in vivo reprogrammed cell clusters in Nanog-GFP mouse skeletal muscle tissue. (a) *Nanog-GFP transgenic mice were i.m. injected with 50µg OKS and 50 µg M or 50 µl 0.9% saline in the GA muscle. Tissues were dissected 2 days after injection and 10 µm-thick sections were obtained by cryotomy.* ***(b)*** *Number of GFP⁺ cell clusters per GA muscle. No GFP⁺ clusters were observed in saline-injected controls (n=3 mice, GA muscles were sectioned sequentially from tendon to tendon and 10 tissue sections/mouse were screened, representative of the different muscle areas). Data are presented as mean ± SD.* ***(c)*** *Clusters of reprogrammed cells in the GA muscle of the pDNA-injected group were identified by H&E and by the green fluorescence triggered by the expression of Nanog (100X, scale bar represents 50 µm).* ***(c)*** *IHC for the expression of pluripotency markers in GFP⁺ cell clusters and quantification (n=1). Images were taken with a confocal microscope (100X). Scale bar represents 50 µm.*

The use of a Pax3-GFP transgenic mouse strain also allowed the identification of bright GFP^+ cell clusters 2 days after injection of the same reprogramming pDNA combination, which were very similar to those observed in Nanog-GFP mouse tissues and did not appear in the saline-injected controls **(Figures 4.10a-b)**. This observation agreed with our gene expression data that evidenced an upregulation of *Nanog* and *Pax3* on day 2 after injection **(Figure 4.8)**, but did not confirm whether both markers were co-expressed by the same cells. To answer such question, we performed anti-NANOG IHC on Pax3-GFP mouse skeletal muscle tissue sections and found precise co-localisation of both signals in cells within the clusters **(Figure 4.10c)**. Such finding suggested that the cells that expressed NANOG expressed also PAX3.

Overall, these observations suggested that *in vivo* reprogrammed cells which grow in clusters of mononucleated cells and express pluripotency and early myogenic progenitor markers, but not those characteristic to satellite cells or pericytes, are generated in the skeletal muscle tissue upon i.m. administration of reprogramming pDNA. While not all the cells within the clusters in Nanog-GFP and Pax3-GFP specimens expressed the green reporter, this heterogeneity might also be explained by the transiency of the reprogramming event, with some cells probably re-differentiating already at the time point investigated (day 2).

4.4.5. Cell proliferation in mouse skeletal muscle after i.m. administration of reprogramming pDNA.

Cell proliferation has been identified as a distinct and indispensable step in the somatic to pluripotent conversion [167, 235], hence we next aimed to investigate whether the clusters of *in vivo* reprogrammed cells showed signs of active division.

To address this question, BALB/c mice were i.m. injected in the GA muscle with 50 μg **OKSM** – which encodes an *eGFP* reporter allowing the identification of transfected cells – or the same volume of vehicle alone. We planned to label the cells actively proliferating in the muscle 18 h after pDNA administration via i.p. injection of BrdU and to collect the tissues 6 h later for investigation **(Figure 4.11a)**. The signal of the *eGFP* reporter co-localised with that of an anti-BrdU antibody in GA muscle tissue sections from the pDNA-injected group. Importantly,

such co-localisation was found in clusters of mononucleated cells morphologically identical to those described in the previous section. This finding confirmed that cells transfected with reprogramming pDNA within the skeletal muscle tissue not only acquired an embryonic-like gene expression profile but also proliferated actively. No cell clusters, eGFP signal or BrdU incorporation were found in tissues from the saline-injected controls **(Figure 4.11b)**.

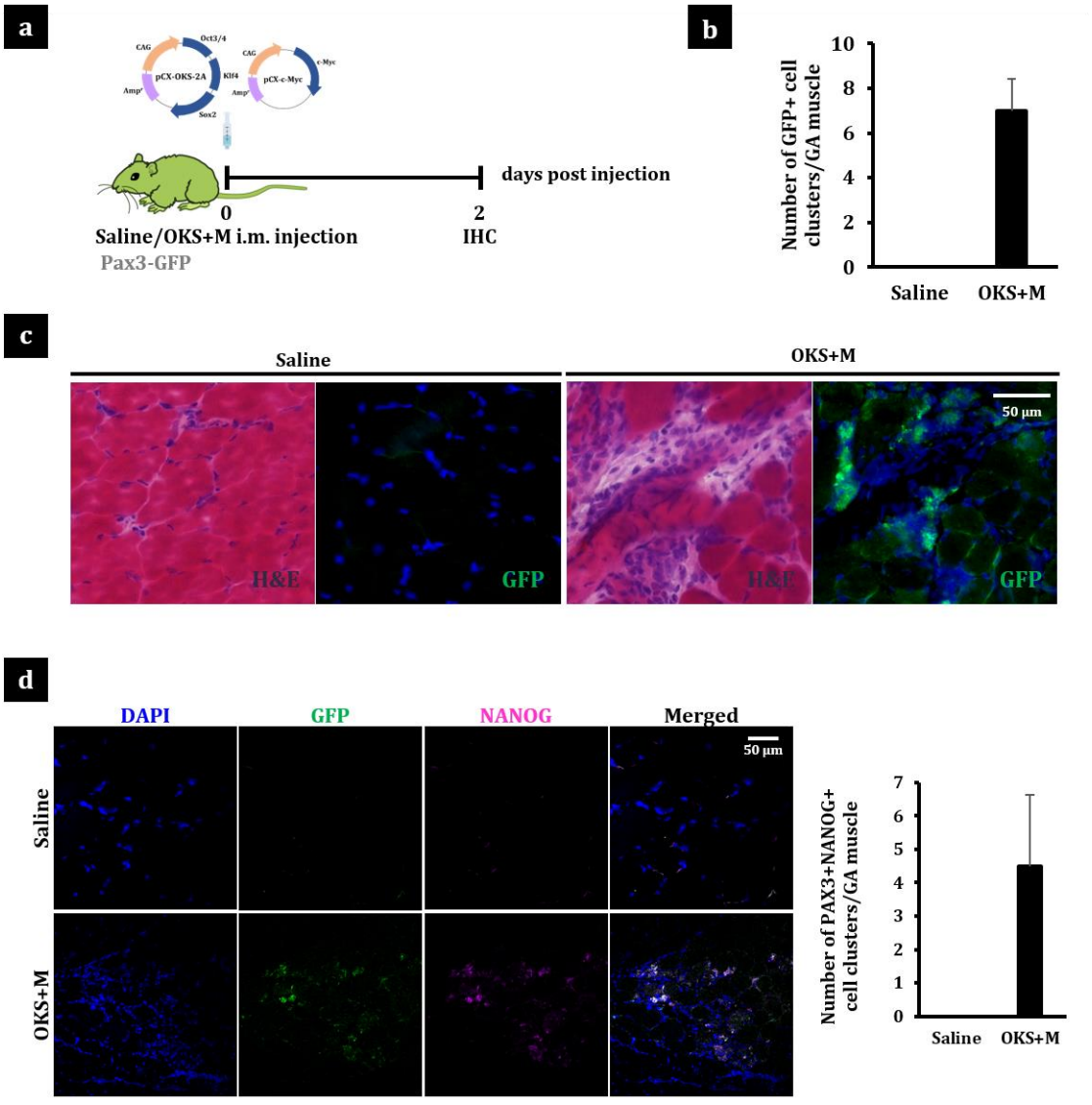

Figure 4. 10. Characterisation of in vivo reprogrammed cell clusters in Pax3-GFP mouse skeletal muscle tissue. (a) *Pax3-GFP transgenic mice were i.m. injected with 50µg OKS and 50 µg M or 50 µl 0.9% saline in the GA muscle. Tissues were dissected 2 days after injection and 10 µm-thick sections were obtained by cryotomy.* ***(b)*** *Number of GFP⁺ cell clusters per GA muscle. No GFP⁺ clusters were observed in saline-injected controls (n=2 mice, GA muscles were sectioned sequentially from tendon to tendon and 10 tissue sections/mouse were screened, representative of the different muscle areas). Data are presented as mean ± SD.* ***(c)*** *Clusters of reprogrammed cells in the GA muscle were identified by H&E and by the green fluorescence triggered by Pax3 expression (100X, scale bar represents 50 µm).* ***(d)*** *IHC for the expression of the pluripotency marker NANOG in GFP⁺ clusters and quantification of PAX3⁺NANOG⁺ cell clusters (n=2). Images were taken with a confocal microscope (100X). Scale bar represents 50 µm. For number of PAX3+NANOG+ cell clusters, data are presented as mean ± SD.*

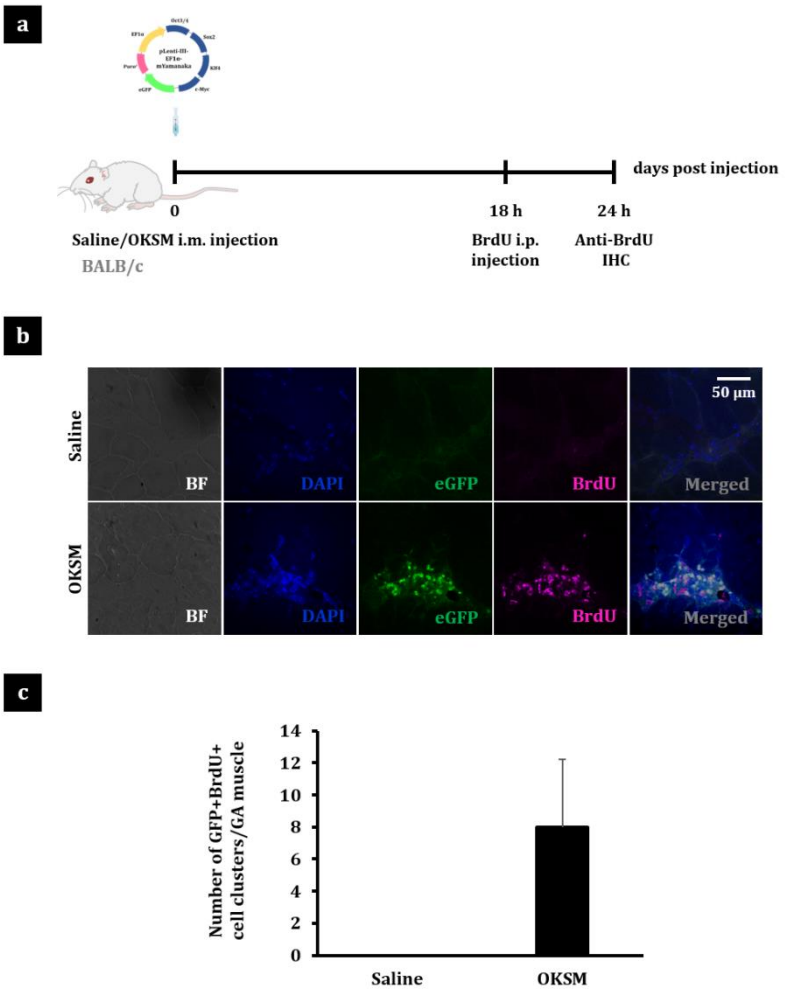

Figure 4. 11. Cell proliferation in mouse skeletal muscle after i.m. administration of reprogramming pDNA. (a) *BALB/c mice were i.m. injected in the GA muscle with 50µg OKSM in 50 µl 0.9% saline or 50 µl 0.9% saline alone and 18 h later administered with 500mg/kg BrdU, i.p. GA muscles were dissected 24 h after pDNA injection.* ***(b)*** *10 µm-thick tissue sections obtained by cryotomy were stained with anti-BrdU antibody. eGFP signal corresponds to the reporter encoded in OKSM pDNA. Images were captured with a confocal microscope (100X). Scale bar represents 50µm.* ***(c)*** *Number of GFP⁺BrdU⁺ cell clusters per GA muscle (n=3 mice, GA muscles were sectioned sequentially from tendon to tendon and at least 10 tissue sections/muscle were screened for the appearance of GFP⁺BrdU⁺ cell clusters, representative of all different muscle areas). Data are presented as mean ± SD.*

4.4.6. Short and long term histological outcomes of *in vivo* reprogramming to pluripotency in mouse skeletal muscle.

The evolution of cell morphology, nuclear position and tissue architecture within and around the clusters of *in vivo* reprogrammed cells was monitored for an extended period of time. BALB/c mice were i.m. injected in the GA muscle with 50 µg **OKSM** in 50 µl 0.9% saline or the same volume of saline alone. GA muscles were dissected 2, 4, 8, 15, 50 and 120 days after injection and processed for histological investigation **(Figure 4.12a)**.

H&E staining confirmed the appearance soon after injection (day 2) of distinct and dense clusters of small mononucleated cells among the myofibers, which appeared only in the pDNA-injected group. On day 4, small calibre fibers with the nucleus in the centralised position and expressing desmin - both characteristics of the regenerating, immature myotube [213, 236] - appeared within such clusters. Only few desmin$^+$ centronucleated myofibers were noted in the tissue on day 8 after injection and none at later time points. From day 15 onwards, we did not observe any differences between the pDNA and saline-injected tissues **(Figures 4.12b and 4.13b)**. Such evolution in the organisation of the clusters, together with the fact that no teratomas were found even at the latest time point of the study (day 120), suggested that the reprogrammed cells could have committed to myogenesis and successfully integrated into the muscle tissue. **Figure 4.12c** provides higher magnification images of these findings.

To further support this hypothesis and to address any concerns that the reprogrammed cells, exhibiting pluripotency features, would not be able to survive within an adult tissue microenvironment, TUNEL assay was performed to label any apoptotic nuclei **(Figure 4.12d)**. TUNEL$^+$ nuclei were only found at the earliest time points after injection and no differences were detected between the pDNA and saline-injected groups Therefore, their occurrence was attributed to marginal tissue damage along the needle track and not to reprogramming.

Finally, changes in morphometric parameters in the tissue were studied in an attempt to indirectly follow the fate of the reprogrammed cells. First, the number of nuclei per mm^2 was counted and found to be moderately but consistently higher in the muscles administered with reprogramming pDNA compared to saline controls **(Figure 4.12e)**, which agreed with our findings in cell proliferation. In addition, the diameter of the myofibers was also larger in the pDNA group **(Figure 4.12f)**, whereas the total number of myofibers per cross-section remained invariable compared to saline controls **(Figure 4.12g)**. These observations suggested that reprogrammed cells proliferated and fused to existing myofibers, enlarging their calibre, but did not form *de novo* fibers. Therefore, the events occurred in the skeletal muscle tissue upon *in vivo* reprogramming to pluripotency seemed to mirror those happening in normal post-natal myogenesis.

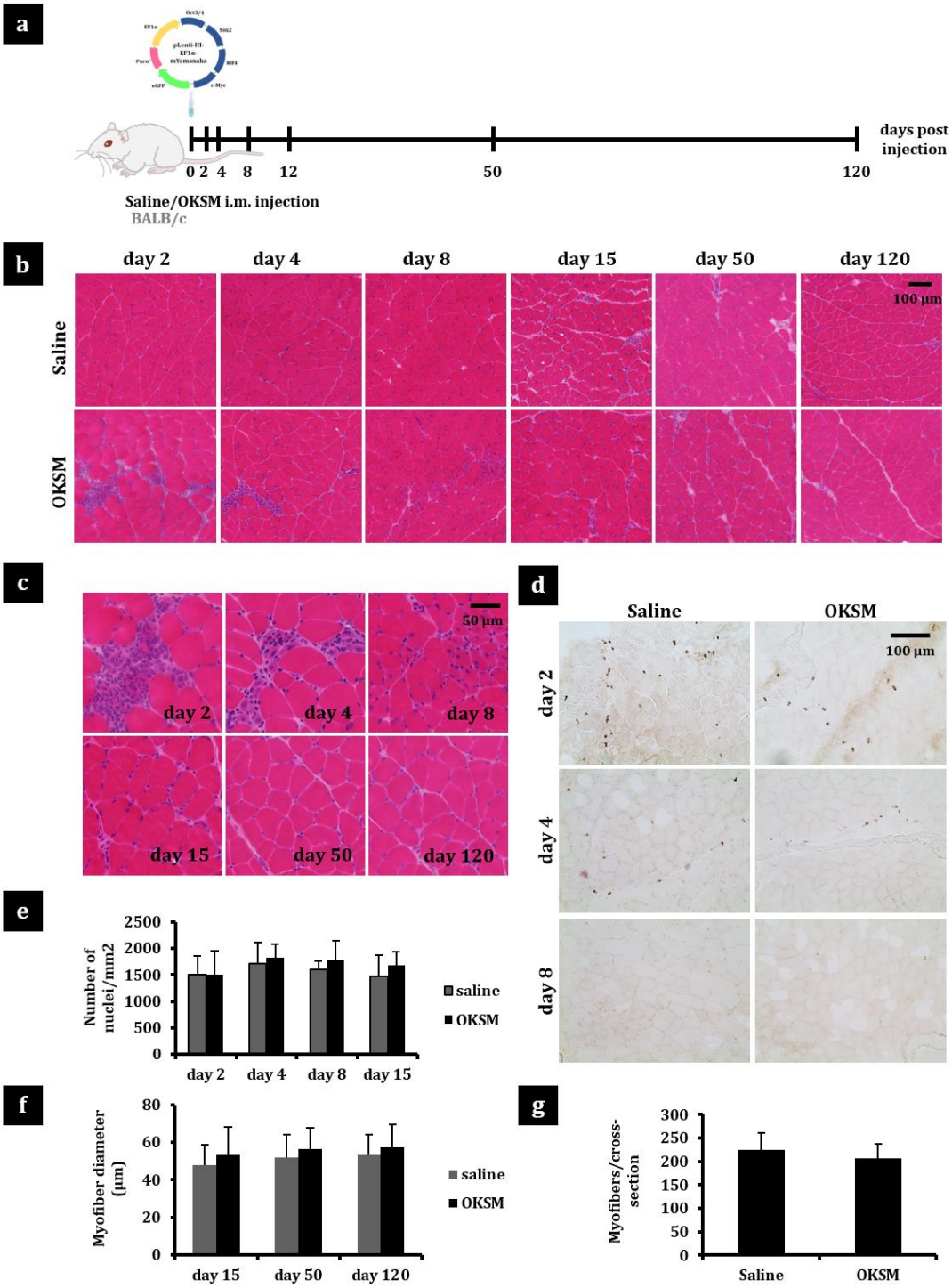

Figure 4.12. Short and long-term outcomes of in vivo reprogramming to pluripotency in mouse skeletal muscle. (a) *BALB/c mice were i.m. injected in the GA muscle with 50µg OKSM in 50 µl 0.9% saline or 50 µl 0.9% saline alone. GA muscles were dissected 2, 4, 8, 15, 50 and 120 days after pDNA injection and 10 µm-thick transverse tissue sections were obtained by cryotomy and stained with H&E.* ***(b)*** *Representative images at low magnification (40X, scale bar represents 100 µm).* ***(c)*** *Representative images at high magnification, focus on cell clusters that appear at the earliest time points after i.m. injection (100X, scale bar represents 50 µm).* ***(d)*** *TUNEL staining to label apoptotic nuclei was performed on days 2, 4 and 8 after injection. Representative images were obtained at 40X, scale bar represents 100 µm. The pattern in all stainings was faithfully recapitulated in pDNA-injected mice compared to saline controls, n=3.* ***(e)*** *Number of nuclei/mm² (n=3 GA muscles per condition, 10-12 sections per muscle).* ***(f)*** *Myofiber diameter (n=3 GA muscles per condition, 5 sections per muscle).* ***(g)*** *Myofiber number/cross-section (n=3 GA muscles per condition, 5 sections per muscle). All data are presented as mean ± SD.*

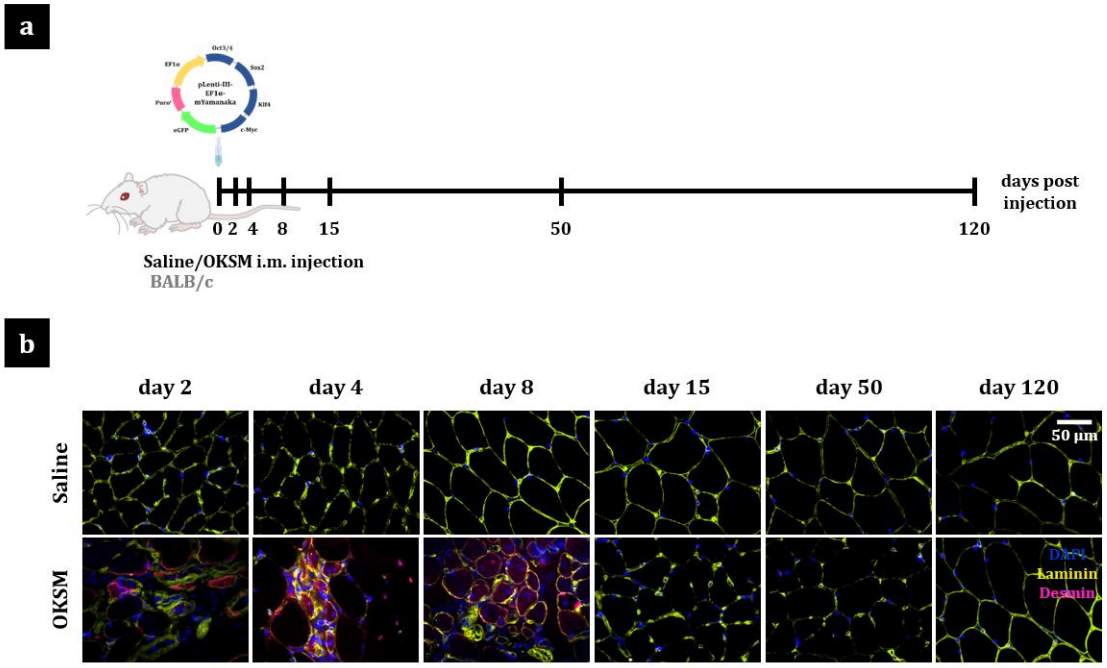

Figure 4.13. Expression of desmin in mouse skeletal muscle after in vivo reprogramming to pluripotency. (a) *BALB/c mice were i.m. injected in the GA muscle with 50µg OKSM in 50 µl 0.9% saline or 50 µl 0.9% saline alone. GA muscles were dissected 2, 4, 8, 15, 50 and 120 days after pDNA injection and 10 µm-thick transverse tissue sections were obtained by cryotomy.* ***(b)*** *IHC for the expression of desmin and laminin. Images were taken with an epi-fluorescence microscope (40X). Scale bar represents 50 µm.*

4.5. Discussion.

In this Chapter, we aimed to verify the universality of the Yamanaka cocktail as a tool to induce somatic cells to pluripotency *in vivo.* We confirmed that adult cells can be reprogrammed to express pluripotency markers in the skeletal muscle, a tissue of entirely different developmental origin from that of the previously reprogrammed liver.

Similar to the effects of HTV administration in liver, i.m. delivery of reprogramming pDNA and subsequent expression of Yamanaka factors led to transient de-differentiation of a subset of cells in the GA muscle. This was evidenced by the expression of pluripotency genes that are otherwise silenced in adult tissues **(Figure 4.8c)** and by the upregulation of *Pax3*, a transcription factor typically expressed in myogenic progenitors, but not in differentiated myotubes, nor in mature myofibers **(Figure 4.8d)**. The same outcome was reproducibly found when the study was repeated in different mouse strains and with different reprogramming pDNA cassettes **(Figures 4.2, 4.3 and S3)**. Notably, we did not find any significant differences in the gene expression levels of pluripotency and

early progenitor markers achieved in the absence of *c-Myc* **(Figure 4.7)**, which could facilitate the prospective clinical translation of this approach.

Gene expression profiles obtained from saline-injected and uninjected controls confirmed that the minor trauma derived from the i.m. injection did not have any input in the expression of pluripotency and muscle-specific genes **(Figure 4.4)**. The contribution of satellite cell and pericyte proliferation, initially suspected from the increase in *Pax3* mRNA levels, was disproved by a number of findings. First, we found that gene expression of several satellite cell and pericyte-specific markers was downregulated in the pDNA-injected muscles compared to saline controls **(Figures 4.8e-f)**. In addition, *MyoD* – which is rapidly upregulated upon satellite cell activation and highly expressed in their proliferating progeny [237] – was significantly downregulated in the reprogrammed group throughout our work **(Figures 4.2, 4.3, 4.7, S4 and 4.8)**. Finally, no differences in the abundance of such cells between the pDNA and saline-injected tissues were observed in histological studies **(Figure S5)**.

Co-localisation studies on a Nanog-GFP transgenic mouse strain confirmed conversely that mononucleated cells growing in clusters among the myofibers expressed several pluripotency markers but not those characteristic of satellite cells or pericytes **(Figures 4.9 and S5)**. Similar studies on a Pax3-GFP mouse strain confirmed that reprogrammed cells expressing *Nanog*, expressed also the myogenic progenitor marker *Pax3* **(Figure 4.10)**.

The relatively rapid decrease in the expression of reprogramming factors after injection **(Figure 4.8b)** was interpreted as an indication of the proliferative status of the transfected cells. I.m. injection of pDNA is known to result instead in long-term transgene expression - at least 2 months, with peak levels reached 14 days after injection as previously described [212] - given the post-mitotic status of the myofibers. Our observation can be explained if post-mitotic cells had re-entered the cell cycle and divided actively upon *in vivo* reprogramming or if dividing cells had been transfected instead, in both cases resulting in the dilution of the pDNA. Importantly, BrdU labelling was able to confirm the proliferative status of the clusters of reprogrammed cells **(Figure 4.11)**. Cells labelled with BrdU and expressing the eGFP reporter encoded in **OKSM** were found when the synthetic nucleoside was administered soon after (18 h) i.m. injection of reprogramming

factors. No incorporation of BrdU was detected in the saline-injected controls, which suggested that proliferation was a result of *in vivo* reprogramming. This observation was pivotal to support that reprogramming towards pluripotency occurred *in vivo*, given that active proliferation is known to be one of the indispensable initial stages in the pluripotent conversion [167].

In addition, the evolution of the cell clusters over time suggested that the pluripotent-like proliferative state was only transient and reprogrammed cells eventually re-differentiated and were successfully integrated into the muscle tissue. Such conclusion was supported by the gradual disappearance of the mononucleated cell clusters (only prominent 2 days after injection), followed by the emergence of small calibre centronucleated muscle fibers expressing desmin from days 4 to 8 (characteristic of the regenerating or newly-formed immature myotube) and the fact that no differences were observed between tissues administered with pDNA or saline after this point **(Figures 4.12b-c and 4.13b)**. These histological observations agreed with our findings at the mRNA level, in which significant upregulation of pluripotency markers was evident 2 days after injection, but not later **(Figure 4.8)**. Likewise, no fluorescence originated from *Nanog* upregulation was observed in Nanog-GFP tissues after the same time point **(Figure S4)**. The lack of significant apoptosis in the tissues administered with reprogramming pDNA and the morphometric information advocated also for the re-integration of the reprogrammed cells into the muscle tissue **(Figures 4.12d-g).** The latter suggested that *in vivo* reprogrammed cells behaved similarly to myogenic precursors such as satellite cells by fusing to neighbouring muscle cells but not forming *de novo* fibers. The final number of myofibers in the mouse skeletal muscle is fixed soon after birth, with little changes after postnatal day 14. During postnatal growth, satellite cell-derived myoblasts fuse to and enlarge the diameter of existing myofibers (hypertrophy) but no new fibers are formed (hyperplasia) [238]. In the reprogrammed tissue, we consistently observed a higher number of nuclei per mm^2 compared to the saline control **(Figure 4.12e)**, in agreement with our findings of cell division. In addition, the myofiber diameter increased **(Figure 4.12f)** but the number of myofibers per cross-sectional area remained invariable by the end of the study (day 120) **(Figure 4.12g).** In spite of the coherence of these observations, specific lineage tracing studies that could allow the permanent labelling of the *in vivo* reprogrammed cells will be required to

fully understand their fate in the tissue and further confirm the observations described here.

A previous study has also reported successful integration of *in vivo* reprogrammed cells in the tissue after a proliferative phase. Ohnishi et al. similarly utilised BrdU labelling to identify proliferative cells upon *in vivo* reprogramming and follow their fate in a doxycycline-inducible reprogrammable mouse [196]. When the expression of reprogramming factors was sustained – via administration of the drug - for no more than 7 days, $BrdU^+$ cells were successfully integrated into the respective tissues. In addition, $BrdU^+$ cells producing insulin were observed within the pancreatic tissue of the treated animals, confirming that reprogrammed cells not only re-differentiated to the appropriate phenotype but were also able to accomplish their normal physiological function. The fact that under such conditions the reprogrammed cells did not progress to dysplasia, but they did when the drug was administered for longer periods of time [196], stressed again the importance of the transient expression of reprogramming factors for the successful re-integration of the reprogrammed cells into the tissue and the avoidance of tumourigenesis. The same conclusion transpired from our experiments in skeletal muscle, in which no teratoma formation was observed in any of the mice sacrificed at different time points over a period of 120 days **(Figures 4.12b and 4.12c)**. This was again in accordance not only with Yilmazer's findings in liver tissue [162] but also with the *in vivo* reprogramming reported in tadpole tail muscle [161].

Many are indeed the common findings between the work presented in this Chapter and the Vivien et al. study using muscle tissue of pre-metamorphic tadpoles. The onset of reprogramming was also rapid in that model, with notable expression of endogenous pluripotency genes as early as 3 days after i.m. administration of **OKS** pDNA in the tail muscle. Similar to our studies, the expression of the reprogramming factors encoded in the pDNA decreased significantly over time, and was not detected from day 14 onwards. Even more interesting were the similarities between the cell clusters that appeared among the myofibers after the administration of reprogramming pDNA in both models. Similar to what we have described in mouse skeletal muscle, the clusters observed by Vivien et al. in the tadpole tail were populated by proliferative mononucleated cells that expressed endogenous pluripotency markers. Finally, the pluripotent

conversion was also transient in the amphibian tissue, the cells within the clusters did not form teratomas but re-differentiated and integrated into the tissue.

Vivien and colleagues were in addition able to isolate the *in vivo* reprogrammed cells from the tail muscle tissue and culture them *in vitro*, where they formed colonies able to differentiate towards the three developmental lineages. We also attempted to isolate such cells from the clusters present in the GA muscle. We based our efforts first on a protocol described to isolate satellite cells and other stem cells resident in skeletal muscle [239] and later on a method reported to isolate individual myofibers retaining their associated satellite cells [240]. While we were able to isolate and culture satellite cells and muscle cells that formed beating myotubes (data not shown), none of the protocols succeeded in the generation of i^2PS cells from skeletal muscle tissue. We attribute this failure to the transiency with which the pluripotent-like cells exist in the tissue, which makes their isolation very challenging. Having already characterised the i^2PS cells generated from liver tissue as a proof of concept that functional pluripotency can be achieved upon *in vivo* reprogramming, we preferred to focus our attention in the fate of the reprogrammed cells *in vivo* and their possible contribution to tissue regeneration as will be described in Chapter V.

An interesting question that remains to be answered is the identity of the cells within the skeletal muscle that are reprogrammed towards pluripotency following this approach. We have not performed studies that identify the cell type or types transfected with reprogramming pDNA. Fully differentiated myofibers are known to spontaneously uptake naked pDNA [208], the reason why they are considered an advantageous target for gene delivery *in vivo*. Indeed, all of the early studies on direct i.m. administration of naked pDNA proved the expression of the relevant transgenes in mature myofibers, although they did not explore systematically the uptake in other cell populations [208, 209, 212, 224]. On the other hand, the feasibility to reprogram mammalian multinucleated and post-mitotic myofibers into pluripotent mononucleated cells remains controversial due to the requirements of cell cycle re-entry and cell fission involved. While it has long been known that myofibers in urodele amphibians can re-enter the cell cycle and cleave into mononucleated progenitors [241], there is no proof of such an event in mammalian fully differentiated muscle cells. Recent studies have attempted to achieve mammalian myofiber de-differentiation and fission via ectopic expression

of transcription factors that mediate such processes in the amphibian organism [242-244] or simply via muscle injury [245, 246]. However, their results are questionable due to the lack of robust lineage tracing tools that confirm the origin of the resulting mononucleated cells.

Myoblasts present in adult skeletal muscle have been successfully reprogrammed into iPS cells *in vitro* [228] and hence could have also been the targets of de-differentiation in our studies. We did not observe a reproducible downregulation of markers associated to fully differentiated myofibers, but we did consistently report the downregulation of the myoblast marker *MyoD* **(Figures 4.2, 4.3, 4.7, 4.8 and S4)**. The downregulation of this gene, mediated by the upregulation of the master regulator of pluripotency *Oct4*, has been determined as mandatory for the pluripotent conversion of myoblasts [218]. We also confirmed downregulation of markers specific to satellite cells, which are also amenable to reprogramming, as demonstrated *in vitro*, and with higher reprogramming efficiencies than other more committed cell types [228]. However, uptake of pDNA by satellite cells upon i.m. injection remains to be confirmed and, in fact, Vivien et al. demonstrated that such cell population was not transfected in their tadpole model [161]. We repeated our reprogramming studies using 2-week-old juvenile mice, under the hypothesis that if satellite cells were reprogrammed the significantly larger population of such cells in the juveniles compared to adult counterparts [229] would result in a higher reprogramming effect. Conversely, even the expression of transgenes encoded in the reprogramming pDNA was lower than that achieved in adult mice with the same dose of pDNA **(Figures 4.5 and 4.6)**, contradicting a previous study [224]. Hence, we currently have no experimental evidence to suggest that satellite cells are reprogrammed to pluripotency *in vivo*. Whether it is the fully differentiated myofibers and/or other cell types resident in the skeletal muscle, the population reprogrammed upon i.m. injection of reprogramming pDNA remains to be demonstrated and this question will have to be answered with the appropriate cell tracking strategies. Alternatively, incorporation of cell-specific promoters in the pDNA cassette might also help to address this question. Given the probably random incorporation of pDNA in a diversity of cells, it is conceivable that different interstitial cells (including satellite cells) were reprogrammed rather than a particular cell type; all down-regulating their specific markers.

In conclusion, the data presented in this Chapter showed that *in vivo* reprogramming towards pluripotency can be achieved in a different somatic tissue (mesoderm origin) from the previously reprogrammed liver (endoderm). Although tri-lineage contribution will have to be tested to confirm that complete reprogramming was achieved, i.m. administration of reprogramming pDNA induced a subset of cells within the tissue to execute an embryonic-like genetic program to then recapitulate features characteristic of normal myogenesis in terms of tissue morphometry and organisation. In light of these observations, we hypothesised that *in vivo* reprogramming towards pluripotency might enhance the regeneration capacity of the tissue in a skeletal muscle injury scenario.

Chapter V.

In vivo reprogramming to pluripotency in two models of skeletal muscle injury.

5.1. Scope of Chapter V.

In Chapter III we demonstrated that the expression of reprogramming factors *in vivo* generates functionally pluripotent cells. In addition, we observed in Chapter IV that cells expressing pluripotency markers proliferated transiently in the skeletal muscle and then seemed to successfully re-integrate into the tissue, enlarging the diameter of existing myofibers, without forming teratomas. In the present Chapter, we aimed to investigate whether the induction of pluripotency within injured skeletal muscle would enhance the endogenous regenerative capacity of the tissue and accelerate rehabilitation at the histological and functional levels.

5.2. Introduction.

The skeletal muscle in some lower vertebrates - including urodele amphibians (newts and axolotls), anuran amphibians (*Xenopus laevis* tadpoles) and zebrafish larvae - has an outstanding capacity to regenerate after severe insults. Such phenomenon occurs either via de-differentiation of mature myofibers, activation of tissue resident stem cells or both mechanisms, and contributes to their ability to regrow amputated body structures [241, 247]. The regenerative capacity of the mammalian skeletal muscle is however less striking and relies mainly on the self-renewal and myogenic potential of resident stem cells, primarily satellite cells [248]. Such cells are normally quiescent but, in the event of an injury, proliferate and differentiate into myoblasts that fuse to existing myofibers or form new fibers to replenish the tissue [216, 217, 249]. The pool of satellite cells varies across species and dramatically decreases with age (from 30-35% in the neonate mouse to <5% in the adult; from 4.5% in the neonate human to <2% in the adult) [229, 250], hence it is normally sufficient to repair minor to moderate injuries but can be easily exhausted if the injury is severe [251]. In this scenario, various resident cell types differentiate into myofibroblasts that generate a collagen-based fibrotic scar unable to meet the contractile requirements of the tissue and that therefore prevents the complete functional rehabilitation of the injured muscle [137, 252]. Therefore, major injuries including severe lacerations, contusions and strains (significantly prevalent in sports medicine and traumatology) are often not

entirely resolved at the anatomical and functional levels, leading to a high frequency of relapse [5].

Also important for the frequent lack of complete rehabilitation upon severe damage to the skeletal muscle is the fact that only conservative treatment is currently clinically available, which consists on the so-called RICE strategy (rest, ice, compression and elevation) at the earliest stages, followed by physical therapy aimed to recover the contractile function in the long term [5]. Anti-inflammatory therapy has additionally been proposed but recent studies have advised against it given the important role that inflammation plays at the earliest stages of the muscle degeneration-regeneration process [253, 254]. The surgical suturing of the defect has reported modest benefits, however it is very limited to particular types of injury [255]. Although other strategies - including the administration of anti-fibrotic drugs [256-259], growth factors [260], replacement cells [261-263], miRNAs involved in muscle development [264] and combinations of these [265-268] - are currently being extensively investigated, they are not devoid of limitations and have not yet reached routine clinical practice [5, 8].

We have previously hypothesised that the generation of pluripotent cells able to transiently proliferate and eventually re-differentiate to the appropriate phenotype within a damaged tissue might help to repopulate the injured site and therefore improve regeneration and functional rehabilitation [164]. This hypothesis became especially sound upon confirmation in Chapter IV that *in vivo* reprogramming to pluripotency in healthy skeletal muscle recapitulates events characteristic of mammalian post-natal myogenesis (fusion to existing myofibers) and possibly of the endogenous regeneration in certain organisms (de-differentiation to an embryonic-like phenotype).

In this Chapter, a chemically-induced (i.m. administration of cardiotoxin, CTX) and a physically-induced (surgical laceration) model of skeletal muscle injury were used to explore the therapeutic potential of *in vivo* reprogramming to pluripotency.

5.3. Materials and methods.

5.3.1. Materials used in Chapter V.

5.3.1.1. Plasmid (pDNA) vectors.

Reprogramming pDNA pCX-OKS-2A (**OKS**, encoding Oct3/4, Klf4, Sox2), pCX-cMyc (**M**, encoding cMyc) and pLenti-lll-EF1α-mYamanaka (**OKSM**, encoding Oct3/4, Klf4, Sox2, cMyc and eGFP) were used in this study. A more detailed description of the cassettes is provided in **Chapter III**, **Section 3.3.1.1**. pDNA maps are illustrated in **Figure S1.**

5.3.1.2. Mouse strains.

Female mice were used in this work that entered the procedures at 7 weeks of age. BALB/c mice were purchased from Harlan (UK) and C57BL/6 mice were obtained from Charles River (UK). All experiments were performed with previous approval from the UK Home Office under a project license PPL 70/7763 and after allowing the mice one week to acclimatise to the facilities.

5.3.1.3. Myotoxic substances.

Cardiotoxin (CTX), snake venom from *Naja mossambica mossambica,* was purchased from Sigma (C9759, UK) as a powder, and dissolved in PBS to a final 10 μM concentration.

5.3.2. Methods involved in Chapter V.

5.3.2.1. Monitoring of endogenous regeneration after CTX injury in different mouse strains.

BALB/c and C57BL/6 mice (n=3) were i.m. administered with 30 μl CTX (10μM) in the left GA muscle. The contralateral hind limb was left uninjected and used as control. Mice were sacrificed on days 3, 6 and 9 after injury and the progress of endogenous regeneration in the two strains was compared via macroscopic observation, changes in moist weight and histological (H&E) investigation of the dissected muscles.

5.3.2.2. Monitoring of gene expression changes in skeletal muscle tissue over time after CTX administration.

BALB/c mice (n=3) were i.m. administered with 30 µl CTX (10µM) in the left GA muscle. The contralateral hind limb was left uninjected and used as control. Mice were sacrificed on days 3, 6 9 and 15 after injury and the expression of inflammation, pluripotency and myogenesis-related genes in the injured muscles was compared to that of the intact controls. Gene expression levels were determined by real-time RT-qPCR, as described in **Chapter IV, Section 4.3.2.2**. Primer sequences used in this Chapter are listed in **Table S8**.

5.3.2.3. CTX injury model and *in vivo* reprogramming to pluripotency.

BALB/c mice (n=3-4, as specified in each study) were i.m. administered with 30 µl CTX (10µM) in the left GA. The time of injury was considered day 0 (d0). Two doses of 50 µg **OKS** and 50 µg **M** each were i.m. administered in the injured muscle on consecutive days, according to one of the following regimens: days 0 and 1 (d0+1), 5 and 6 (d5+6) or 7 and 8 (d7+8) after injury. The injured (left) GA of the control group was administered with the equivalent volume (50 µl) of 0.9% saline. In both groups, the contralateral (right) GA was left intact (uninjured and uninjected) and used as internal control. Mice were sacrificed and GA muscles were dissected 2 and 7 days after the last administration of **OKS**+**M** or saline for further investigations. Schematic representations of the therapeutic regimens included in this study are provided in **Figure 5.4**.

5.3.2.4. Laceration of GA, soleus and plantaris muscles and *in vivo* reprogramming to pluripotency.

BALB/c mice (n=3) were anesthetised with isoflurane and the left hind limb was shaved and prepared for surgery. 0.05 mg/kg buprenorphine were s.c. administered at the start of the procedure. A vertical skin incision (6 mm long) was made overlying the posterior compartment of the calf with a scalpel number 11 and the fascia was exposed and incised with fine scissors at the level of mid GA to release the muscle belly. All the muscles in the posterior compartment of the calf – including lateral and medial GA, soleus and plantaris– were lacerated in the transverse plane, at their mid-point, through the 100% of their width and the 100% of their depth **(Figure 5.9a)**. The contralateral (right) hind limb was left

uninjured. The skin was sutured with 5 interrupted stitches (Vicryl 6-0 absorbable suture, Ethicon, UK) and the mice were allowed to recover in a warm chamber. 100 μg **OKSM** or the equivalent volume (40 μl) of 0.9% saline (control) were i.m. administered in the injured (left) hind limb at the time of surgery (day 0), or 2 days after injury (day2). The contralateral (right) leg was left intact (uninjured and uninjected) and used as internal control. Mice were sacrificed and muscles were dissected 2 and 5 days after the administration of **OKSM** or saline for further investigations. **Figure 5.9b** provides schematic representations of such therapeutic regimens.

5.3.2.5. Laceration of medial GA and *in vivo* reprogramming to pluripotency.

BALB/c mice (n=3-4, as specified in each study) were operated as described above, however only the medial GA was blunt dissected and lacerated with a single incision in the transverse plane. The cut was performed at its mid-point, through the 100% of its width and the 100% of its depth **(Figure 5.12a)**, preserving the lateral GA and all other muscles in the posterior compartment of the calf. The contralateral (right) hind limb was left uninjured. 100 μg **OKSM** or the equivalent volume (40 μl) of 0.9% saline (control) were i.m. administered in the injured (left) GA muscle at the time of surgery (day 0), or 5 or 7 days after injury. The contralateral (right) GA was left intact (uninjured and uninjected) and used as internal control. **Figure 5.12b** provides schematic representations of the therapeutic regimens included in this study. Mice were sacrificed and GA muscles were dissected 2 and 7 days after the administration of **OKSM** or saline for further investigations. The medial and lateral GA were processed separately for moist weight and gene expression studies.

Record of muscle moist weight.

Muscle moist weight was recorded straight after dissection on a precision balance PA114 Pioneer (Ohaus, UK). Changes in muscle weight were either expressed as the mean ± SD of each group or as the mean ± SD of the ratio injured/healthy hind limb of each treatment group.

Analysis of gene expression.

Relative gene expression of *Oct3/4*, *Nanog* and *Pax3* 2 days after the last administration of reprogramming pDNA or saline was analysed by real-time RT-

qPCR as previously described **(Chapter IV, Section 4.3.2.2)**. Livak's method was followed to analyse the data and dCt values were utilized for statistical analysis. Primer sequences are listed in **Table S8**.

Analysis of collagen deposition (picrosirius red/fast green staining).

Muscles were dissected 2 and 7 days after the last administration of reprogramming pDNA or saline and fixed in 10% buffered formalin solution (Sigma, UK). After embedding the tissues in paraffin wax, 5 μm-thick transverse sections were obtained with a microtome (Leica RM2255) and left to dry overnight at 37°C prior to the staining procedure. De-paraffinization using a standard protocol was followed by 1 h incubation in picrosirius red/fast green staining solution (0.1% Sirius red, 0.1% fast green in a saturated aqueous solution of picric acid). Tissue sections were then quickly immersed in 0.5% acetic acid for 6 s and dehydrated in 100% ethanol and xylene to be finally mounted with DPX mountant (Sigma, UK). Sections were imaged on a 3D Histech Pannoramic 250 Flash slide scanner and 40X images were obtained with Pannoramic Viewer Software. The percentage of collagen+ areas around the site of injury was measured with ImageJ 1.48 software in 3 to 5 randomly selected fields per section. The data for each GA muscle were calculated from 3 to 4 sections and we observed 2 to 4 GA muscles in each group. Precise n numbers are specified in each study. The measurements and calculations were performed in a blinded manner.

Analysis of % of centronucleated myofibers.

5 μm-thick transverse tissue sections were obtained as described above from muscles dissected 2 and 7 days after the last administration of reprogramming pDNA or saline. H&E staining was performed following a standard protocol. 40X images were obtained using a 3D Histech Pannoramic 250 Flash slide scanner and Pannoramic Viewer Software. The number of centronucleated myofibers and total number of fibers per cross-sectional area were quantified around the site of injury using ImageJ 1.48 software in 2 to 3 randomly selected fields per section. The data for each GA muscle were calculated from 3 sections, and we observed 2 to 4 GA muscles in each group, as specified in each study. Precise n numbers are specified in each study. The measurements and calculations were performed in a blinded manner.

Electromechanical evaluation.

The function of the GA muscle after injury (2 and 7 days after the last administration of reprogramming pDNA or saline) was assessed by recording the force produced under fast twitch and tetanus contraction triggered by direct stimulation of the sciatic nerve. Such measurements were performed with an Aurora 1300A myograph (Aurora Scientific Inc, Canada) that allowed the recording of muscle forces in terminally anaesthetized mice. In brief, mice were anaesthetised with isoflurane and the GA muscle was exposed and released from the fascia as previously described in **Section 5.3.2.4**. The GA muscle and sciatic nerve were blunt dissected. The femur's head was prepared free from surrounded tissue and fixed to the platform clamp preventing movement of the leg upon stimulation. The Achilles tendon was connected to the force transducer and an electrode was placed directly on the sciatic nerve. The nerve and muscle were kept moist with paraffin oil at 37°C throughout the measurements. A schematic representation of the setup is shown in **Figure 5.1**. Since we aimed to record isometric contractions, optimal muscle length was first determined by repeating twitch measurements with a fixed current of 5V while adjusting the length of the muscle. The maximum twitch force was then assessed by increasing the voltage of stimulation. Finally, tetanus contractions were produced by repeated stimulation at optimal length and current (identified from the twitch measurements) with a 150 Hz frequency. 1 and 5 minutes were allowed between twitch and tetany measurements, respectively, to avoid muscle fatigue that could influence the results. The percentage of recovered force was calculated as the ratio between the force produced by the left (injured) and right (intact) GA muscles and expressed as mean ± SE. n=4 mice per treatment group and time point. This protocol was established in collaboration with Dr. Hans Degens.

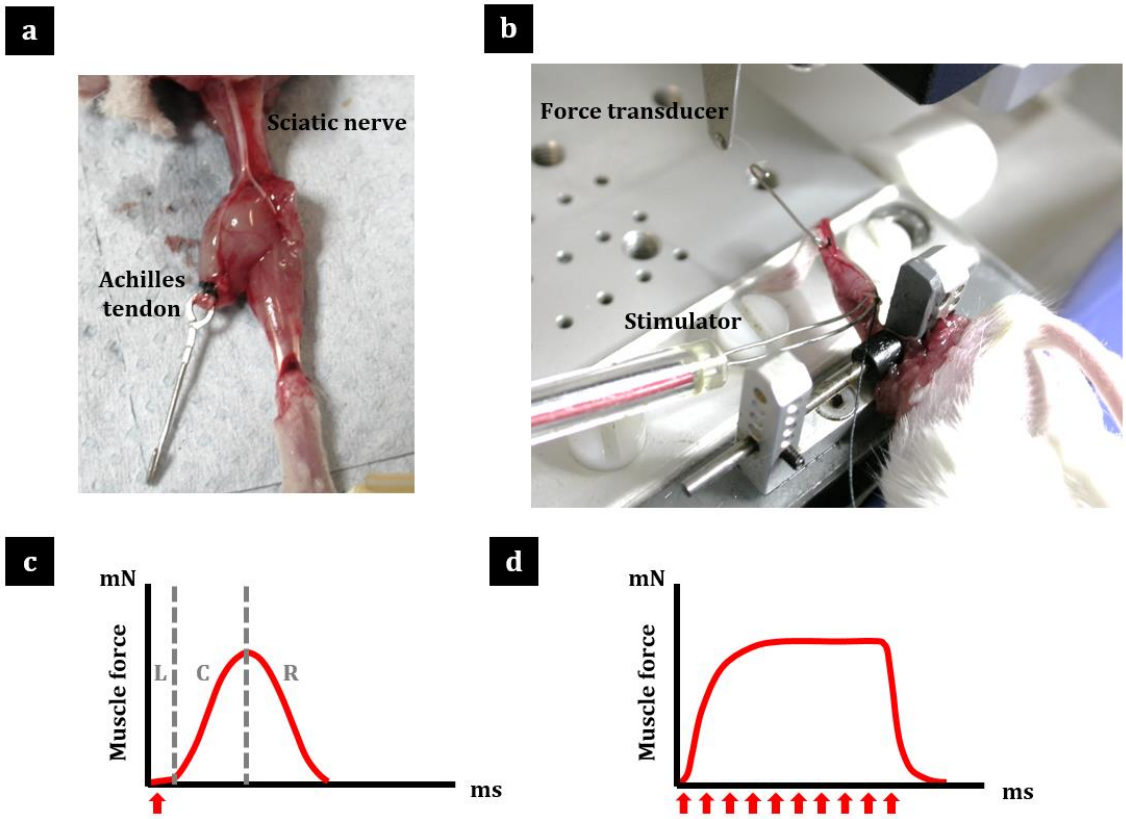

Figure 5. 1. Recording of muscle force under twitch and tetanus contraction. ***(a)*** *GA muscle and sciatic nerve were exposed under terminal anaesthesia and connected to a myograph.* ***(b)*** *In vivo myography setup. An electrode was placed on the sciatic nerve for direct stimulation while the Achilles tendon was tied to a force transducer.* ***(c)*** *Twitch contraction was produced by a single stimulation (red arrow) at the optimal muscle length and current (L= latent period, C= contraction, R=relaxation).* ***(d)*** *Tetanus contraction was produced by repeated stimulations (red arrows) with a frequency of 150 Hz that did not allow the relaxation of the muscle between single contractions.*

5.3.3. Statistical analysis.

N numbers were specified in each particular study. Statistical analysis was performed first by Levene's test to assess homogeneity of variance. When no significant differences were found in the variances of the different groups, statistical analysis was continued by one-way ANOVA and Tukey's post-hoc test. When variances were unequal, the analysis was followed with Welch ANOVA and Games-Howell's post-hoc test. Probability values <0.05 were regarded as significant. SPSS software, version 20.0 was used to perform these analyses.

5.4. Results.

5.4.1. Preparatory work: investigation of endogenous regeneration after skeletal muscle injury.

We first relied on the simplest model of skeletal muscle damage (i.m. administration of CTX) to select the most appropriate mouse strain in which to perform the injury and regeneration studies and to design the treatment regimens, with a special focus on the time of administration of reprogramming pDNA. CTX is a venom produced by the snake *Naja mossambica mossambica* that causes myofiber necrosis [269] and hence has been widely used both to model muscle injury and to study the innate regenerative response triggered upon.

5.4.1.1. Effects of CTX administration in skeletal muscle tissue of BALB/c and C57BL/6 mouse strains.

Driven by studies reporting significant differences in the regeneration capacity of different mouse genetic backgrounds [270, 271], we first aimed to identify the strain that would provide a wider time interval between muscle injury and regeneration to assess the effect of *in vivo* reprogramming to pluripotency. Three days after the i.m. administration of 30 µl CTX in the GA muscle, an inflammatory infiltrate was obvious to the naked eye in the tissues dissected from BALB/c but not C57BL/6 mice **(Figure 5.2b)**. Such observation, together with the significant increase in muscle weight compared to the contralateral (uninjured) hind limb also at day 3 **(Figure 5.2c)** and the incomplete clearance of necrotic fibers and restoration of normal tissue architecture 9 days after injury **(Figure 5.2d)**, illustrated the poorer and slower capacity of BALB/c skeletal muscle to regenerate compared to that of C57BL/6 mice. In light of these findings, the BALB/c strain was selected for the rest of the studies in this Chapter.

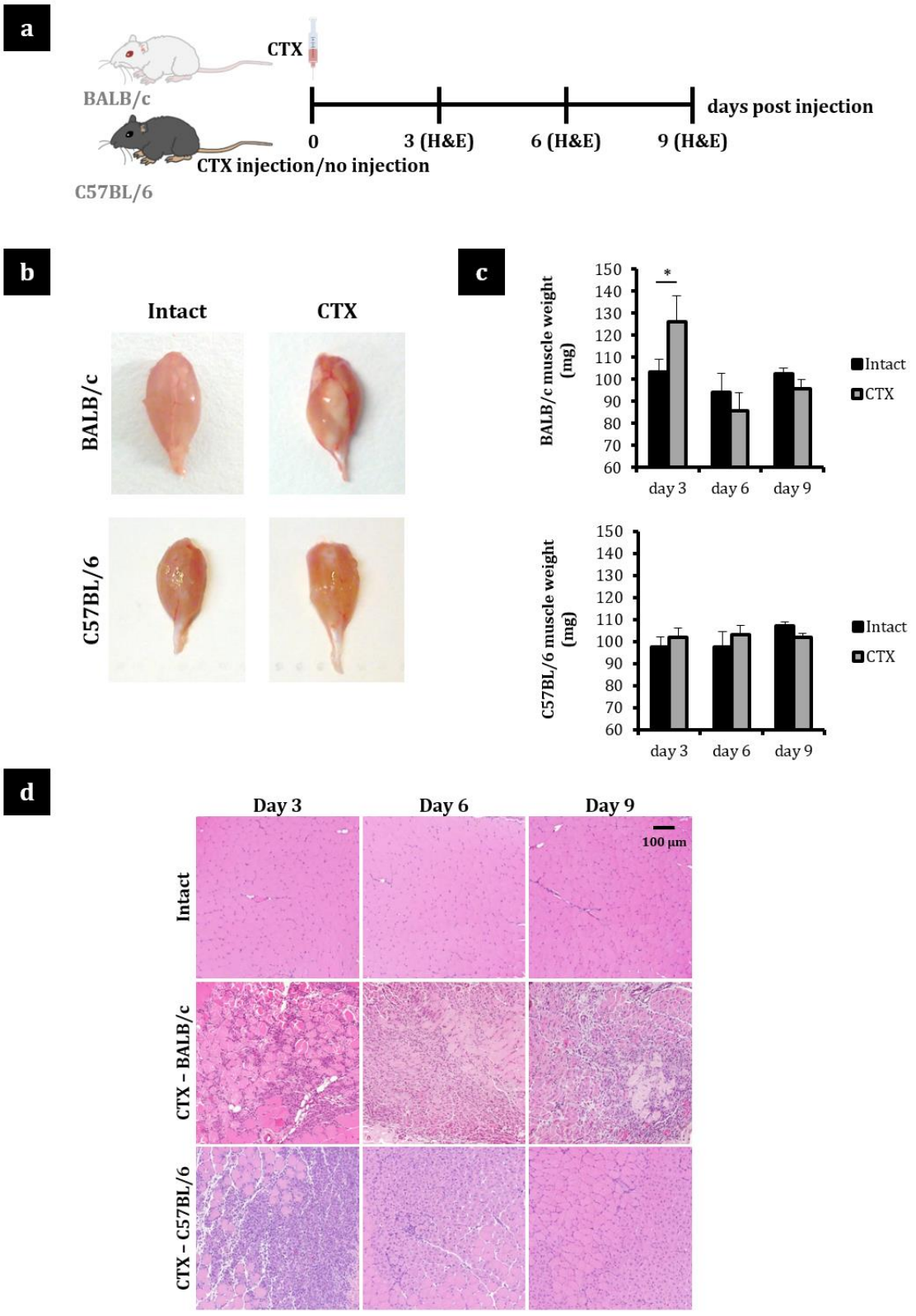

Figure 5. 2. Endogenous regeneration after i.m. injection of CTX in BALB/c and C57BL/6 mouse strains. (a) *30 µl CTX (10 µM) were i.m. administered in the left GA muscle of BALB/c and C57BL/ 6 mice. The right GA was left uninjected and used as control.* ***(b)*** *Macroscopic appearance of GA muscles 3 days after injection.* ***(c)*** *Muscle moist weight. *p<0.05 indicates statistically significant differences between the injured and healthy GA muscles, assessed by one-way ANOVA. Data are presented as mean ± SD, n=3.* ***(d)*** *H&E staining of muscle tissue sections at different time points after CTX injection (30X, scale bar represents 100 µm).*

5.4.1.2. Effects of the i.m. administration of CTX in the gene expression profile of the skeletal muscle over time.

Changes in gene expression at different time points after the injection of CTX in the GA muscle were studied next. This information was particularly relevant to design the therapeutic regimens in accordance to the changes induced by the insult in the muscle tissue. Muscle injury progresses through three defined phases: degeneration, regeneration and muscle remodeling [216], regardless of the nature of the insult. The first phase (degeneration) is characterised by an inflammatory response that takes place promptly after injury [5]. The expression of monocyte/macrophage markers involved in such stage was at its highest 3 days after CTX administration **(Figure 5.3b)**. *Il-6*, essential not only for macrophage infiltration but also for myoblast proliferation and hence for the success of regeneration [272], was highly upregulated on day 3 after injury, but its expression was significantly lower from day 6 onwards. The same trend was found for *Mcp-1*, while the upregulation of *Cd11b* and *Ccr2* was sustained for a longer period after CTX injection and only decreased significantly after day 9. The T cell marker *Cd3*, also typically involved in muscle inflammation and regeneration [272-274], showed a consistent but not significant upregulation compared to the healthy muscle control up to day 9, suggesting a lower contribution of these cells in the infiltration of the injured site.

The expression of the different myosin heavy chain (MyHC) isoforms is commonly used to monitor the progress of regeneration. While at the earliest stages of muscle degeneration embryonic and perinatal forms are highly upregulated, mRNA levels of adult isoforms plummet significantly. Such trend is progressively inverted as the tissue recovers [275]. We found that embryonic (*Myh3*) and perinatal (*Myh8*) isoforms were above 10-fold upregulated in the CTX-injected group throughout the course of the study **(Figure 5.3d)**, while the expression of adult isoforms (*Myh2*, *Myh4* and *Myh7*) was strongly downregulated on day 3 after injury but increased significantly after that time point and reached comparable levels to the intact control by day 15. The greatest change in the expression of these genes took place from days 3 to 6 after CTX administration, which together with the data on muscle weight, histological investigation and expression of inflammation markers pointed at day 3 as the summit of the degeneration phase.

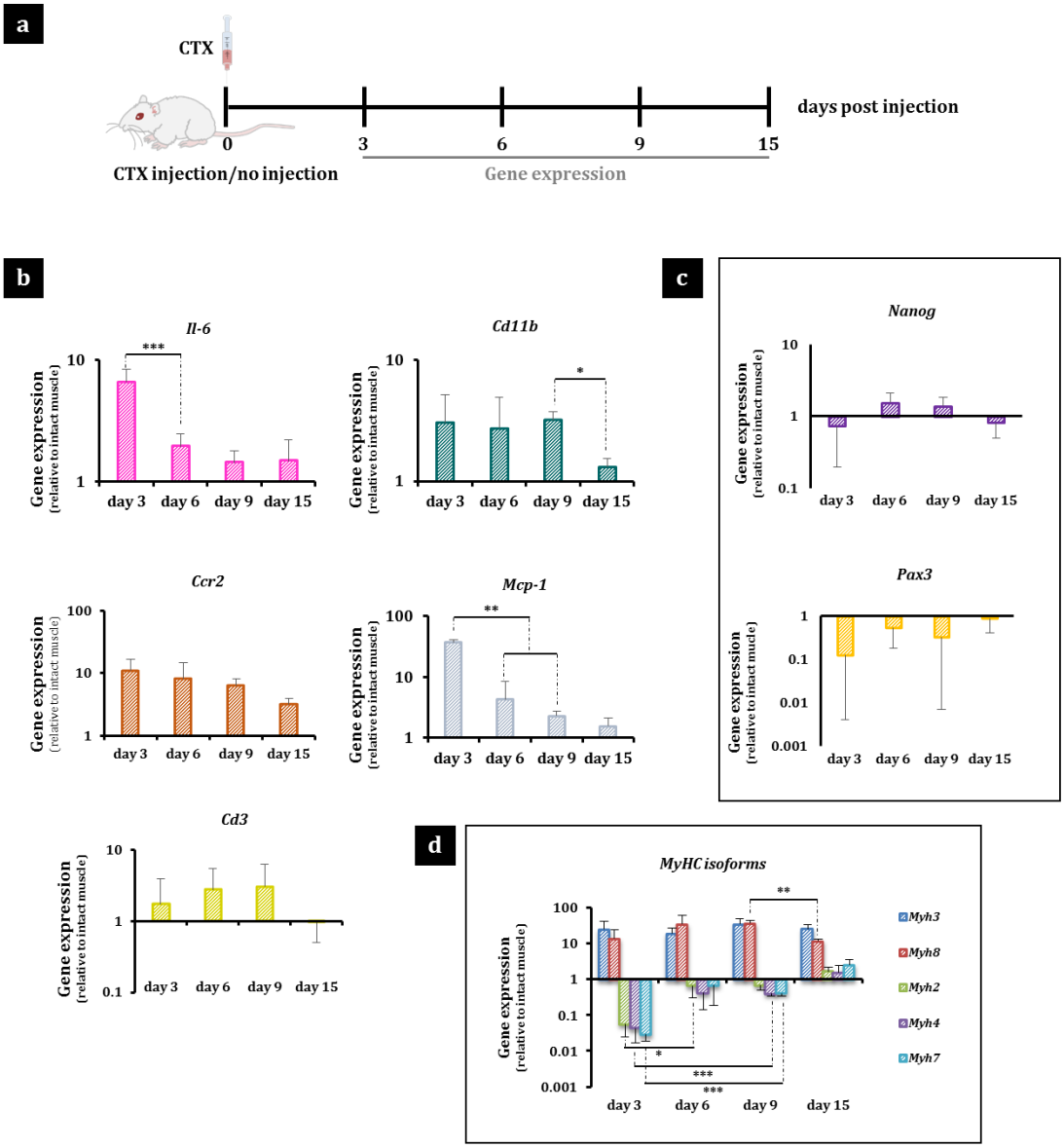

Figure 5. 3. Changes in gene expression in the GA muscle after i.m. administration of CTX. (a) *BALB/c mice were i.m. administered with 30 µl CTX (10 µM) in the left GA. The right GA was left uninjected as control and real-time RT-qPCR was conducted to determine the relative gene expression of* ***(b)*** *inflammation markers* ***(c)*** *genes upregulated upon in vivo reprogramming to pluripotency in healthy skeletal muscle and* ***(d)*** *myosin heavy chain (MyHC) isoforms. Gene expression was normalised to that of uninjected (intact) muscle. *p<0.05, **p<0.01 and ***p<0.001 indicate statistically significant differences in gene expression among different time points after CTX injection. For Pax3 expression, *p<0.05 indicates a statistically significant difference compared to the uninjected control Statistical significance was assessed by one-way ANOVA and Tukey's test or Welch ANOVA and Games-Howell's test. Data are presented as mean ± SD, n=3.*

Finally, it was also of interest to investigate injury-induced changes in the expression of genes involved in *in vivo* reprogramming to pluripotency in healthy skeletal muscle. *Nanog* was upregulated on days 6 and 9 after injury, whereas *Pax3* was downregulated for the duration of the study but more prominently at the earliest time points after injury **(Figure 5.3c)**.

5.4.2. *In vivo* reprogramming to pluripotency in a chemically-induced model of skeletal muscle injury: i.m. administration of CTX.

5.4.2.1. Administration of reprogramming pDNA at different time points after CTX injury: definition of "early intervention" and "late intervention" protocols.

The potential of *in vivo* reprogramming to pluripotency to enhance regeneration was then first interrogated in the CTX injury model. The injection of 30 µl CTX (10 µM) in the left GA was followed by the administration, in the same muscle, of two doses (on two consecutive days) of 50 µg **OKS** and 50 µg **M** each or the equivalent volume (50 µl) of 0.9% saline, as established in a previous work (data not shown). The contralateral hind limb was left uninjured and uninjected and used as internal control. In light of the previous observations, we classified the therapeutic regimens under two groups: "early intervention" protocols, when **OKS**+**M** or saline were administered prior to day 3 and thus during the bulk of the degeneration phase; and "late intervention" protocols, when the administration of reprogramming factors took place after day 3 and hence after the peak of such phase. One "early intervention" protocol - **OKS**+**M** or saline administered at the time of injury and one day later (d0+1) - and two "late intervention" regimens - **OKS**+**M** or saline administered on days 5 and 6 (d5+6) or on days 7 and 8 (d7+8) after CTX injection – were tested **(Figure 5.4)**. Since the peak of reprogramming in healthy skeletal muscle was reached two days after the administration of reprogramming pDNA **(Chapter IV, Figure 4.8)**, muscles were dissected at such time (days 3, 8 and 10 after injury, respectively) for further analysis.

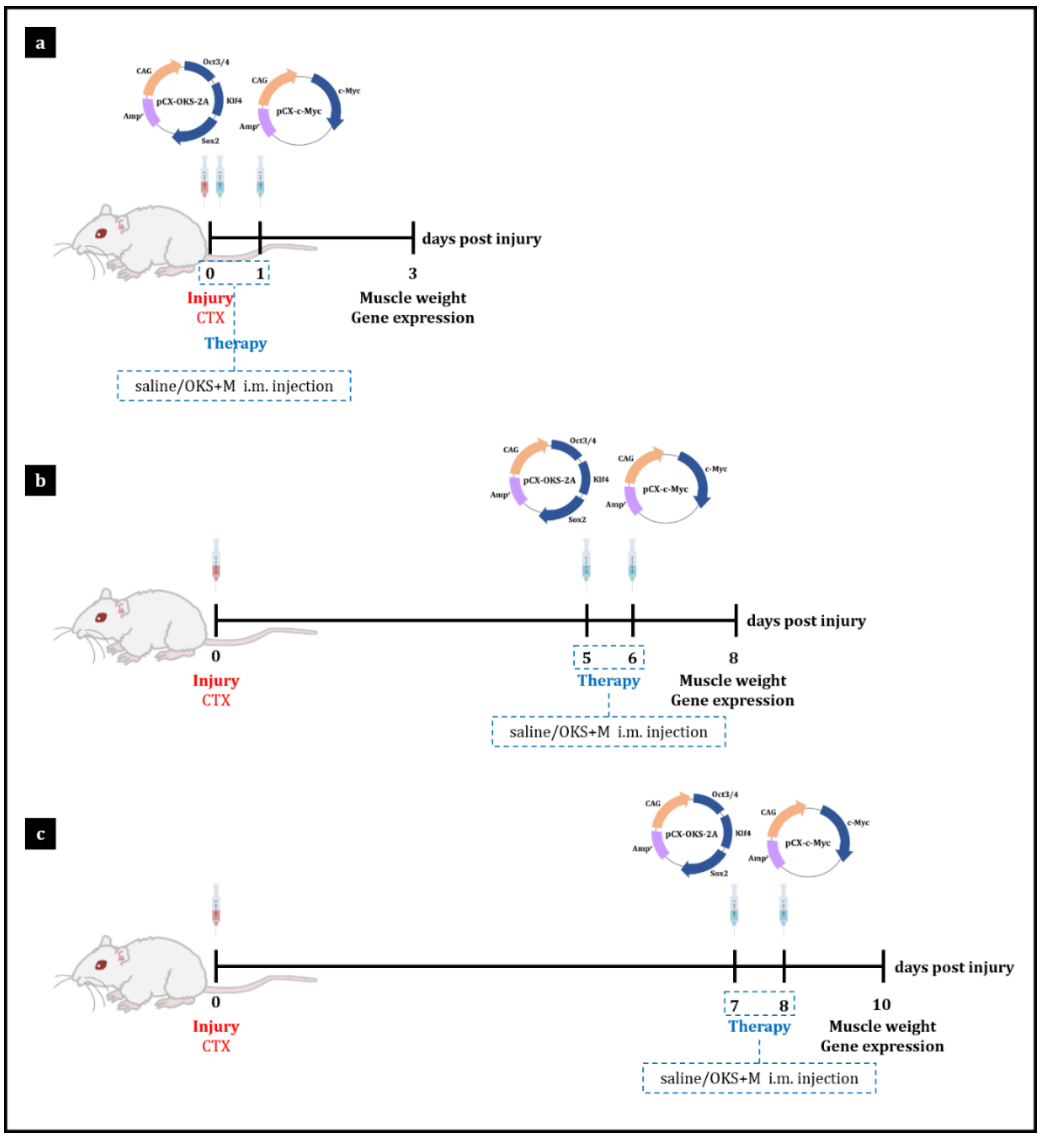

Figure 5. 4. Administration of reprogramming pDNA at different time points after CTX injection. *30 µl CTX (10 µM) were i.m. administered in the BALB/c left GA at day 0. Two doses of 50 µg* ***OKS*** *and 50 µg* ***M*** *each or the equivalent volume (50 µl) of 0.9% saline were i.m. administered in the same muscle on* ***(a)*** *day 0 (immediately after CTX injection) and day 1* ***(b)*** *days 5 and 6 or* ***(c)*** *days 7 and 8 after CTX injection. The right hind limb was left uninjured and uninjected and used as internal control. Tissues were dissected 2 days after the last pDNA or saline administration for gene expression and muscle weight analysis, n=3.*

Macroscopic evaluation and changes in muscle weight.

Macroscopic observation upon dissection revealed the presence of an inflammatory infiltrate in the specimens injected with CTX, which was very prominent for those collected 3 days after injury and was progressively reduced when the tissues were collected at later time points. No obvious differences between saline and **OKS+M** groups were observed **(Figure 5.5a)**. We weighed the GA muscles upon dissection to investigate whether the administration of reprogramming factors would have any effect on the changes in muscle weight

produced by the injury. In agreement with our studies with CTX administration only **(Figure 5.2)**, muscle weight increased in injured specimens compared to intact controls early after injury (day 3). At later time points, a significant decrease in muscle weight was consistently observed in CTX-injected muscles. However, no differences were observed at any time point between **OKS+M** and saline-treated GA muscles **(Figure 5.5b)**.

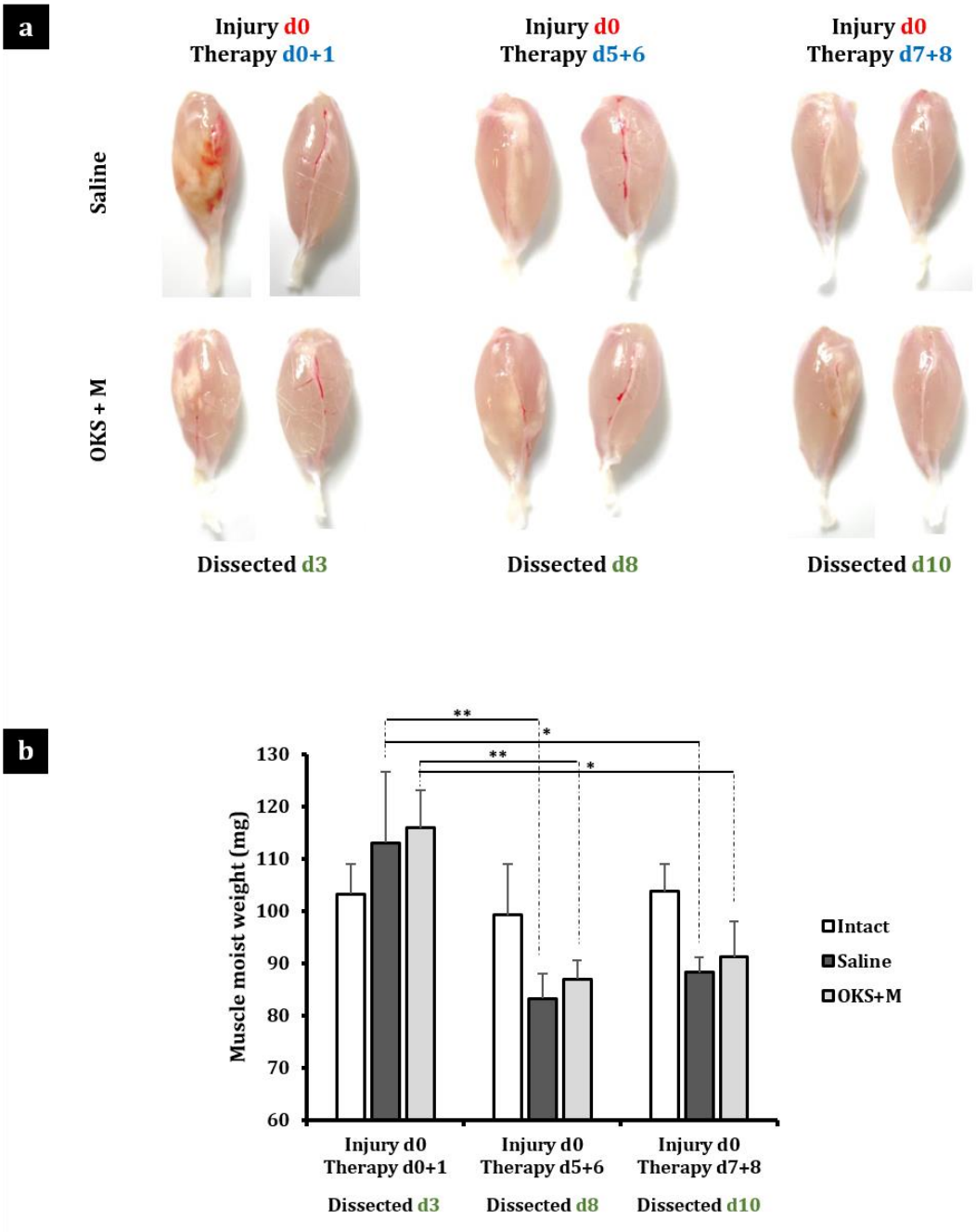

Figure 5. 5. Macroscopic evaluation and changes in muscle moist weight after CTX injury and i.m. administration of reprogramming pDNA. (a) *GA muscles dissected 2 days after the last administration of* ***OKS+M*** *or saline (injured vs. contralateral intact control).* ***(b)*** *Muscle moist weight. *p<0.05 and **p<0.01 indicate statistically significant differences in muscle weight among groups, assessed by one-way ANOVA and Tukey's test. Data are presented as mean ± SD, n=3.*

Changes in gene expression.

The expression of reprogramming factors and induction of pluripotency in the context of an injured microenvironment was then investigated. *Oct3/4* mRNA levels 2 days after the last administration of **OKS**+**M** did not suggest differences in the efficiency of *in vivo* transfection when the reprogramming factors were administered at different time points after injury **(Figure 5.6a)**. A different scenario was however found when the expression of *Nanog* was investigated. While the "early intervention" failed to induce the expression of the pluripotency marker, this gene was upregulated compared to the intact **(Figure 5.6b)** and saline-injured **(Figure 5.6c)** controls when reprogramming factors were administered on d5+6 after the onset of injury, and such upregulation was even higher when the administration took place on d7+8.

Only with the latter intervention were we able to prove statistically significant differences in the expression of *Nanog* between the **OKS**+**M** and saline-injured groups. These results suggested that the time of administration of reprogramming pDNA after injury could be important for the pluripotency outcomes. In addition, the administration of such reprogramming pDNA in the injured scenario failed to reproduce the upregulation of the myogenic progenitor marker *Pax3*, characteristically observed early upon *in vivo* reprogramming to pluripotency in healthy skeletal muscle **(Figure 5.6d)**. On the contrary, and as reported after the administration of CTX alone **(Figure 5.3c)**, this transcription factor was strongly downregulated in all injured groups, irrespective of the administration of saline or **OKS+M**, and for the entire duration of the study (15 days after the injury). As a result, *Pax3* expression could not be used as an indication of successful *in vivo* reprogramming in this injury model.

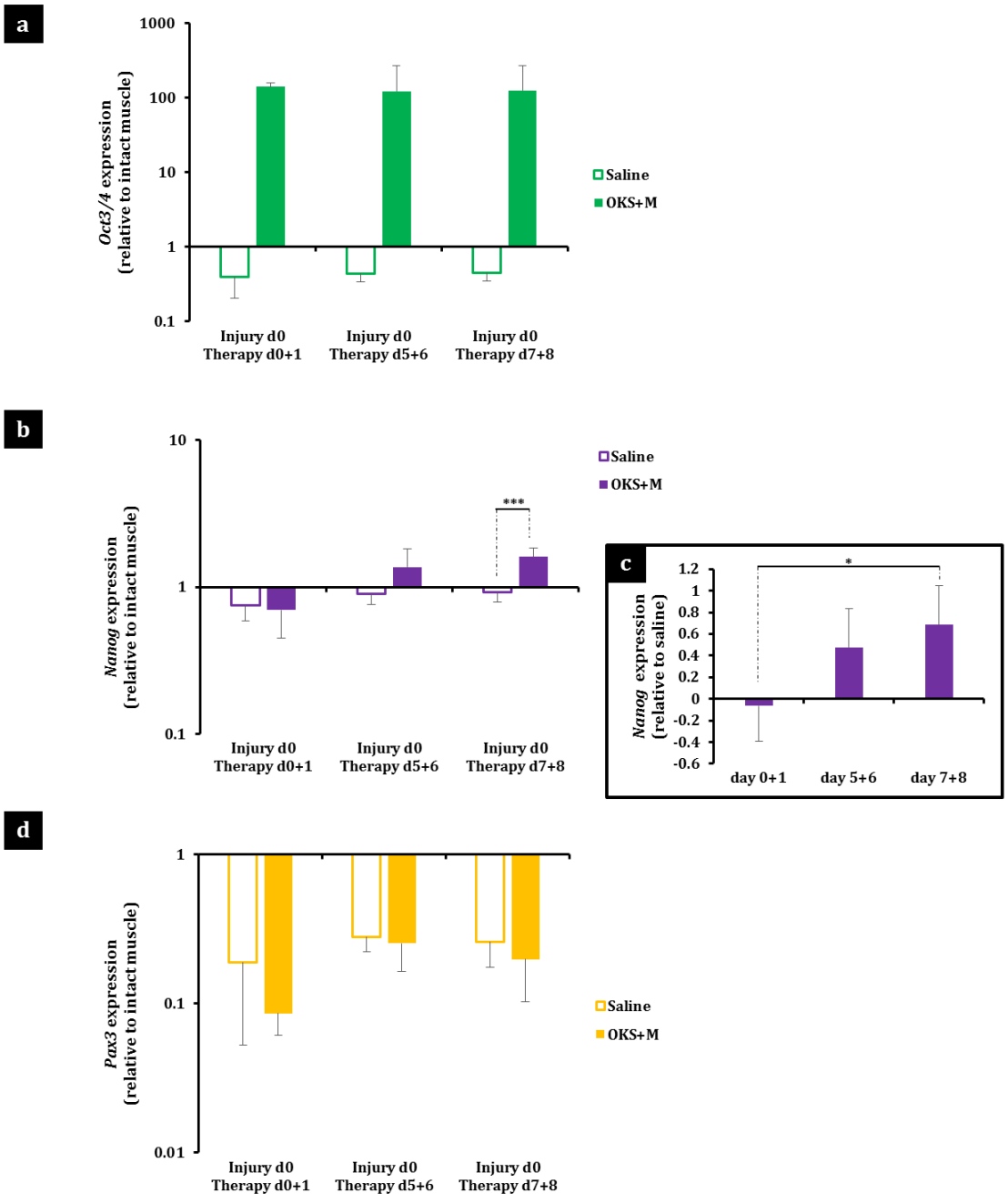

Figure 5. 6. Changes in gene expression after CTX injury and i.m. administration of reprogramming pDNA. *Real-time RT-qPCR was performed 2 days after the last administration of* ***OKS+M*** *or saline (3, 8 or 10 days after injury) to determine the relative gene expression of* ***(a)*** *the reprogramming factor Oct3/4* ***(b)*** *the pluripotency marker Nanog (normalised to uninjured, uninjected controls),* ***(c)*** *the pluripotency marker Nanog (normalised to injured, saline-injected controls) and* ***(d)*** *the myogenic progenitor marker Pax3. Oct3/4 and Pax3 expression was normalised to that of intact muscle controls. *p<0.05 and ***p<0.001 indicate statistically significant differences between groups, assessed by one-way ANOVA and Tukey's test or Welch ANOVA and Games-Howell's test. Data are presented as mean ± SD, n=3.*

5.4.2.2. Tissue regeneration upon i.m. administration of reprogramming pDNA on days 7 and 8 after CTX injury.

We next fixed the administration of **OKS**+**M** or saline at d7+8 after CTX injection ("late intervention" protocol) on the grounds of the higher *Nanong* upregulation. We aimed to investigate the effects of the induction of pluripotency *in vivo* on the regeneration of the skeletal muscle by examining the tissues 2 and 7 days after the last administration of **OKS**+**M** or saline (10 and 15 days after injury, **Figure 5.7a**). Regenerating myofibers are characterised by the centralized position of the nucleous, which migrates to the edges of the cell once they are fully differentiated and mature[216]. The number of centronucleated (regenerating) myofibers around the site of injury was counted on H&E stained tissue sections and expressed as a percentage of the total number of myofibers (mean ± SD, **Figure 5.7b**). No significant differences in the percentage of regenerating myofibers were observed between saline and **OKS**+**M** groups 10 days after the injection of CTX (59.4 ± 12.2 % saline, 63.2 ± 15.4 % **OKS**+**M**) and such numbers remained also invariable 15 days after injury (55.9 ± 21.5 % saline, 65.7 ± 11.1 % **OKS**+**M**).

The generation of a collagen-based fibrotic scar is one of the most important factors precluding the complete functional rehabilitation of injured skeletal muscle tissue [5, 252]. Picrosirius red/fast green staining, which specifically dyes collagen in magenta and myofibers in green, revealed the existence of moderate collagen deposits in the site of injury **(Figure 5.7c)**. However, no differences in the extension of such deposits, expressed as a percentage of the selected area (mean ± SD), were found between treatment groups or time points after injury (**day 10:** 0.6 ± 0.2 % intact, 9.4 ± 3.9 % saline, 9.6 ± 3.2 % **OKS**+**M**, **day 15:** 0.7 ± 0.2 % intact, 11.9 ± 3.2 % saline, 11.6 ± 4.7 % **OKS**+**M**).

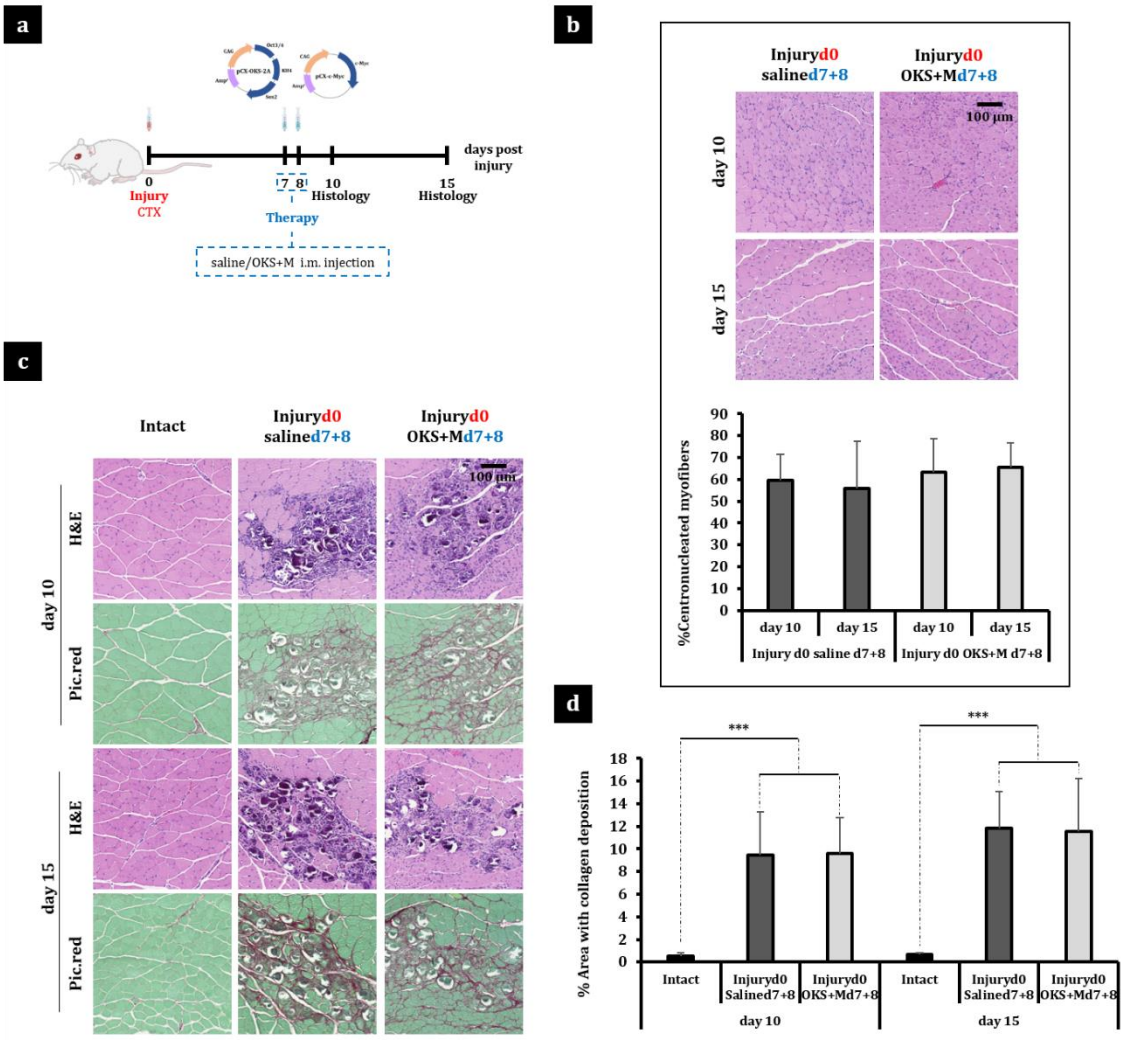

Figure 5. 7. Histological evaluation of skeletal muscle tissues after CTX injury (day 0) and i.m. administration of reprogramming pDNA (days 7 and 8)*. **(a)** 30 µl CTX (10 µM) were injected in the left BALB/c GA and two doses of 50 µg **OKS** and 50 µg **M** each or the equivalent volume (50 µl) of 0.9% saline were administered on days 7 and 8 after injury. The right GA was left uninjured and uninjected and used as control. Tissues were dissected 2 and 7 days after the last pDNA administration (10 and 15 days after injury) and analysed histologically. **(b)** H&E staining (40X, scale bar represents 100 µm) and quantification of % of centronucleated myofibers (n=2-4 GA muscles per condition, 3 sections per muscle, 2 random fields per section; data are presented as mean ± SD). **(c)** Picrosirius red/fast green staining for collagen and H&E staining of the same cross-section (40X, scale bar represents 100 µm). **(d)** Quantification of collagen deposition. ***p<0.001 indicates statistically significant differences between the intact control and the injured groups, analysed by Welch ANOVA and Games-Howell's test, (n=2-4 GA muscles per condition, 4 sections per muscle, 3 random fields per section; data are presented as mean ± SD).*

5.4.2.3. Investigation of functional rehabilitation upon i.m. administration of reprogramming pDNA on days 7 and 8 after CTX injury.

Our final goal was to investigate whether reprogramming the skeletal muscle to pluripotency after injury would improve its functional recovery. Muscle function was investigated in terminally anaesthetised mice by directly stimulating the sciatic nerve and recording the muscle force produced under twitch and

tetanus contraction, as detailed in the Materials and Methods section of this Chapter **(Section 5.3.2.5, Figure 5.1)**. 83.3 ± 15.9 % of the twitch and 72.7 ± 14.5 % of the tetanus force of the contralateral (intact) GA, expressed as mean ± SE, had already been recovered in the **OKS+M** group by day 10 after injury **(Figure 5.8)**, only 2 days after the administration of reprogramming factors. However a very similar result was observed in the saline control (82.6 ± 15.7 % twitch, 68.2 ± 7.6 % tetanus). Even 15 days after CTX injury, 7 days after the last **OKS+M** administration, such intervention did not generate any significant difference in the recovered force compared to saline-injected controls (**OKS+M**: 67.3 ± 9.5 % twitch, 57.4 ± 10.6 % tetanus; saline: 100.7 ± 22.1 % twitch, 60.4 ± 20.5 % tetanus).

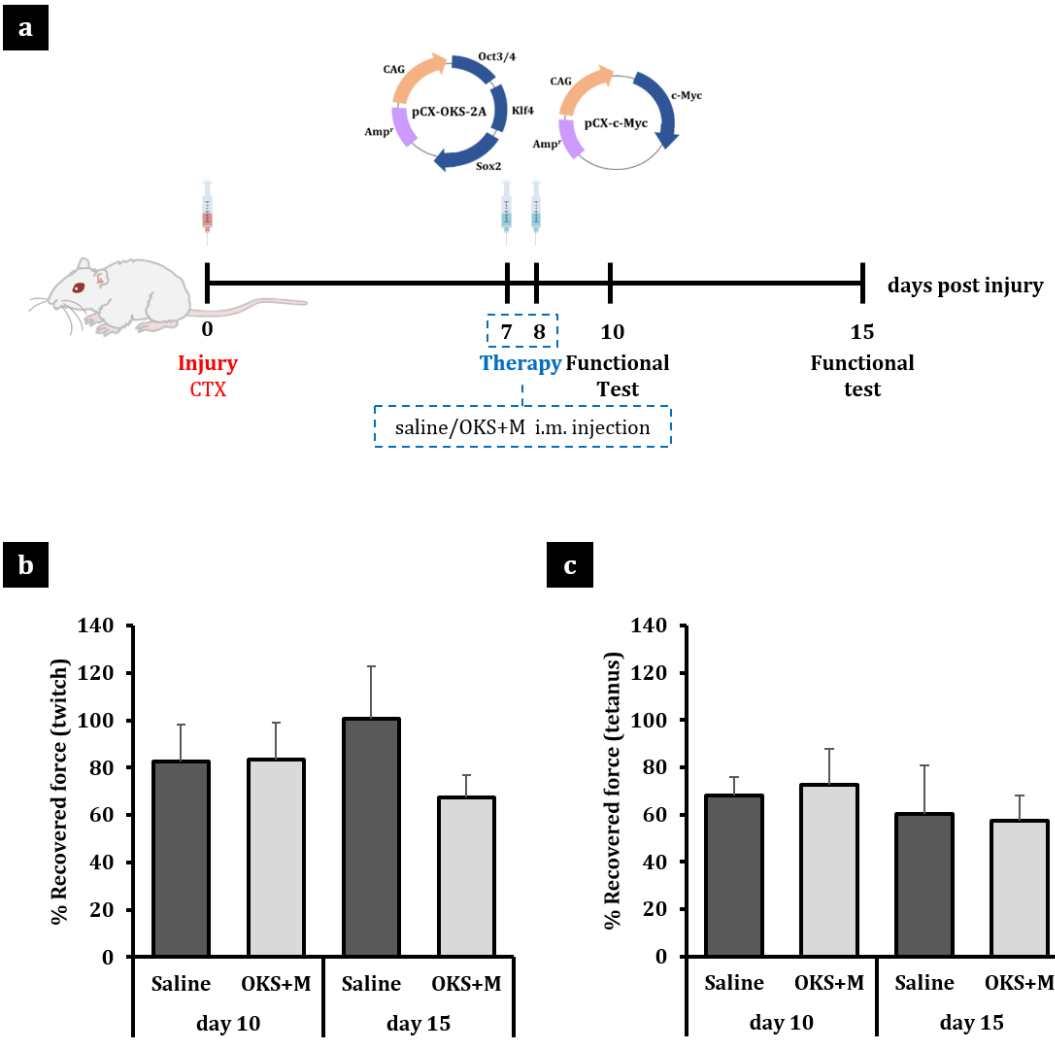

Figure 5. 8. Investigation of functional rehabilitation after CTX injury (day 0) and i.m. administration of reprogramming pDNA (days 7 and 8). (a) *30 µl CTX (10 µM) were injected in the left BALB/c GA and two consecutive doses of 50 µg* ***OKS*** *and 50 µg* ***M*** *each or the equivalent volume (50 µl) of 0.9% saline were administered at days 7 and 8 after injury. The right GA was left uninjured and uninjected and used as control. Muscle function was assessed 2 and 7 days after the last pDNA administration (10 and 15 days after injury).* ***(b)*** *Recovered forces of the injured GA under twitch and tetanus contraction are expressed as a percentage of the contralateral (uninjured) GA force. Data are presented as mean ± SE, n=4.*

5.4.3. *In vivo* reprogramming to pluripotency in a physically-induced model of skeletal muscle injury: laceration of GA, soleus and plantaris muscles.

We next sought to explore the therapeutic potential of *in vivo* reprogramming to pluripotency in a more anatomically localised and clinically relevant injury model. The left GA, soleus and plantaris muscles of BALB/c mice were surgically lacerated in the transverse plane as represented in **Figure 5.9a**. The right hind limb was left uninjured and used as an intact control.

5.4.3.1. Administration of reprogramming pDNA at different time points after laceration of GA, soleus and plantaris muscles.

A single dose of 100 μg **OKSM** or the equivalent volume (40 μl) of 0.9% saline was i.m. administered in the injured (left) hind limb at the time of injury (day 0) or 2 days later (day 2). The uninjured (right) hind limb was left uninjected. Tissues were collected at different time points including 2, 4 and 7 days after injury (2 and 5 days after **OKSM** or saline administration), as indicated in **Figure 5.9b**.

Changes in muscle weight.

When muscles were dissected at different time points after injury, a similar trend was observed for the saline and **OKSM**-injected specimens, without significant differences between the two treatment groups. Overall, the ratio injured/intact was high early after injury but decreased over time and was <1 by day 7 **(Figure 5.9c)**, which agreed with the observations in the CTX model.

Changes in gene expression.

The lack of *Oct3/4* expression when **OKSM** was administered at the time of injury **(Figure 5.10a)** confirmed the technical limitations encountered during the surgical procedure (i.e. impossibility to retain the pDNA solution in the tissue). On the contrary, the administration of reprogramming factors 2 days later resulted in *Oct3/4* mRNA levels comparable to those obtained in the CTX injury model.

As predicted from the above observations, we could not detect a significant upregulation of *Nanog* compared to the intact control when **OKSM** was administered on day 0. More unexpectedly, the administration of reprogramming factors 2 days later also failed to trigger the expression of *Nanog* above the levels

observed in the saline control, hence most probably attributed to the initiation of the endogenous regenerative response. All such mRNA levels were in fact only marginally higher than those of the intact controls **(Figure 5.10b)**. *Pax3* was strongly downregulated early after injury in both treatment groups **(Figure 5.10c)**. Only 7 days after injury were we able to detect significantly higher mRNA levels of such gene in the **OKSM** group compared to the saline control, however, the absence of clear *Nanog* upregulation rested importance to this finding.

5.4.3.2. Tissue regeneration upon i.m. administration of reprogramming pDNA 2 days after laceration of GA, soleus and plantaris muscles.

Histological investigation of the above muscles 7 days after injury (5 days after the administration of **OKSM** or saline, **Figure 5.11a**) reported no differences in the percentage of centronucleated (regenerating) myofibers between treatment groups (47.5 ± 20.8 % saline, 47.3 ± 14.6 % **OKSM**) as illustrated in **Figure 5.11b**. The establishment of severe muscle damage was evidenced by a remarkable inflammatory infiltrate in the injured site and the deposition of collagen, considerably more prominent than in the chemically-induced model **(Figure 5.11c)**. Collagen accumulation was quantitatively similar in all injured specimens **(Figure 5.11d)**, regardless of the treatment group (2.1 ± 1.2 % intact, 28.8 ± 8.1 % saline, 21.3 ± 9.0 % **OKSM**).

Only “early intervention” protocols were investigated in this particular injury model. The severity of the damage precluded further investigations and prompted the development of a more moderate model.

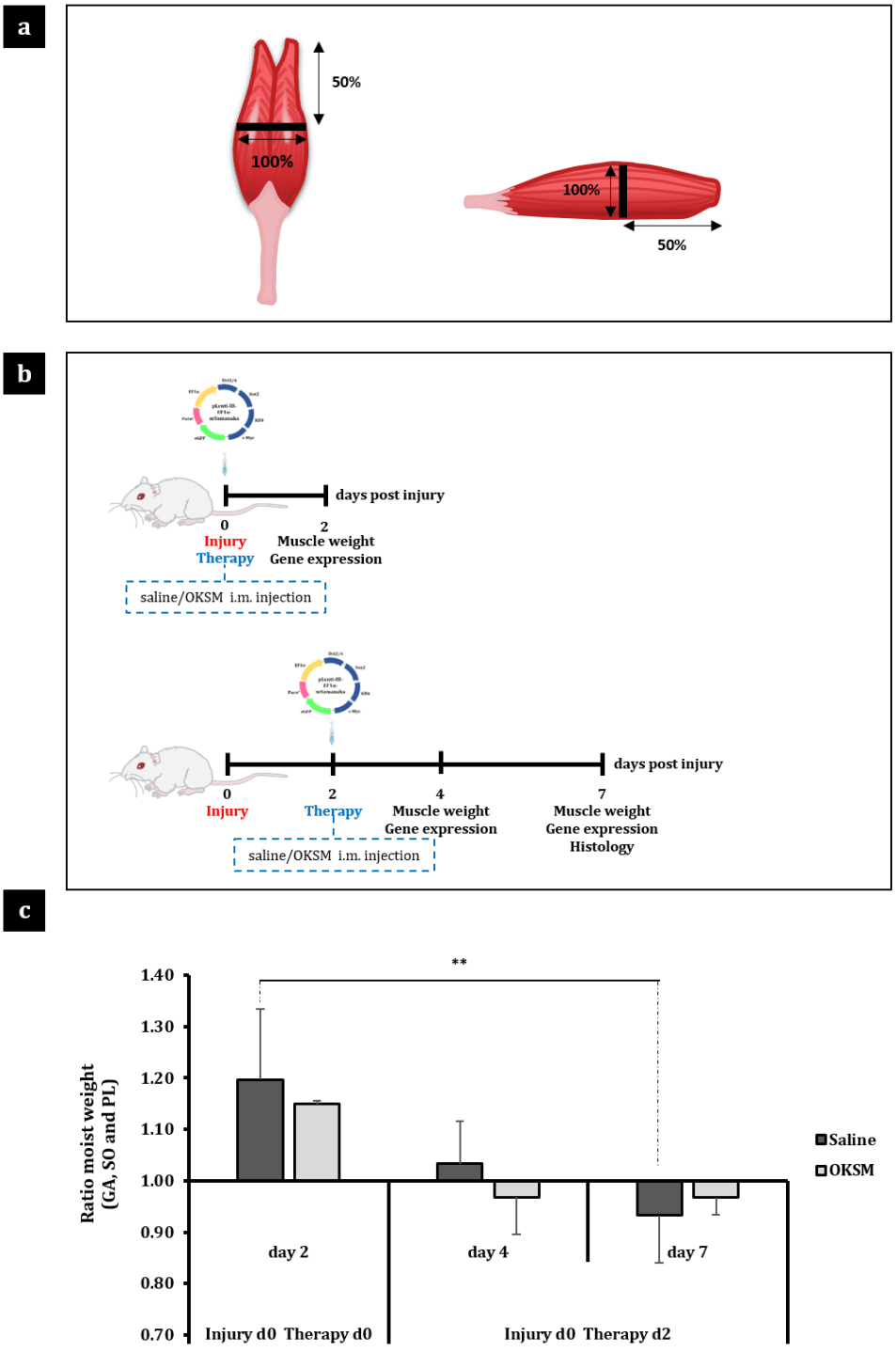

Figure 5. 9. Laceration of GA, soleus and plantaris muscles and i.m. administration or reprogramming pDNA. (a) *The left GA, soleus and plantaris muscles of BALB/c mice were surgically lacerated in the transverse plane. The cut was performed at its mid-point and through the 100% of their width and depth.* ***(b)*** *100 µg* ***OKSM*** *or the equivalent volume (40 µl) of 0.9% saline were administered at the time of injury or 2 days later* ***(c)*** *Muscle weight was recorded 2, 4 and 7 days after laceration (2 and 5 days after pDNA or saline administration) and expressed as a ratio injured/intact. **p<0.01 indicates statistically significant differences in the injured/intact ratio of the saline group between days 2 and 7 after injury, analysed by one-way ANOVA and Tukey's test. Data are presented as mean ± SD, n=3.*

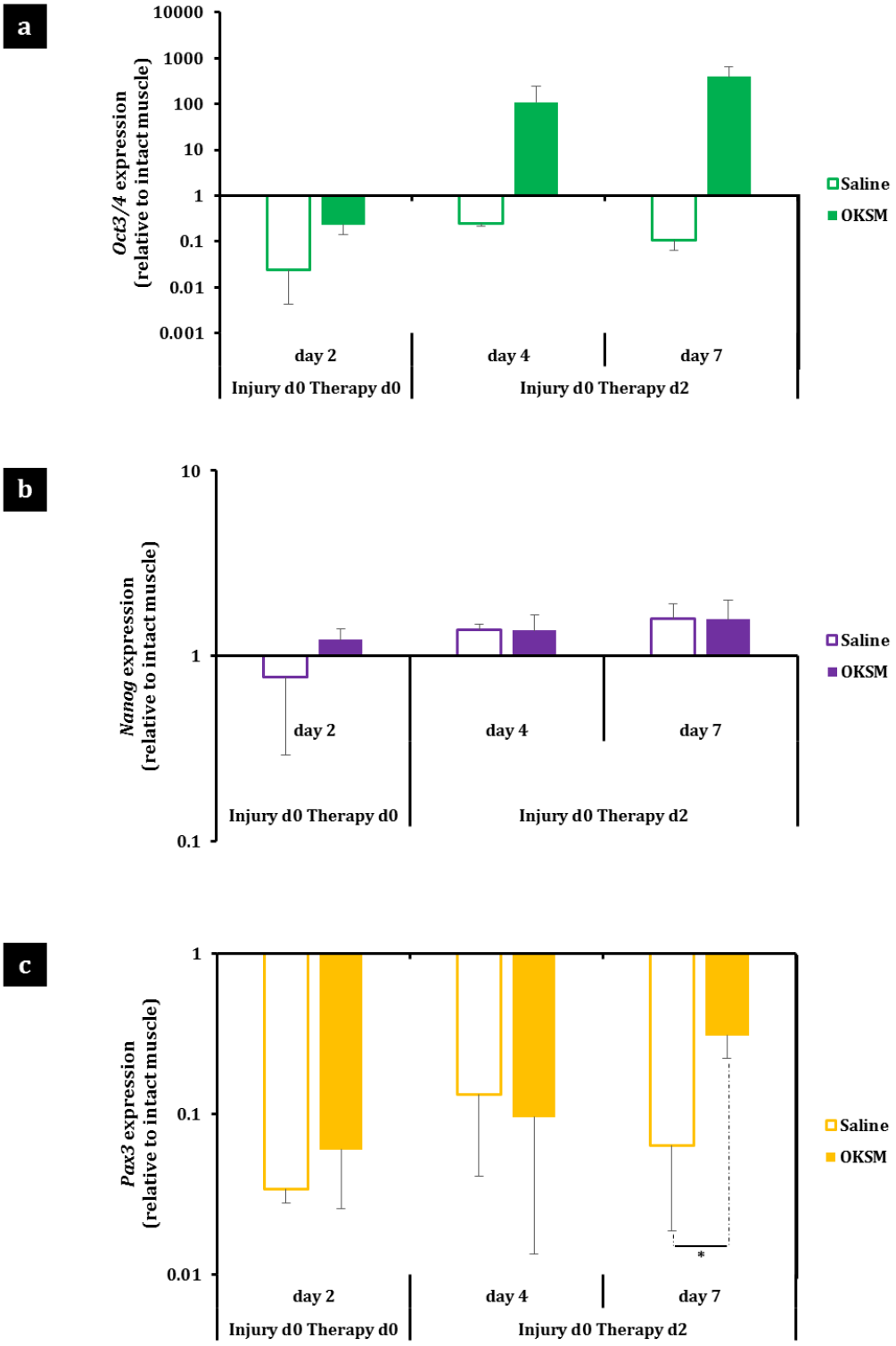

Figure 5. 10. Changes in gene expression after laceration of GA, soleus and plantaris muscles and i.m. administration of reprogramming pDNA. *Real-time RT-qPCR was performed 2 and 5 days after the administration of reprogramming pDNA or saline control (2, 4 and 7 days after laceration) to analyse the relative gene expression of* ***(a)*** *the reprogramming factor Oct3/4* ***(b)*** *the pluripotency marker Nanog* ***(c)*** *the myogenic progenitor marker Pax3. Gene expression was normalised to the intact muscle control. *p<0.05 indicates statistically significant differences in gene expression between groups, assessed by Welch ANOVA and Games-Howell's test. Data are presented as mean ± SD, n=3.*

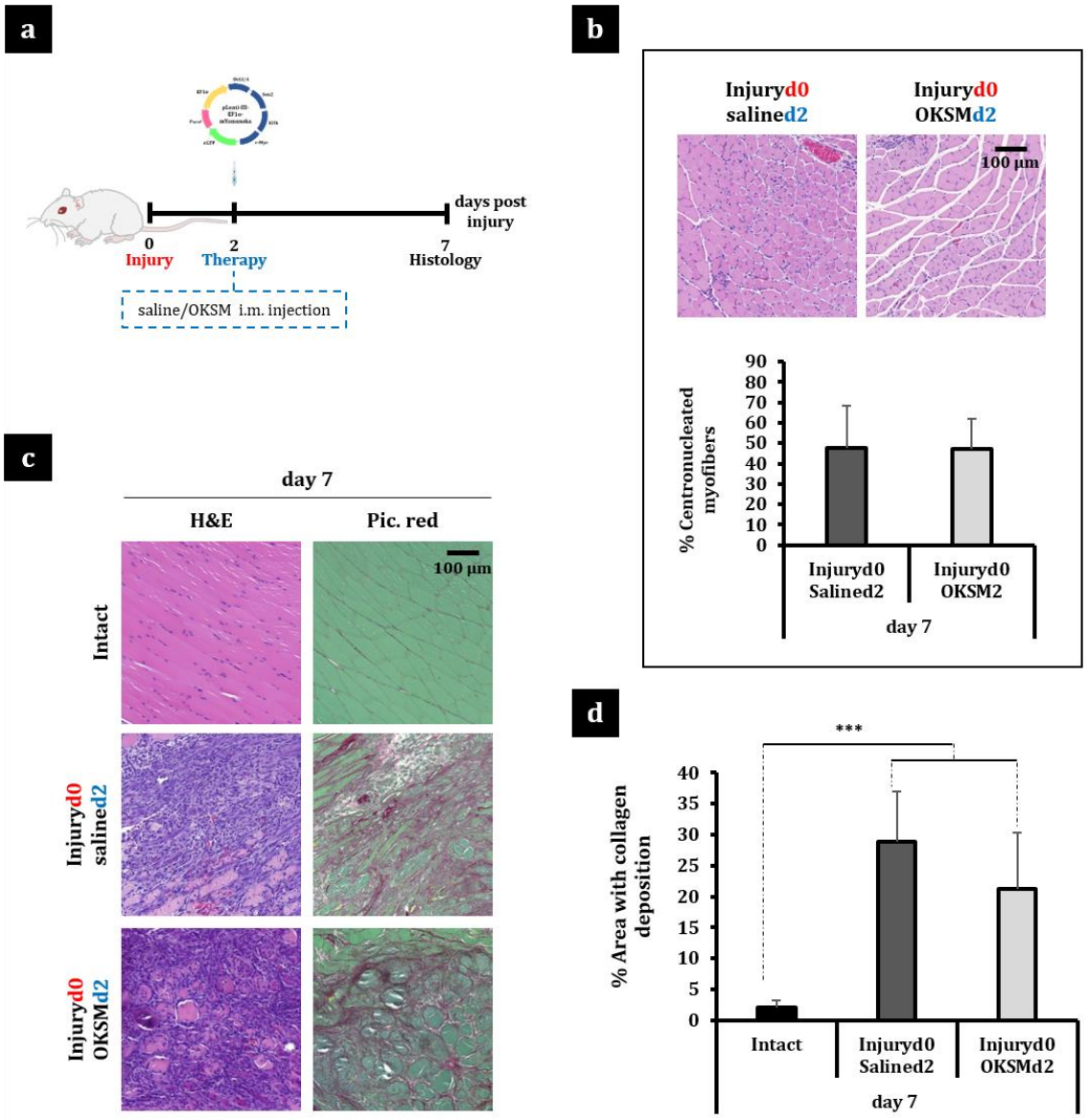

Figure 5. 11. Histological evaluation after laceration of GA, soleus and plantaris muscles (day 0) and i.m. administration of reprogramming pDNA (day 2). (a) *The left GA, soleus and plantaris muscles of BALB/c mice were surgically lacerated and 100 µg* ***OKSM*** *or the equivalent volume (40 µl) of 0.9% saline were i.m. administered 2 days after injury. The right hind limb was left uninjured and uninjected and used as control. Tissues were dissected 7 days after laceration for histological investigation.* ***(b)*** *H&E staining (40X, scale bar represents 100 µm) and quantification of % of centronucleated myofibers (n=3 GA muscles per condition, 3 sections per muscle, 3 random fields per section). Data are presented as mean ± SD.* ***(c)*** *Picrosirius red/fast green staining for collagen and H&E staining of the same cross-section (40X, scale bar represents 100 µm).* ***(d)*** *Quantification of collagen deposition. ***p<0.001 indicates statistically significant differences between the intact control and the injured groups, analysed by Welch ANOVA and Games-Howell's test (n=3 GA muscles per condition, 3 sections per muscle, 3 random fields per section). Data are presented as mean ± SD.*

5.4.4. *In vivo* reprogramming to pluripotency in a physically-induced model of skeletal muscle injury: laceration of medial GA.

Aiming to establish an equally clinically relevant and anatomically localised but more moderate injury model, we transversely lacerated the medial GA in the left BALB/c hind limb, preserving the lateral GA, soleus and plantaris and leaving the contralateral (right) hind limb uninjured as intact control. An illustration of the anatomical localisation and dimensions of the defect is provided in **Figure 5.12a**.

5.4.4.1. Administration of reprogramming pDNA at different time points after laceration of medial GA.

A single dose of 100 μg **OKSM** or the equivalent volume (40 μl) of 0.9% saline was i.m. administered in the injured GA at the time of injury (day 0, "early intervention") or 5 or 7 days later ("late intervention" protocols). The contralateral (right) hind limb was left intact (uninjured and uninjected) and GA muscles were dissected 2 days after the administration of **OKSM** or saline (2, 7 and 9 days after laceration, respectively, **Figure 5.12b**). The medial and lateral GA were then processed separately for muscle weight and gene expression studies.

Macroscopic evaluation.

Macroscopic observation of the GA muscles harvested at different time points after injury suggested the progressive retraction of the medial head, however no obvious differences were confirmed between saline and **OKSM**-injected groups **(Figure 5.13a)**.

Changes in muscle weight.

A significant increase in the moist weight of the whole GA was observed soon after laceration which, in agreement with the findings in previous injury models, decreased at later time points. By day 9 after laceration, the ratio injured/intact was < 1 **(Figure 5.13b)**. The separate analysis of the medial and lateral heads confirmed that the progressive loss of mass took place specifically in the directly injured tissue (medial head, **Figure 5.13c**) and was very significant by day 9 after injury. Conversely, the initial increase in muscle weight was almost exclusively due to the increase in the lateral GA mass **(Figure 5.13d)**. Such findings were however common for both treatment groups.

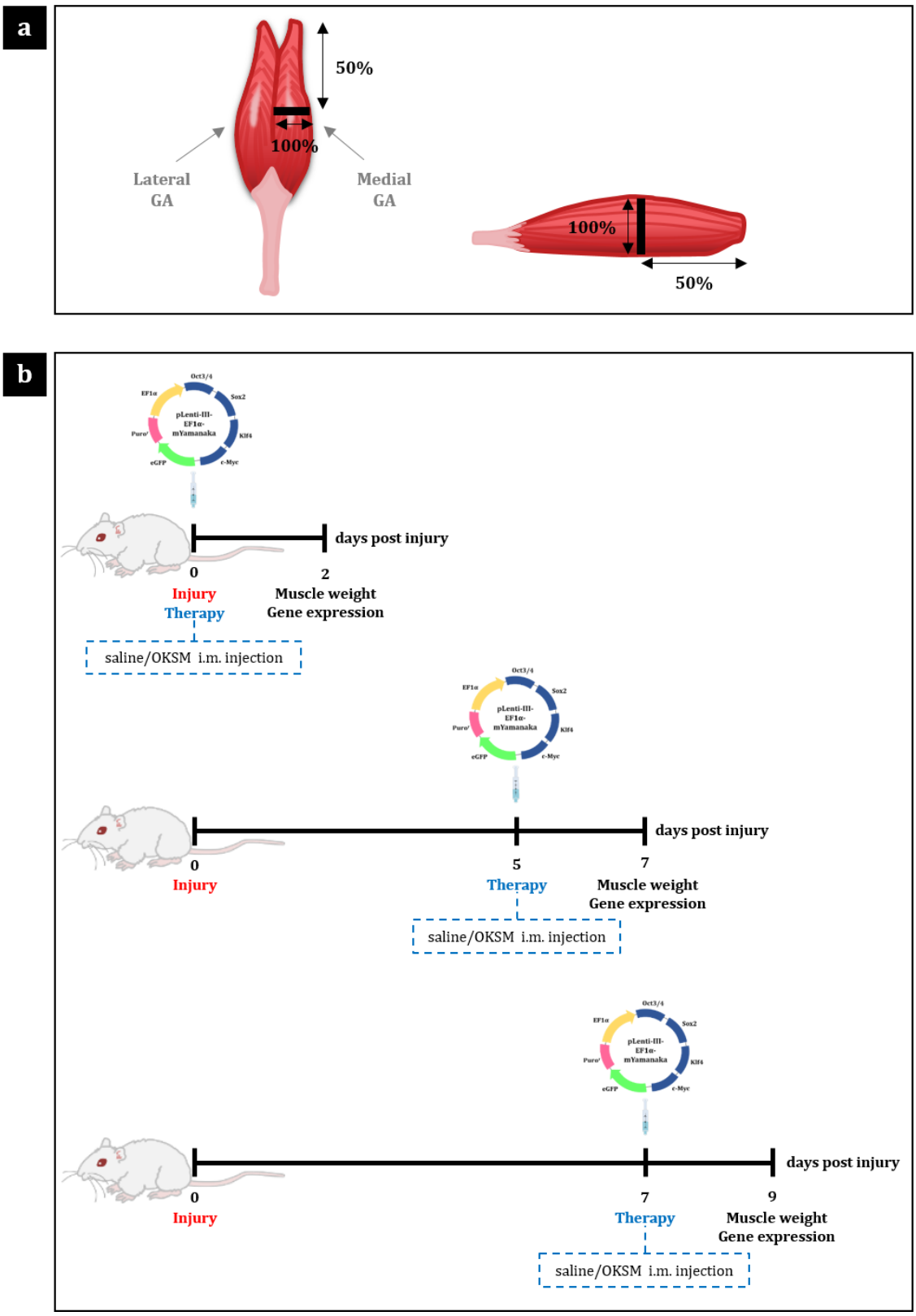

Figure 5. 12. Laceration of medial GA and i.m. administration of reprogramming pDNA. ***(a)*** *The medial head of the left GA muscle of BALB/c mice was surgically lacerated in the transverse plane. The cut was performed at its mid-point and through the 100% of its width and depth.* ***(b)*** *100 µg* ***OKSM*** *or the equivalent volume (40 µl) of 0.9% saline were administered at the time of injury (day 0) or 5 of 7 days later. The right hind limb was left uninjured and uninjected and used as an internal control. Muscles were dissected 2 days after the administration of reprogramming pDNA or saline (2, 7 or 9 days after injury) for gene expression and muscle weight analysis, n=3.*

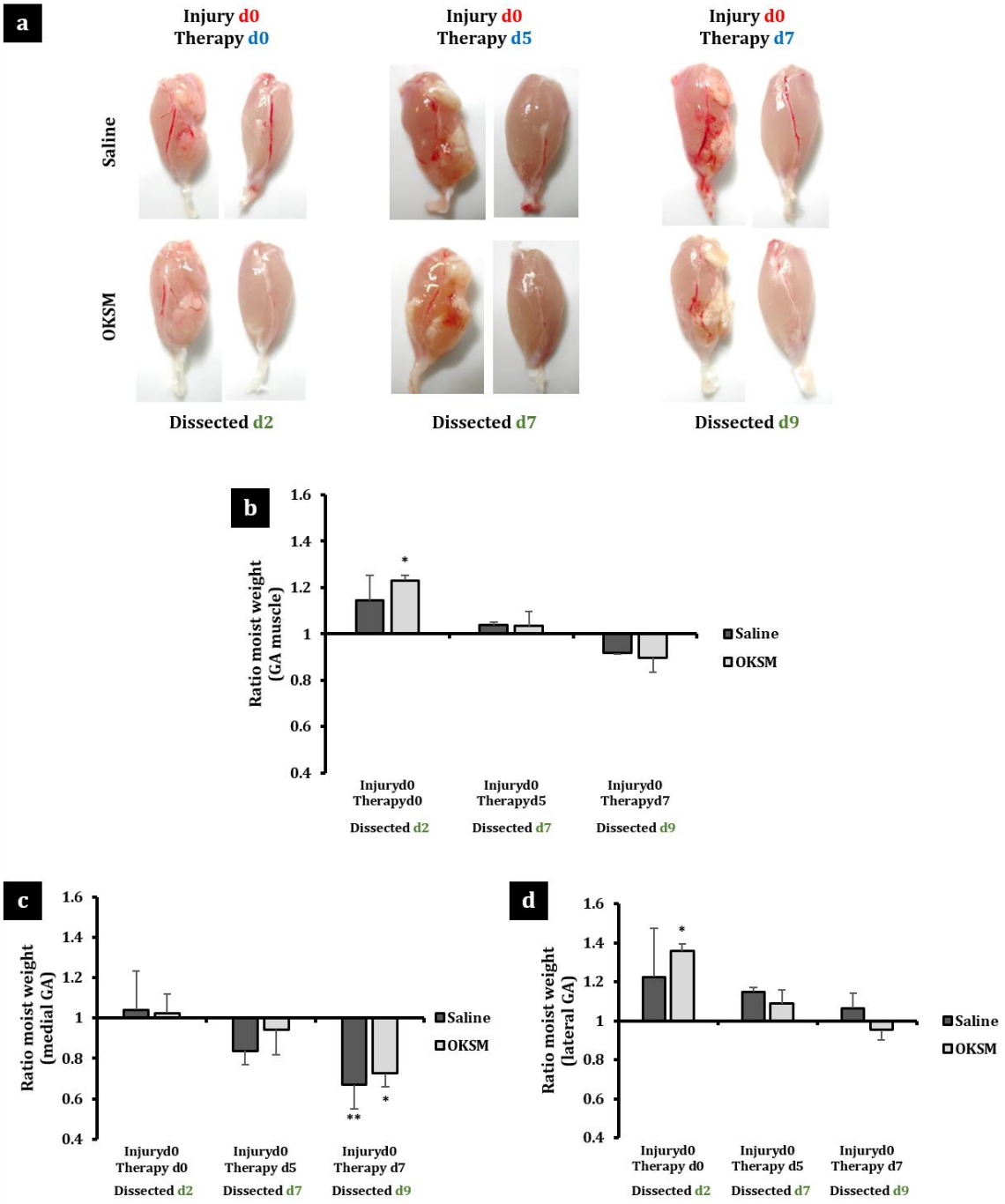

Figure 5. 13. Macroscopic evaluation and changes in muscle moist weight after laceration of medial GA and i.m. administration of reprogramming pDNA. (a) *GA muscles dissected 2 days after pDNA or saline administration (injured vs. contralateral intact control). Muscle moist weight was expressed as an injured/intact ratio for the* ***(b)*** *whole GA muscle,* ***(c)*** *medial GA and* ***(d)*** *lateral GA. *p<0.05 and **p<0.01 indicate statistically significant differences in muscle weight between the injured and intact hind limbs, assessed by one-way ANOVA. Data are presented as mean ± SD, n=3.*

Changes in gene expression.

In agreement to the more severe laceration of GA, soleus and plantaris, the delivery and expression of reprogramming pDNA was technically hindered when the administration took place at the time of injury, which inevitably resulted in the lack of *Nanog* upregulation **(Figures 5.14a-b)**. The expression of *Oct3/4* when **OKSM** was administered 7 days after injury was restricted to the lateral GA, possibly due to the excessive retraction and loss of muscle mass in the medial head that even complicated its dissection. More importantly, and similar to the CTX injury model, the upregulation of *Nanog* compared to the intact control increased with increasing time interval between injury and **OKSM** administration **(Figure 5.14b)**. The difference in upregulation between **OKSM**- and saline-injected injured groups was calculated in order to correct for the endogenous upregulation of the pluripotency marker resulting from innate regeneration. Importantly, such difference increased significantly with the increasing time lapse between injury and therapeutic intervention **(Figure 5.14c)**.

The downregulation of *Pax3*, although persisted throughout the course of the study and showed no significant differences between treatment groups, was more notable in the directly injured medial GA than in the preserved lateral head **(Figure 5.14d)**.

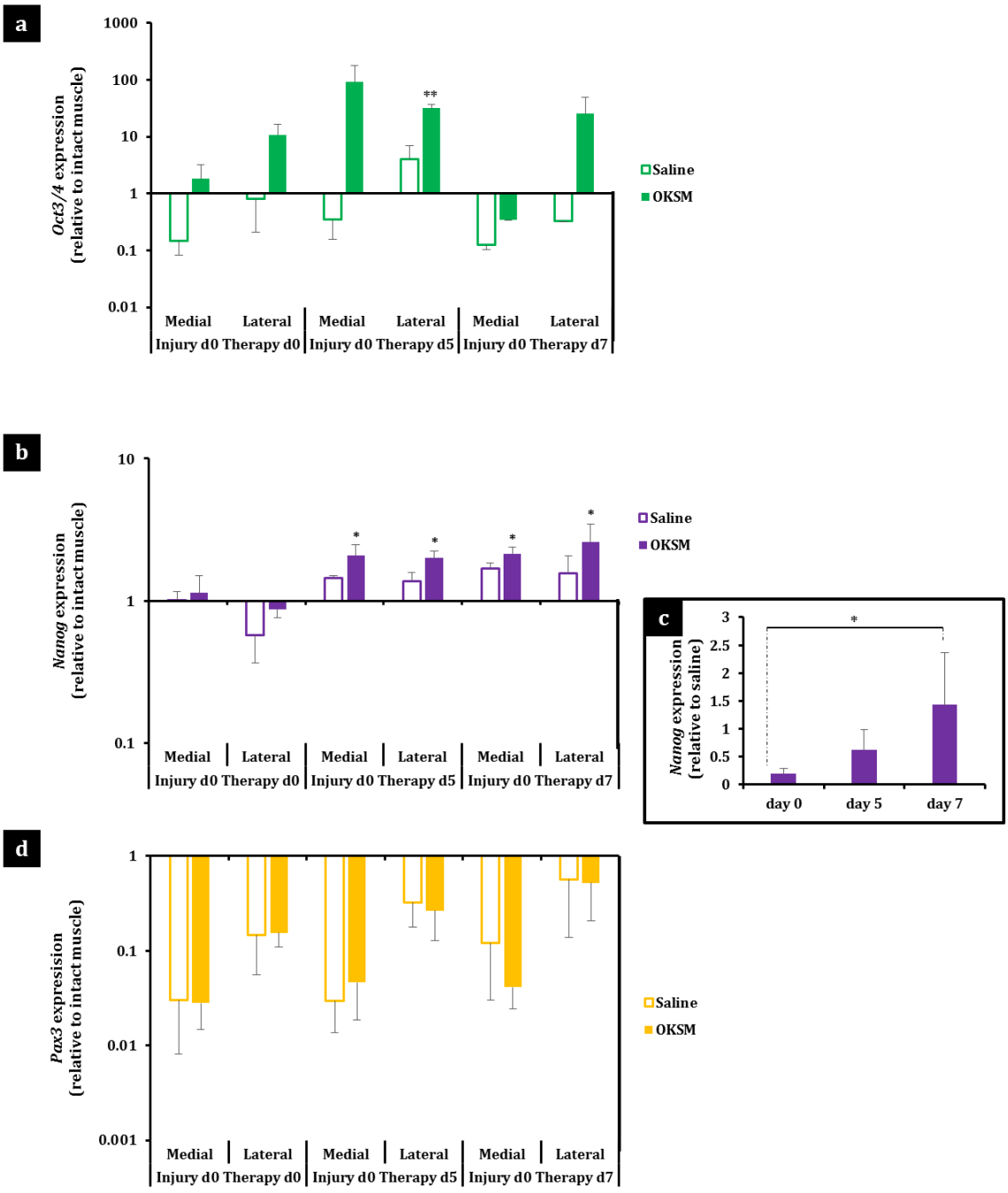

Figure 5. 14. Changes in gene expression after laceration of medial GA and i.m. administration of reprogramming pDNA. *Real-time RT-qPCR was performed 2 days after the administration of pDNA or saline (2, 7 and 9 days after laceration, respectively) to analyse the relative gene expression of* ***(a)*** *the reprogramming factor Oct3/4* ***(b)*** *the pluripotency marker Nanog (normalised to uninjured, uninjected controls),* ***(c)*** *the pluripotency marker Nanog (normalised to injured, saline-injected controls, lateral head) and* ***(d)*** *the myogenic progenitor marker Pax3. For Oct3/4 and Pax3, gene expression was normalised to intact muscle controls. *p<0.05 and **p<0.01 indicate statistically significant differences between groups, assessed by Welch ANOVA and Games-Howell's test. Data are presented as mean ± SD, n=3.*

5.4.4.2. Tissue regeneration upon i.m. administration of reprogramming pDNA 7 days after laceration of the medial GA.

As in the CTX-induced injury model, the administration of reprogramming pDNA was fixed on day 7 after injury to take advantage of the higher *Nanog* upregulation. Tissues were collected 2 and 7 days after **OKSM** or saline administration (9 and 14 days after injury) and analysed histologically **(Figure 5.15a)**. 2 days after injection (9 days after injury), a significantly higher percentage of the myofibers surrounding the injured site were regenerating in the **OKSM** group (56.0 ± 23.4 %) – as evidenced by the centralised position of the nuclei – compared to the saline control (33.9 ± 12.9 %). While in the saline-injected group this figure continued to increase 7 days after the injection (14 days after injury, 45.6 ± 14.6 %), the percentage of fibers still regenerating in the **OKSM** group significantly dropped (18.2 ± 7.7 %). Representative images are shown in **Figure 5.15b**.

H&E staining confirmed the presence of necrotic fibers and inflammatory infiltrate in the vicinity of the injured site, which was very prominent in both groups 9 days after laceration, but diminished considerably by day 14 in the **OKSM** group **(Figure 5.15c)**. Picrosirious red/fast green staining of the same cross-sections evidenced that collagen deposition on day 9 was moderately more extensive in the tissues from saline control animals and that this difference was even more pronounced on day 14. While the percentage of collagen^{+} areas in the vicinity of the injury remained practically invariable in the **OKSM** group (12.3 ± 5.1%, to 15.5 ± 6.5%), it raised from 15.4 ± 5.2% on day 9 to 22.6 ± 6.7% on day 14 in the animals that received saline solution after the injury **(Figure 5.15d)**.

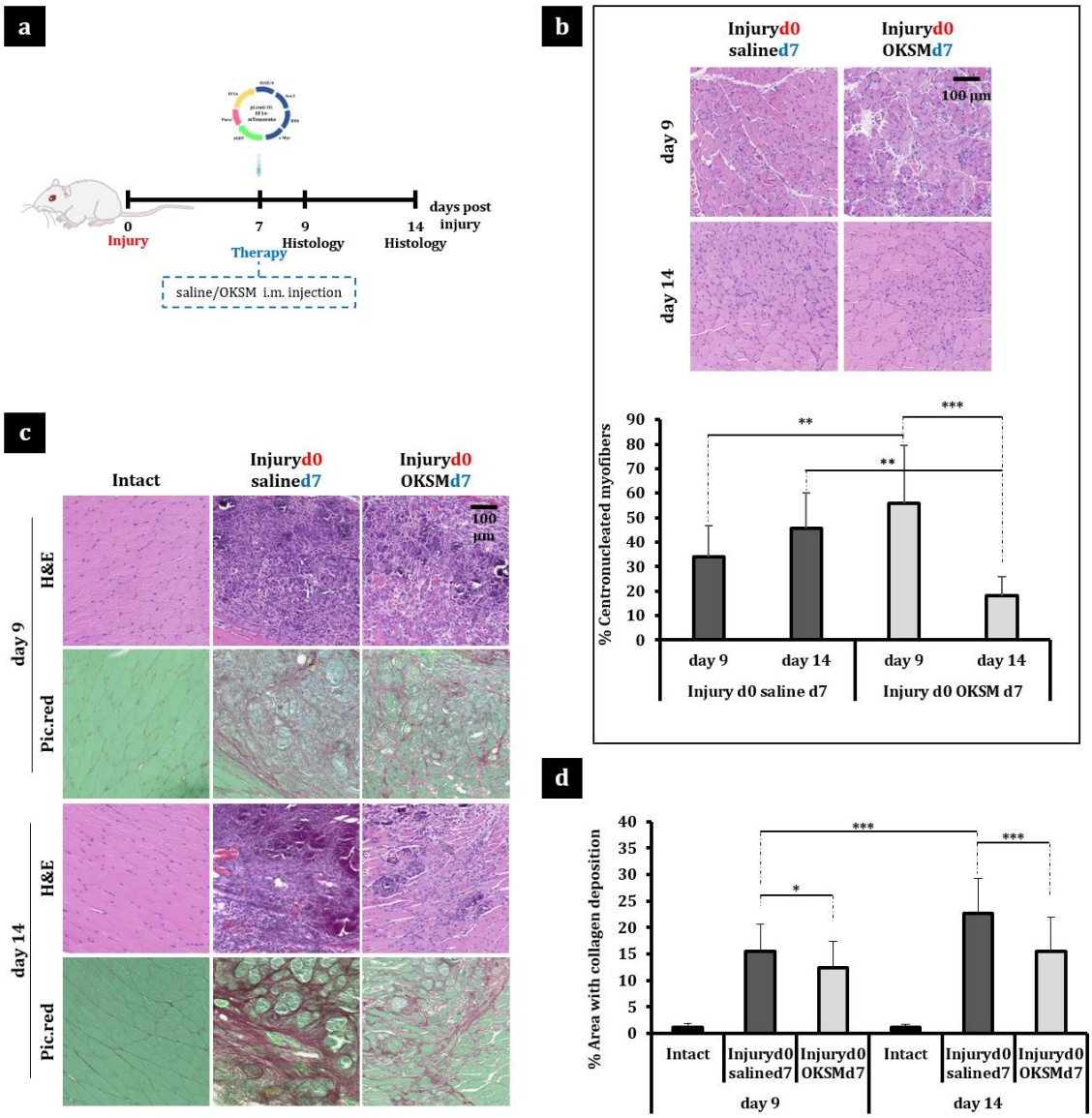

Figure 5. 15. Histological evaluation after laceration of medial GA (day 0) and i.m. administration of reprogramming pDNA (day 7). (a) *The medial head of the left GA muscle of BALB/c mice (n=4) was surgically lacerated and 100 µg* ***OKSM*** *pDNA or the equivalent volume (40 µl) of 0.9% saline were administered 7 days after the injury. The right hind limb was left uninjured and uninjected for control. Tissues were dissected 2 and 7 days after pDNA/saline administration (9 and 14 days after injury) and analysed histologically.* ***(b)*** *H&E staining (40X, scale bars represent 100 µm) and quantification of % of centronucleated myofibers. **p<0.01 and ***p<0.001 indicate statistically significant differences between groups analysed by Welch ANOVA and Games-Howell's test (n=2-4 GA muscles per condition, 3 sections per muscle, 2 random fields per section). Data are presented as mean ± SD.* ***(c)*** *Picrosirius red/fast green staining for collagen and H&E staining of the same cross-section (40X, scale bars represent 100 µm).* ***(d)*** *Quantification of collagen deposition. *p<0.05 and ***p<0.001 indicate statistically significant differences between groups, analysed by Welch ANOVA and Games-Howell's test (n=2-4 GA muscles per condition, 4 sections per muscle, 5 random fields per section). Data are presented as mean ± SD.*

5.4.4.3. Investigation of functional rehabilitation upon i.m. administration of reprogramming pDNA 7 days after laceration of the medial GA.

Finally, functional recovery was investigated 2 and 7 days after **OKSM** or saline administration (9 and 14 days after laceration) by myography as previously described **(Figure 5.16)**. 2 days after the administration of **OKSM** or saline, the percentage of recovered force under twitch and tetanus contraction was low compared to the measurements in the CTX model and no differences were observed between treatment groups (**twitch**: 57.8 ± 11.8 % saline, 57.9 ± 11.6 % **OKSM**, **tetanus**: 47.8 ± 5.5 % saline, 41.5 ± 19.0 % **OKSM**). On the contrary, the analysis on day 7 suggested that **OKSM**-treated animals recovered a higher percentage of the force of the contralateral (intact) GA, compared to the saline-injected controls, when both fast twitch (50.4 ± 12.3% saline, 80.2 ± 18.2% **OKSM**) and tetanus contractions (49.9 ± 19.2% saline, 56.6 ± 20.9% **OKSM**) were induced. However, the number of animals thata entered the procedure was low (n=4) and these results were not supported by statistical significance. Hence, albeit promising, these observations will have to be confirmed in future studies.

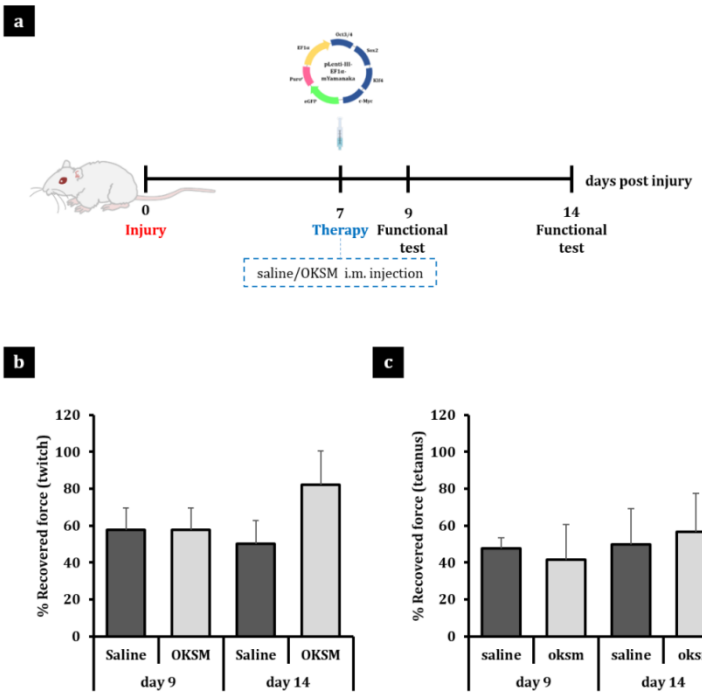

Figure 5. 16. Investigation of functional rehabilitation after laceration of medial GA (day 0) and i.m. administration of reprogramming pDNA (day 7). ***(a)*** *The medial head of the left BALB/c GA was surgically lacerated and 100 μg* ***OKSM*** *or the equivalent volume (40 μl) of 0.9% saline were administered 7 days after injury. The right medial GA was left uninjured and uninjected and used as an internal control. Muscle function was assessed 2 and 7 days after pDNA or saline administration (9 and 14 days after injury).* ***(b)*** *Recovered forces of the injured muscles under twitch and tetanus contractions are expressed as a percentage of the contralateral (uninjured) hind limb force. Data are presented as mean ± SE, n=4.*

5.4. Discussion.

In this Chapter we provide first time evidence of the therapeutic potential of *in vivo* cell reprogramming to pluripotency in a model of skeletal muscle injury. Administration of reprogramming pDNA one week after surgical laceration of the medial GA enhanced myofiber regeneration, prevented fibrosis and modestly improved the recovery of muscle force.

Most of the recent experimental efforts in the treatment of major skeletal muscle injuries have however been directed to the search of appropriate cell sources to replenish the injured muscle. Bone marrow mesenchymal stromal cells (BMMSCs) [261], $CD133^+$ human peripheral blood cells [262], adipose tissue-derived regenerative cells (ADRCs) [263] and adipose tissue-derived stem cells (ADSCs) [266, 267] have been tested in laceration injury models similar to the ones presented here. However, the improvement in muscle regeneration reported in such studies very rarely correlated with the number of transplanted cells that successfully integrated into the host's tissue – which was generally very low – and was often attributed to paracrine effects. Only Shi et al. were able to demonstrate integration, survival and differentiation of $CD133^+$ human peripheral blood cells to the myogenic and endothelial lineages [262]. Mori et al. could only confirm differentiation of very limited numbers of ADRCs [263] while Natsu et al. observed that BMMSCs did not differentiate or fuse to the host's fibers at all [261]. Even myoblast transplantation, theoretically favoured by their natural commitment to the myogenic lineage, was hampered by extremely poor graft survival [276]. Although immune responses against the transplanted cells might have played a role in their poor tissue integration, the use of immunosuppressive drugs or immunodeficient animal models improved graft survival in some [262] but not all the above studies [261, 263]. Therefore, other factors limiting the contribution of the transplanted cells towards the replenishment of the tissue should be investigated. In fact, cell therapy strategies for the treatment of muscle injuries have not always been able to show therapeutic efficacy on their own. A study by Hwang et al. required co-administration of growth factors to achieve sufficient engraftment and differentiation of transplanted ADSCs [267]. Although muscle regeneration modestly improved even when such factors were administered on their own [260], their clinical use suffers from their rapid clearance and, in some

cases, controversial mitogen status. Gene therapy strategies are being explored in order to optimise their delivery and expression [265, 277].

We have proposed here a novel strategy that combines gene and cell therapy in the *in vivo* setup and may overcome some of the hurdles faced by traditional cell therapy thanks to the generation of host-specific replacement cells *in situ.*

Administration of reprogramming pDNA 7 days after surgical laceration of the medial GA resulted in a significant increase in the percentage of regenerating fibers 2 days after the induction of pluripotency. This finding suggested that regeneration was accelerated compared to saline-treated controls **(Figure 5.15b)**. One week later, immature regenerating fibers were still abundant in the saline-injected tissues, indicating that the regeneration process was still ongoing, while the number of fibers in such state had significantly decreased in the reprogrammed group. In addition, a modest – albeit not statistically significant – improvement in recovered muscle force in comparison to saline controls was detected one week after the administration of reprogramming pDNA, but not earlier **(Figure 5.16)**. The timing of these events agreed with our observations in healthy skeletal muscle, in which centronucleated myofibers appeared soon after the administration of reprogramming pDNA and only seemed to mature and integrate into the normal tissue architecture approximately one week after injection **(Chapter IV, Figures 4.12 and 4.13)**. However, cell tracking strategies that indelibly label the *in vivo* reprogrammed cells will be required to fully confirm whether the recovery of muscle force is a direct cause of their re-differentiation to the myogenic lineage and integration in the injured muscle tissue.

The deposition of collagen that ultimately generates a fibrotic scar is normally initiated one week after injury and can continue to accumulate for weeks thereafter, depending on the severity of the damage [252]. As expected, collagen deposition significantly increased in the control group between days 2 and 7 after saline administration (days 9 and 14 after injury, **Figure 5.15d**). However, it remained invariable between these two time points in the reprogrammed group, suggesting that *in vivo* reprogramming to pluripotency was able to prevent fibrosis. Further studies will however be necessary to determine the mechanisms behind this effect. Myofibroblasts originate from the differentiation of various

resident cell types [252], hence we could speculate that reprogramming to pluripotency antagonises such cell fate conversion in a subset of cells. In addition, the reprogrammed cells replenishing the injured site may be able to repress myofibroblast proliferation via paracrine mechanisms, as it has been demonstrated upon MS cell transplantation in other tissues [278].

Regardless of the mechanism, we hypothetise that the attenuation of collagen deposition may act as one of the main contributors to the improved functional rehabilitation in the reprogrammed muscles **(Figure 5.16).** The relevance of the inhibition of fibrosis has also been highlighted by others [256-259, 265, 266, 268, 279] based on the facts that (a) the establishment of a fibrotic scar acts in detriment of the contractile capabilities of the muscle [5, 252] and (b) the inhibition of the TGF-β signaling pathway and subsequent reduction of fibrosis benefits the integration of transplanted cells [266]. In agreement, a study by Lee et al. evidenced that the combination of cell and growth factor therapy was not able to fully restore muscle function in the absence of anti-fibrotic substances [265]. Importantly, we have achieved here enhancement of myofiber regeneration and prevention of fibrosis without co-administration of growth factors or anti-fibrotic agents. Nonetheless, future investigation of synergistic effects will be of interest.

A different strategy also in the crossroads between gene and cell therapy was published by Nakasa et al. in a muscle laceration model similar to ours [264]. A cocktail of three miRNAs involved in muscle development and homeostasis were i.m. administered in the rat tibialis anterior immediately after laceration. Their findings one week after administration were very similar to those observed in our medial GA laceration model, including increased number of centronucleated fibers, attenuation of fibrosis and improved recovery of muscle force. However, the proposed mechanism behind such findings does not involve reprogramming to pluripotency but conversely the enhancement of myoblast proliferation and differentiation. Promoting differentiation towards the myogenic lineage constitutes a more direct approach to repopulate injured muscle, avoiding pluripotent or pluripotent-like intermediates. However, it relies on the presence of sufficient numbers of muscle progenitors, which cannot be taken for granted depending on the pathological condition of the muscle. Muscle progenitors are known to be depleted as a consequence of ageing [250] and in some conditions such as muscular dystrophy, where muscle mass is progressively replaced by

fibrotic and adipose tissue [280]. Therefore, it is conceivable that this approach may not be effective depending on the type of injury. Conversely, we suggest that thanks to the universality of the Yamanaka factors to reprogram different starting cell types, *in vivo* reprogramming towards pluripotency might be a more versatile strategy not only effective in muscle lacerations such as the ones explored here but also in other types of ailments.

Although also limited by the requirements of not only particular cell types but also specific reprogramming cocktails, *in vivo* transdifferentiation strategies have shown encouraging results in the post-injury recovery of a different muscle, the heart, via *in situ* conversion of cardiac fibroblasts into CMs [147-151]. This suggests that similar strategies could also enhance regeneration after skeletal muscle injury. To this respect, the transcription factor MyoD stands out as a potential candidate, thanks to its capacity to transdifferentiate fibroblasts to myoblasts in the culture dish. However, the *in vivo* overexpression of MyoD with therapeutic purposes is still largely unexplored [146, 281] and has not yet been investigated in skeletal muscle injury models.

We could not reproduce the encouraging histological and modest functional rehabilitation results obtained after medial GA laceration when a similar protocol was implemented in the CTX injury model. In the laceration model, we had absolute control of the anatomical localisation and dimensions of the injury and were able to direct the administration of reprogramming pDNA to the periphery of the defect. CTX administration produced a less severe insult – evidenced by the lower percentage of collagen deposition **(Figure 5.7d)** and the less deteriorated muscle function **(Figure 5.8b)** – but it was difficult to control the extension and exact localisation of the injured site within the muscle volume. As a result, we could not control whether the reprogramming pDNAs were administered directly in the injured site or in the periphery of it and suspect that a considerable fraction of the pDNA may have been internalised by cells in the damaged tissue. Since the feasibility to reprogram cells undergoing stress situations is yet to be explored, we speculate that they may be less amenable to the pluripotent-like conversion. In fact, *Oct3/4* mRNA levels were slightly higher in the CTX model while the upregulation of *Nanog* was lower compared to the medial GA laceration model **(Figures 5.6 and 5.14).** Therefore, the reprogramming effect

achieved might have not been enough to enhance significantly the regeneration of the tissue.

Our observations that gene expression in healthy and injured muscle was significantly different might also explain why healthy and injured cells responded differently to reprogramming. The expression of *Nanog* and *Pax3*, characteristically upregulated upon in *in vivo* reprogramming to pluripotency in healthy skeletal muscle, was affected in a temporal manner by the induction of tissue damage. *Nanog* was modestly upregulated after the administration of CTX alone **(Figure 5.3)** as expected from its role in the process of regeneration after injury, unveiled in a previous report [184] and confirmed by our HTV administration experiments in mouse liver tissue **(Chapter III, Figure 3.7)**. *Pax3* was conversely downregulated upon injury **(Figure 5.3c)**, possibly due to its role as survival factor and its negative regulation in apoptotic mechanisms [282, 283]. *Pax3* mRNA levels were more prominently depleted soon after injury and in directly injured tissue (i.e. medial GA vs. lateral GA, in the model in which the latter was preserved, **Figure 5.14d**), which confirmed the links between muscle injury and the downregulation of this gene.

In fact we have identified the timing of the administration of reprogramming pDNA as a critical factor that affects the success of the induction of pluripotency in injured tissue. Lack of reprogramming when OKSM was administered at the time of injury in surgically-induced injury models was explained by technical limitations **(Figures 5.10 and 5.14).** However, successful expression of *Oct3/4* when reprogramming pDNAs were administered at such time point in the CTX model failed as well to upregulate *Nanog* **(Figure 5.6)**. When reprogramming pDNA was administered after the summit of the inflammation/degeneration phase, following what we denominated "late intervention" protocols, the upregulation of *Nanog* increased with the increased time lapse between injury and therapeutic intervention **(Figures 5.6 and 5.14)**. This observation was consistent in CTX and laceration models and would be explained by our hypothesis that injured cells do not respond to the reprogramming stimulus as well as their healthy counterparts. Rather than this being a limitation in our study, we propose that the fact that optimal reprogramming effect was achieved when reprogramming pDNA was administered after the bulk of the inflammation phase, but before muscle

remodeling was established, constitutes and advantage over other approaches in the treatment of skeletal muscle injuries. The cell therapy strategies discussed here and the miRNA study by Nakasa et al. relied on the administration of replacement cells or miRNAs at the time of injury. The absence of data to support the efficacy of the treatment when administered at later time points questions the clinical relevance of these studies, especially given the extended culturing – sometimes close to 4 weeks – required to achieve enough numbers of replacement cells [261, 262, 266, 267]. Very importantly, the strategy we propose here circumvents the need for rapid post-injury intervention, which may facilitate its potential clinical translation.

Overall, we can affirm that a balance was found in the administration of reprogramming pDNA avoiding the peak of the degeneration phase but prior to the establishment of muscle remodeling in a localised and clinically-relevant model of skeletal muscle injury (laceration of medial GA). In such model, the induction of pluripotency has proved to accelerate muscle regeneration, prevent fibrosis and modestly improve functional recovery without the need for rapid intervention or co-administration of growth factors, anti-fibrotic agents or other substances. In addition, this strategy avoids some of the hurdles faced by traditional cell therapies (*in vitro* culture, challenges of cell delivery and engraftment) and *in vivo* transdifferentiation (requirement for specific cell types and reprogramming cocktails). The results presented here are therefore promising for the treatment of major skeletal muscle injuries, although further studies will be necessary to confirm the mechanisms behind the enhancement of regeneration described here (i.e. contribution of reprogrammed cells to the regenerated tissue) and functional rehabilitaton will have to be confirmed with higher animal numbers and longer term studies. In addition, *in vivo* reprogramming to pluripotency may also have a place in the treatment of other ailments thanks to the versatile character of the pluripotent conversion driven by OKSM.

Chapter VI.

Conclusions and Final Remarks

Overall, the studies presented in this thesis confirm that adult somatic cells can be transiently reprogrammed to a functionally pluripotent state *in vivo* in the absence of teratomas and that the induction of pluripotency can enhance regeneration and, albeit modestly, functional rehabilitation of injured tissue. Below are the major findings in this work and their implications for the future directions of the field:

- ***In vivo* reprogramming towards pluripotency can be achieved in different somatic tissues via ectopic expression of Yamanaka factors.** *In vivo* cell reprogramming to a pluripotent or pluripotent-like state has been achieved in two adult tissues of different developmental origin, liver and skeletal muscle. Hence, the versatile character of the Yamanaka factors, able to reverse the differentiated status of a variety of cell types *in vitro* [51, 60], has been validated in the *in vivo* setting. Such attribute constitutes a remarkable advantage over transdifferentiation strategies, which conversely require extensive work towards the identification of specific reprogramming factors for each particular cell fate conversion [49, 144, 147, 158, 159]. Future work will have to address whether complete reprogramming to pluripotency was achieved in the skeletal muscle, as demonstrated upon liver reprogramming. It will also involve the investigation of *in vivo* reprogramming to pluripotency in other tissues as well as studies to determine the specific cell types within the tissue that are reprogrammed to pluripotency.

- **Transient reprogramming to pluripotency *in vivo* does not generate teratomas.** Our observations in liver [162, 163] and skeletal muscle tissue, together with those produced by others [161, 195, 196], pointed at the transiency of the expression of reprogramming factors and of the pluripotent conversion in the tissues as a key factor to avoid the generation of teratomas. Notably, the expression of reprogramming factors was not sustained (only minor signs of integration of the pDNA were observed), we were not able to find cells expressing pluripotency markers in the tissues any later than 4 days after the administration of reprogramming pDNA and no signs of dysplasia were found in the liver or the skeletal muscle for the duration of our studies (120 days). However, future work will necessarily require *ad hoc* toxicity studies to confirm the safety of the approach.

- ***In vivo* reprogrammed liver cells and i²PS cells are *bona fide* pluripotent cells.** The functional pluripotency of *in vivo* reprogrammed cells directly extracted from liver tissue was confirmed through the generation of teratomas in nude mice. Additionally, i²PS cells were able to contribute widespread to the adult tissues of chimeric mice upon blastocyst injection [185]. While the gene expression and differentiation potential of i²PS cells did not suggest reminiscence of major signatures from the tissue of origin, further studies will have to confirm the absolute absence of epigenetic memory in the *in vivo* reprogrammed and i²PS cells. *In vitro* generated iPS cell clones have shown heterogeneity depending on many factors including the starting cell type, choice of reprogramming technology and even the laboratory where they were produced [284]. Hence, it will be interesting to compare epigenetic signatures between *in vivo* reprogrammed cells directly isolated from different tissues to investigate the influence of the tissue of origin.

- ***In vivo* reprogrammed cells proliferate transiently to then re-differentiate and integrate into the tissue.** We have confirmed that cells *in vivo* transfected with reprogramming pDNA divided actively but transiently. After this proliferative stage, the absence of cells expressing pluripotency markers together with morphometric analysis of the tissue indicated that the reprogrammed cells re-differentiated and successfully re-integrated in the tissue without significant apoptosis or any tissue abnormalities. Similar findings have been described by others [161, 196]. While we speculate that the successful re-differentiation of the pluripotent-like intermediates is governed by specific biochemical and mechanical cues in the microenvironment, further studies will be required to address the role of such factors. In addition, lineage tracing strategies able to indelibly label the reprogrammed cells will be necessary to fully confirm these findings.

- ***In vivo* reprogramming towards pluripotency can enhance the regenerative capacity of injured tissues.** Induction of pluripotency one week after surgical laceration of the medial GA muscle was proved able to accelerate myofiber regeneration, prevent fibrosis and modestly improve muscle function. However, the exact mechanism behind this beneficial effect remains to be explained and cell tracking strategies will be necessary to follow the reprogrammed cells and confirm their re-differentiation and integration in

the injury site. In addition, and in light of the different results obtained in different injury models, further work will need to clarify under which exact conditions is this strategy able to enhance regeneration and especially, whether damaged cells are responsive to reprogramming or not.

The above findings support our hypothesis that *in vivo* reprogramming to pluripotency may combine the opportunities offered by both *in vitro* iPS cell generation and *in vivo* transdifferentiation while overcoming some of their respective limitations (i.e. taking advantage of the versatile character of Yamanaka factors while avoiding limitations associated to *in vitro* culture and benefiting from the role of the microenvironment). Although they should be interpreted in the context of very preliminary research, the observations in this thesis indicate that *in vivo* cell reprogramming to pluripotency holds potential to occupy a relevant place in regenerative medicine toolbox.

References

1. Office for National Statistics. *Healthy Life Expectancy (ONS)*. [cited 2015 5 May]; Available from: http://www.ons.gov.uk/ons/taxonomy/index.html?nscl=Healthy+Life+Expectancy#tab-data-tables.
2. Christensen, K., et al., *Ageing populations: the challenges ahead.* Lancet, 2009. **374**(9696): p. 1196-208.
3. Katzenschlager, R. and A.J. Lees, *Treatment of Parkinson's disease: levodopa as the first choice.* J Neurol, 2002. **249 Suppl 2**: p. II19-24.
4. Alexander, G.E., *Biology of Parkinson's disease: pathogenesis and pathophysiology of a multisystem neurodegenerative disorder.* Dialogues Clin Neurosci, 2004. **6**(3): p. 259-80.
5. Huard, J., Y. Li, and F.H. Fu, *Muscle injuries and repair: current trends in research.* J Bone Joint Surg Am, 2002. **84-A**(5): p. 822-32.
6. Mason, C. and P. Dunnill, *A brief definition of regenerative medicine.* Regen Med, 2008. **3**(1): p. 1-5.
7. Lindvall, O. and A. Bjorklund, *Cell therapeutics in Parkinson's disease.* Neurotherapeutics, 2011. **8**(4): p. 539-48.
8. Gharaibeh, B., et al., *Biological approaches to improve skeletal muscle healing after injury and disease.* Birth Defects Res C Embryo Today, 2012. **96**(1): p. 82-94.
9. Freed, W.J., et al., *Restoration of dopaminergic function by grafting of fetal rat substantia nigra to the caudate nucleus: long-term behavioral, biochemical, and histochemical studies.* Ann Neurol, 1980. **8**(5): p. 510-9.
10. Ganz, J., et al., *Cell replacement therapy for Parkinson's disease: how close are we to the clinic?* Expert Rev Neurother, 2011. **11**(9): p. 1325-39.
11. Hughes, R.D., R.R. Mitry, and A. Dhawan, *Current status of hepatocyte transplantation.* Transplantation, 2012. **93**(4): p. 342-7.
12. Madrazo, I., et al., *Open microsurgical autograft of adrenal medulla to the right caudate nucleus in two patients with intractable Parkinson's disease.* N Engl J Med, 1987. **316**(14): p. 831-4.

13. Goetz, C.G., et al., *Multicenter study of autologous adrenal medullary transplantation to the corpus striatum in patients with advanced Parkinson's disease.* N Engl J Med, 1989. **320**(6): p. 337-41.
14. Plunkett, R.J., et al., *Long-term evaluation of hemiparkinsonian monkeys after adrenal autografting or cavitation alone.* J Neurosurg, 1990. **73**(6): p. 918-26.
15. Brunt, K.R., R.D. Weisel, and R.K. Li, *Stem cells and regenerative medicine - future perspectives.* Can J Physiol Pharmacol, 2012. **90**(3): p. 327-35.
16. Martin, G.R., *Isolation of a pluripotent cell line from early mouse embryos cultured in medium conditioned by teratocarcinoma stem cells.* Proc Natl Acad Sci U S A, 1981. **78**(12): p. 7634-8.
17. Evans, M.J. and M.H. Kaufman, *Establishment in culture of pluripotential cells from mouse embryos.* Nature, 1981. **292**(5819): p. 154-6.
18. Nichols, J., E.P. Evans, and A.G. Smith, *Establishment of germ-line-competent embryonic stem (ES) cells using differentiation inhibiting activity.* Development, 1990. **110**(4): p. 1341-8.
19. Nagy, A., et al., *Embryonic stem cells alone are able to support fetal development in the mouse.* Development, 1990. **110**(3): p. 815-21.
20. Thomson, J.A., et al., *Embryonic stem cell lines derived from human blastocysts.* Science, 1998. **282**(5391): p. 1145-7.
21. Wilmut, I., *Consternation and confusion following EU patent judgment.* Cell Stem Cell, 2011. **9**(6): p. 498-9.
22. Evans, M.D. and J. Kelley, *US attitudes toward human embryonic stem cell research.* Nat Biotechnol, 2011. **29**(6): p. 484-8.
23. Wu, D.C., A.S. Boyd, and K.J. Wood, *Embryonic stem cells and their differentiated derivatives have a fragile immune privilege but still represent novel targets of immune attack.* Stem Cells, 2008. **26**(8): p. 1939-50.
24. Swijnenburg, R.J., et al., *In vivo imaging of embryonic stem cells reveals patterns of survival and immune rejection following transplantation.* Stem Cells Dev, 2008. **17**(6): p. 1023-9.
25. English, K. and K.J. Wood, *Immunogenicity of embryonic stem cell-derived progenitors after transplantation.* Curr Opin Organ Transplant, 2011. **16**(1): p. 90-5.

26. Ilic, D. and J.M. Polak, *Stem cells in regenerative medicine: introduction.* Br Med Bull, 2011. **98**: p. 117-26.
27. Ilic, D., C. Miere, and E. Lazic, *Umbilical cord blood stem cells: clinical trials in non-hematological disorders.* Br Med Bull, 2012. **102**: p. 43-57.
28. Phinney, D.G. and D.J. Prockop, *Concise review: mesenchymal stem/multipotent stromal cells: the state of transdifferentiation and modes of tissue repair--current views.* Stem Cells, 2007. **25**(11): p. 2896-902.
29. Volarevic, V., et al., *Human stem cell research and regenerative medicine--present and future.* Br Med Bull, 2011. **99**: p. 155-68.
30. Health, U.N.I.o. *Clinical Trials (US NIH)*. [cited 2015 10 May]; Available from: https://clinicaltrials.gov.
31. Graf, T., *Historical origins of transdifferentiation and reprogramming.* Cell Stem Cell, 2011. **9**(6): p. 504-16.
32. Stadtfeld, M. and K. Hochedlinger, *Induced pluripotency: history, mechanisms, and applications.* Genes Dev, 2010. **24**(20): p. 2239-63.
33. Briggs, R. and T.J. King, *Transplantation of Living Nuclei From Blastula Cells into Enucleated Frogs' Eggs.* Proc Natl Acad Sci U S A, 1952. **38**(5): p. 455-63.
34. King, T.J. and R. Briggs, *Changes in the Nuclei of Differentiating Gastrula Cells, as Demonstrated by Nuclear Transplantation.* Proc Natl Acad Sci U S A, 1955. **41**(5): p. 321-5.
35. Gurdon, J.B., *The developmental capacity of nuclei taken from differentiating endoderm cells of Xenopus laevis.* J Embryol Exp Morphol, 1960. **8**: p. 505-26.
36. Gurdon, J.B., *The developmental capacity of nuclei taken from intestinal epithelium cells of feeding tadpoles.* J Embryol Exp Morphol, 1962. **10**: p. 622-40.
37. Gurdon, J.B., R.A. Laskey, and O.R. Reeves, *The developmental capacity of nuclei transplanted from keratinized skin cells of adult frogs.* J Embryol Exp Morphol, 1975. **34**(1): p. 93-112.
38. Wilmut, I., et al., *Viable offspring derived from fetal and adult mammalian cells.* Nature, 1997. **385**(6619): p. 810-3.
39. Griffin, H. and I. Wilmut, *Seven days that shook the world.* New Sci, 1997. **153**(2074): p. 49.

40. Turner, L., *The media and the ethics of cloning.* Chron High Educ, 1997. **44**(5): p. B4-5.
41. Noggle, S., et al., *Human oocytes reprogram somatic cells to a pluripotent state.* Nature, 2011. **478**(7367): p. 70-5.
42. Egli, D., et al., *Reprogramming within hours following nuclear transfer into mouse but not human zygotes.* Nat Commun, 2011. **2**: p. 488.
43. Tachibana, M., et al., *Human Embryonic Stem Cells Derived by Somatic Cell Nuclear Transfer.* Cell, 2013.
44. Miller, R.A. and F.H. Ruddle, *Pluripotent teratocarcinoma-thymus somatic cell hybrids.* Cell, 1976. **9**(1): p. 45-55.
45. Miller, R.A. and F.H. Ruddle, *Teratocarcinoma X friend erythroleukemia cell hybrids resemble their pluripotent embryonal carcinoma parent.* Dev Biol, 1977. **56**(1): p. 157-73.
46. Stevens, L.C. and C.C. Little, *Spontaneous Testicular Teratomas in an Inbred Strain of Mice.* Proc Natl Acad Sci U S A, 1954. **40**(11): p. 1080-7.
47. Davis, R.L., H. Weintraub, and A.B. Lassar, *Expression of a single transfected cDNA converts fibroblasts to myoblasts.* Cell, 1987. **51**(6): p. 987-1000.
48. Weintraub, H., et al., *Activation of muscle-specific genes in pigment, nerve, fat, liver, and fibroblast cell lines by forced expression of MyoD.* Proc Natl Acad Sci U S A, 1989. **86**(14): p. 5434-8.
49. Zhou, Q., et al., *In vivo reprogramming of adult pancreatic exocrine cells to beta-cells.* Nature, 2008. **455**(7213): p. 627-32.
50. Schneuwly, S., R. Klemenz, and W.J. Gehring, *Redesigning the body plan of Drosophila by ectopic expression of the homoeotic gene Antennapedia.* Nature, 1987. **325**(6107): p. 816-8.
51. Takahashi, K. and S. Yamanaka, *Induction of pluripotent stem cells from mouse embryonic and adult fibroblast cultures by defined factors.* Cell, 2006. **126**(4): p. 663-76.
52. Yamanaka, S., *A fresh look at iPS cells.* Cell, 2009. **137**(1): p. 13-7.
53. Okita, K., T. Ichisaka, and S. Yamanaka, *Generation of germline-competent induced pluripotent stem cells.* Nature, 2007. **448**(7151): p. 313-7.
54. Takahashi, K., et al., *Induction of pluripotent stem cells from adult human fibroblasts by defined factors.* Cell, 2007. **131**(5): p. 861-72.

55. Yu, J., et al., *Induced pluripotent stem cell lines derived from human somatic cells.* Science, 2007. **318**(5858): p. 1917-20.
56. Nakagawa, M., et al., *Generation of induced pluripotent stem cells without Myc from mouse and human fibroblasts.* Nat Biotechnol, 2008. **26**(1): p. 101-6.
57. Loh, Y.H., et al., *Generation of induced pluripotent stem cells from human blood.* Blood, 2009. **113**(22): p. 5476-9.
58. Ruiz, S., et al., *High-efficient generation of induced pluripotent stem cells from human astrocytes.* PLoS One, 2010. **5**(12): p. e15526.
59. Seki, T., et al., *Generation of induced pluripotent stem cells from human terminally differentiated circulating T cells.* Cell Stem Cell, 2010. **7**(1): p. 11-4.
60. Aoi, T., et al., *Generation of pluripotent stem cells from adult mouse liver and stomach cells.* Science, 2008. **321**(5889): p. 699-702.
61. Kim, J.B., et al., *Direct reprogramming of human neural stem cells by OCT4.* Nature, 2009. **461**(7264): p. 649-3.
62. Lowry, W.E., et al., *Generation of human induced pluripotent stem cells from dermal fibroblasts.* Proc Natl Acad Sci U S A, 2008. **105**(8): p. 2883-8.
63. Staerk, J., et al., *Reprogramming of human peripheral blood cells to induced pluripotent stem cells.* Cell Stem Cell, 2010. **7**(1): p. 20-4.
64. Zhang, X.B., *Cellular Reprogramming of Human Peripheral Blood Cells.* Genomics Proteomics Bioinformatics, 2013.
65. Okita, K., et al., *An efficient nonviral method to generate integration-free human-induced pluripotent stem cells from cord blood and peripheral blood cells.* Stem Cells, 2013. **31**(3): p. 458-66.
66. Bellin, M., et al., *Induced pluripotent stem cells: the new patient?* Nat Rev Mol Cell Biol, 2012. **13**(11): p. 713-26.
67. Hanna, J., et al., *Treatment of sickle cell anemia mouse model with iPS cells generated from autologous skin.* Science, 2007. **318**(5858): p. 1920-3.
68. Wernig, M., et al., *Neurons derived from reprogrammed fibroblasts functionally integrate into the fetal brain and improve symptoms of rats with Parkinson's disease.* Proc Natl Acad Sci U S A, 2008. **105**(15): p. 5856-61.
69. Hargus, G., et al., *Differentiated Parkinson patient-derived induced pluripotent stem cells grow in the adult rodent brain and reduce motor*

asymmetry in Parkinsonian rats. Proc Natl Acad Sci U S A, 2010. **107**(36): p. 15921-6.

70. Rhee, Y.H., et al., *Protein-based human iPS cells efficiently generate functional dopamine neurons and can treat a rat model of Parkinson disease.* J Clin Invest, 2011. **121**(6): p. 2326-35.
71. Kawai, H., et al., *Tridermal tumorigenesis of induced pluripotent stem cells transplanted in ischemic brain.* J Cereb Blood Flow Metab, 2010. **30**(8): p. 1487-93.
72. Oki, K., et al., *Human-induced pluripotent stem cells form functional neurons and improve recovery after grafting in stroke-damaged brain.* Stem Cells, 2012. **30**(6): p. 1120-33.
73. Tornero, D., et al., *Human induced pluripotent stem cell-derived cortical neurons integrate in stroke-injured cortex and improve functional recovery.* Brain, 2013. **136**(Pt 12): p. 3561-77.
74. Polentes, J., et al., *Human induced pluripotent stem cells improve stroke outcome and reduce secondary degeneration in the recipient brain.* Cell Transplant, 2012. **21**(12): p. 2587-602.
75. Jensen, M.B., et al., *Survival and differentiation of transplanted neural stem cells derived from human induced pluripotent stem cells in a rat stroke model.* J Stroke Cerebrovasc Dis, 2013. **22**(4): p. 304-8.
76. Filareto, A., et al., *An ex vivo gene therapy approach to treat muscular dystrophy using inducible pluripotent stem cells.* Nat Commun, 2013. **4**: p. 1549.
77. Tedesco, F.S., et al., *Transplantation of genetically corrected human iPSC-derived progenitors in mice with limb-girdle muscular dystrophy.* Sci Transl Med, 2012. **4**(140): p. 140ra89.
78. Nelson, T.J., et al., *Repair of acute myocardial infarction by human stemness factors induced pluripotent stem cells.* Circulation, 2009. **120**(5): p. 408-16.
79. Nori, S., et al., *Grafted human-induced pluripotent stem-cell-derived neurospheres promote motor functional recovery after spinal cord injury in mice.* Proc Natl Acad Sci U S A, 2011. **108**(40): p. 16825-30.
80. Homma, K., et al., *Developing rods transplanted into the degenerating retina of Crx-knockout mice exhibit neural activity similar to native photoreceptors.* Stem Cells, 2013. **31**(6): p. 1149-59.

81. Nature News. *Japanese woman is first recipient of next-generation stem cells*. 2014 [cited 2014 24 Sept]; Available from: http://www.nature.com/news/japanese-woman-is-first-recipient-of-next-generation-stem-cells-1.15915.
82. Cyranoski, D., *Stem cells cruise to clinic.* Nature, 2013. **494**(7438): p. 413.
83. Cyranoski, D., *Stem-cell pioneer banks on future therapies.* Nature, 2012. **488**(7410): p. 139.
84. Hirami, Y., et al., *Generation of retinal cells from mouse and human induced pluripotent stem cells.* Neurosci Lett, 2009. **458**(3): p. 126-31.
85. Kanemura, H., et al., *Tumorigenicity studies of induced pluripotent stem cell (iPSC)-derived retinal pigment epithelium (RPE) for the treatment of age-related macular degeneration.* PLoS One, 2014. **9**(1): p. e85336.
86. Kamao, H., et al., *Characterization of human induced pluripotent stem cell-derived retinal pigment epithelium cell sheets aiming for clinical application.* Stem Cell Reports, 2014. **2**(2): p. 205-18.
87. Tetsuhiro Kikuchi, A.M., Daisuke Doi, Hirotaka Onoe, Takuya Hayashi, Toshiyuki Kawasaki, Hidemoto Saiki, Susumu Miyamoto, Jun Takahashi, *Survival of Human Induced Pluripotent Stem Cell–Derived Midbrain Dopaminergic Neurons in the Brain of a Primate Model of Parkinson's Disease.* Journal of Parkinson's Disease, 2011. **1**(4): p. 395-412.
88. Qin, J., et al., *Transplantation of human neuro-epithelial-like stem cells derived from induced pluripotent stem cells improves neurological function in rats with experimental intracerebral hemorrhage.* Neurosci Lett, 2013. **548**: p. 95-100.
89. Suzuki, H., et al., *Therapeutic angiogenesis by transplantation of induced pluripotent stem cell-derived Flk-1 positive cells.* BMC Cell Biol, 2010. **11**: p. 72.
90. Yoo, C.H., et al., *Endothelial progenitor cells from human dental pulp-derived iPS cells as a therapeutic target for ischemic vascular diseases.* Biomaterials, 2013. **34**(33): p. 8149-60.
91. Lian, Q., et al., *Functional mesenchymal stem cells derived from human induced pluripotent stem cells attenuate limb ischemia in mice.* Circulation, 2010. **121**(9): p. 1113-23.

92. Liu, H., et al., *In vivo liver regeneration potential of human induced pluripotent stem cells from diverse origins.* Sci Transl Med, 2011. **3**(82): p. 82ra39.
93. Li, Y., et al., *Long-term safety and efficacy of human induced pluripotent stem cell (iPS) grafts in a preclinical model of retinitis pigmentosa.* Mol Med, 2012.
94. Li, M., I. Sancho-Martinez, and J.C. Izpisua Belmonte, *Cell fate conversion by mRNA.* Stem Cell Res Ther, 2011. **2**(1): p. 5.
95. Anokye-Danso, F., et al., *Highly efficient miRNA-mediated reprogramming of mouse and human somatic cells to pluripotency.* Cell Stem Cell, 2011. **8**(4): p. 376-88.
96. Kim, D., et al., *Generation of human induced pluripotent stem cells by direct delivery of reprogramming proteins.* Cell Stem Cell, 2009. **4**(6): p. 472-6.
97. Hou, P., et al., *Pluripotent stem cells induced from mouse somatic cells by small-molecule compounds.* Science, 2013. **341**(6146): p. 651-4.
98. Sommer, C.A., et al., *Excision of reprogramming transgenes improves the differentiation potential of iPS cells generated with a single excisable vector.* Stem Cells, 2010. **28**(1): p. 64-74.
99. Awe, J.P., et al., *Generation and characterization of transgene-free human induced pluripotent stem cells and conversion to putative clinical-grade status.* Stem Cell Res Ther, 2013. **4**(4): p. 87.
100. Woltjen, K., et al., *piggyBac transposition reprograms fibroblasts to induced pluripotent stem cells.* Nature, 2009. **458**(7239): p. 766-70.
101. Davis, R.P., et al., *Generation of induced pluripotent stem cells from human foetal fibroblasts using the Sleeping Beauty transposon gene delivery system.* Differentiation, 2013. **86**(1-2): p. 30-7.
102. Hiratsuka, M., et al., *Integration-free iPS cells engineered using human artificial chromosome vectors.* PLoS One, 2011. **6**(10): p. e25961.
103. Sommer, C.A., et al., *Induced pluripotent stem cell generation using a single lentiviral stem cell cassette.* Stem Cells, 2009. **27**(3): p. 543-9.
104. Hamilton, B., et al., *Generation of induced pluripotent stem cells by reprogramming mouse embryonic fibroblasts with a four transcription factor, doxycycline inducible lentiviral transduction system.* J Vis Exp, 2009(33).

105. Tashiro, K., *Optimization of adenovirus vectors for transduction in embryonic stem cells and induced pluripotent stem cells.* Yakugaku Zasshi, 2011. **131**(9): p. 1333-8.
106. Fusaki, N., et al., *Efficient induction of transgene-free human pluripotent stem cells using a vector based on Sendai virus, an RNA virus that does not integrate into the host genome.* Proc Jpn Acad Ser B Phys Biol Sci, 2009. **85**(8): p. 348-62.
107. Okita, K., et al., *Generation of mouse induced pluripotent stem cells without viral vectors.* Science, 2008. **322**(5903): p. 949-53.
108. Okita, K., et al., *Generation of mouse-induced pluripotent stem cells with plasmid vectors.* Nat Protoc, 2010. **5**(3): p. 418-28.
109. Yu, J., et al., *Human induced pluripotent stem cells free of vector and transgene sequences.* Science, 2009. **324**(5928): p. 797-801.
110. Okita, K., et al., *A more efficient method to generate integration-free human iPS cells.* Nat Methods, 2011. **8**(5): p. 409-12.
111. Jia, F., et al., *A nonviral minicircle vector for deriving human iPS cells.* Nat Methods, 2010. **7**(3): p. 197-9.
112. Zhao, T., et al., *Immunogenicity of induced pluripotent stem cells.* Nature, 2011. **474**(7350): p. 212-5.
113. Guha, P., et al., *Lack of immune response to differentiated cells derived from syngeneic induced pluripotent stem cells.* Cell Stem Cell, 2013. **12**(4): p. 407-12.
114. Araki, R., et al., *Negligible immunogenicity of terminally differentiated cells derived from induced pluripotent or embryonic stem cells.* Nature, 2013. **494**(7435): p. 100-4.
115. Kaneko, S. and S. Yamanaka, *To be immunogenic, or not to be: that's the iPSC question.* Cell Stem Cell, 2013. **12**(4): p. 385-6.
116. Cahan, P. and G.Q. Daley, *Origins and implications of pluripotent stem cell variability and heterogeneity.* Nat Rev Mol Cell Biol, 2013. **14**(6): p. 357-68.
117. Puri, M.C. and A. Nagy, *Concise review: Embryonic stem cells versus induced pluripotent stem cells: the game is on.* Stem Cells, 2012. **30**(1): p. 10-4.
118. Kim, K., et al., *Epigenetic memory in induced pluripotent stem cells.* Nature, 2010. **467**(7313): p. 285-90.

119. Silva, J., et al., *Promotion of reprogramming to ground state pluripotency by signal inhibition.* PLoS Biol, 2008. **6**(10): p. 2237-47.
120. Lowry, W.E. and W.L. Quan, *Roadblocks en route to the clinical application of induced pluripotent stem cells.* J Cell Sci, 2010. **123**(Pt 5): p. 643-51.
121. Tucker, B.A., et al., *Use of a synthetic xeno-free culture substrate for induced pluripotent stem cell induction and retinal differentiation.* Stem Cells Transl Med, 2013. **2**(1): p. 16-24.
122. Chen, G., et al., *Chemically defined conditions for human iPSC derivation and culture.* Nat Methods, 2011. **8**(5): p. 424-9.
123. Rajala, K., et al., *A defined and xeno-free culture method enabling the establishment of clinical-grade human embryonic, induced pluripotent and adipose stem cells.* PLoS One, 2010. **5**(4): p. e10246.
124. Bilic, J. and J.C. Izpisua Belmonte, *Concise review: Induced pluripotent stem cells versus embryonic stem cells: close enough or yet too far apart?* Stem Cells, 2012. **30**(1): p. 33-41.
125. Asgari, S., et al., *Differentiation and Transplantation of Human Induced Pluripotent Stem Cell-derived Hepatocyte-like Cells.* Stem Cell Rev, 2013. **9**(4): p. 493-504.
126. Takahashi, K. and S. Yamanaka, *Induced pluripotent stem cells in medicine and biology.* Development, 2013. **140**(12): p. 2457-61.
127. Nakajima, F., K. Tokunaga, and N. Nakatsuji, *Human leukocyte antigen matching estimations in a hypothetical bank of human embryonic stem cell lines in the Japanese population for use in cell transplantation therapy.* Stem Cells, 2007. **25**(4): p. 983-5.
128. Taylor, C.J., et al., *Generating an iPSC bank for HLA-matched tissue transplantation based on known donor and recipient HLA types.* Cell Stem Cell, 2012. **11**(2): p. 147-52.
129. He, J., et al., *Regeneration of liver after extreme hepatocyte loss occurs mainly via biliary transdifferentiation in zebrafish.* Gastroenterology, 2014. **146**(3): p. 789-800 e8.
130. Zhang, R., et al., *In vivo cardiac reprogramming contributes to zebrafish heart regeneration.* Nature, 2013. **498**(7455): p. 497-501.
131. Suetsugu-Maki, R., et al., *Lens regeneration in axolotl: new evidence of developmental plasticity.* BMC Biol, 2012. **10**: p. 103.

132. Wang, T., et al., *Lgr5+ cells regenerate hair cells via proliferation and direct transdifferentiation in damaged neonatal mouse utricle.* Nat Commun, 2015. **6**: p. 6613.
133. Barrett, N.R., *The lower esophagus lined by columnar epithelium.* Surgery, 1957. **41**(6): p. 881-94.
134. Spechler, S.J., *Clinical practice. Barrett's Esophagus.* N Engl J Med, 2002. **346**(11): p. 836-42.
135. Hay, E.D. and A. Zuk, *Transformations between epithelium and mesenchyme: normal, pathological, and experimentally induced.* Am J Kidney Dis, 1995. **26**(4): p. 678-90.
136. Tsukamoto, H., et al., *Anti-adipogenic regulation underlies hepatic stellate cell transdifferentiation.* J Gastroenterol Hepatol, 2006. **21 Suppl 3**: p. S102-5.
137. Li, Y. and J. Huard, *Differentiation of muscle-derived cells into myofibroblasts in injured skeletal muscle.* Am J Pathol, 2002. **161**(3): p. 895-907.
138. Ferber, S., et al., *Pancreatic and duodenal homeobox gene 1 induces expression of insulin genes in liver and ameliorates streptozotocin-induced hyperglycemia.* Nat Med, 2000. **6**(5): p. 568-72.
139. Ber, I., et al., *Functional, persistent, and extended liver to pancreas transdifferentiation.* J Biol Chem, 2003. **278**(34): p. 31950-7.
140. Miyatsuka, T., et al., *Ectopically expressed PDX-1 in liver initiates endocrine and exocrine pancreas differentiation but causes dysmorphogenesis.* Biochem Biophys Res Commun, 2003. **310**(3): p. 1017-25.
141. Kojima, H., et al., *NeuroD-betacellulin gene therapy induces islet neogenesis in the liver and reverses diabetes in mice.* Nat Med, 2003. **9**(5): p. 596-603.
142. Kaneto, H., et al., *PDX-1/VP16 fusion protein, together with NeuroD or Ngn3, markedly induces insulin gene transcription and ameliorates glucose tolerance.* Diabetes, 2005. **54**(4): p. 1009-22.
143. Yechoor, V., et al., *Neurogenin3 is sufficient for transdetermination of hepatic progenitor cells into neo-islets in vivo but not transdifferentiation of hepatocytes.* Dev Cell, 2009. **16**(3): p. 358-73.
144. Banga, A., et al., *In vivo reprogramming of Sox9+ cells in the liver to insulin-secreting ducts.* Proc Natl Acad Sci U S A, 2012. **109**(38): p. 15336-41.

145. Mozaffarian, D., et al., *Heart disease and stroke statistics--2015 update: a report from the American Heart Association.* Circulation, 2015. **131**(4): p. e29-322.
146. Murry, C.E., et al., *Muscle differentiation during repair of myocardial necrosis in rats via gene transfer with MyoD.* J Clin Invest, 1996. **98**(10): p. 2209-17.
147. Qian, L., et al., *In vivo reprogramming of murine cardiac fibroblasts into induced cardiomyocytes.* Nature, 2012. **485**(7400): p. 593-8.
148. Inagawa, K., et al., *Induction of cardiomyocyte-like cells in infarct hearts by gene transfer of Gata4, Mef2c, and Tbx5.* Circ Res, 2012. **111**(9): p. 1147-56.
149. Song, K., et al., *Heart repair by reprogramming non-myocytes with cardiac transcription factors.* Nature, 2012. **485**(7400): p. 599-604.
150. Jayawardena, T.M., et al., *MicroRNA-mediated in vitro and in vivo direct reprogramming of cardiac fibroblasts to cardiomyocytes.* Circ Res, 2012. **110**(11): p. 1465-73.
151. Jayawardena, T.M., et al., *MicroRNA induced cardiac reprogramming in vivo: evidence for mature cardiac myocytes and improved cardiac function.* Circ Res, 2015. **116**(3): p. 418-24.
152. Kapoor, N., et al., *Direct conversion of quiescent cardiomyocytes to pacemaker cells by expression of Tbx18.* Nat Biotechnol, 2013. **31**(1): p. 54-62.
153. Hu, Y.F., et al., *Biological pacemaker created by minimally invasive somatic reprogramming in pigs with complete heart block.* Sci Transl Med, 2014. **6**(245): p. 245ra94.
154. Torper, O., et al., *Generation of induced neurons via direct conversion in vivo.* Proc Natl Acad Sci U S A, 2013. **110**(17): p. 7038-43.
155. Niu, W., et al., *In vivo reprogramming of astrocytes to neuroblasts in the adult brain.* Nat Cell Biol, 2013. **15**(10): p. 1164-75.
156. Niu, W., et al., *SOX2 Reprograms Resident Astrocytes into Neural Progenitors in the Adult Brain.* Stem Cell Reports, 2015.
157. Guo, Z., et al., *In vivo direct reprogramming of reactive glial cells into functional neurons after brain injury and in an Alzheimer's disease model.* Cell Stem Cell, 2014. **14**(2): p. 188-202.
158. Su, Z., et al., *In vivo conversion of astrocytes to neurons in the injured adult spinal cord.* Nat Commun, 2014. **5**: p. 3338.

159. Rouaux, C. and P. Arlotta, *Direct lineage reprogramming of post-mitotic callosal neurons into corticofugal neurons in vivo.* Nat Cell Biol, 2013. **15**(2): p. 214-21.
160. De la Rossa, A., et al., *In vivo reprogramming of circuit connectivity in postmitotic neocortical neurons.* Nat Neurosci, 2013. **16**(2): p. 193-200.
161. Vivien, C., et al., *Non-viral expression of mouse Oct4, Sox2, and Klf4 transcription factors efficiently reprograms tadpole muscle fibers in vivo.* J Biol Chem, 2012. **287**(10): p. 7427-35.
162. Yilmazer, A., et al., *In vivo cell reprogramming towards pluripotency by virus-free overexpression of defined factors.* PLoS One, 2013. **8**(1): p. e54754.
163. Yilmazer, A., et al., *In vivo reprogramming of adult somatic cells to pluripotency by overexpression of Yamanaka factors.* JoVE, 2013. **17**(82).
164. de Lazaro, I. and K. Kostarelos, *In vivo cell reprogramming to pluripotency: exploring a novel tool for cell replenishment and tissue regeneration.* Biochemical Society Transactions, 2014. **42**(3): p. 711-716.
165. Cyranoski, D., *iPS cells in humans.* Nat Biotechnol, 2013. **31**(9): p. 775.
166. Reardon, S. and D. Cyranoski, *Japan stem-cell trial stirs envy.* Nature, 2014. **513**(7518): p. 287-8.
167. Buganim, Y., D.A. Faddah, and R. Jaenisch, *Mechanisms and models of somatic cell reprogramming.* Nat Rev Genet, 2013. **14**(6): p. 427-39.
168. Liu, F., Y. Song, and D. Liu, *Hydrodynamics-based transfection in animals by systemic administration of plasmid DNA.* Gene Ther, 1999. **6**(7): p. 1258-66.
169. Eastman, S.J., et al., *Development of catheter-based procedures for transducing the isolated rabbit liver with plasmid DNA.* Hum Gene Ther, 2002. **13**(17): p. 2065-77.
170. Yoshino, H., K. Hashizume, and E. Kobayashi, *Naked plasmid DNA transfer to the porcine liver using rapid injection with large volume.* Gene Ther, 2006. **13**(24): p. 1696-702.
171. Alino, S.F., et al., *Pig liver gene therapy by noninvasive interventionist catheterism.* Gene Ther, 2007. **14**(4): p. 334-43.
172. Khorsandi, S.E., et al., *Minimally invasive and selective hydrodynamic gene therapy of liver segments in the pig and human.* Cancer Gene Ther, 2008. **15**(4): p. 225-30.

173. Zhang, G., V. Budker, and J.A. Wolff, *High levels of foreign gene expression in hepatocytes after tail vein injections of naked plasmid DNA.* Hum Gene Ther, 1999. **10**(10): p. 1735-7.
174. Andrianaivo, F., et al., *Hydrodynamics-based transfection of the liver: entrance into hepatocytes of DNA that causes expression takes place very early after injection.* J Gene Med, 2004. **6**(8): p. 877-83.
175. Sebestyen, M.G., et al., *Mechanism of plasmid delivery by hydrodynamic tail vein injection. I. Hepatocyte uptake of various molecules.* J Gene Med, 2006. **8**(7): p. 852-73.
176. Si-Tayeb, K., F.P. Lemaigre, and S.A. Duncan, *Organogenesis and development of the liver.* Dev Cell, 2010. **18**(2): p. 175-89.
177. Shin, D. and S.P. Monga, *Cellular and molecular basis of liver development.* Compr Physiol, 2013. **3**(2): p. 799-815.
178. Kheolamai, P. and A.J. Dickson, *Liver-enriched transcription factors are critical for the expression of hepatocyte marker genes in mES-derived hepatocyte-lineage cells.* BMC Mol Biol, 2009. **10**: p. 35.
179. ten Hagen, T.L., W. van Vianen, and I.A. Bakker-Woudenberg, *Isolation and characterization of murine Kupffer cells and splenic macrophages.* J Immunol Methods, 1996. **193**(1): p. 81-91.
180. Michalska, A.E., *Isolation and propagation of mouse embryonic fibroblasts and preparation of mouse embryonic feeder layer cells.* Curr Protoc Stem Cell Biol, 2007. **3**: p. 1C.3.1-1C.3.17.
181. Kang, N.Y., et al., *Embryonic and induced pluripotent stem cell staining and sorting with the live-cell fluorescence imaging probe CDy1.* Nat Protoc, 2011. **6**(7): p. 1044-52.
182. Mochizuki, H., Y. Ohnuki, and H. Kurosawa, *Effect of glucose concentration during embryoid body (EB) formation from mouse embryonic stem cells on EB growth and cell differentiation.* J Biosci Bioeng, 2010. **111**(1): p. 92-7.
183. Park, H.Y., et al., *Efficient generation of virus-free iPS cells using liposomal magnetofection.* PLoS One, 2012. **7**(9): p. e45812.
184. Bhave, V.S., et al., *Genes inducing iPS phenotype play a role in hepatocyte survival and proliferation in vitro and liver regeneration in vivo.* Hepatology, 2011. **54**(4): p. 1360-70.

185. de Lazaro, I., et al., *Generation of induced pluripotent stem cells from virus-free in vivo reprogramming of BALB/c mouse liver cells.* Biomaterials, 2014. **35**(29): p. 8312-20.
186. Maherali, N. and K. Hochedlinger, *Guidelines and techniques for the generation of induced pluripotent stem cells.* Cell Stem Cell, 2008. **3**(6): p. 595-605.
187. Som, A., et al., *The PluriNetWork: an electronic representation of the network underlying pluripotency in mouse, and its applications.* PLoS One, 2010. **5**(12): p. e15165.
188. Kurosawa, H., *Methods for inducing embryoid body formation: in vitro differentiation system of embryonic stem cells.* J Biosci Bioeng, 2007. **103**(5): p. 389-98.
189. Yukawa, H., H. Noguchi, and S. Hayashi, *Embryonic body formation using the tapered soft stencil for cluster culture device.* Biomaterials, 2011. **32**(15): p. 3729-38.
190. Ben-David, U. and N. Benvenisty, *The tumorigenicity of human embryonic and induced pluripotent stem cells.* Nat Rev Cancer, 2011. **11**(4): p. 268-77.
191. Jaenisch, R. and R. Young, *Stem cells, the molecular circuitry of pluripotency and nuclear reprogramming.* Cell, 2008. **132**(4): p. 567-82.
192. Koehler, K.R., et al., *Extended passaging increases the efficiency of neural differentiation from induced pluripotent stem cells.* BMC Neurosci, 2011. **12**: p. 82.
193. Markel, P., et al., *Theoretical and empirical issues for marker-assisted breeding of congenic mouse strains.* Nat Genet, 1997. **17**(3): p. 280-4.
194. Robinton, D.A. and G.Q. Daley, *The promise of induced pluripotent stem cells in research and therapy.* Nature, 2012. **481**(7381): p. 295-305.
195. Abad, M., et al., *Reprogramming in vivo produces teratomas and iPS cells with totipotency features.* Nature, 2013. **502**: p. 340-345.
196. Ohnishi, K., et al., *Premature Termination of Reprogramming In Vivo Leads to Cancer Development through Altered Epigenetic Regulation.* Cell, 2014. **156**(4): p. 663-77.
197. Kawase, E., et al., *Strain difference in establishment of mouse embryonic stem (ES) cell lines.* Int J Dev Biol, 1994. **38**(2): p. 385-90.

198. Dinkel, A., et al., *Efficient generation of transgenic BALB/c mice using BALB/c embryonic stem cells.* J Immunol Methods, 1999. **223**(2): p. 255-60.
199. Carstea, A.C., M.K. Pirity, and A. Dinnyes, *Germline competence of mouse ES and iPS cell lines: Chimera technologies and genetic background.* World J Stem Cells, 2009. **1**(1): p. 22-9.
200. Longenecker, G. and A.B. Kulkarni, *Generation of gene knockout mice by ES cell microinjection.* Curr Protoc Cell Biol, 2009. **44**(19): p. 1-36.
201. Gertsenstein, M., et al., *Efficient Generation of Germ Line Transmitting Chimeras from C57BL/6N ES Cells by Aggregation with Outbred Host Embryos.* PLoS ONE, 2010. **5**(6): p. e11260.
202. Longo, L., et al., *The chromosome make-up of mouse embryonic stem cells is predictive of somatic and germ cell chimaerism.* Transgenic Research, 1997. **6**(5): p. 321-328.
203. Nagy, A., et al., *Derivation of completely cell culture-derived mice from early-passage embryonic stem cells.* Proc Natl Acad Sci U S A, 1993. **90**(18): p. 8424-8.
204. Huang, J., et al., *Association of telomere length with authentic pluripotency of ES/iPS cells.* Cell Res, 2011. **21**(5): p. 779-92.
205. Silva, J., et al., *Nanog is the gateway to the pluripotent ground state.* Cell, 2009. **138**(4): p. 722-37.
206. Mochiduki, Y. and K. Okita, *Methods for iPS cell generation for basic research and clinical applications.* Biotechnol J, 2012. **7**(6): p. 789-97.
207. Ye, L., et al., *Blood cell-derived induced pluripotent stem cells free of reprogramming factors generated by Sendai viral vectors.* Stem Cells Transl Med. **2**(8): p. 558-66.
208. Wolff, J.A., et al., *Direct gene transfer into mouse muscle in vivo.* Science, 1990. **247**(4949 Pt 1): p. 1465-8.
209. Davis, H.L., et al., *Plasmid DNA is superior to viral vectors for direct gene transfer into adult mouse skeletal muscle.* Hum Gene Ther, 1993. **4**(6): p. 733-40.
210. Levy, M.Y., et al., *Characterization of plasmid DNA transfer into mouse skeletal muscle: evaluation of uptake mechanism, expression and secretion of gene products into blood.* Gene Ther, 1996. **3**(3): p. 201-11.

211. Wolff, J.A., et al., *Expression of naked plasmids by cultured myotubes and entry of plasmids into T tubules and caveolae of mammalian skeletal muscle.* J Cell Sci, 1992. **103 (Pt 4)**: p. 1249-59.
212. Wolff, J.A., et al., *Long-term persistence of plasmid DNA and foreign gene expression in mouse muscle.* Hum Mol Genet, 1992. **1**(6): p. 363-9.
213. Buckingham, M., et al., *The formation of skeletal muscle: from somite to limb.* J Anat, 2003. **202**(1): p. 59-68.
214. Buckingham, M., *Myogenic progenitor cells and skeletal myogenesis in vertebrates.* Curr Opin Genet Dev, 2006. **16**(5): p. 525-32.
215. Koch, U., R. Lehal, and F. Radtke, *Stem cells living with a Notch.* Development, 2013. **140**(4): p. 689-704.
216. Charge, S.B. and M.A. Rudnicki, *Cellular and molecular regulation of muscle regeneration.* Physiol Rev, 2004. **84**(1): p. 209-38.
217. Sirabella, D., L. De Angelis, and L. Berghella, *Sources for skeletal muscle repair: from satellite cells to reprogramming.* J Cachexia Sarcopenia Muscle, 2013. **4**(2): p. 125-36.
218. Watanabe, S., et al., *MyoD gene suppression by Oct4 is required for reprogramming in myoblasts to produce induced pluripotent stem cells.* Stem Cells, 2011. **29**(3): p. 505-16.
219. Chambers, I., et al., *Nanog safeguards pluripotency and mediates germline development.* Nature, 2007. **450**(7173): p. 1230-1234.
220. Relaix, F., et al., *A Pax3/Pax7-dependent population of skeletal muscle progenitor cells.* Nature, 2005. **435**(7044): p. 948-53.
221. Davis, H.L., R.G. Whalen, and B.A. Demeneix, *Direct gene transfer into skeletal muscle in vivo: factors affecting efficiency of transfer and stability of expression.* Hum Gene Ther, 1993. **4**(2): p. 151-9.
222. Curran, J., *In Vivo Assay of Cellular Proliferation*. 2001. p. 379-389.
223. Collins, C.A., et al., *Integrated functions of Pax3 and Pax7 in the regulation of proliferation, cell size and myogenic differentiation.* PLoS One, 2009. **4**(2): p. e4475.
224. Danko, I., et al., *High expression of naked plasmid DNA in muscles of young rodents.* Hum Mol Genet, 1997. **6**(9): p. 1435-43.
225. Kim, J.B., et al., *Pluripotent stem cells induced from adult neural stem cells by reprogramming with two factors.* Nature, 2008. **454**(7204): p. 646-50.

226. Eminli, S., et al., *Differentiation stage determines potential of hematopoietic cells for reprogramming into induced pluripotent stem cells.* Nat Genet, 2009. **41**(9): p. 968-76.
227. Kleger, A., et al., *Increased reprogramming capacity of mouse liver progenitor cells, compared with differentiated liver cells, requires the BAF complex.* Gastroenterology, 2012. **142**(4): p. 907-17.
228. Tan, K.Y., et al., *Efficient generation of iPS cells from skeletal muscle stem cells.* PLoS One, 2011. **6**(10): p. e26406.
229. Allbrook, D.B., M.F. Han, and A.E. Hellmuth, *Population of muscle satellite cells in relation to age and mitotic activity.* Pathology, 1971. **3**(3): p. 223-43.
230. Chambers, I., et al., *Nanog safeguards pluripotency and mediates germline development.* Nature, 2007. **450**(7173): p. 1230-4.
231. Dellavalle, A., et al., *Pericytes resident in postnatal skeletal muscle differentiate into muscle fibres and generate satellite cells.* Nat Commun, 2011. **2**: p. 499.
232. Buckingham, M., et al., *Myogenic progenitor cells in the mouse embryo are marked by the expression of Pax3/7 genes that regulate their survival and myogenic potential.* Anat Embryol (Berl), 2006. **211 Suppl 1**: p. 51-6.
233. Relaix, F., et al., *Pax3 and Pax7 have distinct and overlapping functions in adult muscle progenitor cells.* J Cell Biol, 2006. **172**(1): p. 91-102.
234. Gnocchi, V.F., et al., *Further characterisation of the molecular signature of quiescent and activated mouse muscle satellite cells.* PLoS One, 2009. **4**(4): p. e5205.
235. Buganim, Y., et al., *Single-Cell Expression Analyses during Cellular Reprogramming Reveal an Early Stochastic and a Late Hierarchic Phase.* Cell, 2012. **150**(6): p. 1209-1222.
236. Vaittinen, S., et al., *The expression of intermediate filament protein nestin as related to vimentin and desmin in regenerating skeletal muscle.* J Neuropathol Exp Neurol, 2001. **60**(6): p. 588-97.
237. Yablonka-Reuveni, Z., et al., *Defining the transcriptional signature of skeletal muscle stem cells.* J Anim Sci, 2008. **86**(14 Suppl): p. E207-16.
238. White, R.B., et al., *Dynamics of muscle fibre growth during postnatal mouse development.* BMC Dev Biol, 2010. **10**: p. 21.

239. Merrick, D., et al., *Adult and embryonic skeletal muscle microexplant culture and isolation of skeletal muscle stem cells.* J Vis Exp, 2010(43).
240. Pasut, A., A.E. Jones, and M.A. Rudnicki, *Isolation and culture of individual myofibers and their satellite cells from adult skeletal muscle.* J Vis Exp, 2013(73): p. e50074.
241. Morrison, J.I., et al., *Salamander limb regeneration involves the activation of a multipotent skeletal muscle satellite cell population.* J Cell Biol, 2006. **172**(3): p. 433-40.
242. Odelberg, S.J., A. Kollhoff, and M.T. Keating, *Dedifferentiation of mammalian myotubes induced by msx1.* Cell, 2000. **103**(7): p. 1099-109.
243. McGann, C.J., S.J. Odelberg, and M.T. Keating, *Mammalian myotube dedifferentiation induced by newt regeneration extract.* Proc Natl Acad Sci U S A, 2001. **98**(24): p. 13699-704.
244. Yang, Z., et al., *Mononuclear cells from dedifferentiation of mouse myotubes display remarkable regenerative capability.* Stem Cells, 2014. **32**(9): p. 2492-501.
245. Miyoshi, T., et al., *In vivo electroporation induces cell cycle reentry of myonuclei in rat skeletal muscle.* J Vet Med Sci, 2012. **74**(10): p. 1291-7.
246. Mu, X., et al., *Study of muscle cell dedifferentiation after skeletal muscle injury of mice with a Cre-Lox system.* PLoS One, 2011. **6**(2): p. e16699.
247. Rodrigues, A.M., et al., *Skeletal muscle regeneration in Xenopus tadpoles and zebrafish larvae.* BMC Dev Biol, 2012. **12**: p. 9.
248. Mauro, A., *Satellite cell of skeletal muscle fibers.* J Biophys Biochem Cytol, 1961. **9**: p. 493-5.
249. Le Grand, F. and M.A. Rudnicki, *Skeletal muscle satellite cells and adult myogenesis.* Curr Opin Cell Biol, 2007. **19**(6): p. 628-33.
250. Bareja, A. and A.N. Billin, *Satellite cell therapy - from mice to men.* Skelet Muscle, 2013. **3**(1): p. 2.
251. Sirabella, D., L. Angelis, and L. Berghella, *Sources for skeletal muscle repair: from satellite cells to reprogramming.* Journal of Cachexia, Sarcopenia and Muscle, 2013. **4**(2): p. 125-136.
252. Lieber, R.L. and S.R. Ward, *Cellular mechanisms of tissue fibrosis. 4. Structural and functional consequences of skeletal muscle fibrosis.* Am J Physiol Cell Physiol, 2013. **305**(3): p. C241-52.

253. Bondesen, B.A., et al., *The COX-2 pathway is essential during early stages of skeletal muscle regeneration.* Am J Physiol Cell Physiol, 2004. **287**(2): p. C475-83.
254. Shen, W., et al., *NS-398, a cyclooxygenase-2-specific inhibitor, delays skeletal muscle healing by decreasing regeneration and promoting fibrosis.* Am J Pathol, 2005. **167**(4): p. 1105-17.
255. Menetrey, J., et al., *Suturing versus immobilization of a muscle laceration. A morphological and functional study in a mouse model.* Am J Sports Med, 1999. **27**(2): p. 222-9.
256. Fukushima, K., et al., *The use of an antifibrosis agent to improve muscle recovery after laceration.* Am J Sports Med, 2001. **29**(4): p. 394-402.
257. Chan, Y.S., et al., *Antifibrotic effects of suramin in injured skeletal muscle after laceration.* J Appl Physiol (1985), 2003. **95**(2): p. 771-80.
258. Foster, W., et al., *Gamma interferon as an antifibrosis agent in skeletal muscle.* J Orthop Res, 2003. **21**(5): p. 798-804.
259. Negishi, S., et al., *The effect of relaxin treatment on skeletal muscle injuries.* Am J Sports Med, 2005. **33**(12): p. 1816-24.
260. Menetrey, J., et al., *Growth factors improve muscle healing in vivo.* J Bone Joint Surg Br, 2000. **82**(1): p. 131-7.
261. Natsu, K., et al., *Allogeneic bone marrow-derived mesenchymal stromal cells promote the regeneration of injured skeletal muscle without differentiation into myofibers.* Tissue Eng, 2004. **10**(7-8): p. 1093-112.
262. Shi, M., et al., *Acceleration of skeletal muscle regeneration in a rat skeletal muscle injury model by local injection of human peripheral blood-derived CD133-positive cells.* Stem Cells, 2009. **27**(4): p. 949-60.
263. Mori, R., et al., *Promotion of skeletal muscle repair in a rat skeletal muscle injury model by local injection of human adipose tissue-derived regenerative cells.* J Tissue Eng Regen Med, 2012.
264. Nakasa, T., et al., *Acceleration of muscle regeneration by local injection of muscle-specific microRNAs in rat skeletal muscle injury model.* J Cell Mol Med, 2010. **14**(10): p. 2495-505.
265. Lee, C.W., et al., *BIOLOGICAL INTERVENTION BASED ON CELL AND GENE THERAPY TO IMPROVE MUSCLE HEALING AFTER LACERATION.* Journal of Musculoskeletal Research, 2000. **04**(04): p. 265-277.

266. Park, J.K., et al., *Losartan improves adipose tissue-derived stem cell niche by inhibiting transforming growth factor-beta and fibrosis in skeletal muscle injury.* Cell Transplant, 2012. **21**(11): p. 2407-24.
267. Hwang, J.H., et al., *Combination therapy of human adipose-derived stem cells and basic fibroblast growth factor hydrogel in muscle regeneration.* Biomaterials, 2013. **34**(25): p. 6037-45.
268. Sato, K., et al., *Improvement of muscle healing through enhancement of muscle regeneration and prevention of fibrosis.* Muscle Nerve, 2003. **28**(3): p. 365-72.
269. CHARGÉ, S.B.P. and M.A. RUDNICKI, *Cellular and Molecular Regulation of Muscle Regeneration.* Physiological Reviews, 2004. **84**(1): p. 209-238.
270. Grounds, M.D. and J.K. McGeachie, *A comparison of muscle precursor replication in crush-injured skeletal muscle of Swiss and BALBc mice.* Cell Tissue Res, 1989. **255**(2): p. 385-91.
271. Mitchell, C.A., J.K. McGeachie, and M.D. Grounds, *Cellular differences in the regeneration of murine skeletal muscle: a quantitative histological study in SJL/J and BALB/c mice.* Cell Tissue Res, 1992. **269**(1): p. 159-66.
272. Zhang, C., et al., *Interleukin-6/signal transducer and activator of transcription 3 (STAT3) pathway is essential for macrophage infiltration and myoblast proliferation during muscle regeneration.* J Biol Chem, 2013. **288**(3): p. 1489-99.
273. Warren, G.L., et al., *Mechanisms of skeletal muscle injury and repair revealed by gene expression studies in mouse models.* J Physiol, 2007. **582**(Pt 2): p. 825-41.
274. Martinez, C.O., et al., *Regulation of skeletal muscle regeneration by CCR2-activating chemokines is directly related to macrophage recruitment.* Am J Physiol Regul Integr Comp Physiol, 2010. **299**(3): p. R832-42.
275. Czerwinska, A.M., et al., *Mouse gastrocnemius muscle regeneration after mechanical or cardiotoxin injury.* Folia Histochem Cytobiol, 2012. **50**(1): p. 144-53.
276. Fan, Y., et al., *Rapid death of injected myoblasts in myoblast transfer therapy.* Muscle Nerve, 1996. **19**(7): p. 853-60.

277. Schertzer, J.D. and G.S. Lynch, *Comparative evaluation of IGF-I gene transfer and IGF-I protein administration for enhancing skeletal muscle regeneration after injury.* Gene Ther, 2006. **13**(23): p. 1657-64.
278. Wu, Y., et al., *Mesenchymal Stem Cells Suppress Fibroblast Proliferation and Reduce Skin Fibrosis Through a TGF-beta3-Dependent Activation.* Int J Low Extrem Wounds, 2015. **14**(1): p. 50-62.
279. Li, Y., et al., *Decorin gene transfer promotes muscle cell differentiation and muscle regeneration.* Mol Ther, 2007. **15**(9): p. 1616-22.
280. Wallace, G.Q. and E.M. McNally, *Mechanisms of muscle degeneration, regeneration, and repair in the muscular dystrophies.* Annu Rev Physiol, 2009. **71**: p. 37-57.
281. Kocaefe, Y.C., et al., *Myogenic program induction in mature fat tissue (with MyoD expression).* Exp Cell Res, 2005. **308**(2): p. 300-8.
282. Borycki, A.G., et al., *Pax3 functions in cell survival and in pax7 regulation.* Development, 1999. **126**(8): p. 1665-74.
283. Hirai, H., et al., *MyoD regulates apoptosis of myoblasts through microRNA-mediated down-regulation of Pax3.* J Cell Biol, 2010. **191**(2): p. 347-65.
284. Planello, A.C., et al., *Aberrant DNA methylation reprogramming during induced pluripotent stem cell generation is dependent on the choice of reprogramming factors.* Cell Regen (Lond), 2014. **3**(1): p. 4.

Appendices

Supplementary Figures and Tables

Figure S 1. Maps of the DNA plasmids employed in the study. (a) *pCX-OKS-2A (**OKS** pDNA),* ***(b)*** *pCX-cMyc (**M** pDNA),* ***(c)*** *pLenti-III-EF1α-mYamanaka (**OKSM** pDNA).*

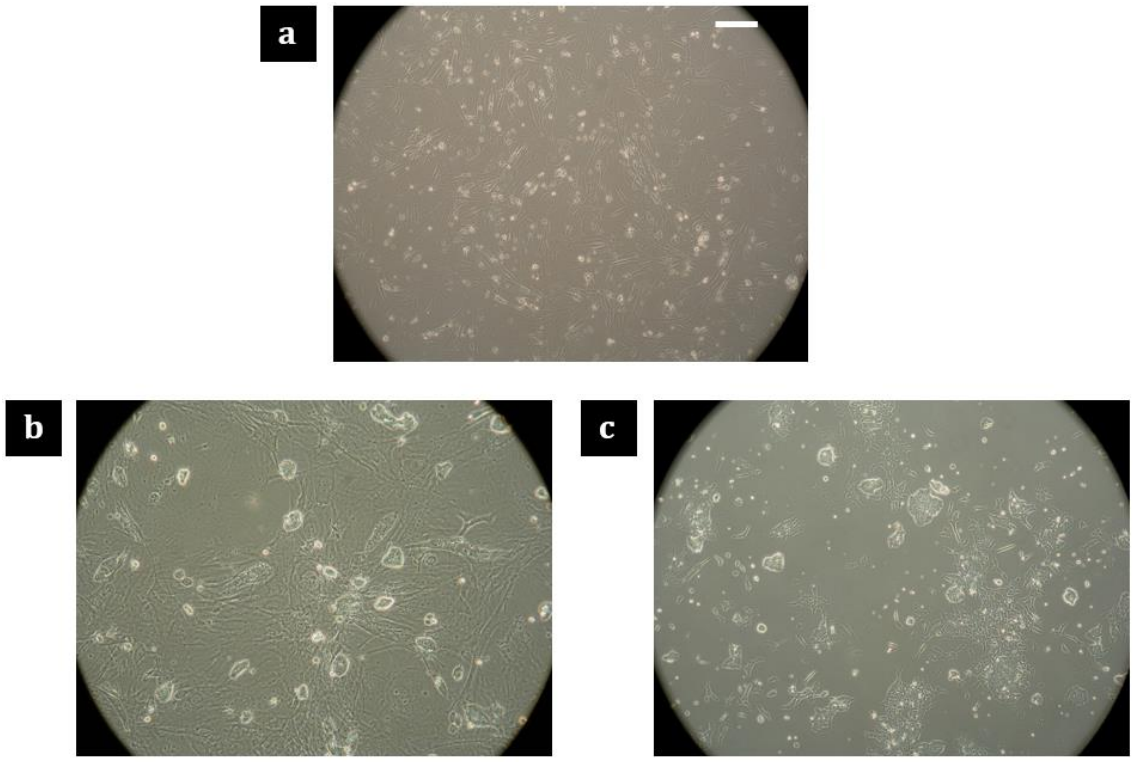

Figure S 2. Isolation of MEFs and preparation of feeder layers for the culture of pluripotent stem cells. *MEFs were isolated from E12.5-14.5 CD1 mouse embryos after removal of internal organs and cell dissociation.* ***(a)*** *MEFs were cultured as monolayers in tissue culture vessels and mitotically inactivated with mitomycin C. The morphology E14TG2A cell colonies was compared when cultured on* ***(b)*** *MEFs feeder layers and* ***(c)*** *gelatin-coated surfaces. Images were acquired with an optical microscope. Scale bar represents 100µm.*

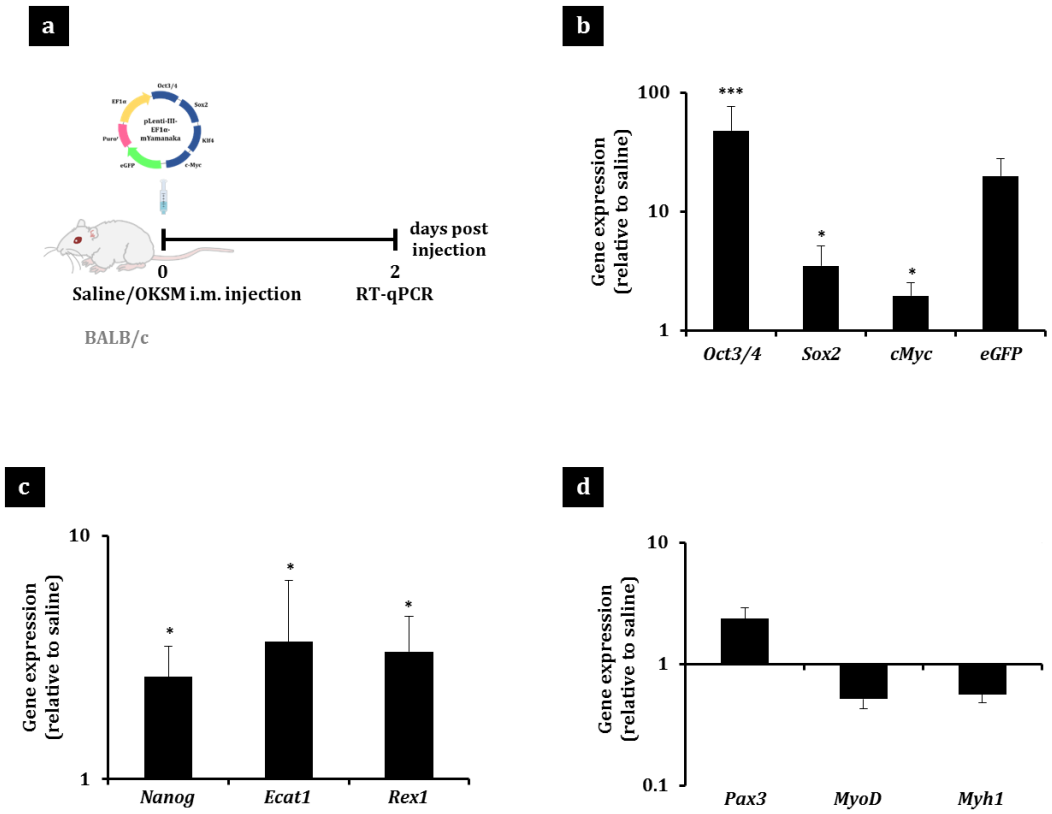

Figure S 3. Gene expression in BALB/c mouse skeletal muscle after i.m. administration of OKSM reprogramming pDNA. ***(a)*** *BALB/c mice were i.m. injected in the GA muscle with 50µg* ***OKSM*** *in 50 µl 0.9% saline or 50 µl 0.9% saline alone. GA muscles were dissected 2 days after injection and real-time RT-qPCR was performed to determine the relative gene expression of* ***(b)*** *reprogramming factors,* ***(c)*** *endogenous pluripotency markers and* ***(d)*** *genes involved in myogenesis. Gene expression levels were normalised to the saline-injected group. *p<0.05 and ***p<0.001 indicate statistically significant differences in gene expression between pDNA and saline-injected groups, assessed by one-way ANOVA. Data are presented as mean ± SD, n=3. This experiment was performed with Dr. Acelya Yilmazer.*

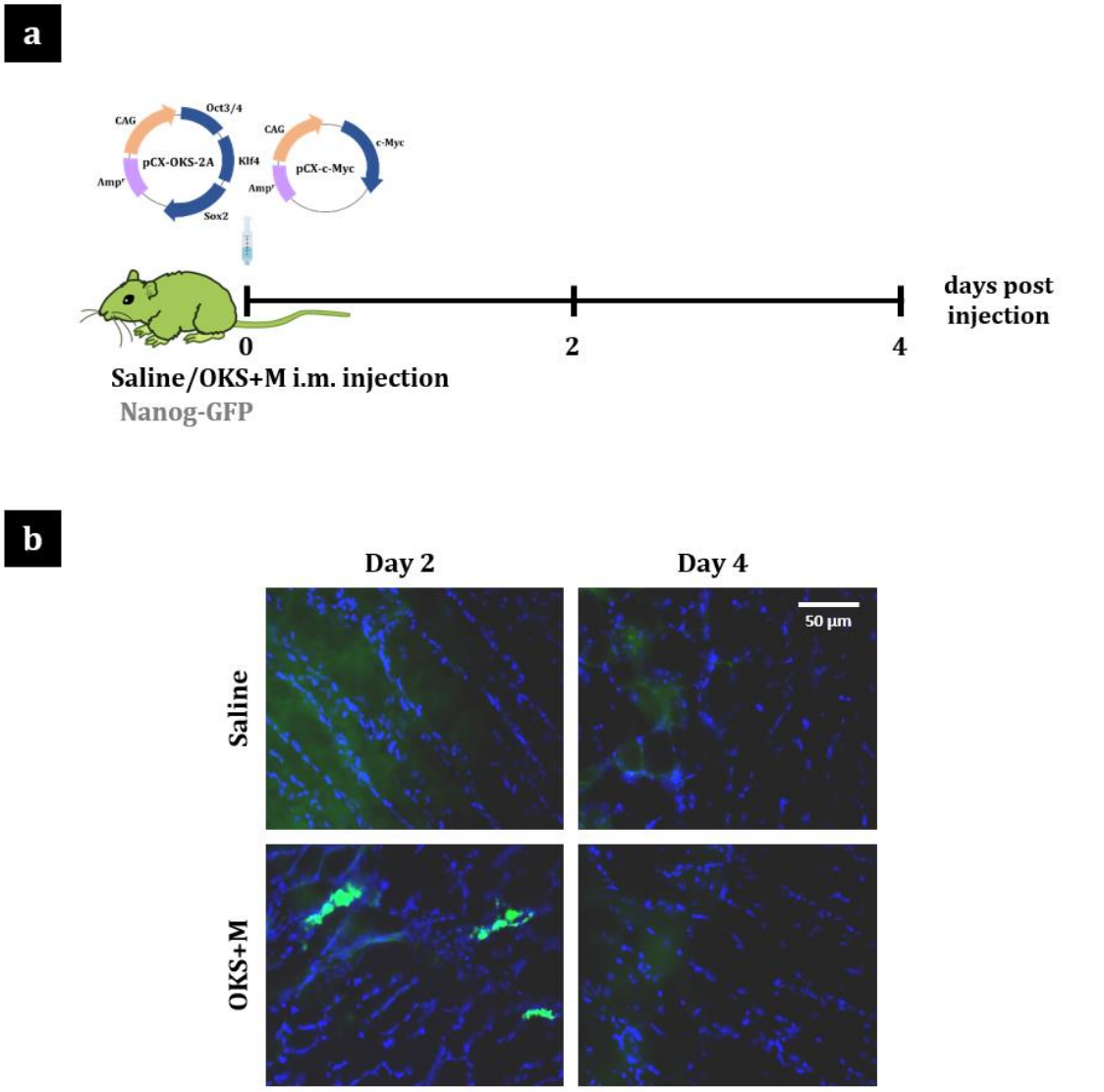

Figure S 4. Characterisation of GFP⁺ cell clusters in the GA muscle of Nanog-GFP mice. (a) *Nanog-GFP transgenic mice were i.m. injected with 50µg* ***OKS*** *and 50 µg* ***M*** *or 50 µl 0.9% saline in the GA muscle. Tissues were dissected 2 and 4 days after injection.* ***(b)*** *10 µm-thick tissue sections were obtained by cryotomy and the green fluorescence resulting from the expression of Nanog was observed with an epi-fluorescence microscope. Representative images were taken at 100X, scale bar represents 50 µm. This experiment was performed by Dr. Acelya Yilmazer.*

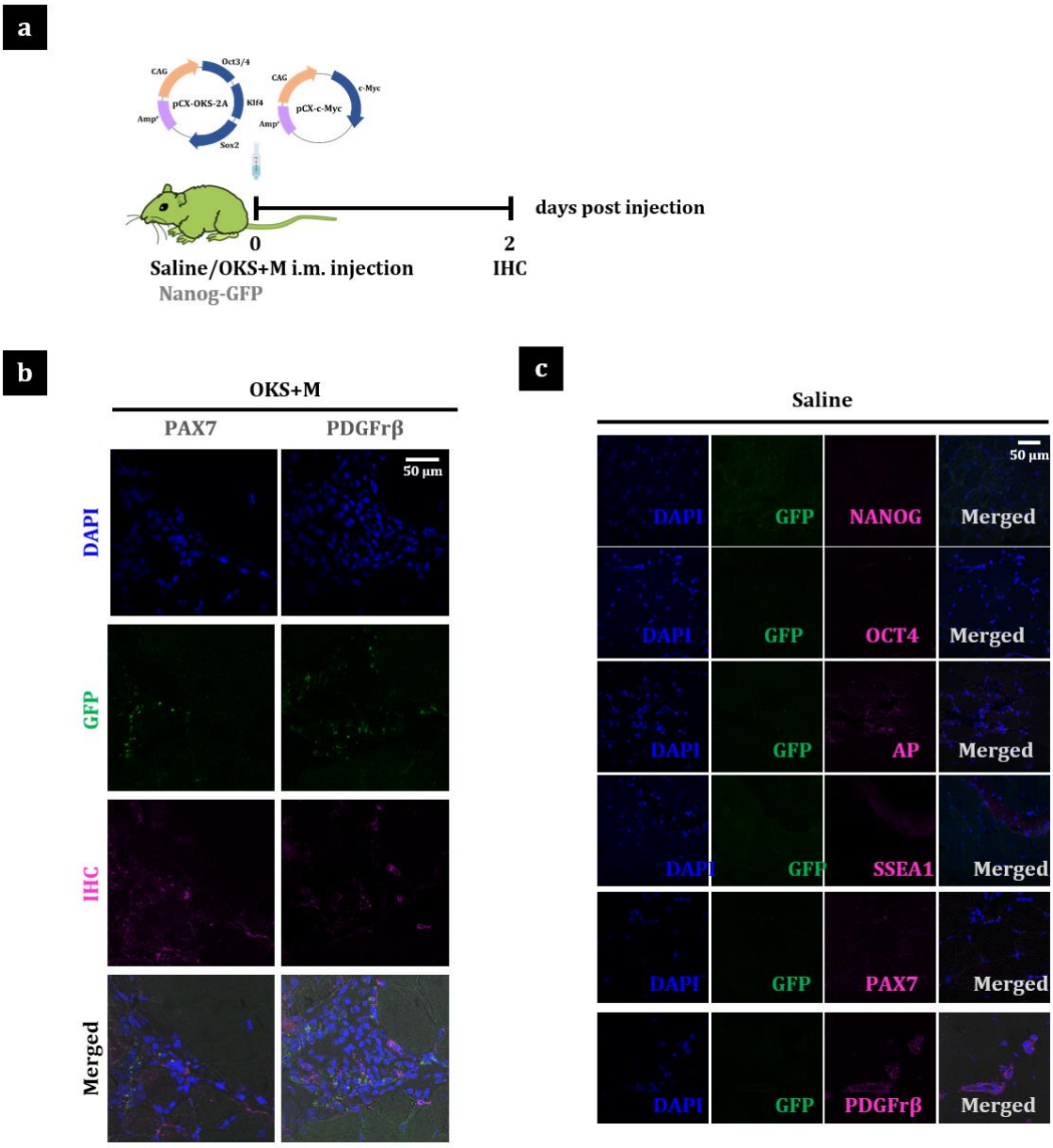

Figure S 5. Characterisation of in vivo reprogrammed cell clusters in the GA muscle of Nanog-GFP mice. (a) *Nanog-GFP transgenic mice were i.m. injected with 50μg* ***OKS*** *and 50 μg* ***M*** *or 50 μl 0.9% saline (control) in the GA muscle. Tissues were dissected 2 days after injection and 10 μm-thick tissue sections were obtained by cryotomy.* ***(b)*** *IHC for the expression of a satellite cell (PAX7) and a perycite (PDGFrβ) marker in Nanog⁺ cell clusters.* ***(c)*** *IHC for the expression of pluripotency, satellite cell and perycite markers in saline-injected controls.. Images were taken with a confocal microscope (100X). Scale bars represent 50 μm.*

Tissue	Disease model	Starting cell	Induced cell	Reprogramming factors	Vector	Administration	Outcomes	Ref.
Liver	Diabetes	Liver (cell type not determined)	Mixed phenotype (Insulin and glucagon producing cells)	*Pdx1*	Adenovirus	Intravenous	Endocrine and exocrine pancreatic markers Insulin production Long term amelioration of hyperglycaemia	[138, 139]
Liver	None	Hepatocyte Cholangiocyte	Mixed phenotype (not complete reprogramming)	*Pdx1*	N/A (conditional *Pdx1* transgenic model)	N/A	Endocrine and exocrine pancreatic markers Liver dysmorphogenesis and jaundice	[140]
Liver	Diabetes	Liver (cell type not determined)	Induced β-islet	*NeuroD, β-cellulin*	Adenovirus	Intravenous	Appearance of β-islet like structures in liver Long term amelioration of diabetes	[141]
Liver	Diabetes	Liver (cell type not determined)	Insulin-producing cell (hepatocyte phenotype remained)	*Pdx1VP16, NeuroD1*	Adenovirus	Intravenous	Insulin production in liver Amelioration of hyperglycaemia	[142]
Pancreas	Diabetes	α-cell	Induced β-cell	*Pdx1, Ngn3, MafA*	Adenovirus	Intrapancreatic	Generation of induced β-cells that secrete insulin in response to glucose. Long term alleviation of diabetes.	[49]
Liver	Diabetes	Hepatic progenitor/oval cells (not confirmed)	Induced (periportal) β-islet	*Ngn3, β-cellulin*	Adeno-associated virus	Intravenous	Transdetermination of hepatic progenitors No hepatocyte transdifferentiation Amelioration of diabetes	[143]
Liver	Diabetes	$Sox9^{+}$ cell	Insulin-secreting duct	*Pdx1, Ngn3, MafA*	Adenovirus	Intravenous	Generation of long-lasting insulin secreting ducts in liver. Long term alleviation of diabetes.	[144]

Table S 1. In vivo transdifferentiation studies in pancreas and liver. All studies were performed in mice.

Species	Disease model	Starting cell	Induced cell	Reprogramming factors	Vector	Administration	Outcomes	Ref.
Rat	Freeze-thaw injury	Cardiac fibroblasts	Skeletal myofibers	*MyoD*	Adenovirus	Intramyocardial	Immature myofibers in tissue	[146]
Mouse	MI	Cardiac fibroblast	Cardiomyocyte	*Gata4, Mef2c, Tbx5*	Retrovirus	Intramyocardial	Decreased infarct size. Significant attenuation of cardiac dysfunction	[147]
Mouse	MI	Cardiac fibroblast	Cardiomyocyte	*Gata4, Mef2c, Tbx5*	Retrovirus	Intramyocardial	Cardiomyocyte-like cells in fibrotic area No functional data	[148]
Mouse	MI	Cardiac fibroblast	Cardiomyocyte	*Gata4, Hand2, Mef2c, Tbx5*	Retrovirus	Intramyocardial	Decreased infarct size. Significant attenuation of cardiac dysfunction	[149]
Mouse	MI	Cardiac fibroblast	Cardiomyocyte	*microRNAs 1, 133, 208 and 499*	Lentivirus	Intramyocardial	Fibroblast to cardiomyocyte conversion in the infarct area Modest attenuation of cardiac dysfunction	[150, 151]
Guinea pig	Complete heart block	Ventricular cardiomyocyte	Pacemaker cell- induced sinoatrial node (iSAN) cell	*Tbx18*	Adenovirus	Intramyocardial	Establishment of a biological pacemaker Correction of bradycardia	[152]
Pig	Complete heart block	Ventricular cardiomyocyte	Pacemaker cell- induced sinoatrial node (iSAN) cell	*Tbx18*	Adenovirus	Percutaneous, to heart ventricule	Establishment of a biological pacemaker Correction of bradycardia	[153]

Table S 2. In vivo transdifferentiation studies in heart tissue.

Tissue	Disease model	Starting cell	Induced cell	Reprogramming factors	Vector	Administration	Outcomes	Ref.
Brain	None	Fibroblast Astrocyte	Induced neuron (iN)	*Ascl1, Brn2a, Myt1l*	Lentivirus doxycycline inducible	Transduced *in vitro* Doxycycline in drinking water	iNs in tissue	[154]
Brain	None	Astrocyte	Induced adult neuroblast (iANB)	*Sox2*	Lentivirus	Stereotactic (brain)	iANBs in tissue Mature neurons (+ BNTP/Noggin or VPA)	[155, 156]
Brain	Stab injury Alzheimer's disease	Astrocyte NG2 cell	Induced neuron (iN)	*NeuroD1*	Retrovirus	Stereotactic (brain)	Mature iN in tissue No functional or behavioural data	[157]
Brain	None	Callosal projection neuron (CPN)	Corticofugal projection neuron (CFuPN)	*Fezf2*	Plasmid DNA	*In utero* electroporation	Changes in morphology, gene and protein expression (until P3) Changes in axon connectivity (until E17.5)	[159]
Brain	None	L4 neuron	L5B neuron	*Fezf2*	Plasmid DNA	*In utero* Iontoporation	Changes in morphology, gene and protein expression and axon connectivity (until P1)	[160]
Spinal cord	Spinal cord injury	Astrocyte	Induced adult neuroblast (iANB)	*Sox2*	Lentivirus	Stereotactic (spinal cord)	iANBs in tissue Mature neurons (+VPA) Synapses with resident neurons No functional data	[158]

Table S 3. In vivo transdifferentiation studies in the CNS. All studies were performed in mice.

Nomenclature	Composition (for 50 ml medium)	Use
DMEM/LIF medium	DMEM.....42 ml FBS (15%).....7.5 ml NEAAs (1%).....0.5 ml 2-mercaptoethanol.....50 µl LIF.....5 µl	• Culture of E14TG2a cells. • Culture of i²PS cells. • Generation of i²PS cells from primary hepatocytes (add 2500 U Penicilin + 2500 µg Streptomycin).
KO-DMEM/2i/LIF medium	KO DMEM.....35.5 ml KSR.....7.5 ml NEAAs (1%).....0.5 ml Glutamine(1%).....0.5 ml 2-mercaptoethanol.....50 µl LIF.....5 µl GSK-3.....70 µg Mek1/2.....24 µg	• Culture of E14TG2a cells. • Culture of i²PS cells.
MEF medium	DMEM.....41 ml FBS (15%).....7.5 ml NEAAs (1%).....0.5 ml Penicilin.....2500 U Streptomycin.....2500 µg	• Isolation of primary MEFs. • MEF feeder layers.
MEF inactivation medium	DMEM.....41 ml FBS (15%).....7.5 ml NEAAs (1%).....0.5 ml Mitomycin C.....500 µg Penicilin.....2500 U Streptomycin.....2500 µg	• Inactivation of MEFs.
EBs medium	DMEM.....38.5 ml FBS (20%).....10 ml NEAAs (1%).....0.5 ml 2-mercaptoethanol.....50 µl	• EB generation. • Differentiation of cells from EBs.

Table S 4. Composition of cell culture media used in this thesis.

Group	Gene	Forward primer	Reverse primer
Housekeeping gene	*β-Actin*	GACCTCTATGCCAACACAGT	AGTACTTGCGCTCAGGAGGA
Reporter gene	*eGFP*	GACGGCGACGTAAACGGCCA	CAGCTTGCCGGTGGTGCAGA
Reprogramming factors	*Oct3/4*	TGAGAACCTTCAGGAGATATGCAA	CTCAATGCTAGTTCGCTTTCTCTTC
	Sox2	GGTTACCTCTTCCTCCCACTCCAG	TCACATGTGCGACAGGGGCAG
	c-Myc	CAGAGGAGGAACGAGCTGAAGCGC	TTATGCACCAGAGTTTCGAAGCTGTTCG
Pluripotency markers	*Nanog*	CAGAAAAACCAGTGGTTGAAGACTAG	GCAATGGATGCTGGGATACTC
	Ecat1	TGTGGGGCCCTGAAAGGCGAGCTGAGAT	ATGGGCCGCCATACGACGACGCTCAACT
	Rex1	ACGAGTGGCAGTTTCTTCTTGGGA	TATGACTCACTTCCAGGGGGCACT
	Cripto	ATGGACGCAACTGTGAACATGATGTTCGCA	CTTTGAGGTCCTGGTCCATCACGTGACCAT
	Gdf3	GTTCCAACCTGTGCCTCGCGTCTT	AGCGAGGCATGGAGAGAGCGGAGCAG
	Endo-Oct3/4	TCTTTCCACCAGGCCCCCGGCTC	TGCGGGCGGACATGGGGAGATCC
	Endo-Sox2	TAGAGCTAGACTCCGGGCGATGA	TTGCCTTAAACAAGACCACGAAA
	Endo-Klf4	GCGAACTCACACAGGCGAGAA ACC	TCGCTTCCTCTTCCTCCGACACA
Hepatocyte markers	*Alb*	GTTCGCTACACCCAGAAAGC	CCACACAAGGCAGTCTCTGA
	Aat	CAGAGGAGGCCAAGAAAGTG	ATGGACAGTCTGGGGAAGTG
	Trf	ACCATGTTGTGGTCTCACGA	ACAGAAGGTCCTTGGTGGTG
Early differentiation markers	*Afp*	AGCGAAATGTAGCAGGAGGA	AAACATCCCACTTCCAGCAC
	Fgf-5	AGTCAATGGCTCCCACGAAG	TGACGGTGAAGGAAAGTTCC
	Brachyury	CATGTACTCTTTCTTGCTGG	GGTCTCGGGAAAGCAGTGGC
Chimerism studies	*H2Kb*	GTGATCTCTGGCTGTGAAGTG	GTCGCGTTCCCGTTCTT
	H2Kd	GTTCCAGCGGATGTTC	TAGGTAGGCCCTGTAATA
	D19Mit59	CTCTAACTATCCTCTGACCTTCACA	TTTTAAGCAGAACATTGAGGACC

Table S 5. Primer sequences used for the characterisation of in vivo reprogrammed liver tissue and i²PS cells (Chapter III).

Group	Region	Forward primer	Reverse primer
Primers for PCR-based integration study	*O-1*	CGGAATTCAAGGAGCTAGAACAGTTTGCC	CTGAAGGTTCTCATTGTTGTCG
	O-2	GATCACTCACATCGCCAATC	CTG GGAAAGGTGTCCTGTAGCC
	K	GCGGGAAGGGAGAAGACACTGCGTC	TAGGAGGGCCGGGTTGTTACTGCT
	K-S	CCTTACACATGAAGAGGCACTTT	CAGCTCCGTCTCCATCAT GTT AT
	M	ACACTCCCCCAACACCAGGACGTTT	GAGATGAGCCCGACTCCGACCTCTT
		GCTCGCCCAAATCCTGTACCTCGTCCGAT	
	1	AGGTGCAGGCTGCCTATC	TTAGCCAGAAGTCAGATGCTC
	2	CTGGATCCGCTGCATTAATGA	CCGAGCGCAGCGAGTCA
	3	GAAAAGTGCCACCTGGTCGACATT	GGGCCATTTACCGTAAGTTATGTA
	4	TATCATATGCCAAGTACGC	TAGATGTACTGCCAAGTAGGAA
	5	TCTGACTGACCGCGTTACT	AGAAAAGAAACGAGCCGTCATT
	6	GCGAGCCGCAGCCATTGCCTTTTA	CCCAGATTTCGGCTCCGCCAGAT
Primers for Southern blot probes	**Transgene**	**Forward primer**	**Reverse primer**
	Oct3/4	AAGTTGGCGTGGAGAC	CTGAAGGTTCTCATTGTTGTCG
	Sox2	GGAGTGGAAACTTTTGTCC	TTGACCACAGAGCCCATGGA
	Klf4	GCGGGAAGGGAGAAGACACTGCGTC	GCCCGAGGGGCTCACGTCATTGATG
	c-Myc	GCTCGCCCAAATCCTGTACCTCGTCCGA	GCAACGCAATTAATGTGAGTTAG

Table S 6. Primer sequences used in genomic integration studies (Chapter III).

Group	Gene	Forward primer	Reverse primer
Housekeeping gene	*β-Actin*	GACCTCTATGCCAACACAGT	AGTACTTGCGCTCAGGAGGA
Reporter gene	*eGFP*	GACGGCGACGTAAACGGCCA	CAGCTTGCCGGTGGTGCAGA
Reprogramming factors	*Oct3/4*	TGAGAACCTTCAGGAGATATGCAA	CTCAATGCTAGTTCGCTTTCTCTTC
	Sox2	GGTTACCTCTTCCTCCCACTCCAG	TCACATGTGCGACAGGGGCAG
	c-Myc	CAGAGGAGGAACGAGCTGAAGCGC	TTATGCACCAGAGTTTCGAAGCTGTTCG
Pluripotency markers	*Nanog*	CAGAAAAACCAGTGGTTGAAGACTAG	GCAATGGATGCTGGGATACTC
	Ecat1	TGTGGGGCCCTGAAAGGCGAGCTGAGAT	ATGGGCCGCCATACGACGACGCTCAACT
	Rex1	ACGAGTGGCAGTTTCTTCTTGGGA	TATGACTCACTTCCAGGGGGCACT
Myogenesis markers	*Pax3*	GGGAACTGGAGGCATGTTTA	GTTTTCCGTCCCAGCAATTA
	MyoD	AGCACTACAGTGGCGACTCA	GCTCCACTATGCTGGACAGG
	Myf5	GAGCTGCTGAGGGAACAGGTGG	GTTCTTTCGGGACCAGACAGGG
	Myh1	CAGGTCAACAAGCTGCGGGTG	GATCTTCACATTTTGCTCATC
	Myog	TGTTTGTAAAGCTGCCGTCTGAC	AAAAATTGGCAAAACCACACAATGC
Satellite-cell markers	*Pax7*	GACGACGAGGAAGGAGACAA	CGGGTTCTGATTCCACATCT
	Caveolin-1	AGCAAAAGTTGTAGCGCCAG	TGGGCTTGTAGATGTTGCCC
	Integrin a 7	CAATCTGGATGTGATGGGTG	CTCAGGGGACAAGCAAAGAG
	Jagged-1	AGCTCACTTATTGCTGCGGT	CCGCTTCCTTACACACCAGT
Pericyte markers	*TN-AP*	GTGGATACACCCCCCGGGGC	GGTCAAGGTTGGCCCCAATGCA
	PdgfrB	AAGTTTAAGCACACCCATGACAAG	ATTAAATAACCCTGCCCACACTCT
	Rgs5	GCTTTGACTTGGCCCAGAAA	CCTGACCAGATGACTACTTGATTAGC

Table S 7. Primer sequences used in Chapter IV.

Group	Gene	Forward primer	Reverse primer
Housekeeping gene	*β-Actin*	GACCTCTATGCCAACACAGT	AGTACTTGCGCTCAGGAGGA
Reprogramming factor	*Oct3/4*	TGAGAACCTTCAGGAGATATGCAA	CTCAATGCTAGTTCGCTTTCTCTTC
Pluripotency marker	*Nanog*	CAGAAAAACCAGTGGTTGAAGACTAG	GCAATGGATGCTGGGATACTC
Myogenesis marker	*Pax3*	GGGAACTGGAGGCATGTTTA	GTTTTCCGTCCCAGCAATTA
Inflammation markers	*Il-6*	ATGGATGCTACCAAACTGGA	CCTCTTGGTTGAAGATATGA
	Cd11b	TGTCCTAGGGAATGGAGGCA	ACCACAGAACATGCCCATCC
	Mcp-1	CATGCTTCTGGGCCTGCTGTTC	CCTGCTGCTGGTGATCCTCTTGTAG
	Ccr2	TCCTGTAAAGACCTCAGCCCAA	AGTTTCCTGCAGAAAGAGAAGG
	Cd3	AGGGTGATTAGGATGGTGGGA	ACAATTGGGCTCCTCCTGAC
Myosin heavy chain isoforms	*Myh3*	AGAGGCAGGCTGAGGAGGCT	CCGGCTAGAGGTGAAGTCACGGG
	Myh8	ACACATCTTGCAGAGGAAGG	TAAACCCAGAGAGGCAAGTG
	Myh2	AAGCGAAGAGTAAGGCTGTC	GTGATTGCTTGCAAAGGAAC
	Myh4	ACAAGCTGCGGGTGAAGAGC	CAGGACAGTGACAAAGAACG
	Myh7	CCAAGGGCCTGAATGAGGAG	GCAAAGGCTCCAGGTCTGAG

Table S 8. Primer sequences used in Chapter VI.

Publications

- **de Lázaro I**, Yilmazer A, Nam Y, Degens H, Cossu G and Kostarelos K. ***In vivo* reprogramming to pluripotency leads to enhanced regeneration and functional rehabilitation of injured skeletal muscle.** (In preparation).
- **de Lázaro I** and Kostarelos K (2015) **Engineering cell fate for tissue regeneration by *in vivo* transdifferentiation**. Stem Cell Rev and Rep, Epub ahead of print.
- Yilmazer A, **de Lázaro I**, Taheri H (2015) **Reprogramming cancer cells: a novel approach for cancer therapy or a tool for disease-modelling?** Cancer Letters, 369(1): 1-8.
- Mazza M, Hadjidemetriou M, **de Lázaro I**, Bussy C, Kostarelos, K (2015) **Peptide Nanofiber Complexes with siRNA for Deep Brain Gene Silencing by Stereotactic Neurosurgery.** ACS Nano, 9(2), 1137-49.
- **de Lázaro I**, Bussy C, Yilmazer A, Jackson MS, Humphreys NE, Kostarelos K (2014) **Generation of induced pluripotent stem cells from virus-free *in vivo* reprogramming of BALB/c mouse liver cells.** Biomaterials, 35(29): 8312-20.
- **de Lázaro I**, Yilmazer A, Kostarelos K (2014) **Induced pluripotent stem (iPS) cells: a new source for cell-based therapeutics?** J Control Release, 185: 37-44.
- **de Lázaro I**, Kostarelos K (2014) ***In vivo* cell reprogramming to pluripotency: exploring a novel tool for cell replenishment and tissue regeneration.** Biochem Soc Trans, 42(3), 711-716.
- Yilmazer A, **de Lázaro I,** Bussy C, Kostarelos K (2013) ***In vivo* reprogramming of adult somatic cells to pluripotency by overexpression of Yamanaka factors.** J Vis Exp, 17(82).
- Yilmazer A, **de Lázaro I**, Bussy C, Kostarelos K (2013) ***In Vivo* Cell Reprogramming towards Pluripotency by Virus-Free Overexpression of Defined Factors.** PLoS ONE, 8(1): e54754.

Conferences and seminars

- Gordon Research Conference. **Exploring Innovations in Tissue Repair and Regeneration: From Bench to Therapies** (7-12.06.2015) New London, USA. **Poster presentation:** "Teratoma-free *in vivo* reprogramming to pluripotency in the mouse liver and generation of i²PS cells".
- Gordon Research Seminar. **Exploring Innovations in Tissue Repair and Regeneration: From Bench to Therapies** (6-7.06.2015) New London, USA. **Poster presentation and oral communication:** "*In vivo* reprogramming to pluripotency enhances regeneration and functional rehabilitation of injured skeletal muscle".
- Wellcome Trust Conference. **The Biology of Regenerative Medicines** (22-24.04.2015) Cambridge, UK. **Poster presentation:** "*In vivo* reprogramming to pluripotency enhances regeneration and functional rehabilitation of injured skeletal muscle". **Poster presentation and oral communication:** "Teratoma-free *in vivo* reprogramming to pluripotency in the mouse liver and generation of i²PS cells".
- **UCL School of Pharmacy PhD Research Day** (19.09.2014) London, UK. **Oral communication:** "Reprogramming the skeletal muscle to pluripotency *in vivo*".
- Gordon Research Conference. **Reprogramming cell fate: Understanding the Mechanisms of Nuclear Reprogramming and Its Potential in Cell Therapy** (02-07.03.2014) Galveston, Texas, US. **Poster presentation:** "*In vivo* reprogramming to pluripotency in BALB/c mice and generation of i²PS cells".
- Biochemical Society Annual Symposium. **Biochemical Determinants of Tissue Regeneration.** (11-13.12.2013) Macclesfield, UK. **Poster presentation and oral communication:** "*In vivo* reprogramming to pluripotency as a strategy for tissue regeneration".
- Wellcome Trust Conference. **Regenerative Medicine: from Biology to Therapy** (30.10-01.11.2013) Cambridge, UK. **Poster presentation and oral communication:** "Generation and characterisation of *in vivo* induced pluripotent stem (i²PS) cells".
- **UCL School of Pharmacy PhD Research Day** (20.09.2013) London, UK. **Poster presentation:** "Generation and characterisation of *in vivo* induced pluripotent stem (i²PS) cells".
- **International Conference on Stem Cells and Regenerative Medicine** (11-13.07.2012) jointly organised by inStem (Bangalore, India) and University College London (London, UK).
- **Young Embryologist (YEM) Network: Meeting 2012** (01.06.2012) Institute of Child Health (ICH), University College London, UK.
- **Driving Stem Research towards Therapy** (21-22.05.2012) MRC Centre for Regenerative Medicine, Edinburgh, UK.

Awards

- Wellcome Trust Conference. The Biology of Regenerative Medicines (22-24.04.2015) Cambridge, UK. **Best Poster Prize,** awarded by **Faculty of 1000.**
- Wellcome Trust Conference. The Biology of Regenerative Medicines (22-24.04.2015) Cambridge, UK. **Bursary Award.**
- UCL School of Pharmacy PhD Research Day (19.09.2014) London, UK. **Best Lecture Award.**
- Biochemical Determinants of Tissue regeneration (11-13.12.2013) Macclesfield, UK. **Best Poster Award.**
- UCL School of Pharmacy PhD Research Day (20.09.2013) London, UK. **Best Poster Award.**